Vol. 102 December 1, 1978
Complete in one issue

ISSN 0003-2670

ANALYTICA CHIMICA ACTA

International journal devoted to all branches of analytical chemistry

ELSEVIER SCIENTIFIC PUBLISHING COMPANY

ANALYTICA CHIMICA ACTA

International journal devoted to all branches of analytical chemistry
Revue internationale consacrée à tous les domaines de la chimie analytique
Internationale Zeitschrift für alle Gebiete der analytischen Chemie

PUBLICATION SCHEDULE FOR 1978 (incorporating the section on Computer Techniques and Optimization).

	J	F	M	A	M	J	J	A	S	O	N	D
Analytica Chimica Acta	96/1	96/2	97/1	97/2	98/1	98/2	99/1	99/2	100	101/1	101/2	102
Section on Computer Techniques and Optimization			103/1			103/2			103/3			103/4

Scope. *Analytica Chimica Acta* publishes original papers, short communications, and reviews dealing with every aspect of modern chemical analysis, both fundamental and applied. The section on *Computer Techniques and Optimization* is devoted to new developments in chemical analysis by the application of computer techniques and by interdisciplinary approaches, including statistics, systems theory and operation research. The section deals with the following topics: Computerized acquisition, processing and evaluation of data. Computerized methods for the interpretation of analytical data including chemometrics, cluster analysis, and pattern recognition. Storage and retrieval systems. Optimization procedures and their application. Automated analysis for industrial processes and quality control. Organizational problems.

Submission of Papers. Manuscripts (three copies) should be submitted to:
for *Analytica Chimica Acta:* Dr. A. M. G. Macdonald, Department of Chemistry, The University, P.O. Box 363; Birmingham B15 2TT, England;
for the section on *Computer Techniques and Optimization:* Dr. J. T. Clerc, Laboratorium für Organische Chemie, Swiss Federal Institute of Technology, Universitätstrasse 16, CH-8092 Zürich, Switzerland.

Information for Authors. Papers in English, French and German are published. There are no page charges. Manuscripts should conform in layout and style to the papers published in this Volume. Authors should consult Vol. 102, p. 253 for detailed information. Reprints of this information are available from the Editors or from: Elsevier Editorial Services Ltd., Mayfield House, 256 Banbury Road, Oxford OX2 7DE (Great Britain).

Reprints. Fifty reprints will be supplied free of charge. Additional reprints (minimum 100) can be ordered. An order form containing price quotations will be sent to the authors together with the proofs of their article.

Advertisements. Advertisement rates are available from the publisher.

Subscriptions. Subscriptions should be sent to: Elsevier Scientific Publishing Company, P.O. Box 211, 1000 Amsterdam, The Netherlands. The section on *Computer Techniques and Optimization* can be subscribed to separately.

Publication. *Analytica Chimica Acta* (including the section on *Computer Techniques and Optimization*) appears in 8 volumes in 1978. The subscription for 1978 (Vols. 96–103) is Dfl. 1000.00 plus Dfl. 120.00 (postage) (Total approx. US $486.96). The subscription for the *Computer Techniques and Optimization* section only (Vol. 103) is Dfl. 125 plus Dfl. 15.00 (postage) (Total approx. US $60.87). Journals are sent automatically by air mail to the U.S.A. and Canada at no extra cost and to Japan, Australia and New Zealand for a small additional postal charge. All earlier volumes (Vols. 1–95) except Vols. 23 and 28 are available at Dfl. 144.00 (U.S. $63.00), plus Dfl. 10.00 (U.S. $4. postage and handling, per volume.

Claims for issues not received should be made within three months of publication of the issue, otherwise they cannot be honoured free of charge.

Customers in the U.S.A. and Canada who wish to obtain additional bibliographic information on this and other Elsevier journals should contact our Journal Information Center, 52, Vanderbilt Avenue, New York, NY 10017. Tel: (212) 867-9040.

valuation and ptimization of Laboratory [ethods and nalytical Procedures

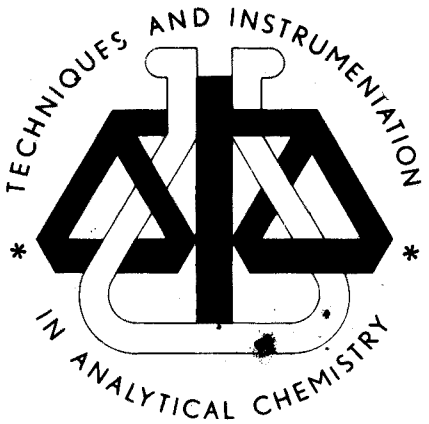

;urvey of Statistical and thematical Techniques

.. MASSART, A. DIJKSTRA *and* L. KAUFMAN.

h contributions by S. Wold, B. Vandeginste *and* Y. Michotte

chniques and Instrumentation in Analytical Chemistry - Volume 1

s book provides detailed treatment, in a single volume, of formal methods for imization in analytical chemistry. It is a comprehensive and practical handbook ich no analytical laboratory will want to be without.

aspects of optimization are discussed, from the simple evaluation of procedures the organization of laboratories or the selection of optimal complex analytical grammes. Quantitative discrete analysis as well as qualitative and continuous asurement techniques are evaluated.

; book consists of 30 chapters divided into 5 main parts.The main sections are: luation of the Performance of Analytical Procedures, Experimental Optimization, mbinatorial Problems, Requirements for Analytical Procedures, and Systems proach in Analytical Chemistry.

s work will be of practical value not only to those involved with optimization blems in analytical chemistry, but also to those in related fields such as nical chemistry or specialized fields such as chromatography. Because it cusses the application of many mathematical techniques in analytical chemistry, ; book will also serve as a general introduction to the new field of Chemometrics.

:. 1978 xvi + 596 pages US $57.75/Dfl. 130.00 ISBN 0-444-41743-5

ELSEVIER

Dutch guilder price is definitive. US $ prices are subject to exchange rate fluctuations.

P.O. Box 211,
1000 AE Amsterdam
The Netherlands

52 Vanderbilt Ave
New York, N.Y. 10017

7113

nouncing new volumes in two series:

iomolecular Information Theory

SERAFIN FRAGA, K.M.S. SAXENA, *and* MANUEL TORRES, *Department of Chemistry, iversity of Alberta.*

udies in Physical and Theoretical Chemistry 4

vances in computer technology have led to unforeseeable possibilities in the theoretical dy of biological processes. The purpose of the present work is to review, update and sum-rize the applicability of molecular recognition theory in quantum biology and quantum bio-emistry. The book will be particularly valuable because of its comprehensive summary (in ular form and in figures) of all the practical information required for the theoretical con-uction of biopolymers and the evaluation of their interactions.

BREVIATED CONTENTS: **I. Introduction. II. Biomolecular Information.** Chapters: 1. The Code d its Origins. **III. Molecular Information Theory.** 2. Recognition Processes. 3. Interaction ergies. 4. Computational Simulations. **IV. Appendices:** Coordinates. Transformation of Coordi-es. Determination of Cartesian Coordinates. Spherical Harmonics. Basic Statistical-rmodynamical Formulas. Electric Fields and Moments. Density Distributions: Population alysis and Properties. Bond-Energy Analysis. **V. References. VI. Author Index. VII. Subject dex.**

pt. 1978 × + 272 pages US $48.75/Dfl. 112.00 ISBN 0-444-41736-2

---

ritium in Organic Chemistry

topes in Organic Chemistry, Volume 4

ted by E. BUNCEL, *Queen's University, Kingston, Ontario, Canada, and* C.C. LEE, *University Saskatchewan, Saskatoon, Saskatchewan, Canada.*

h a foreword by Lars Melander.

s series is rapidly gaining recognition as an indispensible work, of value to lecturers, dents, and research workers alike.

BREVIATED CONTENTS: Chapters: 1. Tritium Nuclear Magnetic Resonance Spectroscopy *. Elvidge, J.R. Jones, V.M.A. Chambers and E.A. Evans).* 2. The Use of Tritium and Deuterium Photochemical Electrophilic Aromatic Substitution *(W.J. Spillane).*3. Reactions of Energetic ium Atoms with Organic Compounds *(Y.-N Tang).*4. Stereospecific Synthesis of Tritium belled Organic Compounds Using Chemical and Biological Methods *(D.W. Young).* bject Index.

t. 1978 xvi + 300 pages US $66.75/Dfl. 150.00 ISBN 0-444-41741-9

ELSEVIER

Dutch guilder price is definitive. US $ prices are subject to exchange rate fluctuations

P.O. Box 211,
1000 AE Amsterdam
The Netherlands

52 Vanderbilt Ave
New York, N.Y. 10017

7106

Announcing two new volumes in the series:

Journal of Chromatography Library

Volume 13

INSTRUMENTATION FOR HIGH-PERFORMANCE LIQUID CHROMATOGRAPHY

J.F.K. HUBER (Editor), Institute of Analytical Chemistry, University of Vienna, Austria.

A practical guide for all those involved in the application of column liquic chromatography, this book provides a valuable, up-to-date review of the large selection of instrumentation currently available. Special emphasis is given to discussion of the general principles of design which will remain relevant even i new technical solutions are found in the future. The final chapter comprises a useful compilation of commercially available chromatographs together with their specifications.

Aug. 1978 xii + 204 pages US $34.75/Dfl. 80.00 ISBN 0-444-41648-X

Volume 16

POROUS SILICA

Its Properties and Use as Support in Column Liquid Chromatography

KLAUS K. UNGER, *Professor of Chemistry at the University of Mainz, West Germany.*

This book provides the chromatographer with full information on the properties of silica and its chemically bonded derivatives in context with its chromatographic behaviour. The first part of the book deals with the physical and chemical properties of silica including pore structure, surface chemistry, particle preparation and characterization, while the second part surveys the wide-spread application of untreated and chemically modified silica as absorbent, support and ion exchanger in the four modes of HPLC, i.e. adsorption, partition, ion exchange and size exclusion chromatography. The book will be useful to all those who use silica in HPLC and who seek to choose the optimum silica packing for a given separation problem.

Jan. 1979 ca. 300 pages US $52.25/Dfl. 120.00 ISBN 0-444-41683-8

ELSEVIER

The Dutch guilder price is definitive. US $ prices are subject to exchange rate fluctuations.

P.O. Box 211,
1000 AE Amsterdam
The Netherlands

52 Vanderbilt Ave
New York, N.Y. 10017

7111

ANALYTICA CHIMICA ACTA
VOL. 102 (1978)

ANALYTICA CHIMICA ACTA

International journal devoted to all branches of analytical chemistry

ELSEVIER SCIENTIFIC PUBLISHING COMPANY

Anal. Chim. Acta, Vol. 102 (1978)

Printed in The Netherlands

Analytica Chimica Acta, 102 (1978) 1—13

THE EFFECT OF SAMPLE ENVIRONMENT ON THE ROOM-TEMPERATURE PHOSPHORESCENCE OF SEVERAL POLYNUCLEAR AROMATIC HYDROCARBONS

ESTHER LUE-YEN BOWER** and J. D. WINEFORDNER*

Department of Chemistry, University of Florida, Gainesville, FL 32611 (U.S.A.)

(Received 10th July 1978)

SUMMARY

Room-temperature phosphorescence (r.t.p.) of numerous molecules has been studied with emphasis on several polynuclear aromatic hydrocarbons (PAH). The heavy atom effect has led to a significant enhancement of r.t.p. signals for the PAH studied with the trend being $Tl^+ > Ag^+ > Pb^{2+} > Hg^{2+}$. The Tl^+ also resulted in enhanced spectral features of emission bands. R.t.p. could be induced from PAH on a sodium acetate sample support as well as on filter paper. A study of the effect of different gaseous environments provided anomalous results.

Polynuclear aromatic hydrocarbons (PAH) have been investigated extensively in recent years because of their occurrence in automobile exhaust, coal tars, meat products, and cigarette smoke, and their relationship with cancer in man. The presence of PAH has become so widespread that even green vegetables and fruits have been found to be contaminated, especially when grown in the vicinity of heavy traffic [1]. Scientific evidence has led to a correlation between smoking and lung cancer [2] and since then a great deal of effort, time, and money have been spent in identifying and attributing carcinogenic activity to the PAH components. These have been mainly tri-, tetra-, penta-, and hexa-cyclic compounds, although the carcinogenic activity of the larger ring structures has been less studied only because of their limited availability and the difficulty of separating and characterizing them in complex mixtures.

The carcinogenicity of a particular compound is extremely dependent on its structure; shape, size, steric factor, and substituent position are all important. For example, chrysene and 1-, 2-, 4-, and 6-methylchrysenes are moderately carcinogenic, while 3- and, especially 5-methylchrysene, are strong tumor initiators [3].

Among the techniques used for determination and characterization of PAH in cigarette smoke are gas chromatography [4, 5], gas chromatography—mass spectrometry and Fourier-transform n.m.r. [6]. The presence of PAH in meat

**Present address: Materials Science & Engineering, University of Florida, Gainesville, FL 32611, U.S.A.

products is also of great concern and has been determined mainly by liquid-solid or liquid-liquid extraction followed by further purification and identification with column chromatography [7—9]. Sawicki et al. [10] separated PAH from airborne particulates by thin-layer chromatography with fluorescence detection, while others [11, 12] have chosen gas chromatography with fluorescence, electron capture or flame ionization detectors.

Several workers [13—15] have shown the usefulness of low-temperature luminescence for the determination of several PAH. Hood and Winefordner [16] found the combination of thin-layer chromatography with low-temperature luminescence detection to be extremely useful and sensitive for studying PAH. Others have used capillary column chromatography [17—20], gel filtration chromatography [21], adsorption chromatography followed by ultraviolet, visible or mass spectrometric detection [22], supercritical fluid chromatography [23], dry-column and thin-layer chromatography with fluorescence detection [24, 25], and the Shpol'skii effect at 77 K [26].

Since the initial observation of room-temperature phosphorescence [27] of ionic compounds adsorbed on filter paper and its rediscovery several years later [28, 29], the technique as described in recent articles [28—35] has swiftly developed to a simple, sensitive, and rapid method of analysis. However, its application to non-ionic compounds have so far been limited [32] and the importance of PAH has instigated further work in this area. This article reports a more detailed study of PAH, and of the effects of sample environment on signal-to-background intensities with room-temperature phosphorimetry (r.t.p.) The results obtained should provide further insight as to the mechanism prevailing.

EXPERIMENTAL

Chemicals

The compounds determined were obtained from commercial sources (Table 1) and were used without further purification. Ethanol (U.S. Industrial Chemicals Co., New York,), silver nitrate, sodium acetate, sodium malonate, and sodium citrate (Mallinckrodt Chemical Works), sodium hydroxide (Fisher Scientific) and sodium iodide (Alfa Products) were used to prepare the solutions and reagents. Lead nitrate (Mallinckrodt Chemical Works), mercury(II) chloride and mercury(II) nitrate (J. T. Baker Chemical Co.), thallium(I) acetate (PCR Inc., Gainesville, FL) and thallium(I) chloride (Alfa Products) were used in the heavy atom study as received. Schleicher and Schuell 591-C and S & S 604 were the filter papers used as the sample support.

Apparatus and procedure

All phosphorescence measurements were performed on an Aminco-Bowman spectrophotofluorimeter (American Instrument Co., Inc., Silver Spring, MD); the experimental details have already been described [30—32].

TABLE 1

Compounds studied by phosphorescence and their sources

Compound	Source	Compound	Source
Anthracene 1,2-Benzanthracene Chrysene Fluoranthene Naphthalene Pyrene	Chem Service, Media, PA	Benzo[a]pyrene Coronene Rubrene	Fluka AG, Buchs, Switzerland
		Benzo[e]pyrene 1,2,5,6-Dibenzanthracene 2,3,6,7-Dibenzanthracene	K & K Laboratories, Inc., Plainview, NY
Acridine 7,12-Dimethylbenzanthracene Phenanthrene	Eastman Kodak, Rochester, NY	1,2,7,8-Dibenzphenanthrene 1,2,4,5-Dibenzpyrene Perylene	
Triphenylene	Technam, Inc., Park Forest, S., IL	*p*-Aminobenzoic acid	Nutritional Biochemicals Corp., Cleveland, OH

RESULTS AND DISCUSSION

Solutions of pyrene and phenanthrene in ethanol and of silver nitrate were placed on 0.25-in. circles of Teflon tape to provide an inert support. No phosphorescence emission developed even in the presence of silver(I). The same procedure was repeated on asbestos tape and spectrographic emulsions impregnated with silver. No signal was seen on the asbestos tape, while only weak signals were observed on the spectrographic emulsions. Since it was earlier observed [32] that a heavy atom perturber was necessary for the observation of r.t.p. emission of PAH adsorbed on filter paper, the weak signal could be due to the unavailability of Ag^+ on the plates. This seemed to indicate that the functional groups on the paper were necessary for the r.t.p. phenomenon to be observed, as well as available Ag^+ or other heavy metal ion.

The effect of sodium acetate on r.t.p.

Von Wandruszka and Hurtubise [33] have shown that certain molecules such as *p*-aminobenzoic acid and folic acid give intense phosphorescence emission at room temperature when embedded in a sodium acetate matrix. Their experiments resulted in an extremely selective method for these compounds and a few others. Indications were that the molecules were adsorbed flatly, and the overlap of functional groups of the analyte molecule and sodium acetate that occurred led to rigid adsorption.

Filter paper was therefore treated by moistening with 1 M sodium acetate and allowing it to dry. The same was done for solutions of 1 M sodium citrate and malonate to see if increasing the number of carbonyl groups would lead to an increase in phosphorescence. These pretreated papers were then used as supports for r.t.p. analyses.

Two compounds, *p*-aminobenzoic acid and phenanthrene, were selected for this study because both were known to give good signals at low temperature as well as at room temperature [15, 31]. Also, it was thought necessary to have a representative of both ionic and non-ionic compounds since their

behavior appears to be different under r.t.p experimental conditions [27–35]. A comparison was done with *p*-aminobenzoic acid in 1 M NaOH–1 M sodium iodide (1:1) and phenanthrene in 0.05 M $AgNO_3$ on untreated filter paper as well as pretreated paper. R.t.p. emission approximately 3-fold greater was seen with the sodium acetate-pretreated paper with a concurrent 4-fold increase in the background emission of the blank, so that the calculated limit of detection was about 2-fold worse (Table 2). Approximately the same results were obtained with sodium citrate and sodium malonate.

Because there was no significant improvement in the limit of detection and because of the complicated matrix created for the analyte (acetate, hydroxide and iodide), this was considered to be of limited analytical merit and no further work was done on this procedure. Also, silver nitrate solution could not be used because darkening of the sample occurred, and no signals were seen.

It has also been reported [33] that r.t.p. emission could not be observed from any non-ionic compounds adsorbed on sodium acetate. In order to verify this and to see if emission could be induced, several PAH were examined on sodium acetate pellets with and without a heavy atom. Analytical reagent-grade sodium acetate was dried overnight at 110°C. The dried powder was then pressed into pellets of 0.25-in. diameter. The same compounds were measured under similar conditions on S & S 591-C filter paper. There was no darkening of the pellets when silver nitrate was added. The results are summarized in Table 3.

No r.t.p. emission was observed when ethanolic solutions were dried on sodium acetate pellets, but, as with the filter paper, intense emission was seen from several PAH when silver nitrate was added as in the case of fluoranthene (see Fig. 1). At the wavelength of excitation, there was no background emission from the pellets beyond 400 nm even when ethanol and silver nitrate were added to determine the blanks. This seemed to make it an ideal support except that considerably lower signals were obtained for the pellets compared to the signal levels on the paper; therefore, poorer limits of detection were obtained with the pellets. Additional drying was of no help in increasing signal levels. It was also curious that pyrene gave no r.t.p. emission from the sodium acetate pellets even in the presence of silver nitrate.

TABLE 2

p-Aminobenzoic acid (PABA) and phenanthrene on S & S 591-C filter paper with and without sodium acetate

Solution	Condition	Limit of detection (ng)[a]
PABA in 1 M NaOH–1 M NaI	With sodium acetate	0.2
PABA in 1 M NaOH–1 M NaI	Without sodium acetate	0.1
Phenanthrene in 0.05 M $AgNO_3$	With sodium acetate	—[b]
Phenanthrene in 0.05 M $AgNO_3$	Without sodium acetate	1.8

[a]The limit of detection is defined as the concentration resulting in a signal-to-noise ratio of three and is calculated for a 3-μl sample.
[b]Paper darkened. No signal seen.

TABLE 3

Limits of detection for several polyaromatic hydrocarbons on sodium acetate pellets and filter paper

Compound	Sodium acetate pellets			Filter paper		
	λ_{ex} (nm)	λ_{em} (nm)[a]	LOD[b] (ng)	λ_{ex} (nm)	λ_{em} (nm)[a]	LOD[b] (ng)
Anthracene	250	— —	—	290	—	—
Benzo(a)pyrene	325	— —	—	310	—	—
Chrysene	280	480, 505, 560	6.0	272	515,550	0.45
Coronene	300	515, 550	15.3	310	525, 560	1.1
1,2,5,6-Dibenz-anthracene	300	565	19.2	300	500, 555	8.4
1,2,4,5-Dibenz-pyrene	334	—	—	280	—	—
Fluoranthene	363	560	19.2	284	500, 555	1.7
Perylene	332	—	—	310	—	—
Phenanthrene	290	480, 505	6.9	260	505	0.9
Pyrene	336	—	—	322	590	2.7
Rubrene	316	—	—	286	—	—
Acridine	—	—	—	290	—	—
1,2-Benzanthracene	—	—	—	290	515	—
7,12-Dimethylbenz-anthracene	—	—	—	320	—	—
2,3,6,7-Dibenz-anthracene	—	—	—	290	—	—
1,2,7,8-Dibenz-phenanthrene	—	—	—	290	510, 540	—
1,2-Benzpyrene (Benzo(e)pyrene)	—	—	—	348	420, 470, 548	—
Naphthalene	—	—	—	340	—	—
Triphenylene	—	—	—	268	395, 465, 490	—

[a]The underlined wavelengths represent the peak of greatest intensity and are the ones used for the limits of detection.
[b]LOD = limit of detection; defined as the concentration of analyte resulting in a signal-to-noise ratio of 3. The estimations were for 3-μl samples.

Another striking feature was that pyrene in ethanol (no heavy atom) gave r.t.p. emission under the experimental conditions used. The only differences between this and a previous study [32] involving pyrene were (i) the filter paper was changed from ED 613 filter paper to S & S 591-C filter paper because this paper gave better signal-to-background ratios [34], and was available in filter paper rolls to be used later in a continuous sampling system [36]; (ii) warm, dry nitrogen was used to flush the sample compartment instead of air. The concentrations of the solutions in both cases were approximately the same. The experiment was therefore repeated with, first, S & S 591-C as the sample support and a flow of air through the sample compartment,

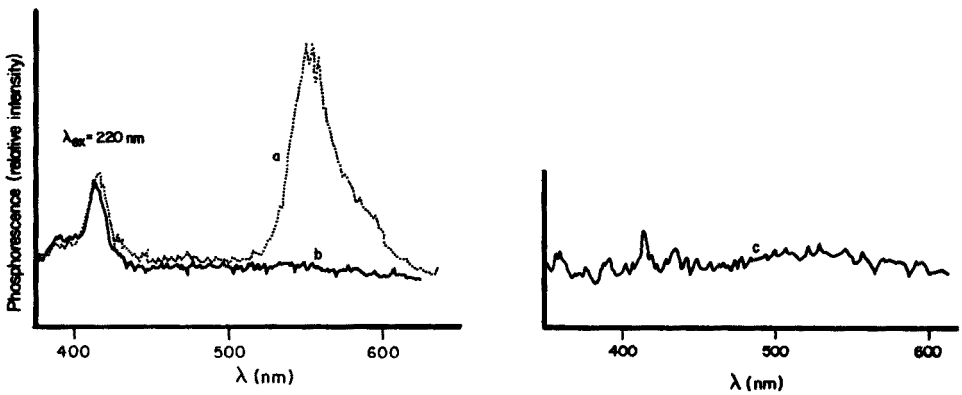

Fig. 1. Spectra of fluoranthene on sodium acetate pellet: (a) 60 ppm ethanolic solution + 0.2 M $AgNO_3$; (b) 60 ppm ethanolic solution only; (c) Blank for (a) (ethanol + 0.2 M $AgNO_3$

and secondly, ED 613 and a flow of nitrogen. In the first case, no emission was seen at room temperature while in the second case, a significant signal was observed. These results led to a study of different flow gases.

The limits of detection proved to be also better for all cases where samples were on filter paper compared with sodium acetate pellets. Chrysene, coronene, and fluoranthene had limits of detection lower by more than an order of magnitude so that the use of sodium acetate did not lead to any significant advantage other than the lower background emission compared with paper. It should be pointed out that the pellets were not prepared quantitatively, i.e., arbitrary amounts of sodium acetate were used and the pressure applied was manual and, therefore, variable. However, a certain amount of variability would also be expected on the surface of the filter paper.

Of the three 5-ringed compounds (benzo(a)pyrene, 1,2,5,6-dibenzanthracene and perylene) investigated, only 1,2,5,6-dibenzanthracene gave any phosphoresecence under room temperature conditions. The structural arrangement of the 5 rings was thought to be of importance with regard to whether r.t. phosphorence would occur or not. Compounds such as 2,3,6,7-dibenzanthracene, 1,2,7,8-dibenzphenanthrene, and other PAH were investigated on paper in order to observe any possible structural dependence. These results are listed at the end of Table 3. No correlation between the energy separations ($\Delta E_{S,T}$) for these compounds (compare Morgan et al. [37]) was observed. However, it would appear that if the lifetime of the compound was $\leqslant$ 0.1 s at 77 K then r.t. phosphorescence would not be seen under the experimental conditions used. The lifetime values for these compounds at 77 K were found in the literature [37—39]. One would expect the lifetime at room temperature (actually 60°C), and under the influence of a heavy atom to be considerably shorter than that at low temperature without a heavy atom. Work is presently being carried out to verify this.

Because the maximum speed of the rotating-can phosphoroscope is approximately 160 Hz, any compound with a lifetime of about 1 ms and mediocre

quantum efficiency ($Y_p < 0.01$) could possibly have completely decayed before the slot of the rotating can had moved to the viewing position. This perhaps accounted for the results obtained with compounds such as benzo(a)pyrene ($\tau_{77\,K}$ = 0.11 s) and 7,12-dimethylbenzanthracene ($\tau_{77\,K}$ = 0.11 s) which are known [37] to phosphoresce at 77 K but do not phosphoresce under room temperature conditions.

Triphenylene (9,10-benzophenanthrene) exhibited an anomaly not seen with the other PAH. Emission (both fluorescence and phosphorescence) was observed under the experimental conditons used (Fig. 2) even without silver nitrate. The emission peak at 395 nm was attributed to delayed fluorescence or other long-lived fluorescence, i.e., longer than the usual time of about 10^{-9} s. The peak at 457 nm was attributed to phosphorescence. Normal room-temperature fluorescence of triphenylene occurs at 357 nm in pentane and the phosphorescence is seen at 460 nm in ethanol at 77 K [40]. The large red shift of the fluorescence cannot immediately be accounted for, but could possibly be due to dimer (excimer) formation and the different circumstances under which emission was being observed. The interesting observation was that when silver nitrate was added, the peak at 395 nm was reduced to about half its original intensity while the peak at 457 nm was shifted to 465 nm and became clearer. Under the experimental conditions used, normal fluorescence was not previously observed because of the gating effect of the rotating can. It is possible that delayed fluorescence could occur because reverse intersystem crossing from the first triplet state back to the excited singlet at the temperatures used in r.t.p. analysis (60°C) would be possible.

The influence of different heavy atoms on the r.t.p. of PAH

The effect of different heavy atoms on the r.t.p. of several PAH was examined. The heavy atom perturbers selected were Ag^+ as $AgNO_3$; Pb^{2+} as

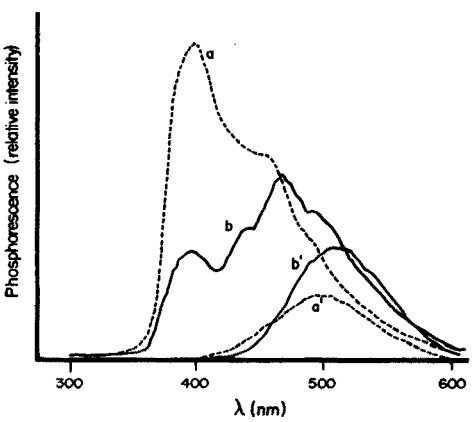

Fig. 2. R.t. phosphorescence of triphenylene with and without heavy atom (λ_{ex} = 268 nm) on S & S 591-C filter paper: (a) in ethanol only; (a') blank for (a); (b) 0.1 M $AgNO_3$ added; (b') blank for (b).

$Pb(NO_3)_2$; Hg^{2+} as 0.1 M $HgCl_2$ or 0.1 M $Hg(NO_3)_2$; and Tl^+ as 0.1 M CH_3COOTl. It was most desirable to have all the anions the same, but their immediate availability prevented this. In this study, S & S 591-C filter paper was used for the reasons already stated.

Of the four heavy ions, thallium(I) seemed to be the greatest enhancer of r.t.p. signals for all PAH with the trend being $Tl^+ > Ag^+ > Pb^{2+} > Hg^{2+}$. In addition to producing greater signals, the presence of thallium(I) resulted in narrower bands and enhanced spectral features in some cases (see Fig. 3 and 4). The narrower bands were at first attributed to the acetate anion which was suspected of contributing a matrix effect similar to that in the sodium acetate matrix. This idea was rejected when a saturated solution (12 mM or approximately 3%) of thallium(I) chloride gave the same band narrowing effect and enhanced special features. Phosphorescence intensity with thallium chloride was not as intense as with thallium acetate because of the lower concentration of the thallium ion. The results for all PAH investigated are listed in Table 4 where all intensities are normalized with respect to signals obtained with thallium acetate.

A shoulder at 550 nm was seen for chrysene and at 590 nm for fluoranthene with thallium acetate which was absent in the presence of Ag^+, Pb^{2+}, and Hg^{2+}. Phenanthrene had two peaks (475 nm and 505 nm) with thallium(I) or lead(II), whereas only the 505-nm peak was obtained with silver(I). At the other end

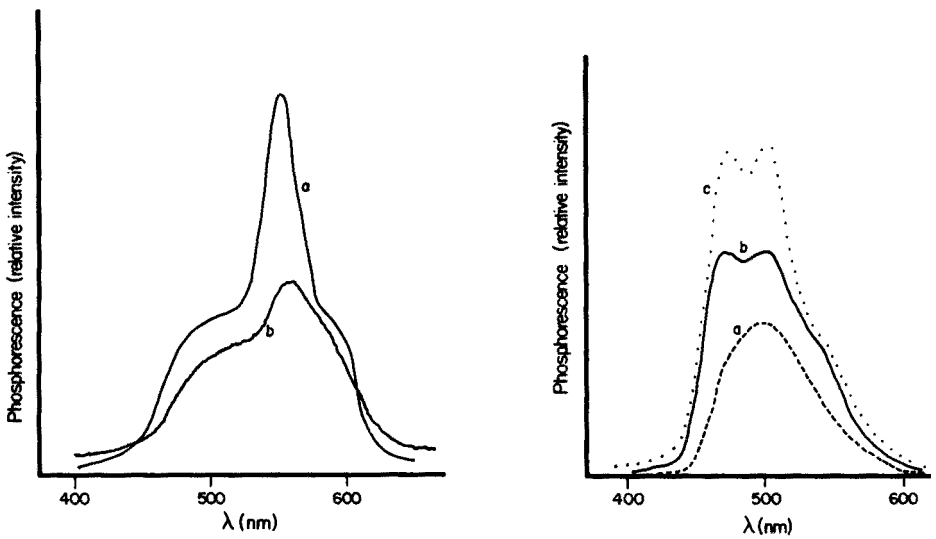

Fig. 3. R.t. phosphorescence of fluoranthene (60 ppm in ethanol) with Ag^+ and Tl^+: (a) with 0.1 M thallium acetate (× 5); (b) with 0.1 M silver nitrate. Spectra were recorded with different sensitivity scales.

Fig. 4. R.t. phosphorescence of phenanthrene with Ag^+ and Tl^+ (110 ppm in ethanol): (a) with 0.1 M $AgNO_3$ added (× 3.3); (b) with 0.1 M thallium acetate added (× 10); (c) with 12 mM thallium chloride added (× 1). Spectra were recorded with different sensitivity scales

TABLE 4

Summary of the effect of different heavy atoms on the r.t. phosphorescence of PAH

Compound	λ_{ex} (nm)	λ_{em} (nm)	I_{Pb}^{a}/I_{Tl}	I_{Hg}^{a}/I_{Tl}	I_{Ag}^{a}/I_{Tl}
Chrysene	272	515	0.071	0.011	0.29
Coronene	310	525	0.054	0.051	0.44
1,2,5,6-Dibenzanthracene	300	555	0.05	0.013	0.28
Fluoranthene	284	550	0.17	0.019	
Phenanthrene	260	505	0.046	—	0.23
Pyrene	322	590	0.067	0.015	0.16

[a] I/I_{Tl} represents the ratio of the phosphorescence signal intensity with a heavy atom (Pb, Hg, or Ag) to the signal intensity obtained in the presence of Tl. All solutions used were of the same concentration.

of the scale, mercury(II) led to a single peak which showed no enhancement in signal intensities and in a few cases caused quenching of the paper background emission.

As demonstrated earlier, the heavy atom effect makes it possible to induce emission from PAH resulting in low limits of detection. These limits can now be further lowered by up to 6-fold by using a thallium(I) salt (Table 4). In addition, narrowing of the emission bands and additional "fine" structure in the emission peaks further enhance the attractiveness of exploring the use of the heavy atom effect in analysis.

Effect of different flow gases on room temperature phosphorescence

It was noted earlier that when a solution of pyrene in ethanol was examined on paper, no r.t.p. emission was seen when air was flowed through the sample compartment but that emission was observed when nitrogen was used. A study of the effect of different flow gases on signal levels was therefore carried out. A plot of phosphorescence signal growth of pyrene in ethanol—0.1 M $AgNO_3$ (1:1) with time is shown in Fig. 5(A). Use of nitrogen led to an almost 3-fold increase over air. The curve labelled "N_2 low T" was constructed from data obtained when dry nitrogen was passed through copper coils immersed in a dry ice—acetone bath (—78.5°C). The experiment was repeated with phenanthrene in ethanol—0.1 M $AgNO_3$ (1:1) and again the same trend was seen (Fig. 5(B)) though the differences in relative intensities were not the same. Argon and nitrogen at low temperature have apparently switched places but their relative positions are within the experimental error of the technique (r.s.d. 15%) so that, when the test was repeated, nitrogen (low T) was highest with argon slightly below.

The rates at which the phosphorescence increased with time varied from sample to sample for a particular solution but when the signal levelled off, the relative intensities were found to be within 10% of each other. Figure 6

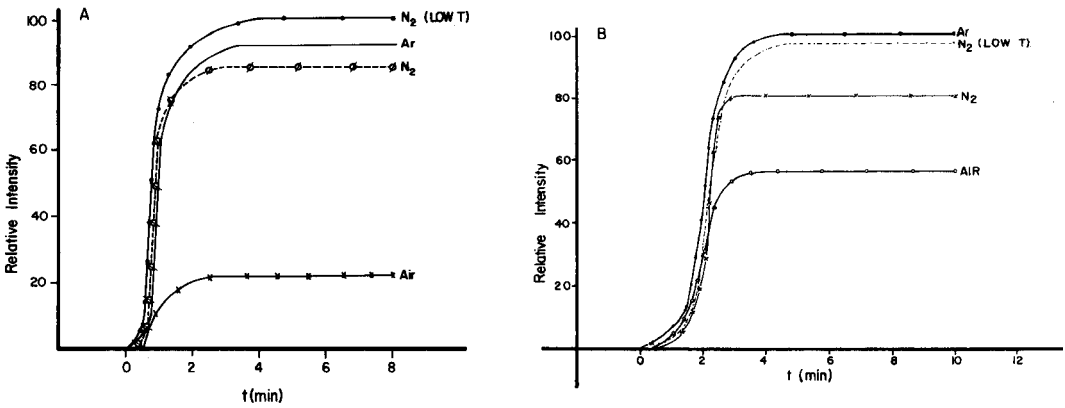

Fig. 5. Growth of phosphorescence signal with time for different flow gases. (a) Pyrene in ethanol—0.1 M $AgNO_3$(1:1) with λ_{ex} = 330 nm and λ_{em} = 590 nm. (b) Phenanthrene in ethanol—0.1 M $AgNO_3$ (1:1) with λ_{ex} = 260 nm and λ_{em} = 505 nm.

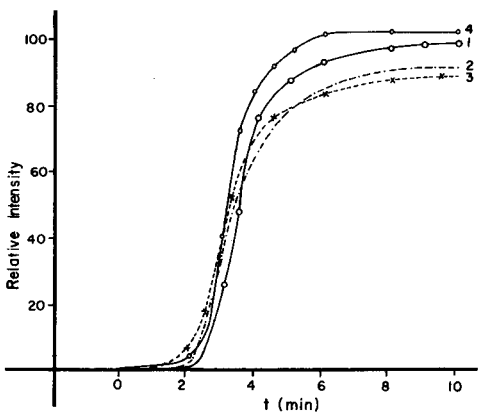

Fig. 6 Variation of the growth of phosphorescence signal with sampling for a series of solutions. All samples (1—4) were 3 μl of a 50-ppm solution of phenanthrene in ethanol—0.1 M $AgNO_3$ (1:1). λ_{ex} = 260 nm; λ_{em} = 505 nm; low rate of nitrogen = 2 l min^{-1}; temperature of nitrogen = 60°C.

shows a plot of four different samples of the same solution and their varying growth rates, which is unimportant in this technique if the samples are dried before they are analyzed and remain dry during the analysis. The rate of phosphorescence signal growth reflects the rate of drying; this will depend on the porosity and thickness of the filter paper, the manner in which it was mounted in the sample holder, the solvent used, and the particular analyte being investigated. The rate of gas flow and the temperature of the gas used to flush the sample compartment are also important in the rate of drying, but these were maintained constant throughout the studies described here.

An ionic compound, *p*-aminobenzoic acid, was subjected to the different flow gases; the data are plotted in Fig. 7. Surprisingly, air, argon, and nitrogen at 60°C all gave the same phosphorescence intensity on drying. Atmospheric carbon dioxide was suspected of forming a $NaOH—Na_2CO_3$ matrix thereby providing an added matrix rigidity in addition to adsorption on the paper. However, when carbon dioxide was passed through the sample compartment, approximately the same signal level was obtained, though the signal level was attained more quickly, possibly because of quicker formation of sodium carbonate. It appeared that nitrogen or argon was a suitable gas for both ionic and non-ionic compounds for obtaining optimum signals. A thorough explanation of the behavior of the gases cannot be offered.

The data presented in this portion were obtained from repeating the experiments until duplicate intensities were obtained within 10% of each other. The higher values for all cases were used in plotting the curves in Figs. 5 and 7.

CONCLUSIONS

It is difficult to conclude from this study the exact mechanism which prevails. Studies involving even greater variation in conditions and of the effects of different parameters on r.t. phosphorescence are necessary to arrive at conclusive results. It is known that silver(I) can form π-complexes with the π-electron cloud of aromatic hydrocarbons. It is therefore proposed that this might be the case here. The silver ions could be considered to be bonded to the molecule and to the functional groups on the paper, perhaps the hydroxyl groups, because cellulose consists of D-(+)-glucose units each of which contains three free OH-groups. This would create links between the analyte molecule and the support, providing the necessary rigidity for observation of phosphorescence.

The silver(I) is believed not only to provide an internal heavy atom effect, but to create a matrix effect as well by presenting a rigid environment for the

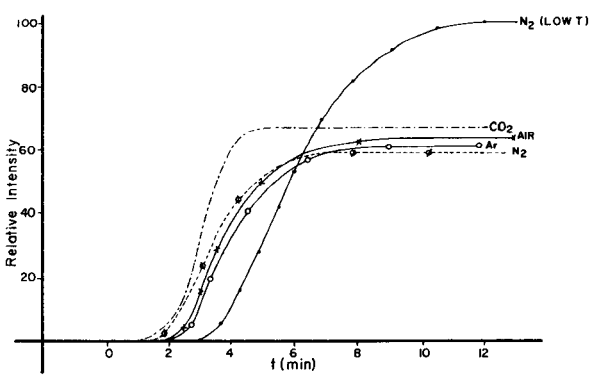

Fig. 7. Growth of phosphorescence signal with time for *p*-aminobenzoic acid in 1 M NaOH—1 M NaI (1:1) with λ_{ex} = 280 nm and λ_{em} = 430 nm.

phosphorescing molecule. Restriction of movement (translational, vibrational and rotational) and resistance to penetration by oxygen was then assumed to be responsible for the lack of susceptibility to quenching. Presence of moisture would serve to weaken the matrix rigidity and allow oxygen to be dissolved in the solvent in a similar manner to the proposition by Schulman and Parker [35] for ionic compounds. These results seem to support the growing amount of data which indicate that room-temperature phosphorescence will find its place among routinely used techniques. An obvious advantage of the r.t.p. technique for analytical purposes, besides its simplicity, is the small amount of sample required for every measurement. Only 3 μl is usually needed to prepare a sample, whereas low-temperature phosphorimetry usually requires 100 μl to1 ml and conventional fluorimetry requires as much as 4 ml. Therefore, the absolute detection limits (in ng) of r.t.p. are in some cases much better than those of the more conventional techniques.

Use of the external and internal heavy atom effect leads to an increase in phosphorescence emission signal levels at room temperature. However, in several cases, compounds known to phosphoresce at 77 K still did not show appreciable phosphorescence under room temperature conditions. Probably, the decrease in the lifetime of the molecule brought about by the heavy atom resulted in such a shortened lifetime that phosphorescence can no longer be detected when the rotating can is operating at conventional speeds. Unfortunately, the maximum speed of the commercial rotating can is about 160 Hz and cannot be run faster. Because of the poor stray light rejection characteristics of the monochromators used and the large fluorescence background emission from the paper sample support, use of a gated detector to observe the phosphorescence would require a relatively long gate delay time, again resulting in the inability to detect appreciable phosphorescence.

This work was solely supported by NIH GM-11373-15.

REFERENCES

1 E. A. Walker, Pure Appl. Chem., 49 (1977) 1673.
2 E. L. Wynder, E. A. Graham and A. B. Croninger, Cancer Res., 13 (1953) 855.
3 D. Hoffman, W. E. Bondinell and E. L. Wynder, Science, 183 (1974) 215.
4 R. F. Severson, M. E. Snook, R. F. Arrendale and O. T. Chortyk, Anal. Chem., 48 (1976) 1866.
5 H. J. Davis, Talanta, 16 (1969) 621.
6 M. L. Lee, M. Novotny and K. D. Bartle, Anal. Chem., 48 (1976) 405.
7 L. Toth, J. Chromatogr., 50 (1970) 72.
8 W. Lijinsky and A. E. Ross, Food Cosmet. Toxicol., 5 (1967) 343.
9 K. Potthast and G. Eigner, J. Chromatogr., 103 (1975) 173.
10 E. Sawicki, T. W. Stanley, W. C. Elbert and J. D. Pfaff, Anal. Chem., 36 (1964) 497.
11 T. D. Searl, F. J. Cassidy, W. H. King and R. A. Brown, Anal. Chem., 42 (1970) 954.
12 K. A. Schulte, D. J. Larson, R. W. Harnung and J. V. Crable, Am. Ind. Hyg. Assoc. J., 36 (1975) 131.
13 J. F. McKay and D. R. Latham, Anal. Chem., 44 (1972) 2132.

14 B. L. Van Duuren, Anal. Chem., 32 (1960) 1436.
15 S. P. McGlynn, B. T. Neely and C. Neely, Anal. Chim. Acta, 28 (1963) 472.
16 L. V. S. Hood and J. D. Winefordner, Anal. Chim. Acta, 42 (1968) 199.
17 N. Carugno and S. Rossi, J. Gas Chromatogr., 5 (1967) 103.
18 M. Novotny, M. L. Lee and K. D. Bartle, J. Chromatogr. Sci., 12 (1974) 606.
19 T. Doran and N. C. McTaggert, J. Chromatogr. Sci., 12 (1974) 715.
20 M. L. Lee, K. D. Bartle and M. Novotny, Anal. Chem., 47 (1975) 540.
21 M. E. Snook, W. J. Chamberlain, R. F. Severson and O. T. Chortyk, Anal. Chem., 47 (1975) 1155.
22 W. Giger and M. Blumen, Anal. Chem., 46 (1974) 1663.
23 R. E. Jentoft and T. H. Gouw, Anal. Chem., 48 (1976) 2195.
24 R. J. Hurtubise, J. F. Schabron, J. D. Feaster, D. H. Therkildsen and R. E. Poulson, Anal. Chim. Acta, 89 (1977) 377.
25 R. J. Hurtubise, G. T. Skar and R. E. Poulson, Anal. Chim. Acta, 97 (1978) 13.
26 G. F. Kirkbright and C. G. DeLima, Analyst, 99 (1974) 338.
27 M. Roth, J. Chromatogr., 30 (1967) 276.
28 E. M. Schulman and C. Walling, Science, 178 (1972) 53.
29 E. M. Schulman and C. Walling, J. Phys. Chem., 77 (1973) 902.
30 R. A. Paynter, S. L. Wellons and J. D. Winefordner, Anal. Chem., 46 (1974) 736.
31 T. Vo Dinh, E. Lue Yen and J. D. Winefordner, Anal. Chem., 48 (1976) 1186.
32 T. Vo Dinh, E. Lue Yen and J. D. Winefordner, Talanta, 24 (1977) 146.
33 R. M. A. von Wandruszka and R. J. Hurtubise, Anal. Chim. Acta, 93 (1977) 331.
34 T. Vo Dinh, G. L. Walden and J. D. Winefordner, Anal. Chem., 49 (1977) 1126.
35 E. M. Schulman and R. T. Parker, J. Phys. Chem., 81 (1977) 1932.
36 E. Lue Yen-Bower and J. D. Winefordner, Appl. Spectrosc., in press.
37 D. D. Morgan, D. Warshawsky and T. Atkinson, Photochem. Photobiol., 25 (1977) 31.
38 G. W. Robinson, J. Mol. Spectrosc., 6 (1961) 58.
39 S. P. McGlynn, M. P. Padhyde and M. Kasha, J. Chem. Phys., 22 (1954) 593.
40 G. G. Guilbault, Practical Fluorescence, Theory, Methods and Techniques, M. Dekker, New York, 1963.

Analytica Chimica Acta, 102 (1978) 15—23

DETERMINATION OF TRACES OF LEAD, CADMIUM AND ZINC IN COPPER BY AN ARC-NEBULIZATION AND FLAME ATOMIC ABSORPTION TECHNIQUE

T. KANTOR*, P. FODOR and E. PUNGOR

Institute for General and Analytical Chemistry, Technical University of Budapest (Hungary)

(Received 11th May 1978)

SUMMARY

Arc-nebulization (a thermal nebulization technique) is used to form an aerosol of cadmium, lead and zinc. An open arc chamber of simple operation and an ejector of high efficiency are described which are adaptable for use with any flame atomic absorption spectrometer. Limits of detection better by one or two orders of magnitude than those achieved by conventional flame a.a.s. methods were obtained viz., 43 ng Pb, 5 ng Cd, 7 ng Zn (equivalent to 0.7, 0.08 and 0.11 ppm, respectively, in copper). Calibration with matrix-free solutions was possible for lead and cadmium but not for zinc. The spectral interference of copper on absorbance at the most sensitive zinc line (213.856 nm) and the efficiency of arc nebulization of cadmium are also discussed.

The determination of volatile trace elements in copper used in the manufacture of electronic devices is of particular importance. Among these elements only cadmium can be determined by conventional flame atomic absorption spectrometry (a.a.s.) down to 2 ppm without chemical enrichment [1]. For determinations of lead at the ppm level, sodium diethyldithiocarbamate extraction has been suggested [2]; for determinations of zinc, an ion-exchange separation has been proposed [1]. By non-dispersive [3, 4] and dispersive [5] atomic fluorescence (a.f.s.) procedures, > 0.1 ppm zinc, and > 0.06 ppm cadmium can be determined if careful correction is made for scattered radiation. Larkins and Willis [4] compared experimentally the performance of flame a.f.s. and a.a.s. and gave the reason for the relative insensitivity of a.a.s. for determining zinc in copper, i.e., that the most sensitive zinc line is overlapped by a copper line which makes it practically impossible to determine zinc in copper below 6 ppm with conventional spectrometric systems. This interference was eliminated by Zander et al. [6] who used continuum-source, echelle wavelength-modulated a.a.s.

In arc emission spectrometry, the metal globule procedure has been one of the best suited to copper analysis, being highly sensitive especially for elements which are completely distilled from the sample during a short arcing time. Thus Publicover [7] achieved approximate detection limits of

0.1 ppm for Pb and Cd and 0.5 ppm for Zn when a 2-g copper sample was arced. Similar detection limits for these elements were found by Tymchuk et al [8] who used 60-mg samples and copper fluoride as fluorinating agent. Obviously, halogenation is more important for those elements which are not volatile in alloyed metallic form (e.g. Fe, Mn, Cr) and its utilization with the arc—flame technique is likely to be important.

The arc-nebulization and flame-atomization technique is a combination of the equipment and procedures of two well established techniques of atomic spectrometry [9, 10]. The advantage of this solid-sample atomic absorption method in the analysis of copper lies in the elimination of the spectral interference of copper on zinc determination by the selective evaporation of zinc and in the possibility of avoiding contamination from acids used for sample dissolution.

EXPERIMENTAL

Arc nebulizer

When an ejector is used for sucking the aerosol into an air-supported flame (see below) an open arc chamber may be used, making the operation simple and convenient (Fig. 1). In this chamber a d.c. arc is operated between vertical and horizontal graphite electrodes. The sample fills a graphite cup fitting the bore of a necked graphite rod (anode). This double supporting electrode

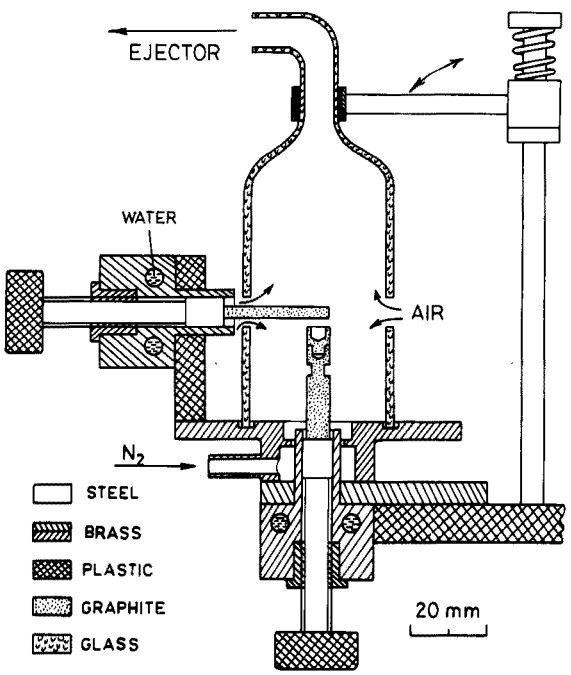

Fig. 1. Diagram of the arc nebulizer.

ensures a greater sample heating rate and the cups can be replaced easily. The electrode holders are threaded spindles screwed into inserts in water-cooled copper sockets. The electrode gap is adjusted by turning the insulated knobs fixed to the spindle terminals. The nut of the vertical spindle is provided with a spring (not shown) which allows a vertical shift of 2 mm. In this way the d.c. arc can be ignited by a vertical push on the insulated knob. The upper glass dome can be removed simply with a retainer spring during replacement of samples. To reduce the burning rate of the graphite electrodes, nitrogen sheath gas is introduced into the chamber at 1.5 l min^{-1}. A d.c. power source (Hungarian Optical Works) with 110-V total available voltage and 15-A arc current is used, providing arc timing of 1—100 s.

Transporting system and flame conditions

The pneumatic sprayer used conventionally for the nebulization of solutions is replaced by an ejector shown in Fig. 2. This is made from a plastic T-shaped junction and a metal capillary tube with a nozzle of 0.6 mm i.d. At an air flow rate of 5 l min^{-1} this ejector produces an equal gas intake rate, indicating a rather high efficiency. The ejector outlet is inserted into the premixing chamber of the flame and its upper inlet port is connected to the arc nebulizer by a plastic tube (30-cm long, 8-mm i.d.) Owing to the suction of the ejector, air flows laterally into the dome and thence to the mixing chamber together with the nitrogen sheath gas, the rate of which is not indicated by the ratemeter of the basic instrument. This, however, does not cause difficulties provided that the flow rate of acetylene is adjusted so as to produce a non-luminous flame (1.8 l min^{-1} in this work). The optimum flame composition and the observation flame height with the arc—flame

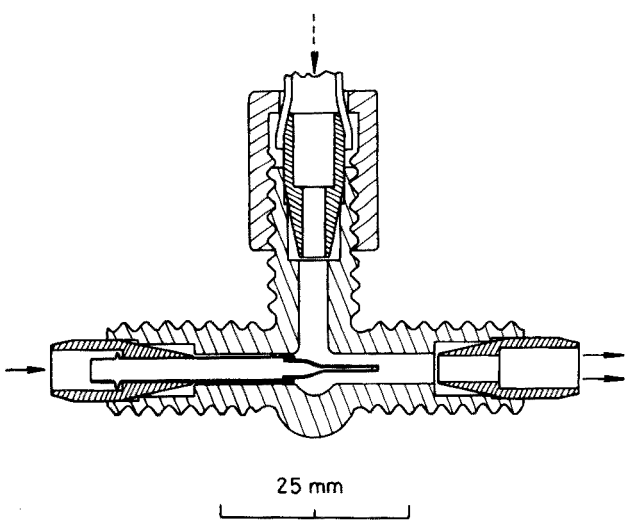

Fig. 2. Ejector for transportation of the aerosol.

method are usually the same as with the conventional flame methods. An acetylene—air, single-slot (10 cm) burner was used in the measurements.

Basic instrument

There are no special demands in respect of the optical and electronic properties of the flame atomic absorption spectrometer, other than that it should be equipped with an electronic integrator. In this work a Spectromom Model 190 A (Hungarian Optical Works) instrument was used, which provided integration over 1—100 s. When the arc gases from a pure carbon arc enter the flame, the absorbance decreases slightly by about 0.01 at 210—230 nm. As the integrator used works only in the positive signal region, the base line should be adjusted to above zero. In practice integrated blank signals were measured at a base-line absorbance of 0.02 and their average was subtracted from the signals obtained from samples (see Table 1). The transit time of the aerosol through the transporting and mixing system was about 2 s under the conditions used. The integration time was chosen to be 4 s longer than the arcing time. The most sensitive absorption line was selected for each element.

Electrodes and standards

Supporting electrodes and cups (Fig. 1) were made of spectrally pure graphite rods (6.15 mm diam.) with a Rank-Hilger Electrode Sharpener. Experience has shown that in spite of the high purity of the graphite materials used, the electrodes must be thermally purified from lead and zinc before sample loading. This was carried out by pre-arcing them in the arc chamber under analytical conditions, so that the purification process could be monitored. The vertical supporting electrode and the horizontal counter electrode have a lifetime of 30—40 arcings (15—20 s each) in nitrogen sheath gas, while the pre-arced cups are used only for single measurements. In the arc-nebulization of solutions used for preliminary calibration (see below) 5 μl

TABLE 1

Experimental data for 3 ppm lead and calculation of weight-normalized absorbances (The average apparent blank absorbance $\bar{A}_B$ was 261 ± 32 (37 replicates). $A = A' - \bar{A}_B$.)

Sample weight G (mg)	Integrated absorbance		
	Uncorr. (A')	Corr. (A)	Norm. (A/G)
51.4	484	223	4.34
52.2	484	223	4.27
53.6	470	209	3.90
45.0	478	217	4.82
50.8	462	201	3.96
45.5	471	210	4.62
		Average:	4.32 ± 0.36

was applied onto the top of pre-arced graphite heads similar in size to the cups but without the hole.

Earlier experiments with the arc—flame method [10] have shown that standardization for solid sample analysis may be carried out with matrix-free standard solutions in certain cases. However, the validity of this simple calibration must be confirmed by solid standards in every special case, as will be shown later. Stock solutions (1 mg ml^{-1}) of lead, cadmium and zinc were prepared from high-purity metals dissolved in nitric acid and were used to make serial aqueous standards. Synthetic powder standards for lead were also prepared from high-purity graphite powder (Ringsdorff RWA) and lead nitrate. Solid copper standards from Johnson-Matthey (U.K.), Bundesanstalt für Materialprüfung (G.F.R.) and Csepel Works (Hungary) were used. Standards and samples were cut into small pieces that weighed several mg. These metal chips were washed in petroleum ether and digested with (1+1) hydrochloric acid to remove surface contamination. After 15 min some drops of nitric acid were added until attack on the metal was apparent. Preparation was finished by washing with deionized water and drying.

As the arcing of samples was continued until complete distillation of the analytes, the remaining globule could be considered as a blank sample to be used in blank measurements. These pre-arced copper globules could also be used as diluents for pieces of copper standards used for zinc determination (see below). These possibilities have been utilized earlier in arc emission spectrometry [8].

RESULTS AND DISCUSSION

Determination of lead

Preliminary studies were performed with a copper standard containing 52 ppm lead to estimate the proper arcing time and the amount of standard for which the peak absorbance does not exceed 0.7. It was found that within 20 s the signal diminished to the base line and less than 10 mg of standard should be used at this concentration. Appropriate amounts of the standards of lower concentrations could be calculated on this basis. The green coloration of the flame (CuOH etc. emission) appeared before total distillation of lead, i.e. lead vaporization was not completely selective, as was also found for cadmium and zinc.

A linear plot of integrated absorbance vs. amount of lead in copper standards and graphite powder/lead nitrate mixtures is shown in Fig. 3. As can be seen, an identical graph is obtained independent of the sample size and of the presence of copper. Similar characteristics were found with matrix-free lead nitrate solutions in earlier studies [10]. Linear regression analysis gave correlation coefficients of r^2 (mixture) = 0.982 and r^2 (metal) = 0.987, while the ratio of slopes was 1.01.

The absorbance values plotted in Fig. 3 were corrected for the "apparent blank value" as can be seen numerically in Table 1. This blank value is due

predominantly to the fact that the base line was adjusted above zero because of the base line shift mentioned. In Table 1, the calculation of weight-normalized absorbances and their reproducibility (8.3% for 3 ppm of lead) are also demonstrated. The absolute detection limit (calculated as the concentration corresponding to twice the standard deviation of the blank) is 43 ng of lead, equivalent to 0.7 ppm for a 60-mg sample, which can readily be accommodated in the cups used. (Performance data for the other elements were calculated in the same way.)

The dynamic range can be extended to higher concentrations by decreasing the sample weight and also by repeated arcing. In the latter method an arcing time shorter than that necessary to reach 0.7 peak absorbance is used and the arcing with the appropriate integration time is repeated until the signal decreases to the base line. The sum of these subsequent integrations is used for evaluation. In Fig. 4 a logarithmic plot of weight-normalized absorbances vs. lead concentration is shown with standards of different origin. Each point represents the mean of 4—6 replicate measurements with variable loadings. Above 52 ppm, the method of repeated arcing and integration was used.

Determination of cadmium

Preliminary studies with copper containing 28 ppm of cadmium indicated the use of 15-s arcing and less than 5-mg samples. Because this copper standard was that with the lowest cadmium concentration in the laboratory, in order

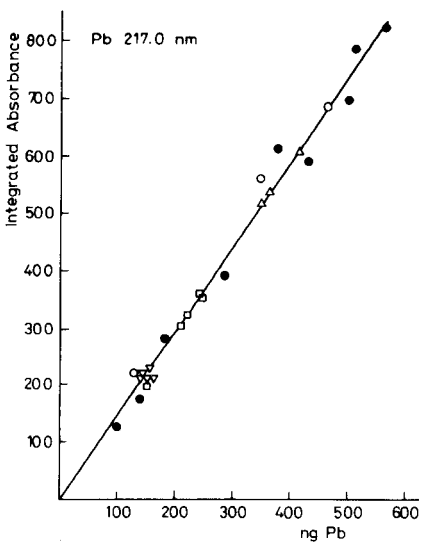

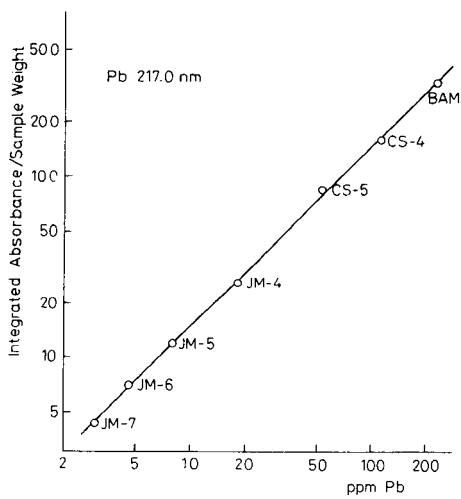

Fig. 3. Calibration graph for lead with different standards of variable weight. (•) Graphite powder and lead nitrate mixture; (○) 52, (△) 8.0, (□) 4.5, (▽) 3.0 ppm lead in copper.

Fig. 4. Calibration graph for lead with weight-normalized absorbances and standards of different origin.

to carry out standardization down to 0.5 ppm, pre-arced copper globules weighing 30—60 mg had to be added to 1—4 mg of standard samples.

In Fig. 5, the calibration graph for cadmium is shown for matrix-free cadmium nitrate solutions (average of three replicates), for various amounts of neat copper standard (28 ppm Cd) and for the copper standard diluted with cadmium-free copper. These measurements show a similar independence of the amount of matrix and chemical form of the analyte to that found for lead determination. Linear regression analysis gave correlation coefficients r^2 (solutions) = 0.984 and r^2 (solids) = 0.995; the ratio of the slopes was 1.05.

Normalized absorbances showed a relative standard deviation of 7.5% for six measurements of 1.3 ppm of cadmium. The absolute detection limit was 5 ng of cadmium, corresponding to 0.08 ppm in 60 mg of copper. The 1.3 ppm of cadmium found in the copper sample could not be determined with an acceptable degree of certainty by pneumatic nebulization of a 1% (w/v) solution of the copper, all other conditions being equal.

An effort was made to determine the efficiency of arc-nebulization of cadmium [11]. The principle of the method applied was to relate the integrated absorbance obtained when the arc—flame technique was used to that by a direct sample introduction technique, 100% efficiency of introduction being assumed for the latter. It was found that 53% of the total amount of cadmium evaporated by the arc could be transported into the flame. This value may be considered as nebulization efficiency.

Determination of zinc

Absorbance vs. arcing time recordings for 13 ppm of zinc, showed that a peak appeared soon after arc ignition. However, the signal did not diminish to the base line but increased after 15 s. During prolonged arcing the signal varied in accordance with the intensity of the green flame colour, i.e. with the vaporization rate of the copper. This absorbance was extremely high (0.1—0.2) when the arc directly attacked the globule. To avoid the possibility of this direct arcing, the electrode arrangement shown in Fig. 1 was modified. The supporting electrode was lifted so that the orifice of the cup was above the horizontal electrode. Thus a horizontal arc could be operated between the outer wall of the cup and the tip of the counter electrode. In this way, the interference of copper decreased appreciably but it was not completely eliminated towards the end of the distillation of zinc. However, it could be kept constant if the sample weight was not varied by more than 5 mg and it could be measured as a blank signal with pre-arced copper globules.

The interference by the Cu 213.853-nm line on the Zn 213.856-nm line was also investigated by pneumatic nebulization of copper solutions prepared from zinc-free globules, as has been studied previously [4, 6]. The lower level of the copper transition originates from the excitation of an inner electron ($3d^{10}\ 4s \rightarrow 3d^9\ 4s^2$) with an excitation energy of 1.39 eV [12]. From Boltzmann's equation, a relative population of 0.36% was calculated

for this anomalous level, assuming a flame temperature of 2400 K. Theoretical predictions on the degree of interference, however, meet several difficulties. Presumably, the interference is enhanced also by the fact that the cathode of "zinc hollow-cathode lamps" is usually made of brass, so that a partial, unresolvable spectral overlap exists. With pneumatic nebulization of zinc-free copper solutions a linear calibration graph was obtained for 0.5—2% (w/v) copper solutions, measured at 213.856 nm, with a characteristic concentration (1% absorption) of 890 μg Cu ml^{-1}. At the same wavelength and under the same conditions, the characteristic concentration of copper-free zinc was 0.016 μg ml^{-1}. Considering a 1% (w/v) copper concentration in the sample solutions usually prepared, the copper interference corresponds to an apparent zinc concentration of 18 ppm. This interference is three times greater than that found by other authors [4], which might be due to the differences in instrumentation and experimental conditions.

In Fig. 6, the calibration graph for zinc is shown for different standards and loadings when their weight was adjusted to 55—60 mg with zinc-free copper globules, and the dilutions were taken into account. The linear correlation coefficient was $r^2 = 0.989$ ($n = 17$). Relative standard deviations were 6.0% at 1 ppm and 11% at 0.4 ppm zinc concentrations ($n = 8$). The absolute detection limit was 7 ng of zinc corresponding to 0.11 ppm in a 60-mg sample.

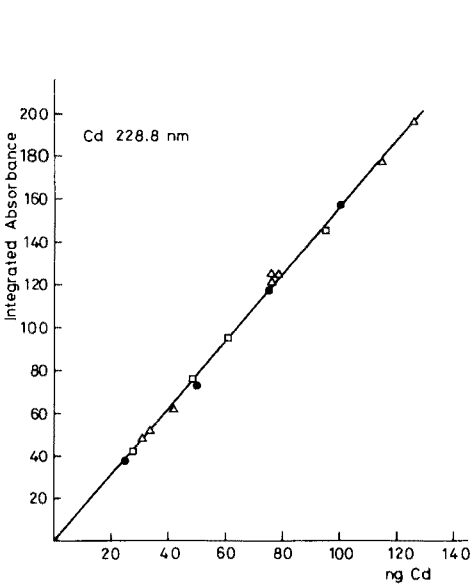

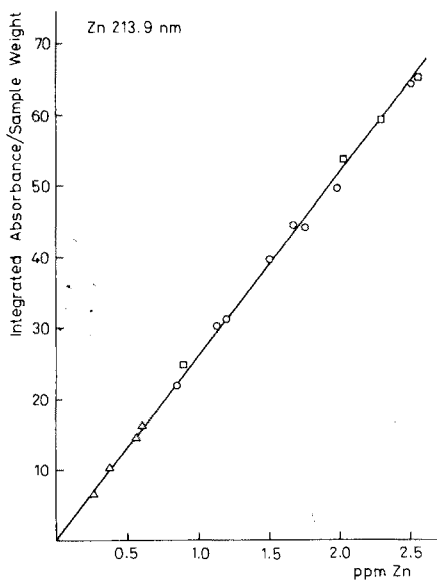

Fig. 5. Calibration graph for cadmium. (•) Matrix-free cadmium nitrate solutions, (△) solid copper standard (28 ppm Cd) of various weights, (□) the copper standard diluted to 30—60 mg with pre-arced copper.

Fig. 6. Calibration graph for zinc, with solid copper standards diluted to 55—60 mg with pre-arced copper. Original concentrations: (□) 13, (○) 11, (△) 1.8 ppm zinc.

Calibration with solutions was unsuccessful. As well as the difference in blank values with and without copper, the slope of the calibration graph for solutions was smaller by a factor of 1.5 than that for solid standards. Investigations of this matrix effect are in progress; at present it seems to be connected with an alteration of the nebulization efficiency.

CONCLUSIONS

The analytical results provide further experimental evidence of the quantitative nature of the "thermal nebulization" process even if it is non-stationary and not well understood at present. These theoretical deficiencies, and the existence of other ways of analysing solids by a.a.s. [13, 14] which do not involve this kind of problem might raise doubts about the present technique. However, thermal nebulization techniques are highly versatile in their analytical applications and for studying high-temperature, condensed-phase processes [11], which are sufficient reasons for continuing their investigation.

REFERENCES

1 J. D. McCrackan, M. C. Vecchione and S. L. Longo, At. Absorpt. Newsl., 8 (1969) 102.
2 W. T. Elwell and I. R. Scholes, Analysis of Copper and Its Alloys, Pergamon Press, Oxford, 1967.
3 P. D. Warr, Talanta, 18 (1971) 234.
4 P. L. Larkins and J. B. Willis, Spectrochim. Acta, Part B, 29 (1974) 319.
5 P. Marugaiyan, S. Natarjan and Ch. Venkateswarlu, Anal. Chim. Acta, 75 (1975) 221.
6 A. T. Zander, T. O. O'Haver and P. Keliher, Anal. Chem., 49 (1977) 838.
7 W. E. Publicover, Anal. Chem., 37 (1965) 1680.
8 P. Tymchuk, A. Mykytiuk and D. S. Russel, Appl. Spectrosc., 22 (1968) 268.
9 T. Kántor and E. Pungor, Proc. XVII Coll. Spectrosc. Int., Florence, Vol I, 1973, pp. 83—88.
10 T. Kántor, P. Fodor, Y. S. Youssef and E. Pungor, Hungarian Scientific Instruments, 36 (1976) 19.
11 T. Kántor and E. Pungor, International Symposium on Microchemical Techniques, Davos, 1977, Switzerland.
12 A. R. Striganov and N. S. Sventickii, Tables of Spectral Lines, Atomizdat, Moscow, 1966.
13 B. V. L'vov, Talanta, 23 (1976) 109.
14 D. D. Siemer and Horng-Yih Wei, Anal. Chem., 50 (1978) 147.

Analytica Chimica Acta, 102 (1978) 25—32

A DEMOUNTABLE BOOSTED-OUTPUT SPECTRAL LAMP FOR ATOMIC ABSORPTION AND FLUORESCENCE MEASUREMENTS‡

J. V. SULLIVAN* and J. C. VAN LOON**

CSIRO Division of Chemical Physics, P.O. Box 160, Clayton, Victoria 3168 (Australia)

(Received 25th July 1978)

SUMMARY

A demountable boosted-output spectral lamp is described that permits easy exchange of the cathode, which is in the form of a disc pressed from the appropriate powder or machined from rod. The new lamp overcomes to a large extent the major disadvantage of the conventional boosted hollow-cathode lamp, namely the interaction of the sputtering and boosting discharges. In flame atomic absorption spectrometry it yields calibration curves more nearly linear than those obtained with commercial hollow-cathode lamps. In non-dispersive flame atomic fluorescence it permits the attainment of detection limits rather better than those obtained with other high-intensity light sources.

Boosted hollow-cathode lamps of the sealed-off type have already been described [1, 2]. These lamps, which combine high spectral output of the resonance line with narrow line width, have found useful application in absorption and fluorescence spectroscopy.

The principal feature of these lamps is the use of two electrical discharges: the first to produce, by cathodic sputtering, the metal atoms whose spectral lines are required, the second to excite these atoms. It is then possible to minimize resonance broadening by controlling the sputtering current and, at the same time, maintain effective excitation by increasing the boosting current.

A limitation in the performance of this type of lamp arises from the electrical interaction between the two discharges. The boosting discharge, which is one of high current, produces a high density of charged species in the region of the sputtering discharge. The latter can then be maintained at any given current by a voltage lower than that needed for efficient atom production. This leads to the situation that an increase in boosting current results in no further increase in spectral output and may even be accompanied by loss of signal. In general, the upper limit on the boosting current is approximately 100 mA.

‡Presented at the 5th International Conference on Atomic Spectroscopy, Melbourne, Australia, August 1975.

**On leave from the Institute of Environmental Studies, University of Toronto, Toronto M5S 1A1, Ontario, Canada.

LAMP DESIGN

The lamp design is shown schematically in Fig. 1. Argon gas, purified by passage through a column of molecular sieves, is allowed to flow through the lamp under reduced pressure.

The flow is so arranged that the argon gas is directed over the cathode, then away from it and toward the region of the boosting discharge, thereby preventing too high a concentration of ions and electrons forming near the sputtering discharge. Electrical interaction is minimized and the spectral output of the lamp increases with boosting current up to currents of approximately 500 mA.

The lamp is made from glass tubing 4 cm in diameter and 8 cm long. One end is sealed with a silica window. The other end, which is ground flat, has two openings, one centred and 10 mm in diameter, the other 3 mm in diameter, to enable the gas inlet tube to reach through the silica arrester to ensure that the flow of argon is confined to the region required.

The cathode of the metal whose resonance lines are to be excited is in the form of a disc, 12 mm in diameter and 3 mm thick, pressed from the appropriate powder or machined from rod. It is press-fitted into an aluminium block. A nut, sealed with a neoprene washer, is provided at the back of the block. Removal of the nut and washer permits easy removal of the cathode.

The block containing the cathode is sealed to the end of the lamp by means of an O-ring which is prevented from collapsing by a disc of silica, also shown in Fig. 1. This disc, or arrester, which is a simplified form of that used by Gough, Hannaford and Walsh [3], is used also to confine the discharge to the region of the cathode and to direct the gas-flow as required. The arrester is 2 mm thick and 25 mm in diameter. The central hole is 10 mm in diameter

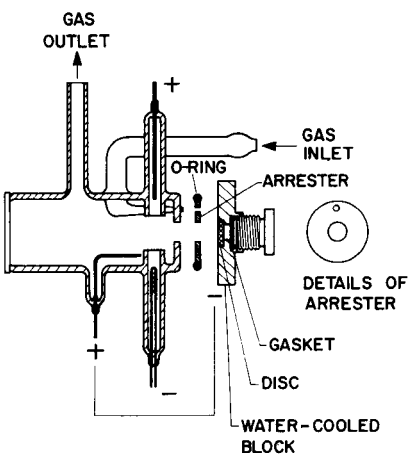

Fig. 1. Schematic diagram of the demountable boosted-output spectral lamp.

whilst the off-centred hole is 3 mm diameter and 10 mm centre-to-centre from the other hole.

The electrodes of the sputtering discharge are the disc of metal in the block (cathode) and a rod of nickel (anode). For the boosting discharge a separate anode is used and the cathode is a helical rhenium filament in which are placed pieces of lanthanum hexaboride [4]. This compound replaces the oxide coatings used in the earlier lamps because it can withstand repeated exposure to air and is readily reprocessed.

As shown in Fig. 1, the side arms housing the secondary electrodes extend into the body of the lamp to ensure that the discharge is confined as much as possible to the region of maximum metal atom concentration.

The lamp operates in a continous flow of argon filler gas whose pressure and flow-rate are maintained at pre-determined values by means of an automatic gas-control unit designed and built by Larkins [5]. The pressure used is approximately 2—3 torr and the flow-rate is 0.4 l min^{-1}.

RESULTS

Atomic absorption measurements

An AA-4 atomic absorption spectrometer (Varian Techtron, North Springvale, Victoria, Australia) was used, with a standard nebulizer-spray chamber assembly and a 10-cm air—acetylene flame (air—hydrogen for the measurement of tin).

Calibration curves were obtained for aqueous solutions of nickel, lead, tin, copper and magnesium. Those for the first three metals are shown in Figs. 2—4; those for copper and magnesium, though not shown, exhibit

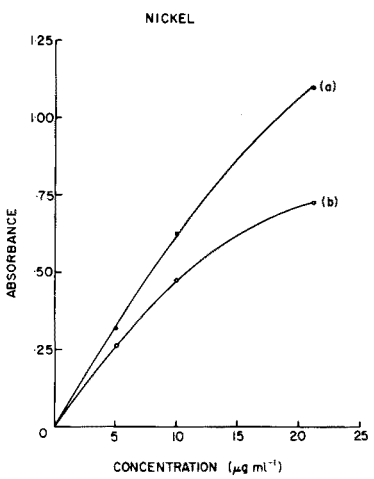

Fig. 2. Calibration curves for nickel obtained from atomic absorption measurement of aqueous solutions. (a) Demountable lamp at 232.0 nm, bandpass 0.1 nm, lamp currents 500 mA (booster) and 8 mA; (b) hollow-cathode lamp at 232.0 nm, bandpass 0.2 nm, lamp current 5 mA.

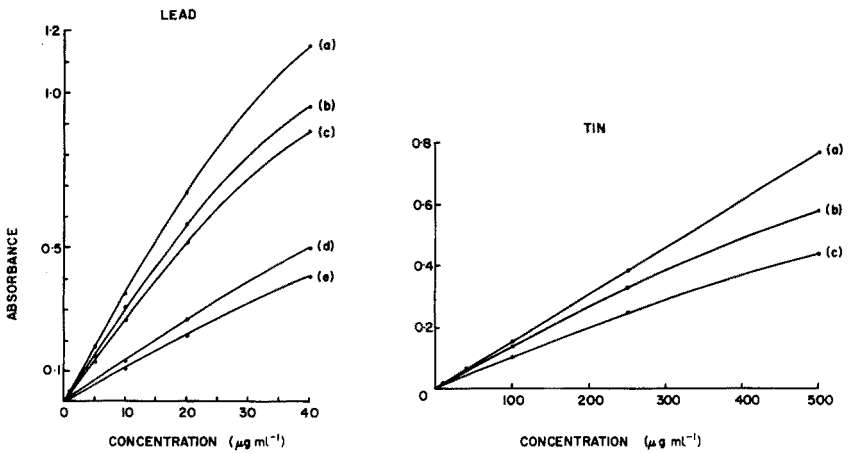

Fig. 3. Calibration curves for lead obtained from atomic absorption measurements of aqueous solutions. (a) Demountable lamp at 217.0 nm, bandpass 0.3 nm, lamp currents 500 mA (booster) and 4 mA; (b) demountable lamp at 217.0 nm, bandpass 0.3 nm, lamp currents 500 mA and 10 mA; (c) hollow-cathode lamp at 217.0 nm, bandpass 0.3 nm, lamp current 6 mA; (d) demountable lamp at 283.3 nm, bandpass 0.2 nm, lamp currents 500 mA and 10 mA; (e) hollow-cathode lamp at 283.3 nm, bandpass 0.2 nm, lamp current 6 mA.

Fig. 4. Calibration curves for tin obtained from atomic absorption of aqueous solutions, with an air—hydrogen flame. (a) Demountable lamp at 224.6 nm, bandpass 0.2 nm, lamp currents 500 mA (booster) and 20 mA; (b) demountable lamp at 224.6 nm, bandpass 0.2 nm, lamp currents 500 mA and 30 mA; (c) hollow-cathode lamp at 224.6 nm, bandpass 0.2 nm, lamp current 7 mA.

similar features. It can be seen from the figures that the curves obtained with the demountable lamp show better sensitivity and greater linearity than those with hollow-cathode lamps run under their recommended conditions; this is due to the narrower line-width resulting from the low sputtering current used in the demountable lamp.

This dependence of sensitivity on line-width is shown in Fig. 5, where the absorbance of a solution containing nickel (20 μg ml^{-1}) was measured at different values of the sputtering current. The boosting current was 500 mA in each case, and experiments showed that changes in this current did not affect absorption. The importance of spectrometer bandpass in the measurement of nickel is also shown in Fig. 5.

Figure 6 shows the short-term stability of the output of a demountable boosted-output lead lamp.

Atomic fluorescence measurements

The non-dispersive flame fluorescence instrument described by Larkins [6] was used, with a nitrogen-sheathed air-acetylene flame. For zinc, cadmium,

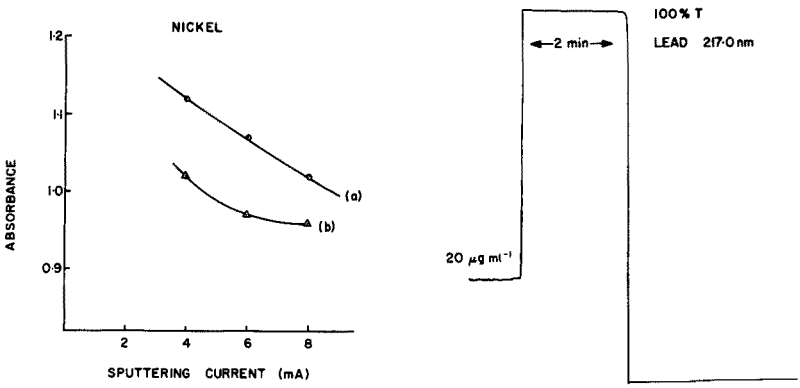

Fig. 5. Dependence of measured nickel absorbance at 232.0 nm on sputtering current, with 500 mA boosting current. (a) Spectrometer bandpass 0.1 nm; (b) spectrometer bandpass 0.2 nm.

Fig. 6. Recorder trace illustrating the stability achieved with a demountable boosted-output lead lamp.

and nickel a solar-blind photomultiplier type R166 (Hamamatsu TV Company, Hamamatsu, Japan) was used, while for silver and copper a broad-response photomultiplier type R106 by the same manufacturer was used in conjunction with a glass absorption filter (Schott UG2).

Figure 7 illustrates the sensitivity obtained with a demountable cadmium lamp. The recorder trace (a) was obtained by using 500 V on the dynode chain of the photomultiplier, while trace (b) was obtained with a dynode voltage of 400 V. Figure 8 shows recorder traces for five metals near the

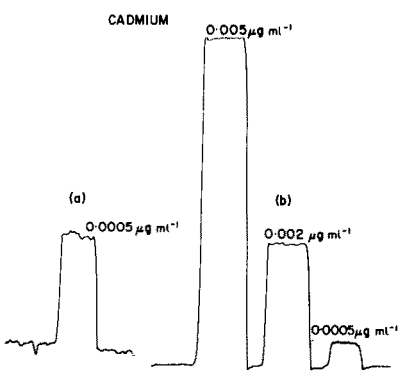

Fig. 7. Recorder traces illustrating the sensitivity of fluorescence measurements on cadmium with the demountable lamp. Photomultiplier dynode voltage: (a) 500 V; (b) 400 V.

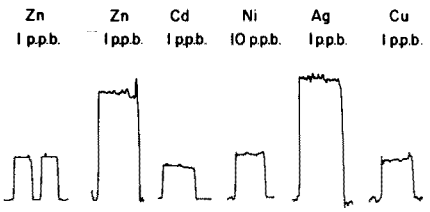

Fig. 8. Recorder traces showing fluorescence signals for zinc, cadmium, nickel, silver and copper near the limits of detection.

limits of detection. Table 1 shows limits of detection compared with those found by Larkins [6], who used earlier types of lamp.

Measurements were made on samples of river water supplied by the Central Scientific Laboratory, State Electricity Commission of Victoria, where they had been analyzed by the techniques of differential pulse anodic stripping voltammetry and flame atomic absorption after chelation and concentration of the metals into an organic solvent [7].

The concentrations of the elements zinc, cadmium, nickel and copper were generally in the range 0—10 parts per billion, and were measured by spraying the samples directly into the flame without any pre-concentration. The total dissolved solid levels of the samples lay in the range 60—300 mg l^{-1}, and presented no problem except with nickel, when a scattering correction was made for particulate scattering in the flame by using a gold boosted hollow-cathode lamp in the manner described by Larkins and Willis [8].

Table 2 shows the results of the measurements, together with those obtained by the Central Scientific Laboratory of the SEC.

TABLE 1

Limits of detection in non-dispersive flame atomic fluorescence[a]

Element	Larkins [6] (ng ml^{-1})	Present work (ng ml^{-1})
Zn	0.3[b]	0.1
Cd	0.2[c]	0.1
Ni	2[d]	1.5
Ag	0.15[d]	0.1
Cu	1[d]	0.2

[a]The limits of detection follow the very conservative definition used by Larkins [6], viz. the concentration giving a signal equal to twice the peak-to-peak fluctuation when only water or dilute acid is aspirated. [b]Sullivan—Walsh-type [1] boosted hollow-cathode lamp. [c]Metal-vapour discharge lamp (Philips). [d]Lowe-type [2] boosted hollow-cathode lamp.

TABLE 2

Concentration of metals in river water, (ng ml^{-1})

Sample No.	Total dissolved solids (mg l^{-1})	Nickel		Cadmium		Zinc		Copper	
		This work	SEC	This work	SEC	This work	SEC	This work	SEC
1	280	3	4	0.8	2	25	24	6	4
2	140	5	2	2.2	2	5	2	6	4
3	185	7	3	0.6	0.5	5	2	6	5
4	60	4	1	0.4	0.4	3	2	2	1
5	120	4	1	0.4	<0.5	4	6	2	1

DISCUSSION

Flow-through demountable boosted-output lamps have several advantages over boosted hollow-cathode lamps. The reduction in electrical interaction between primary and secondary discharges allows higher boosting currents to be used, thus permitting higher output intensities at lower sputtering currents and the emission of narrower lines. This property makes the lamps extremely useful for atomic absorption determinations.

In atomic fluorescence, too, the new lamps give excellent limits of detection, and can be used for the analysis of river waters by non-dispersive flame fluorescence without the need for laborious pre-concentration procedures. With correction for particulate scattering in the flame, this technique could be extended to more complex sample types.

Multi-element operation can be envisaged with cathodes made up of a mixture of elements, and the use of neon instead of argon as the filler-gas should lead to further gains in spectral output.

In general, the demountable boosted-output lamp is easy to use and results in detection limits in non-dispersive flame fluorescence at least as good as those obtained with other high-intensity light sources. Its output is stable and reproducible.

The present demountable boosted-output lamp is well suited for use with cathodes whose physical dimensions are small, thereby conserving pure material. It could be adapted for emission studies as is the lamp described by Lowe [9] and used by Gough and Sullivan [10] for simultaneous, multi-element analysis by emission spectroscopy.

The authors are indebted to Mr. P. L. Boar, of the State Electricity Commission of Victoria, for provision of the analyzed samples of river water. They also thank Sir Alan Walsh and Dr. J. B. Willis for discussion and advice.

REFERENCES

1 J. V. Sullivan and A. Walsh, Spectrochim. Acta, 21 (1965) 721.
2 R. M. Lowe, Spectrochim. Acta, Part B, 26 (1971) 201.
3 D. S. Gough, P. Hannaford and A. Walsh, Spectrochim. Acta, Part B, 28 (1973) 197.
4 J. M. Lafferty, J. Appl. Phys., 22 (1951) 299.
5 P. L. Larkins, unpublished work.
6 P. L. Larkins, Spectrochim. Acta, Part B, 26 (1971) 477.
7 A. T. Phillip, R. W. Pettis, J. E. Harris, G. J. Fabris, P. L. Boar and K. M. Bone, Proc. Roy. Aust. Chem. Inst., 42 (1975) 209.
8 P. L. Larkins and J. B. Willis, Spectrochim Acta, Part B, 29 (1974) 319.
9 R. M. Lowe, Spectrochim. Acta, Part B, 31 (1976) 257.
10 D. S. Gough and J. V. Sullivan, Analyst, in press (1978).

Analytica Chimica Acta, 102 (1978) 33—39

DETERMINATION OF BISMUTH IN NICKEL-BASE ALLOYS BY ATOMIC ABSORPTION SPECTROMETRY WITH INTRODUCTION OF SOLID SAMPLES INTO AN INDUCTION FURNACE

JAMES B. HEADRIDGE* and ROBERT THOMPSON

Department of Chemistry, The University, Sheffield S3 7HF (Gt. Britain)

(Received 4th May 1978)

SUMMARY

Atomic absorption spectrometry with an induction furnace is applicable to the determination of bismuth at 0.02—10 $\mu g\ g^{-1}$ levels in 1—30-mg samples of nickel-base alloys dropped into the furnace. Calibration graphs of peak absorbance versus mass of bismuth are constructed by use of standardised alloys. Samples of alloys can be added to the furnace at 2.5-min intervals. Calibration graphs, accuracy, precision and limits of detection of the method are discussed for 26 alloys. Accuracy is assessed by comparing the induction furnace results with results supplied with the alloys, and with results obtained for solutions of the alloys by atomic absorption spectrometry in association with hydride generation or a mini-Massmann furnace. With alloys containing more than 0.1 μg Bi g^{-1}, relative standard deviations by the induction furnace method are usually < 15%. The limit of detection for bismuth is 0.02 $\mu g\ g^{-1}$

The hot ductility, workability and rupture life of nickel-base alloys are adversely affected by the presence of trace levels of bismuth as low as 0.3 $\mu g\ g^{-1}$ [1—4]. For this reason, stringent specifications have been set for the maximum concentration of bismuth in nickel-base alloys. For example, the SAE Aerospace Metal Specification (AMS) 2280 [5] lists the maximum permissible bismuth content as 0.5 $\mu g\ g^{-1}$, and the DIN 17 01 Preliminary Standard (1974) [6] stipulates a maximum bismuth concentration of 0.2 $\mu g\ g^{-1}$ for primary nickel.

The accurate determination of bismuth at such low concentrations is a challenging task for the metallurgical analyst. Methods that have been reported for the determination of bismuth in nickel-base alloys at concentrations less than 1 $\mu g\ g^{-1}$ are summarized in Table 1, which includes information on the limits of detection for each method.

Undoubtedly the most convenient and sensitive methods described in the literature for the determination of bismuth in nickel-base alloys are hollow-cathode emission spectrometry with solid samples [11] and atomic absorption spectrometry of metallic samples added directly to a resistively-heated graphite furnace [16]. However, Andrews and Headridge [17] have reported that bismuth can be determined in steels by the direct addition of metal turnings or millings (chips) to a constant-temperature induction furnace with

TABLE 1

Methods for the determination of bismuth in nickel-base alloys

Method	Limit of detection for bismuth ($\mu g\ g^{-1}$)	Ref.
D.c. arc emission after preconcentration by precipitation of Bi_2S_3 in CuS	0.5	[7]
D.c. arc emission with LiF—AgCl carrier	0.5	[8]
D.c. arc emission after preconcentration by precipitation of Bi_2S_3 in MoS_3	0.1	[9]
D.c. arc emission of chips mixed with Li_2CO_3	0.2	[10]
Hollow-cathode emission spectrometry	0.02	[11]
Square-wave polarography after solvent extraction	0.5	[12]
Flame a.a.s. after solvent extraction	0.5	[12]
Flame a.a.s. after electrodeposition	0.1	[13]
A.a.s. with graphite furnace atomization after dissolution of alloy	0.1	[14]
A.a.s. following hydride generation	0.1	[15]
A.a.s. of chips in graphite furnace	0.02	[16]

a limit of detection of 0.004 $\mu g\ g^{-1}$, and this method has now been adapted to the determination of bismuth in nickel-base alloys. The accuracy of the method was assessed by comparing the results with those obtained from solutions of the alloys by atomic absorption spectrometry after hydride generation and after atomization in a mini-Massmann furnace, and with those obtained by independent analyses.

EXPERIMENTAL

Materials

Standardized nickel-base alloys were supplied by Henry Wiggin and Co. Ltd., Rolls Royce Ltd. (Derby and Filton) and Ross and Catherall, Ltd.

Apparatus and method for obtaining absorbances for a series of solid samples.

These were identical to those previously described [17] except that the graphite core and side arms were made from AGTS Grade Graphite (British Acheson Electrodes) and the flow rate of the stir gas was 0.08 $dm^3\ min^{-1}$. Graphite cores and side arms were baked under vacuum for 30 min at ca. 1500°C before use. The resonance line at 306.8 nm from a bismuth hollow-cathode lamp (Pye-Unicam) was used with a slit width of 0.2 nm on a Perkin-Elmer 300 S atomic absorption spectrometer. When samples within the concentration range of 0.02—10 μg Bi g^{-1} were handled, the masses of samples added to the furnace lay within the range 1—30 mg and were determined with a 5-place balance. The core temperature was 2250°C. For the determination of bismuth at concentrations below 1.1 $\mu g\ g^{-1}$, × 2 or × 5 scale expansion was used on the 300 S for samples and standards.

Calibration graphs

For the determination of bismuth in nickel-base alloys containing 0.3—10 μg Bi g^{-1}, calibration graphs of peak absorbances versus amount of bismuth were obtained by dropping increasing amounts of alloy R 3386 (2.0 μg Bi g^{-1}) into the graphite core under conditions capable of producing absorbances up to 1.0. For nickel-base alloys containing < 1.0 μg Bi g^{-1}, calibration graphs were prepared in a similar way with alloys R 3385 (0.98 μg Bi g^{-1}) or RRF1 (0.61 μg Bi g^{-1}), which were standardized against alloy R 3386.

Procedures for the determination of bismuth in nickel-base alloys

Induction furnace method. When a series of nickel-base alloys is to be analysed, suitable masses are dropped into the graphite core over a period of 2—3 h; during the same run but generally at the start of the run, various masses of R 3385, R 3386 or RRF 1 are also added for the purpose of constructing a calibration graph. When the run is completed, the calibration graph is drawn and the mass of bismuth in each sample is obtained from the graph. The concentrations of bismuth in the samples are then calculated.

Hydride generation method. A method similar to that of Drinkwater [15] was used. The hydride was dissociated to bismuth atoms within a quartz tube (8 mm i.d. × 17.5 cm long) heated electrically and maintained at a temperature of ca. 900°C. A Unicam SP90A atomic absorption spectrometer and the bismuth resonance line at 223.1 nm were employed. Calibration graphs of peak absorbance versus ng of bismuth were prepared by adding known masses of bismuth to a solution of alloy DTA which was known to contain very little bismuth.

Graphite tube method. A method similar to that of Welcher et al. [14] was employed. The alloys were dissolved in concentrated hydrofluoric acid—concentrated nitric acid—water (1:3:5, v/v) to give 1% or 2% (w/v) solutions of metal. Aliquots (5 μl) were pipetted into the Varian CRA 63 tube furnace to obtain peak absorbances at the bismuth resonance line (223.1 nm). A hydrogen background corrector was used. The bismuth concentrations in these solutions were determined by a standard additions method.

RESULTS

The resonance line at 306.8 nm was employed to construct calibration graphs for 0—65 ng of bismuth for the determination of bismuth between 0.02 and 10 μg g^{-1} with the induction furnace. These calibration graphs were straight lines through the origin. The mass of bismuth producing 1% absorption was approximately 0.3 ng.

Several series of nickel-base alloys were dropped into the furnace to determine their bismuth contents under the conditions outlined in the Experimental Section. The results (Table 2) indicate that the relative standard deviations are usually less than 15%, when the alloys contain more than 0.1 μg Bi g^{-1}. The limit of detection, defined as twice the standard deviation of several series of samples producing absorbances between 0.01 and 0.03, was 0.02 μg Bi g^{-1}.

TABLE 2

Results for the determination of bismuth in nickel-base alloys

Alloy	Induction furnace			BiH_3	CRA 63	Company result
	Bi found ($\mu g\ g^{-1}$)	No. of samples analysed	R.s.d. (%)	Bi found ($\mu g\ g^{-1}$)	Bi found ($\mu g\ g^{-1}$)	Bi content ($\mu g\ g^{-1}$)
RRF2	1.9	5	8	1.7	1.8	1.9[e]
TT3	2.9	6	11	2.2	3.1	2.9[f]
TT4	5.8	6	6	5.4	4.7	7[f]
TT5	8.1	6	10	7.4	6.9	10[f]
DTB	2.5	6	9	2.4	2.1	2.5[g]
DTC	5.7	8	17	6.2	5.1	5.8[g]
DTD	6.7	8	9	6.2	5.8	6.6[g]
DTE	7.9	7	19	7.1	7.0	8.0[g]
DTF	10.2	7	11	10.1	9.3	10[g]
R 3387	8.5	8	9	8.4	7.1	8.5[g]
R 3388	3.9	7	10	3.6	3.0	3.9[g]
R 6286	9.9	8	6	8.3	9.7	9.0[g]
R 7248[a]	6.0	8	4			5.3[g]
RRF1	0.61	8	18	0.5	0.6[d]	0.5[e]
TT2	0.78	8	12		0.7	0.9[f]
	0.82[c]	8	9			
DTA	0.03[b]	8	39			<0.2[g]
	0.05[c]	8	30			
R 3385	0.98	8	7	0.8	0.9[d]	1.0[g]
	0.99[c]	8	14			
R 6285	0.83	7	11	0.5	0.8	0.9[g]
	0.79[c]	8	15			
R 6287	0.11[b]	8	10	<0.2		<0.2[g]
R 7247[a]	0.56	8	10			0.5[g]
BCS 310	0.24[b]	7	12	<0.2		<0.5[g]
BCS 310/1	0.17[b]	7	9	<0.2		<0.5[g]
ST1	0.39	7	6	0.3	0.4	0.30[h]
	0.35[c]	8	12			
ST2	0.96	8	11	0.9	0.8	0.78[h]
	1.01[c]	7	5			
ST3	1.42	8	11	1.4	1.3	1.07[h]
	1.35[c]	11	13			
TT1	0.02[b]	8	32			<0.1[f]
R 3386	-	-	-	2.0	1.6	2.0[g]

[a] Iron-base alloys containing about 30% nickel. [b,c] R 3386 was used as a standard for constructing the calibration graphs except for the alloys marked[b] and [c]where R 3385 and RRF1 were used, respectively. [d]Without background correction. [e]By a.a.s. after hydride generation. [f]By hollow-cathode emission. [g]By square-wave polarography after solvent extraction. [h]By electrothermal atomization of solutions in the CRA 63 cup.

Results for the determination of bismuth in these alloys by atomic absorption after hydride generation are also shown in Table 2. For these results, duplicate samples of the alloys were taken into solution. The peak

absorbances from three aliquots of each solution were averaged and the average absorbances converted to masses of bismuth from a calibration graph. The calculated results of bismuth concentration from the two dissolved samples were then averaged. A statistical assessment of the results indicated that the limit of detection was 0.2 $\mu g\ g^{-1}$.

Results for the determination of bismuth by electrothermal atomization of bismuth from solutions of the alloys are also presented in Table 2. These results are the average of two determinations of the bismuth in 5-μl aliquots of solution, obtained by a single dissolution of each alloy, based on peak absorbances and standard additions.

DISCUSSION

Alloy R 3386 was selected as a reliable standard because it has been stated to contain 2.0 μg Bi g^{-1} and 1.9 μg Bi g^{-1} when analysed by square-wave polarography after solvent extraction and by hollow-cathode emission spectrometry, respectively. Its bismuth content was taken as 2.0 $\mu g\ g^{-1}$ for induction furnace work.

There is good agreement between company results and those obtained on the induction furnace (Table 2) except for samples TT4 and TT5, where all three methods employed in this work indicate that the company results were too high. The results obtained for the bismuth contents of alloys R 7247 and R 7248 with the induction furnace are probably slightly high, because these alloys are actually iron-base alloys containing ca. 30% of nickel, and bismuth is certainly released more readily from iron-base alloys than from nickel-base alloys at 2050°C, the temperature used in the preliminary investigations here. This resulted in a larger peak absorbance for the same mass of bismuth from a molten iron-base alloy than from a molten nickel-base alloy. The effect was very pronounced at 2050°C, the ratio of peak absorbances for the same mass of bismuth from iron- and nickel-base alloys being 4:3, and it is probably not completely eliminated at 2250°C, the temperature used for these determinations.

The results obtained here for samples ST1, ST2 and ST3 are slightly higher than those reported by the company. However, half the present results were based on a bismuth content of 0.61 $\mu g\ g^{-1}$ for alloy RRF1 which was used to prepare the calibration graph. If the company value of 0.5 for RRF1 is more correct and the bismuth contents of ST1, ST2 and ST3 are calculated on this value, then bismuth contents of 0.29, 0.83 and 1.11 $\mu g\ g^{-1}$ are obtained for ST1, ST2 and ST3, respectively, and these values are in good agreement with the company results.

The precision of the induction furnace method is acceptable for these very low concentrations. Relative standard deviations were seldom in excess of 15% when the bismuth content was more than 1 $\mu g\ g^{-1}$. Where higher relative standard deviations were obtained, e.g. 17% for DTC and 19% for DTE, it is suspected that there is a less homogeneous distribution of bismuth

in the samples. The limit of detection of 0.02 $\mu g\ g^{-1}$ could probably be improved further by using the 223.1-nm resonance line from a high-intensity hollow-cathode lamp. The 223.1-nm line from the Pye-Unicam hollow-cathode lamp used in this study was of relatively low intensity, and the 306.8-nm line was used instead.

The limit of detection for bismuth of 0.02 $\mu g\ g^{-1}$ is the same as that obtained by Marks et al. [16], who added chips to a Perkin-Elmer model HGA 2100 device. However, a much more extensive range of bismuth concentrations has been investigated in the present study.

The results obtained by hydride generation (Table 2) are usually slightly lower than those obtained with the induction furnace; the reason for this is not obvious. The limit of detection of 0.2 $\mu g\ g^{-1}$ is not so good as that obtained by Drinkwater [15] probably because the flask in which the hydride was generated was of greater volume and the optical path through the heated quartz tube was less than that used by Drinkwater.

The results obtained with the mini-Massmann furnace (Table 2) are generally also slightly lower than those obtained with the induction furnace. These slightly low results arise because the sensitivity of the method for bismuth falls by approximately 2% for each heating cycle of the furnace. It was our usual practice to spike solutions from alloys with x ng and $2x$ ng of bismuth and to analyse these in the following order: (i) alloy solution + $2x$ ng of bismuth in duplicate, (ii) alloy solution + x ng of bismuth in duplicate and (iii) alloy solution without bismuth addition in duplicate. The best straight line was then drawn through the averages of the duplicate results, and the intercept on the concentration axis was taken as the concentration of bismuth in the 5-μl aliquot of alloy solution. However, because of the decrease in sensitivity with each heating cycle, the calibration graph should actually be a slight curve with an intercept about 10% further along the concentration axis from the origin. The shape of this curve will vary slightly from one alloy to another and it is only practical to extrapolate a straight line. For this reason, the results by the mini-Massmann method will be about 10% low. If these results are raised by 10%, they are in quite good agreement with the results obtained with the induction furnace and with the results from the companies. With hindsight, this drop in sensitivity leading to curvature in the graph could have been corrected for, by adding the solutions in the order (i), (ii), (iii), (iii), (ii), (i),and drawing the best straight line through the averages of the duplicate results. The limit of detection of the mini-Massmann method was 0.1 $\mu g\ g^{-1}$, taken as twice the signal to noise ratio.

Of the three methods investigated, the induction furnace method seems preferable, as it does not require dissolution of the alloy samples and has a much better limit of detection. However, a reliable nickel-base standard is necessary before the method can be used reliably.

We are indebted to the Science Research Council and Materials Quality Assurance Directorate, Woolwich, for a CASE Studentship (for R. T.); to Mr. K. Cowey of M.Q.A.D. for helpful advice concerning the mini-Massmann method for bismuth; to the British Steel Corporation for the gift of the Perkin-Elmer 300 S atomic absorption spectrometer; to Mr. K. Thornton of Henry Wiggin & Co. Ltd., Mr. R. A. Mostyn of M.Q.A.D., Mr. R. D. Evans of Rolls Royce Ltd. (Derby), Mr. J. Drinkwater of Rolls Royce Ltd., (Filton) and Mr. D. J. Allen of Ross and Catherall Ltd. for analysed samples and very useful discussions; and to Mr. A. M. Aziz-Alrahman of this laboratory for the second analyses of samples of ST1, ST2 and ST3.

REFERENCES

1 D. R. Wood and R. M. Cook, Metallurgia, 67 (1963) 109.
2 J. Heslop and A. R. Knott, Met. Mater., 5 (1971) 59.
3 R. S. Cremisio and D. A. Shinn, Proc. 4th Int. Symp. on Electroslag Remelting Processes, Iron and Steel Institute of Japan, 1973, p. 276.
4 W. B. Kent, J. Vac. Sci. Technol., 11 (1974) 1038.
5 R. T. Holt and W. Wallace, Int. Metals Rev., 21 (1976) 1.
6 G. Mayer and C. A. Clark, Metall. Mater. Technol., (1974) 491.
7 B. E. Balfour, D. Jukes and K. Thornton, Appl. Spectrosc., 20 (1966) 168.
8 M. G. Atwell and G. S. Golden, Appl. Spectrosc., 24 (1970) 362.
9 G. S. Golden and M. G. Atwell, Appl. Spectrosc., 24 (1970) 514.
10 M. G. Atwell and G. S. Golden, Appl. Spectrosc., 27 (1973) 464.
11 K. Thornton, Analyst, 94 (1969) 958.
12 K. Thornton and K. E. Burke, Analyst, 99 (1974) 469.
13 J. A. White, W. L. Harper, A. P. Friedman and V. E. Banas, Appl. Spectrosc., 28 (1974) 192.
14 G. G. Welcher, O. H. Kriege and J. Y. Marks, Anal. Chem., 46 (1974) 1227.
15 J. E. Drinkwater, Analyst, 101 (1976) 672.
16 J. Y. Marks, G. G. Welcher and R. J. Spellman, Appl. Spectrosc., 31 (1977) 9.
17 D. G. Andrews and J. B. Headridge, Analyst, 102 (1977) 436.

Analytica Chimica Acta, 102 (1978) 41—59

THE BEHAVIOUR OF AN ELECTROCHEMICAL DETECTOR USED IN LIQUID CHROMATOGRAPHY AND CONTINUOUS FLOW VOLTAMMETRY

Part 2. Evaluation of Low-temperature Isotropic Carbon for use as an Electrode Material

BRADFORD R. HEPLER, STEPHEN G. WEBER and WILLIAM C. PURDY*

Department of Chemistry, McGill University, 801 Sherbrooke St. W., Montreal, Quebec, H3A 2K6 (Canada)

(Received 22nd May 1978)

SUMMARY

Unalloyed Pyrolyte, a low-temperature isotropic carbon (LTIC) material is evaluated electrochemically for use as an electrode material in h.p.l.c. thin-layer electrochemical detection cell systems. LTIC is compared to carbon paste electrode material in all systems studied, and to glassy carbon impregnated with ceresin wax in the hexacyanoferrate(II)/(III) redox system. Electrode areas, residual currents, and potential windows are described. Quantitative kinetic studies are reported for the hexacyanoferrate(II)/(III) redox pair in 2.0 M KCl, and rate constants are given. Quantitative rate constant studies are also reported for *o*-dianisidine in 1.0 M H_2SO_4. Finally, qualitative rate comparisons are made by cyclic voltammetric techniques between carbon paste and LTIC electrode materials for metanephrine, normetanephrine, adrenaline, noradrenaline, dopamine, 3,4-dihydroxyphenylalanine, 5-hydroxytryptophan, and chlorpromazine in chemical systems reflecting previous applications of h.p.l.c. with electrochemical detection.

A recent report [1] has presented an expression which may be useful for the design and construction of thin-layer electrochemical detection (TLED) cells for use in flow-through analysis. The equations presented allow for the prediction of steady-state current by knowledge of cell geometry and flow rate, as well as the usual parameters of concentration, diffusion coefficient and number of electrons transferred. To extract optimum performance from TLED cells, the thickness of the cell must be vanishingly small and thus the electrode must exhibit a flatness that is difficult to obtain with the currently available solid electrode materials. Glassy carbon requires a high degree of polishing and still exhibits deviations from flatness when utilized in TLED systems [2]. Carbon paste electrodes may perhaps be "flattened" sufficiently, but only after very tedious manipulations for relatively small electrode areas. It is difficult to prepare a flat carbon paste electrode with a surface flush to the cell material surrounding the electrode; also the edge of this electrode often

becomes eroded in flowing streams, especially in thin channels where fluid velocity is high. This channeling becomes a more important problem as the perimeter/area ratio of the electrode increases. Additionally, use of organic solvent systems with carbon paste electrode materials has acknowledged limitations [3]. In attempts to resolve these problems, a new material, Pyrolyte, has been examined for use as a solid electrode material.

Pyrolyte is the trade name for a series of products available from the General Atomic Company; these isotropic pyrolytic carbon materials are prepared by deposition from pure hydrocarbon gas at relatively low temperatures in fluidized beds, i.e. low-temperature isotropic carbons (LTIC) onto a preformed refractory substrate such as graphite [4]. Beilby et al. [5] have prepared pyrolytic carbon film electrodes by a similar process, i.e. low temperature leading to deposition of randomly stacked crystallites. LTIC surfaces, however, can be polished to a flat and uniform (mirror-like) appearance both macro- and microscopically [4]. LTIC have found important applications as materials for prosthetic devices that exhibit biocompatibility, strength, fatigue and wear characteristics that are highly desirable [4]. These materials can also be alloyed with silicon to increase density and strength. In the present experiments, unalloyed material was utilized.

It was considered that the introduction of this material to the electrochemical literature required a more extensive examination than the basic items suggested by Mueller and Adams [6]. First, comparison with existing electrode material(s) under similar experimental conditions was essential in order to present a frame of reference. Carbon paste was chosen as the main reference material in this study, because of the extensive literature [3, 7, 8], its general availability, low cost, and familiarity. Secondly, beyond comparisons of potential windows and standard voltammograms of well-studied redox systems, the electrochemical abilities of these materials should be compared in a specific context. One general approach would be to compare apparent rate constants determined under similar conditions by techniques appropriate for the magnitude of the constant. These comparisons may be qualitative or quantitative, as it is the relative differences that are analytically important. Since carbon materials have been very widely applied in organic electrochemical oxidations involving a variety of functional groups, a suitable series of compounds is readily chosen. For this work, current activity in several clinical TLED cell applications [9—11], and acknowledgement of traditionally utilized reversible and quasi-reversible redox systems in voltammetry, guided the selection of "model" compounds. Finally, the data observed must only be interpreted within the framework of specified conditions. Adams [3] has noted that comparability between the various electrochemical techniques is at best difficult. Blaedel and Schieffer [12] in a recent study on the electrode kinetics of the hexacyanoferrate(II)/(III) system, pointed out the difficulty in comparing the literature values for kinetic data obtained on various electrode materials. They observed that the presence of adsorbed ionic or oxide layers on given electrode materials should be ascertained before rate parameters

can be determined and compared. Additionally, as an extension of the above observations, faster electrode kinetics under one set of conditions with a particular compound at a given electrode material may not infer generally faster kinetics for that material. The basic point is that care is needed in selection of techniques and experimental parameters before rate comparisons can be made. Therefore, each electrode material and electrochemical reaction must be considered and interpreted on its own merits.

In this study both positive and negative potential limits were determined for LTIC in a series of aqueous solvent systems by the technique of Lindquist [13]. Kinetic studies and comparisons were done by cyclic voltammetry [19]. Apparent rate constants were obtained with LTIC, carbon paste and glassy carbon impregnated with ceresin wax (WIGC) for the hexacyanoferrate(II)/(III) couple in 2.0 M KCl. Additionally, rate constants for this system were obtained at LTIC by cyclic voltammetry and perturbation techniques [15]. The oxidation of *o*-dianisidine (3,3′-dimethoxybiphenyl-4,4′-diamine) was studied by cyclic voltammetry, and rate constants were determined where possible.

Finally, by inspection of the position and shape of redox peaks obtained at LTIC and carbon paste electrodes, the oxidations of adrenaline, noradrenaline, dopamine, 3,4-dihydroxyphenylalanine (L-dopa), metanephrine, normetanephrine, 5-hydroxytryptophan, and chlorpromazine, were studied. Electrolyte systems for these compounds that reflected either analytical utility, e.g. mobile phases in high-pressure liquid chromatography (h.p.l.c.) or solvent systems useful in mechanism studies, were used.

From data compiled in both the qualitative and quantitative approaches, conclusions were formed about the utility of LTIC for use in TLED cells in particular, and as an electrode material in general. Finally, the concept of utilizing electrode kinetics as an additional means of influencing system sensitivity and selectivity is discussed.

EXPERIMENTAL

Instrumentation

Cyclic voltammetry was done in quiet solutions with a Princeton Applied Research (PAR) model 173 potentiostat. A triangular potential wave with scan rates of 0.001, 0.002, 0.005, 0.010, 0.020, 0.050, 0.100, 0.200, and 0.500 V s^{-1} was applied with a PAR 175 Universal Programmer. The current signal was measured with a PAR 179 current-to-voltage converter. The voltammograms were recorded on an Omnigraphic X—Y recorder model 2000.

The potentiostatic potential-step rate constants were determined with a Telequipment DM63 oscilloscope to record the current response as a result of the potential perturbations. The PAR 173 potentiostat was used with equal concentrations of both parts of the redox couple of interest present in the cell; the cell potential was measured, and the potentiostat was set to apply exactly that potential between the reference and working electrodes. Potential pulses were then applied, moving in a positive direction from the equilibrium

potential in increments of 0.005 V. The current was again measured by use of the PAR 179 current-to-voltage converter. The signal from the converter was fed to one (model V4) amplifier on the oscilloscope. The oscilloscope was triggered at each stepwise change in applied potential by the potential change itself. By using the differential (model V3) amplifier and a variable source of voltage (PAR 175), the equilibrium cell potential was bucked out, and the small applied potential pulse could be amplified sufficiently to cause triggering. The first 5 ms of current was recorded on the storage screen.

Electrode areas were determined in duplicate by chronoamperometry [3], from the mean $it^{1/2}$ value for 20 pairs of current values (from which blank values had been subtracted) recorded at specific points in time up to 1 min. The PAR 173 potentiostat and PAR 179 current—voltage converter were again used, and a Heath-Schlumberger model SR-204 strip-chart recorder was utilized to record i—t curves.

Electrode resistances were measured with a Fluka model 8030A multimeter.

Electrodes

The LTIC electrode material, as rods (length 26.24 mm, diameter 5.64 mm) and plates (20 × 51 × 1.0 mm), was donated by the General Atomic Company, San Diego, California. Glassy carbon was donated by the Carbone Lorraine Corp. (Valleyfield, Quebec). Graphite (Ultra "F" purity) for the carbon paste electrodes was purchased from the Ultra Carbon Corp. (Bay City, Michigan). Carbon paste was prepared as described by Kissinger et al. [16].

The working electrode holder for the LTIC and carbon paste is outlined in Fig. 1(a). Carbon paste electrodes were prepared, with an LTIC rod in the holder, by packing a small amount of paste into the small well (G), and polishing the surface flush on a flat IBM card, after which the edge of the Teflon cylinder was carefully wiped, and the Lucite shield was threaded onto the cylinder. The electrode holder for glassy carbon is shown in Fig. 1(b).

The prepared working electrodes were placed centrally in either a PAR KOO6O clear glass cell, or in a PAR KOO63 amber glass cell. All reported potentials are against a saturated calomel electrode (SCE). A platinum foil electrode (1.74 × 0.85 mm) was utilized as the auxiliary electrode in all measurements. Each electrode was fixed rigidly within the cell to insure reproducible cell geometry. A PAR nitrogen purge device was also rigidly fixed within the cell to deaerate and purge as necessary. All measurements were made at room temperature.

Impregnation of glassy carbon

A glassy carbon disc was placed in a clean, heated, dry 100-ml flask and heated over a bunsen for 10 min. About 100 ml of solid ceresin wax (BDH), and a stirring bar were added to the flask under a stream of dry nitrogen. Still under dry nitrogen the flask was attached to a preflushed rotary evaporator (Büchi R), which was then evacuated and steam-heated until the wax had melted. Heating was stopped, the vacuum broken and under dry nitrogen an

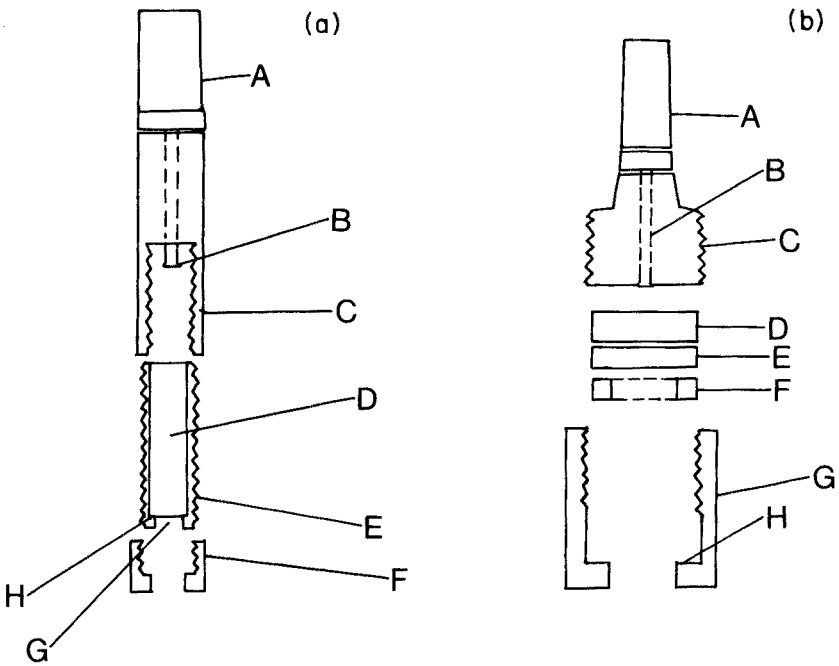

Fig. 1. Electrode holders. (a) For LTIC and carbon paste: (A) banana plug, (B) point of contact with LTIC rod, (C) Teflon jacket, (D) LTIC rod, (E) Teflon cylinder, (F) Lucite cap, (G) well for carbon paste, (H) Teflon lip. (b) For WIGC: (A) banana plug, (B) banana plug post, (C) Teflon plug, (D) brass disc, (E) WIGC disc, (F) Tygon washer, (G) Teflon jacket, (H) internal lip.

equal volume of methylene chloride was added carefully. After evacuation, heating was maintained such that the distillation of methylene chloride was minimal. After 1 h, vacuum and heating were increased until the methylene chloride was distilled off completely, after which heating, mixing and vacuum were maintained constant for another hour. The impregnated disc was then carefully removed from the flask and wiped to a shiny finish with a Kimwipe.

Electrode preconditioning

Electrodes were preconditioned in a suitable electrolyte (without depolarizer) by cyclic scanning through a given potential window (dependent on the electrochemical system) for 3.5 min at 0.100 V s^{-1}. When electrode filming proved to be a problem, e.g. with the catecholamines, their methoxy metabolites, and 5-hydroxytryptophan, fresh paste electrodes were prepared for each scan, and the LTIC rod was cleaned with methylene chloride.

Reagents

All reagents utilized were reagent grade; distilled water was used unless otherwise specified. Stock potassium hexacyanoferrate(II) and (III) standards

were prepared at 0.1000 M concentrations and stored at 4°C. Dilutions were made prior to use in 2.0 M KCl at millimolar concentrations. Other standards (see Table 8, Fig. 7) were prepared as needed at millimolar concentration levels.

Procedures

Potential limits for LTIC electrodes were obtained at scan rates of 0.005, 0.050 and 0.500 V s^{-1} in both positive and negative regions for the electrolytes listed in Tables 3 and 4. For scans into negative potential regions, the solutions were deoxygenated as recommended by Sawyer and Roberts [17].

In kinetic studies for the determination of apparent rate constants, the techniques of Nicholson [14] were used, noting the observations of Perone [18] and Adams [3]. For the hexacyanoferrate(II)/(III) system in 2.0 M KCl, potential windows of —0.300 ↔ 1.250 V were used for blanks, and —0.300 ↔ 1.100 V for the analytes. Scans were initiated in both positive and negative directions with 0.500 V as the initial potential for hexacyanoferrate(III) and 0.000 V for hexacyanoferrate(II). For voltammetry at LTIC, with this redox pair present, all scans were started at the empirically determined equilibrium potential (0.258 V) and scanned through a potential window of 0.728 ↔ —0.258 V for three cycles. Experiments involving scan direction were carried out through a range of scan rates from 0.020 to 0.200 V s^{-1}. In the perturbation experiment, i—t curves were recorded for pulses of 0.005-V increments, from 0.005 to 0.015 V on the positive side of the equilibrium potential (0.258 V). An apparent rate constant was then determined by data analysis as reviewed by Delahay [15].

Scan rates from 0.002 to 0.200 V s^{-1} were used for all systems with the exception of the iron cyanides, which were also studied at 0.001 V s^{-1}. The potential windows and starting potentials used with the organic depolarizers are given in Tables 7 and 8.

RESULTS AND DISCUSSION

Resistance and electrode area measurements

In the initial studies, LTIC was compared to both carbon paste and WIGC electrode materials. The working electrode configurations are shown in Fig. 1. The measured resistances of the three electrode materials in these holders were 0.6 ohms for LTIC, 1.6 ohms for WIGC, and 1.6 ohms for carbon paste. Electrode areas for these three materials are presented in Table 1. As indicated, areas were obtained independently by using each half of the hexacyanoferrate(II)/(III) redox couple in 2.0 M KCl. The $it^{1/2}$ values determined over the 1-min interval used in measurement demonstrated no trends, with a maximum variation of 1.5% about a mean value. These results indicate the general 1:1 relationship between the effective electrochemical and geometrical areas that is expected for useful analytical application. The independence of $it^{1/2}$ with t also demonstrates the effectiveness of electrode shielding in the electrode holders.

TABLE 1

Electrode area

Electrode material	Geometrical area[a] (cm^2)	Electrochemical area[b] (cm^2)	Electrochemical area[c] (cm^2)
LTIC	0.159	0.150	0.148
C paste	0.172	0.172	0.171
WIGC	0.669	0.651	0.668

[a]Geometrical areas are the average of ten measurements.
[b]Determined chronoamperometrically with hexacyanoferrate(III) in 2 M KCl [3].
[c]Determined chronoamperometrically with hexacyanoferrate(II) in 2 M KCl [3].

Residual current

Pretreatment of the LTIC electrode proved to be quite minimal as compared to the packing-finishing and impregnation necessary with the carbon paste and glassy carbon products. Although filming did occur with LTIC in specific oxidative processes (the same ones where filming was observed with carbon paste), the material was readily cleaned with treatment by organic solvent (i.e. methylene chloride) between each voltammogram. It was found that E_p and i_p values were not reproducible with untreated glassy carbon, and residual currents were large and variable. After impregnation of the glassy carbon, i_p values were reproducible within 2.5%; residual currents became reproducible and were lowered by a factor of 5 to 6 (Fig. 2). Residual currents at carbon paste improved with the preconditioning process described above, and therefore this process was beneficial. LTIC, on the other hand, could be used directly as supplied, as little if any improvement in residual current levels was observed with the cyclic preconditioning. This is demonstrated by the difference in background currents after the preconditioning process between the third and sixty-ninth scan taken with the LTIC electrode (Fig. 3).

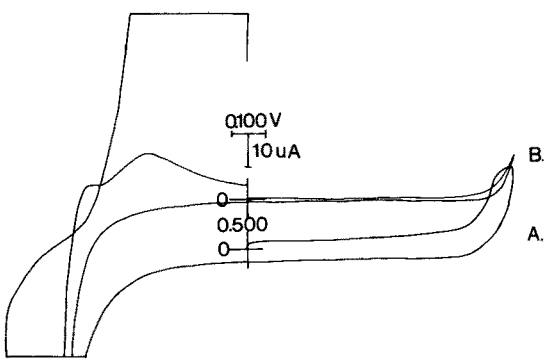

Fig. 2. Residual currents for glassy carbon (A) before impregnation, (B) after impregnation with ceresin wax. Conditions: electrolyte, 2.0 M KCl; scan rate, 0.005 V s^{-1} from 0.500 to −0.300 V to 1.250 V and back to 0.500 V. Flat horizontal areas on voltammograms are areas where pen went off scale. Voltage and current scales are in the polarographic context.

Detailed residual current studies were performed in 2.0 M KCl for all three electrode materials in the hexacyanoferrate(II)/(III) study. Carbon paste provided the lowest residual current values. Residual current values for LTIC and WIGC electrodes relative to carbon paste were determined at scan rates of 0.005, 0.010, 0.020 and 0.050 V s^{-1}. The residual current densities for LTIC and WIGC relative to carbon paste (CP), presented in Table 2, are comparable and both are much higher than one. The change in the initial potential from 0.000 to 0.500 V produced a change in the ratio, but the initial scan direction, was without effect.

Potential windows

The results of the potential window studies for LTIC are presented in Tables 3 and 4. As can be seen, these values compare quite favorably to positive and negative limits reported for a variety of other carbon materials [3, 5, 6, 13, 19—23]. The determined LTIC ranges seem to compare most closely to carbon paste products at both ends of the potential range.

The ranges reported in the present work represent a compilation of values determined from three scan rates, 0.005, 0.050, 0.500 V s^{-1}. Residual current values at the extrapolated cut-off point for the 0.005-V s^{-1} scan rate range from 1.0 to 3.5 μA. This compares with the 2-μA residual current criterion utilized by Adams [3, 19], and Lindquist's observation [13] that use of the extrapolation technique results in cut-off values approximately the same as potential levels at 2 μA on cyclic voltammograms at scan rates of 0.00833 V s^{-1} This indicates that not only the magnitude but the shape of the background of LTIC compares well to those of other carbon products. The potential values in Tables 3 and 4 for each carbon material show a tendency to increase down each column. This indicates, as one might expect, generally consistent characteristics for hydrogen and oxygen overvoltages (and/or solvent decomposition) at carbon-based solid electrodes in given electrolytes.

TABLE 2

Residual current density ratios[a]

Scan rate (V s^{-1})	LTIC/CP[b]	LTIC/CP[c]	WIGC/CP[b]	WIGC/CP[c]
0.005	3.5	7.5	2.5	6.9
0.010	4.9	6.2	3.2	5.4
0.020	4.3	7.2	3.3	5.4
0.050	5.1	6.8	4.0	6.2
Mean	4.4	6.9	3.2	6.0
σ[d]	0.7	0.6	0.6	0.7

[a]Residual currents determined in 2.0 M KCl from cyclic voltammograms based on the difference between anodic and cathodic currents at 0.250 V. Currents have been divided by electrode area, i.e., i/area. [b]Initial potential 0.500 V. [c]Initial potential 0.000 V. [d]Standard deviation.

TABLE 3

Positive potential limits of carbon electrode materials[a]

Electrolyte	LTIC[b]	Carbon paste[c]							CP[d]	SRG[e]	GC[f]	PG[g]	PEG[h]	GR[i]	WIG[j]	PCF[k]
		BN[l]	N_J[l]	MS200[l]	MS555[l]	FIL[l]	Kel-F[l]	DLM[l]								
0.10 M KOH	0.53—0.70	0.68[m]	0.68[m]	0.42[m]	0.68[m]	0.53[m]	0.67[m]	0.62[m]	0.87[n]	0.70[m]	—	—	—	0.68	—	—
0.10 M HCl	1.14—1.21	1.07	1.15	1.05	1.15	0.93	1.14	1.08	1.02	1.30	1.06	1.00	1.1	1.12	—	—
1.0 M KCl	1.17—1.28	0.93[o]	0.88[o]	0.93[o]	0.97[o]	0.86[o]	0.87[o]	0.90[o]	1.10	1.32	—	—	0.95	—	—	1.3[s]
0.10 M KCl	1.18—1.43	—	—	—	—	—	—	—	—	1.35	—	—	0.95	—	1.0	—
0.10 M HNO_3	1.22—1.72	—	—	—	—	—	—	—	—	—	1.24	1.00	1.1	—	—	—
PO_4^{3-} buffer pH 7.00	1.39—1.52	1.26[p]	1.18[p]	1.08[p]	1.27[p]	0.87[p]	1.16[p]	0.99[p]	—	1.25	—	—	—	—	1.35[r] —	—
0.033 M H_3PO_4	1.44—1.68	—	—	—	—	—	—	—	—	—	1.35	—	—	—	—	—
0.10 M $HClO_4$	1.53—1.69	—	—	—	—	—	—	—	—	—	1.20	—	0.92	—	—	—
0.050 M H_2SO_4	1.58—1.79	1.34[q]	1.30[q]	1.13[q]	1.29[q]	0.93[q]	1.21[q]	1.18[q]	1.30[q]	1.40	1.33	—	1.3	1.19	—	—

[a] All values reported in V vs. SCE.
[b] This study.
[c] Lindquist [13].
[d] Carbon paste [19].
[e] Silicone-rubber graphite [20].
[f] Glassy carbon [21].
[g] Pyrolytic graphite [22].
[h] Polythene graphite [23].
[i] Graphite [3; p. 25].
[j] Wax-impregnated graphite [3; p. 27].
[k] Pyrolytic carbon film [5].
[l] Carbon (graphite) binder.
[m] In 0.10 M NaOH.
[n] In 0.2 M NaOH.
[o] In 2 M KCl.
[p] pH 6.80.
[q] In 0.10 M H_2SO_4.
[r] pH 7.02.
[s] 0.5 M KCl.
[t] Adams [3; p. 27].
[u] Concentrations in 1 M.

TABLE 4

Negative potential limits of carbon electrode materials[a]

Electrolyte	LTIC[b]	CP[t]	GC[f]	PG[g]	PEG[h]	GR[i]	WIG[j]	PC
0.10 M HNO_3	—(0.95—1.24)	—	—0.62	—0.8	—0.25	—	—	-
0.10 M HCl	—(1.07—1.27)	—0.90[u]	—(0.81—0.83)	—0.8	—0.30	—0.32	—	-
0.050 M H_2SO_4	—(1.13—1.58)	—	—(0.81—0.83)	—	—0.25	—0.24	—	-
0.033 M H_3PO_4	—(1.22—1.39)	—	—(0.81—0.83)	—	—	—	—	-
0.10 M $HClO_4$	—(1.24—1.39)	—0.90[u]	—(0.81—0.83)	—	—0.20	—	—	-
PO_4^{3-} buffer pH = 7.00	—(1.43—1.71)	—	—	—	—	—	—1.38[r]	-
0.10 M KCl	—(1.51—1.83)	—	—	—	—0.24	—	—1.3	-
0.10 M KOH	—(1.68—1.85)	—	—	—	—	—0.34[m]	—	-
1.0 M KCl	—(1.69—1.84)	—1.1	—	—	—0.24	—	—	—

[a]For footnotes, see Table 3.

Kinetic evaluations

Choice of method. The use of the cyclic voltammetric technique of Nicholson [14] in apparent rate constant determination proved quite reasonable for demonstrating the kinetic abilities of the electrode materials studied. Additionally, the use of the potentiostatic pulse technique as reviewed by Delahay [15], for the hexacyanoferrate system at LTIC helped to establish the validity of the quantitative results obtained by cyclic voltammetry. One of the basic premises of the present approach was that relative differences do indeed exist from system to system, and the importance of the technique utilized therefore lies only in the ability to identify the differences. Other methods of rate constant measurements such as the hydrodynamic approaches of Levich [24], Jordan [25] and Randles [26], as well as other relaxation methods reviewed by Delahay [15], would be just as valid. The important point is that the method must be compatible with the magnitude of the rate parameter sought. Although cyclic voltammetry is less precise than the other methods mentioned, with a larger data sample this quality can be improved (see Table 5). In the present work, the cyclic voltammetric method readily demonstrated the kinetic differences of the various depolarizers at the electrodes indicated. The precision of the apparent rate constants reported is similar to previous data reported by this technique [14, 18], and rivals the precision in recent data reported for the hexacyanoferrate(II)/(III) redox couple in phosphate buffer based on hydrodynamic techniques [12]. Finally, besides being convenient for the systems and rates studied in the present work, cyclic voltammetry provides the most general method of qualitatively evaluating the overall electrode process.

Hexacyanoferrate(II)/(III) redox couple. The apparent rate constant data determined for this couple in 2.0 M KCl are presented in Table 5. These values represent data taken from scan rates over three orders of magnitude where the values of Ψ (which is a numerically derived value relating rate constant and peak separation of a given redox couple determined by cyclic voltammetry [14]) were greater than 0.1.

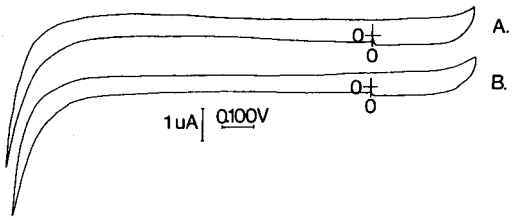

Fig. 3. Residual current for LTIC: (A) at third scan, (B) at sixty-ninth scan. Conditions: electrolyte 2.0 M KCl, scan rate, 0.010 V s^{-1} from 0.000 V to +1.000 V to −0.300 V back to 0.000 V. Voltage and current axes in the polarographic context.

TABLE 5

Apparent rate constants, k_a, (in cm s^{-1}) for hexacyanoferrate(II) and hexacyanoferrate(III) in 2.0 M KCl

	LTIC		Carbon paste[c]		WIGC	
	II[a]	III[b]	II[a]	III[b]	II[a]	III[b]
k_a	5.2×10^{-3}	5.8×10^{-3}	1.6×10^{-3}	1.4×10^{-3}	1.5×10^{-3}	1.7×10^{-3}
S.d. (σ)	$\pm 1.3 \times 10^{-3}$	$\pm 1.3 \times 10^{-3}$	$\pm 0.27 \times 10^{-3}$	$\pm 0.10 \times 10^{-3}$	$\pm 0.13 \times 10^{-3}$	$\pm 0.10 \times 10^{-3}$
σ/k_a	0.25	0.22	0.19	0.074	0.087	0.060
N	17	15	32	37	38	45

[a] $[Fe(CN)_6]^{4-}$ oxidation studied at three separate series of scan rates.
[b] $[Fe(CN)_6]^{3-}$ reduction studied at three separate series of scan rates.
[c] Fresh electrode prepared for each series of scan rates studies.

Cyclic scans in these studies were initiated in both positive and negative directions, in both blanks and analyte solutions. For each carbon material tested for the given starting potentials, there were no observed differences in i_p, E_p, $E_{p/2}$ or residual current values at the electrode materials studied. This includes data taken in the presence of both halves of the redox pair. These observations indicate that hysteresis effects caused by oxide films inhibiting electron transfer is not a factor in these systems under the conditions specified [12]. The reproducibility of the i_p values was within 4.5%.

Values for the rate constant obtained at LTIC by the potentiostatic pulse technique [15] in the presence of equal millimolar concentrations of the hexacyanoferrate redox couple are presented in Table 6. These values are contrasted to rate constants determined by cyclic voltammetric techniques in the same solution, which are also presented in Table 6, and as can be seen compare to an order of magnitude. The rate constants in the presence of both halves of the redox pair are larger than the values obtained with only one member of the pair present (Table 5). This reinforces the concept [12] that adsorbed hexacyanoferrate(II) and (III) ions joined by a cation bridge, produce an entity which is then stabilized by the electrode surface, allowing electrons to be transferred at a faster rate. It is interesting to note that, although the

TABLE 6

Apparent rate constants (in cm s^{-1}) for hexacyanoferrate(II)/(III) determined in the presence of equal concentrations (4.00×10^{-3} M) of both halves of the redox couple

Depolarizer	Rate constants		Ratio (CV)[c]	Ratio (HD)[d]
	PP[a]	CV[b]		
Cyanoferrate(II)		12.6×10^{-3}		
S.d. (σ)	—	$\pm 1.4 \times 10^{-3}$		
σ/k_a		0.11	2.4	2.7
N		10		
Cyanoferrate(III)	8.9×10^{-3}	13.1×10^{-3}		
S.d. (σ)	$\pm 0.48 \times 10^{-3}$	$\pm 0.88 \times 10^{-3}$		
σ/k_a	0.054	0.067	2.2	2.2
N	3	10		

[a]Potentiostatic pulse technique [15].
[b]Cyclic voltammetric technique [14].
[c]Ratio of rate constant value determined in presence of both halves of redox pair to that determined with only given member of redox couple present (Table 5).
[d]Same ratio as above from Blaedel and Schieffer's [12] work on this system by hydrodynamic techniques at glassy carbon in phosphate buffer.

absolute value of rate constants are different, presumably because of different media, electrode materials, methods, etc., the relative increase in rate constant is approximately the same as that obtained at glassy carbon by Blaedel and Schieffer [12] (Table 6).

Finally, for the hexacyanoferrate redox system in 2.0 M KCl, the relationship between peak current, i_p, and the square root of scan rate, $\nu^{1/2}$, is presented

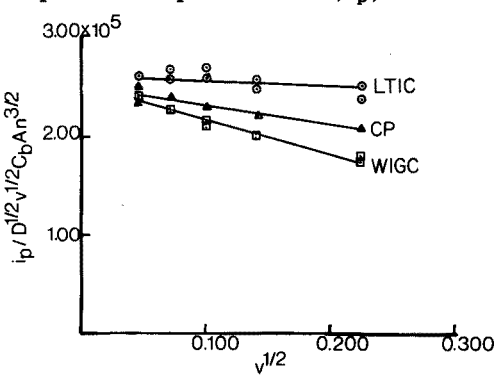

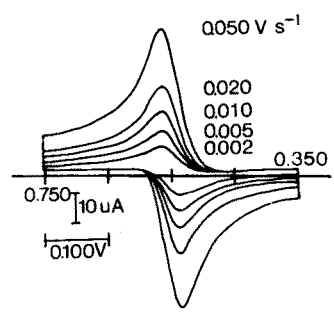

Fig. 4. Graph of $i_p/(\nu^{1/2}D^{1/2}A\ C_b\ n^{3/2})$ vs. $\nu^{1/2}$ for the hexacyanoferrate system in 2.0 M KCl. (All the symbols have their conventional meanings.) All plots include data independently obtained from each member of the redox pair. Each point represents the average of three separate determinations.

Fig. 5. Cyclic voltammograms of 7.39×10^{-4} M *o*-dianisidine in 1.0 M H_2SO_4. Scan rates are indicated on the curves; all scans began at 0.000 V towards positive potentials. Under the conditions used, the potential window was −0.4 ↔ 1.0 V. Voltage axis is in the polarographic context; on the current axis, however, anodic currents are above the axis.

in Fig. 4. The lines are drawn by linear regression analysis from data taken independently from both halves of the redox pair. The intercepts of these plots should approach the Randles—Sevcik constant [27, 28]. The values found were 2.64×10^5 for LTIC, 2.52×10^5 for carbon paste and 2.52×10^5 for WIGC, which are similar to the values reported by Adams [3] at platinum electrodes (2.64×10^5 for hexacyanoferrate(II) in 2 M KCl and 2.59×10^5 for hexacyanoferrate(III) in 2 M KCl) when a combination of chronoamperometric and chronopotentiometric techniques was used. Carbon paste electrodes utilized in this work were prepared fresh for each blank and analyte determination. Electrode area reproducibility was within 3.90%.

o-Dianisidine

The two-electron oxidation of this depolarizer in 1.0 M H_2SO_4 is reversible at carbon paste, as indicated by the cyclic voltammograms presented in Fig. 5. The ΔE_p values were 0.026 ± 0.002 V through scan rates of 0.050 V s^{-1}. This same system studied at LTIC proved to be quasi-reversible by cyclic voltammetric techniques, allowing a rate constant to be determined. The apparent rate constant found was 7.8×10^{-3} ($\pm 1.5 \times 10^{-3}$) cm s^{-1}, for $n = 17$ with a relative standard deviation of 0.20. Neither material demonstrated problems of electrode filming under these conditions, which is consistent with observations by Adams [3]. Table 7 shows the i_p values obtained for *o*-dianisidine at carbon paste electrodes when a fresh electrode was used for each scan and when the same electrode was used throughout. Finally, these two materials are compared graphically as $i_p/(\nu^{1/2}D^{1/2}AC_b\ n^{3/2})$ is plotted vs. $\nu^{1/2}$ in Fig. 6; the intercepts were 2.67×10^5 for carbon paste, and 2.69×10^5 for LTIC, which are similar to values ($2.69—2.72 \times 10^5$) at boron carbide reported by Mueller and Adams [39]. Although the LTIC material is kinetically slower in this system than carbon paste, it still proves to be a useful solid electrode material.

Studies with selected organic compounds

The kinetics of the oxidations of the compounds listed in Table 8 were studied and compared qualitatively by cyclic voltammetric analysis. Voltammograms at LTIC and carbon paste electrodes, representative of these studies are shown in Fig. 7(a—h). The electrolyte systems utilized for these studies reflect those previously reported in the literature for either mechanism studies or applied h.p.l.c. analysis with electrochemical detection.

TABLE 7

Peak currents for 7.39×10^{-4} M *o*-dianisidine. Potential window is —0.400 ↔ 1.000 V. Initial potential 0.000 V scanning in a positive direction.

Scan rate (V s^{-1})	0.002	0.005	0.010	0.020	0.050
$i_p(\mu A)$[a]	9.41	14.5	20.8	29.6	47.6
$i_p(\mu A)$[b]	9.35	14.5	21.0	29.3	47.9

[a]Fresh electrode prepared for each scan rate evaluation.
[b]Same electrode utilized for all determinations.

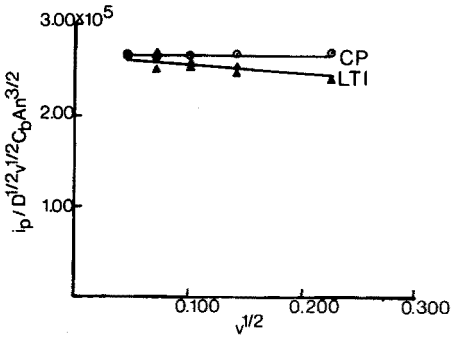

Fig. 6. Graph of $i_p/(v^{1/2}D^{1/2}A\ C_b\ n^{3/2})$ vs. $v^{1/2}$ for *o*-dianisidine in 1.0 M H_2SO_4. Each point represents a single determination.

TABLE 8

E_p and $E_{p/2}$ values for selected organic oxidations at LTIC and carbon paste electrodes (For the first 7 compounds the potential window was —0.20 ↔ 1.00 V; for chlorpromazine, the potential window was —0.10 ↔ 1.10 V. In all cases, scanning was done in a positive direction from 0.00 V. All values reported are to ± 10 mV).

Compound	LTIC		Carbon paste	
	E_p (V)	$E_{p/2}$ (V)	E_p (V)	$E_{p/2}$ (V)
Metanephrine[a]	0.765	0.66	0.775	0.675
Normetanephrine[a]	0.77	0.65	0.735	0.655
Adrenaline[b]	0.66	0.58	0.725	0.64
Noradrenaline[b]	0.66	0.57	0.73	0.64
Dopamine[b]	0.59	0.52	0.675	0.58
L-Dopa[b]	0.62	0.54	0.64	0.56
5-Hydroxytryptophan[c]	0.545[e]	0.42[e]	0.675[e]	0.445[e]
Chlorpromazine[d]	0.53	0.475	—[f]	—[f]
	1.00	0.94	—[f]	—[f]

[a]In 0.10 M citric acid—0.10 M Na_2HPO_4—methanol (10:10:1). [b]In 0.010 M H_2SO_4—0.040 M Na_2SO_4. [c]In pH 5.2 acetate—citrate buffer. [d]In 3.0 M H_2SO_4. [e]The values used are from potentials determined at i_{max}, and $i_{max/2}$. [f]Electrode decomposed at these concentrations of H_2SO_4.

The oxidation of chlorpromazine was carried out in 3.0 M H_2SO_4, under which conditions two one-electron steps are involved [30]. The first 1-e loss produces a highly colored radical cation that is quite stable in the strong acid medium. The second electron loss occurs at a more positive potential and produces the sulfoxide of the parent compound. Analysis by chronopotentiometry [31] and at a rotating platinum microelectrode [32] have shown that the first oxidation step is electrochemically reversible, and it is therefore of interest for rate comparisons. In the present studies with LTIC in the system described, cyclic voltammetric scans of chlorpromazine showed two distinct

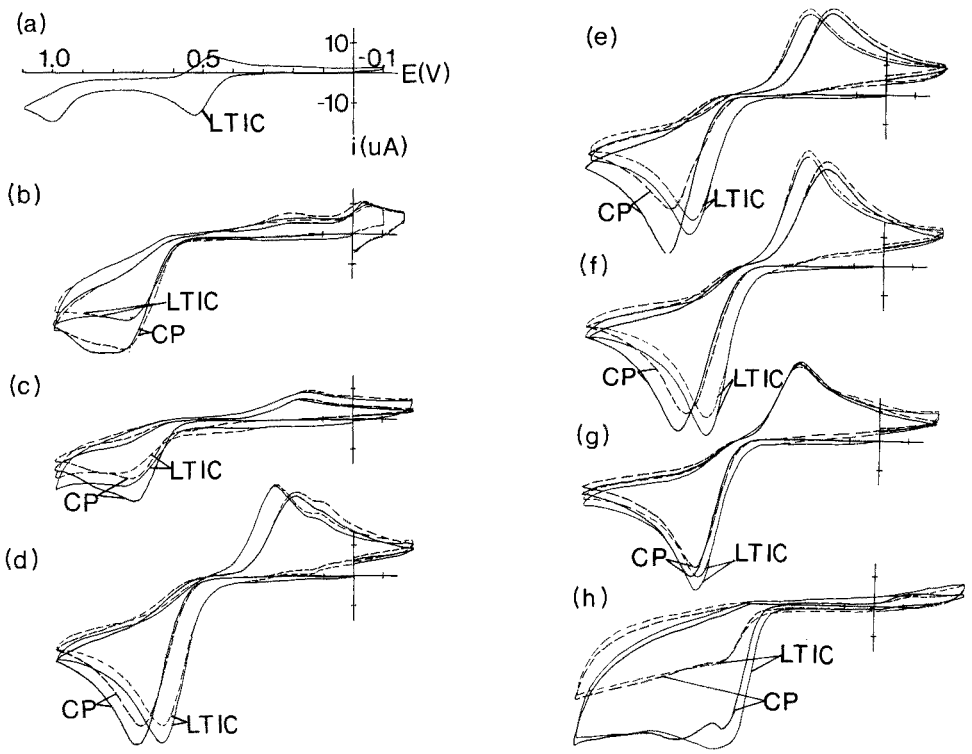

Fig. 7. Cyclic voltammograms at LTIC and carbon paste (CP) electrodes: (a) 1.1×10^{-3} M chlorpromazine in 3.0 M H_2SO_4 at a scan rate of 0.020 V s^{-1}; (b) and (c) 7.1×10^{-4} M metanephrine and 5.3×10^{-4} M normetanephrine, respectively, in 0.10 M citric acid—0.10 M Na_2HPO_4—methanol (10:10:1); (d), (e), (f), (g) 9.9×10^{-4} M adrenaline, 1.1×10^{-3} M noradrenaline 1.1×10^{-3} M dopamine, 9.1×10^{-4} M L-Dopa, respectively, in 0.010 M H_2SO_4 —0.040 M Na_2SO_4; (h) 9.4×10^{-4} M 5-hydroxytryptophan in pH 5.0 citric acid-acetate buffer pH 5.0 [11]. All scans begin at 0.000 V and go towards positive potentials; the scan rate for voltammograms (b)—(h) was 0.050 V s^{-1}. (—) First scan; (---) second scan.

1-e oxidation peaks separated by 0.470 V (Fig. 7a; Table 8). The first peak proved reversible by cyclic voltammetric criteria at the scan rates studied, thus supporting previous reports [30, 31]. Carbon paste could not be evaluated in this system, because of electrode decomposition in the strongly acidic medium.

The 2-e oxidations of the catecholamine metabolites, metanephrine and normetanephrine, were carried out in 0.10 M citric acid—0.10 M Na_2HPO_4—methanol (10:10:1). This solvent system has been used as mobile phase for the reverse-phase h.p.l.c. separation of these metabolites in urine with electrochemical detection [32]. Voltammograms of these metabolites are presented in Fig. 7(b, c). The shapes of the cyclic voltammograms for these oxidations are similar to those in the original work [32], but it can be seen that with LTIC

the ΔE_p values between the oxidation and reduction peaks for metanephrine and normetanephrine are slightly greater, indicating slower kinetics. This is best demonstrated by comparison of the respective peak potentials, E_p and $E_{p/2}$, presented in Table 8. Similar results were noted for all scan rates studied. At the concentration levels used (ca. 10^{-3} M), electrode filming was present with both electrode materials, indicated by a decrease in i_p of the oxidation peak on the second scan. This is again consistent with previous work [32], and as pointed out by Kissinger [7], is generally avoided in h.p.l.c. applications, where contamination of the electrode by adsorption or coating with free radical polymerization products is minimized by having the analyte concentrations below the 10^{-6} M level. In the present work, a fresh carbon paste electrode was utilized with each scan, and the LTIC rod was cleaned with methylene chloride between each voltammogram. Under these conditions, LTIC becomes as convenient to use in h.p.l.c. applications as carbon paste.

Similarly, the oxidations of adrenaline, noradrenaline, dopamine and L-Dopa in 0.010 M H_2SO_4—0.040 M Na_2SO_4 were studied at 10^{-3} M concentration levels. The voltammograms shown in Fig. 7(d—g), and the E_p and $E_{p/2}$ values summarized in Table 8, indicate qualitatively that the kinetics for these processes at LTIC are slightly faster; the less positive E_p and $E_{p/2}$ values and the smaller spread between the oxidation and reduction peaks provide the evidence. The choice of the solvent system was once again determined by previous h.p.l.c. applications with electrochemical detection [33, 34]. Figure 7(d, e, f, and g) indicates that filming of the electrode surface occurred with both LTIC and carbon paste. Solvent cleaning of the LTIC and a fresh carbon paste electrode for each voltammogram provided reproducible results.

As might be expected, similarities of reaction rate exist in this series of compounds. The same trends can be noted as with the metanephrine and normetanephrine oxidations. The 2-e oxidations for the catecholamines and their methoxy metabolites proceed by essentially the same mechanism [32, [32, 35], and therefore similarity in the voltammograms for the same electrolyte system is marked (Fig. 8, b—g). The basic reason for considering these compounds independently, rather than as a group, was to document the ability of LTIC to function effectively as an alternative material for electrodes in existing applications of electrochemical detectors.

The oxidation of 5-hydroxytryptophan was carried out in pH 5.0 acetate—citrate buffer, which was chosen because of its prior use as the mobile phase in h.p.l.c. with a voltammetric detector [10]. Voltammograms are presented in Fig. 7(h). The potential values at i_{max} and $i_{max/2}$ (Table 8) indicate that LTIC exhibits faster kinetics. The i_{max} values were utilized in this case because of the difficulty in determining which hump in the cyclic voltammogram was the actual i_p for these oxidations.

CONCLUSIONS

The data presented have proved that LTIC is a useful material for application as a working electrode in a variety of specific systems. Redox processes in

four general groups of compounds — aromatic hydroxy compounds, aromatic amines, sulfides and hexacyanoferrate complexes — were studied qualitatively and/or quantitatively to demonstrate that kinetic differences do exist between given electrode materials in these systems. For some reactions (hexacyanoferrate(II)/(III), adrenaline, noradrenaline, L-Dopa, dopamine and 5-hydroxytryptophan), LTIC gave faster kinetics. For others (metanephrine, normetanephrine, *o*-dianisidine), carbon paste gave the higher reaction rates. The influence of kinetics is an important consideration for TLED cell application and thereby merits further discussion.

In electrochemical detection systems, there are two factors which affect sensitivity, the electrochemical reaction rate and the mass transport efficiency. The nature of the electrochemical reaction rate, its exponential dependence on applied potential, is an impressive property when viewed as a means of controlling sensitivity. In order to exploit this property the mass transfer must be efficient. The most accessible controls of mass transport efficiency for a TLED chromatographic detector are electrode area and the thickness of the cell itself; the flow-rate is presumed to be governed by chromatographic needs. The largest current densities are obtained as these two parameters approach zero [1]. It is easy to construct a cell with an electrode of small area, but the construction of a very thin cell can be difficult because of non-uniform flatness of electrode material [2]. The criteria that appear as important in choosing an electrode material for maximum sensitivity in a TLED are a high specific rate constant and uniform flatness of the material. Of course, the specific rate constant of any electrode—depolarizer system depends on the depolarizer as much as the electrode, so that the electrode material yielding the highest sensitivity in one application may not be the best for another application.

High specific rate constants with low overvoltage become a more important factor as potential window limits are pressed, and plateaux (in the case of forced convection) or E_p values (in static systems) are not obtained before solvent decomposition occurs. Additional factors, such as electrochemical contaminants (or other electroactive components of interest) in a given system can become significant contributors to the measured current as potentials are varied. These factors may lead to losses in both sensitivity and selectivity.

The LTIC plates seem to possess the required flatness to construct cells thinner than previously possible: TLED cells with cell thicknesses on the order of 3 μm can be prepared. The question of electrochemical reaction rate remains. Current materials exhibit differences under specified conditions as demonstrated in part by this work. Other groups [36—42] are also working with synthetic modifications of electrode materials, with the aim of designing electrodes that provide both high sensitivity (i.e. high specific rate constants) and selectivity (specific electrochemical reactions). Current work in this laboratory is involved in exploration of this type of electroanalytical approach, as well as studying TLED cells quantitatively for given electroanalytical h.p.l.c. applications.

We are grateful to Axel Haubold, W. H. Ellis and Dr. J. C. Bokros of the General Atomic Co. for supplying the Pyrolyte material prepared according to our specifications in this project; to Alfred Kluck for help in the design and construction of the electrode holders; to Dr. Simon N. Young, Allan Memorial Institute, Montreal, for providing the catecholamines and their methoxy metabolites tested; and to Poulenc Ltd., Montreal, for the gift of chlorpromazine. We also thank the National Research Council of Canada for their support.

REFERENCES

1 S. G. Weber and W. C. Purdy, Anal. Chim. Acta, 100 (1978) 531.
2 J. Lankelma and H. Poppe, J. Chromatogr., 125 (1976) 375.
3 R. N. Adams, Electrochemistry at Solid Electrodes, M. Dekker, New York, 1969.
4 J. C. Bokros, R. J. Akins, H. S. Shim, A. D. Haubold and N. K. Agarwar, Chem. Techn. 7 (1977) 40.
5 A. C. Beilby, W. Brooks and G. L. Lawrence, Anal. Chem., 36 (1964) 22.
6 T. R. Mueller and R. N. Adams, Anal.Chim. Acta., 23 (1960) 467.
7 P. T. Kissinger, Anal. Chem., 49 (1977) 447A; 48 (1976) 17R; 46 (1974) 15R.
8 S. Piekarski and R. N. Adams, in A. Weissberger and W. B. Rossiter (Eds.), Techniques of Chemistry, Physical Methods, Wiley-Interscience, New York, 1971, Vol-1, Part IIA, p. 531.
9 P. T. Kissinger, C. S. Bruntlett, G. C. Davis, L. J. Felice, R. M. Riggin and R. E. Shoup, Clin. Chem., 23 (1977) 1449.
10 U. R. Tjaden, J. Lankelma, H. Poppe and R. G. Muusze, J. Chromatogr., 125 (1976) 275.
11 S. Sasa and C. L. Blank, Anal. Chem., 49 (1977) 354.
12 W. J. Blaedel and G. W. Schieffer, J. Electroanal. Chem., 80 (1977) 259.
13 J. Lindquist, J. Electroanal. Chem., 80 (1977) 259.
14 R. S. Nicholson, Anal. Chem., 37 (1965) 1351.
15 P. Delahay in P. Delahay and C. W. Tobias (Eds.), Advances in Electrochemistry and Electrochemical Engineering, Interscience, New York, N.Y., 1961, Vol 1, pp. 233—318.
16 P. T. Kissinger, C. Refshauge, R. Dreiling and R. N. Adams, Anal. Lett., 6 (1973) 465.
17 D. T. Sawyer and J. L. Roberts, Experimental Electrochemistry for Chemists, J. Wiley, New York, N.Y., 1974, p. 134.
18 S. P. Perone, Anal. Chem., 38 (1966) 1158.
19 R. N. Adams and C. Olson, Anal. Chim. Acta, 22 (1960) 582.
20 E. Pungor and E. Szepesvary, Anal. Chim. Acta, 43 (1968) 289.
21 H. E. Zittel and F. J. Miller, Anal. Chem., 37 (1965) 200.
22 F. J. Miller and H. E. Zittel, Anal. Chem., 35 (1963) 1866.
23 M. Mascini, F. Pallozzi and A. Liberti, Anal. Chim. Acta, 66 (1973) 126.
24 V. G. Levich, Physicochemical Hydrodynamics, Prentice-Hall, Englewood Cliffs, New Jersey, 1962, p. 72.
25 J. Jordan, Anal. Chem., 27 (1955) 1708.
26 J. E. B. Randles, Can. J. Chem., 37 (1959) 238.
27 J. E. B. Randles, Trans. Faraday Soc., 44 (1948) 327.
28 A. Sevcik, Collect. Czech. Chem. Commun., 13 (1948) 349.
29 T. R. Mueller and R. N. Adams, Anal. Chim. Acta, 25 (1961) 482.
30 G. J. Patriarche and J. J. Lingane, Anal. Chim. Acta, 49 (1970) 25.
31 F. A. Merkle and C. A. Discher, Anal. Chem., 36 (1964) 1639.
32 R. E. Shoup and P. T. Kissinger, Clin. Chem., 23 (1977) 1268.
33 P. T. Kissinger, R. M. Riggin, R. L. Alcorn and Rau Leh-Daw, Biochem. Med., 13 (1975) 299.
34 R. M. Riggin, R. L. Alcorn and P. T. Kissinger, Clin. Chem., 22 (1976) 782.
35 M. D. Hawley, S. V. Tatawavadi, S. Piekarski and R. N. Adams, J. Am. Chem. Soc., 89 (1967) 447.

36 J. F. Evans and T. Kuwana, J. Electroanal. Chem., 80 (1977) 409.
37 C. A. Koval and F. C. Anson, Anal. Chem., 50 (1978) 223.
38 P. R. Moses and R. W. Murray, J. Am. Chem. Soc., 98 (1976) 7435; J. Electroanal. Chem., 77 (1977) 393.
39 B. F. Watkins, J. R. Behling, E. Kariv and L. L. Miller, J. Am. Chem. Soc., 97 (1975) 3549.
40 B. E. Firth, L. L. Miller, M. Mitani, T. Rogers, J. C. Lennox and R. W. Murray, J. Am. Chem. Soc., 98 (1976) 8271.
41 R. J. Burt, G. J. Leigh and C. J. Pickett, J. Chem. Soc. Chem. Commun., (1976) 1940.
42 M. Fujihira, T. Matsue and T. Osa, Chem. Lett., (1976) 875.

Analytica Chimica Acta, 102 (1978) 61—83

DYNAMIC RESPONSE OF THE FLUORIDE ION-SELECTIVE ELECTRODE

R. C. HAWKINGS*, L. P. V. CORRIVEAU, S. A. KUSHNERIUK and P. Y. WONG

Atomic Energy of Canada Limited, Chalk River Nuclear Laboratories, Chalk River, Ontario KOJ IJO (Canada)

(Received 8th March 1978)

SUMMARY

The dynamic response of the fluoride-selective electrode is shown to result from four distinct processes: ion diffusion, an undefined reaction, LaF_3 dissolution and a calibration drift. Empirical equations are derived which describe the time—e.m.f. relationship over times of the order of days. Dissolution of LaF_3 is shown to be a minor factor in determining the lower limit for measurement of fluoride concentration. The calibration drift process is the main obstacle. The time to thermodynamic equilibrium when the fluoride concentration is reduced becomes very long. A model is given for the calibration drift process. This model explains many of the anomalies reported in the literature for the behaviour of the fluoride-selective electrode. A much more detailed understanding of the calibration drift process is a prerequisite to general application of the fluoride electrode to the measurement of very low concentrations of fluoride.

Electrochemical measurement with the lanthanum trifluoride crystal electrode, developed by Frant and Ross [1], is the most specific and rapid method for the determination of fluoride ion activity. The relationship between the electrode potential and the ion activity is given by the Nernst equation. Implicit in this relationship are the assumptions of electrode reversibility and of a state of thermodynamic equilibrium. Most applications of the fluoride-selective electrode have assumed that the electrode response is sufficiently fast that a near equilibrium potential is attained within a few minutes. However, the literature abounds with observations of much longer times to equilibrium [2—14]. The consensus is that the response time increases with decreasing fluoride ion concentration and that the time to equilibrium could be very long (of the order of hours) for fluoride ion concentrations below 20 ng $F^- g^{-1}$.

The recent surge of interest in the kinetics of the response of ion-selective electrodes [15—24] coincided with our interest in accurate determinations of fluoride down to the lowest levels possible. At such low levels (< 20 ng $F^- g^{-1}$) the time to reach equilibrium is impracticably long. This obstacle

*Author for correspondence. Present address: P.O. Box 1087, Deep River, Ont., Canada KOJ 1PO.

would be overcome if the equilibrium potential could be computed from time—e.m.f. data.

This paper presents the results of investigations into the factors which influence the electrode response at low concentrations, and some empirical relationships between time and electrode potential that yield a satisfactory value for the computed equilibrium potential. The desirability of such investigations was emphasized by Tóth and Pungor [25].

EXPERIMENTAL

The time—response data were obtained under conditions considered applicable to the determination of fluoride by immersion of the electrode in stirred aqueous media of limited volume (10—100 ml) with possible variations in the ionic strength, pH, and impurity content of the samples. To offset the expected variations in sample composition, the total ionic strength adjustment buffer (TISAB) used contained 1 g kg^{-1} of 1,2-diaminocyclohexane-*N*,*N*,*N*′,*N*′-tetraacetic acid (DCTA).

Reagents

Triple-distilled water and reagent-grade chemicals were used for all solutions, unless otherwise mentioned. A modified TISAB stock was prepared in 2-l batches by mixing, with water in a large polypropylene beaker, 108.5 g of quadruple-distilled acetic acid, 116.0 g of sodium chloride recrystallized from triple-distilled water, and 2.0 g of DCTA recrystallized three times from triple-distilled water. The pH was adjusted to 5.5 with 5 M sodium hydroxide and the volume was finally adjusted to 2 l at 20°C. Blank samples were prepared by mixing 21.3 g of stock TISAB with 40 g of water. The fluoride content of blank samples was altered as required by the addition of weighed amounts of standard fluoride solutions prepared by weight from oven-dried analytical-grade sodium fluoride and water. All solutions were stored in polypropylene bottles.

Instrumentation

Two Orion Model 96-09 combination electrodes were used. A Corning Scientific Instruments Model 104 four-channel digital electrometer, with an input impedance greater than 10^{14} ohms, was used to read the cell potentials to the nearest 0.1 mV with interpolation, when possible, to 0.05 mV. Stability of the electrometer was monitored with a standard Weston cell.

Procedure

All samples were prepared, about one hour in advance, in 100-ml polypropylene beakers and immediately covered with a thin sheet of polyethylene to minimize loss by evaporation and contamination from air-borne fluoride. The sealed beakers were transferred to a thermostat, controlled at 25.0 ± 0.1°C, to reach operating temperature. A polypropylene-covered magnetic

stirring bar was dropped in, through a slit in the plastic film, with the aid of a second polypropylene-covered bar used exclusively for handling purposes. This was followed by a precision mercury-in-glass thermometer and finally by the fluoride electrode. A timer was started at the instant of immersion of the electrode.

The fluoride electrodes were kept immersed in a buffered solution at all times except for the brief interval (< 5 s) required to transfer from one sample to the next. The electrodes were not rinsed or wiped between samples, as such procedures had been shown in earlier work here to result in undesirable perturbations on the response. Adhering droplets were removed by shaking the electrode during transfer. The fluoride content of solutions was adjusted in situ by spiking with a standard fluoride solution delivered from a polyethylene weighing bottle [26] through a small hole in the plastic film cover. The timer was restarted when the first drop of spike solution entered the sample. Although such additions were usually complete within 0.3 min, this procedure introduced a slight uncertainty in the effective starting time. Solution temperature was recorded to the nearest 0.05°C along with the time—e.m.f. data. The observed e.m.f. was then partially corrected for minor fluctuations in the solution temperature by normalization of the Nernst slope to 25°C [27]. The upper portion of the electrode was exposed to ambient temperature. This temperature was also recorded, but no adjustments to the observed e.m.f. data were made. The effect of such "pseudo-isothermal" operation is discussed by Hawkings et al. [28].

RESULTS AND DISCUSSION

Basic model

Rangarajan and Rechnitz [16] investigated the dynamic response of Br^-, Cl^- and I^- electrodes in a flowing stream. Their observations were reported to be consistent with an approximate diffusion model of electrode response such as that derived by Markovic and Osburn [17] from measurements of the dynamic response of two H^+-electrodes, a Ca^{2+}-electrode, and a Cl^--electrode, by pulse-testing techniques. Similar results were reported by Rechnitz and Hameka [29] for the glass electrode, and by Tóth et al. [30] from a study of Cl^-, Br^-, CN^- and I^--selective electrodes. Cammann and Rechnitz [18] examined the kinetics of charge-transfer processes occurring at the phase boundaries of Ag_2S-based membrane and LaF_3 crystal electrodes, to determine whether or not thermodynamic equilibrium is established at these boundaries. For the case of the fluoride-selective membrane electrode, they concluded that OH^- does not enter the LaF_3 lattice appreciably, but rather that OH^- interference involves a chemical equilibrium of the type

$$LaF_3 + 3OH^- \leftrightarrows La(OH)_3 + 3F^- \qquad (1)$$

They concluded further that La^{3+} is not involved in the charge-transfer step, and that adsorption and desorption processes of other ions dominate the effect of F^- at very low concentrations.

Morf et al. [19] derived an expression for the dynamic response of an ion-exchange membrane electrode on the basis of a diffusion model with the simplifying assumption that any interfering ions are excluded. In qualitative agreement with experimental data, response times calculated from this expression are longer for an activity decrease than for an activity increase. Lindner et al. [20] investigated the response characteristics of a number of different types of ion-selective electrodes. The LaF_3 single crystal i.s.e. was classed as an electrode operating on chemisorption or precipitate exchange reactions. They expressed the electrode response in terms of an activity change in the boundary layer of the electrode.

Shatkay [21] emphasized the dangers inherent in assuming that the electrode response is fast relative to the velocity of a process under investigation and that, following a step change in concentration, a time-independent reading can be safely postulated. From an analysis of various physical models for the mechanism of the transient response, he concluded that the transients describe a complex phenomenon, and that several models have to be applied simultaneously to account for them satisfactorily. This conclusion is supported by the investigations of Mertens et al. [22] on the kinetics of the i.s.e. in fast flow and automatic systems. They concluded that in the concentration range 0.19—190 $\mu g\ F^- g^{-1}$ the intrinsic response of the Orion 94-09A fluoride electrode is rapid enough to permit its use as a sensing element in automated potentiometric systems, but that its actual response is limited by a film diffusion process. They found that an empirical relationship derived by Müller [31] on the basis of measurements with an Orion Ag_2S membrane electrode best described the time response over time intervals of several minutes. This empirical equation is expressed by

$$E = t/(a + bt) \tag{2}$$

where E is the increase in potential resulting from a sudden incremental change in Ag^+ concentration. A plot of t/E vs. t yields a straight line of slope b and intercept a. The maximum value of E (for $t = \infty$) is equal to $1/b$. It is interesting to note that this equation, postulated on an empirical basis and reported to have a relationship to the Langmuir adsorption isotherm, is identical to an ad hoc equation which Shatkay found gave the best fit to his data (eqn. 14, [21]). This equation was expressed as

$$E_t = E_1 + (E_2 - E_1)\frac{Kt}{1 + Kt} \tag{3}$$

where E_t, E_1, E_2 are the potentials at times $t = t$, $t = 0$ and $t = \infty$, respectively, while K is a constant with units of reciprocal time. By making the transformations $K = b/a$ and $b = 1/(E_2 - E_1)$, eqn. (3) becomes the Müller eqn. (2), $E_t - E_1$ being the potential increase. Again, Buffle, Parthasarathy and Haerdi [23, 24] established an empirical relation for the potential—time curves of both fluoride and chloride i.s.e.:

$$E_t = E_2 - 1/(At + B) \tag{4}$$

where E_t is the potential at time t, E_2 is the equilibrium potential and A and B are empirical constants. This relation is identical to the Müller eqn. (2) when $B = b = 1/(E_2 - E_1)$ and $A = b^2/a$. The ratio $B/A = a/b$ is seen to be the half-time $t_{1/2}$. A mathematical model, analogous to the empirical eqn. (4), was derived by Buffle and Parthasarathy [23] on the basis of a second-order dissolution reaction and the surface electrochemical properties of the membrane.

The Müller and associated relations for the e.m.f. may be alternatively expressed as

$$e_t = e_\infty \exp(\eta/(1 + Kt)); e_i = e_\infty \exp(\eta) \quad (5)$$

in which e_t is proportional to the apparent fluoride ion concentration and is defined by $e_t = \exp(-FE_t/RT)$, where F, R and T represent the Faraday, the gas constant and the absolute temperature, and the subscripts t, i, ∞ refer to the times $t = t$, $t = 0$ and $t = \infty$.

Orion [32] markets a special paper for the graphical extrapolation of time—response data to obtain the equilibrium e.m.f. from low fluoride concentrations. On this paper, the ordinate and abscissa are such that one effectively plots e_t, as defined above, vs. $1/t$. At the lower fluoride concentrations this plot is reputed to be linear.

The present investigations on the kinetics of the fluoride i.s.e. have identified four distinct processes which contribute to the overall dynamic response of the electrode. Each of these processes is consistent with the elementary model for the LaF_3 crystal—solution interface shown schematically in Fig. 1. The processes identified are: (a) a reaction process; (b) ion diffusion; (c) a LaF_3 dissolution process; and (d) a calibration drift process.

In the discussion which follows, it is assumed that electrical equilibrium is attained very rapidly across the solid membrane through the action of charge carriers, and that the overall slow response is the result of processes taking place on the sample solution side of the LaF_3 membrane. These may include

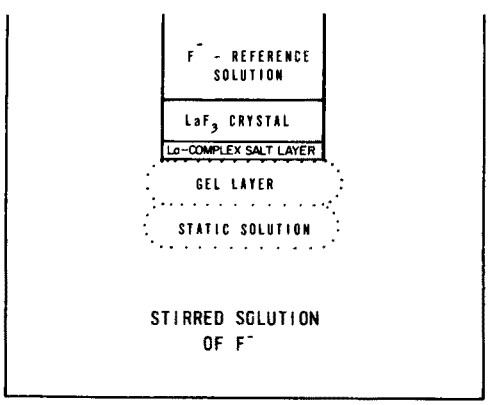

Fig. 1. A schematic view of an elementary model of the crystal—solution interface of the LaF_3 electrode, showing the working zones.

the formation of mixed salts on the surface [33], a gel layer of La-complexes [34], and the effects of a static layer of solution [22]. All of these processes could be expected to influence the approach to equilibrium both by changes in overall potential with change in composition and by controlling diffusion of ions during the approach to equilibrium.

The reaction process and our basic empirical equation

The time—e.m.f. response of the LaF_3 electrodes was investigated over the time range 0.5 to $> 10^4$ min and fluoride concentrations from about 0.7 ng g^{-1} to 15 μg g^{-1}. Typical time—e.m.f. curves for increasing concentrations of fluoride (Fig. 2) confirm that the time to equilibrium increases with decrease in concentration and that times of the order of hours or even tens of hours may be required to reach equilibrium at the lower concentrations. Plots of $\exp(-FE_t/RT)$ vs. $1/t$ [32] gave good straight-line relationships only when t exceeded some value t_l. The value of t_l increased with decreasing concentration to such an extent that this procedure for determining the equilibrium e.m.f. proved impractical. Investigation of the deviation from this linear relationship for a wide range of time and concentration changes resulted in the adoption of the empirical equation

$$e_t = e_\infty + (e_i - e_\infty)\,(1 - e^{-\lambda t})/\lambda t \qquad (6)$$

to describe the time dependence of the approach to equilibrium, e_t being $\exp(-FE_t/RT)$ as defined above. The time constant, λ, has a complex relationship to the concentration change seen by the electrode and is best determined for each sample.

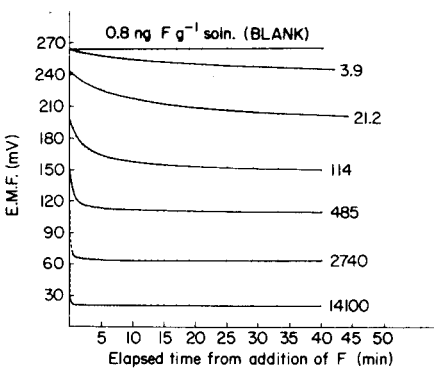

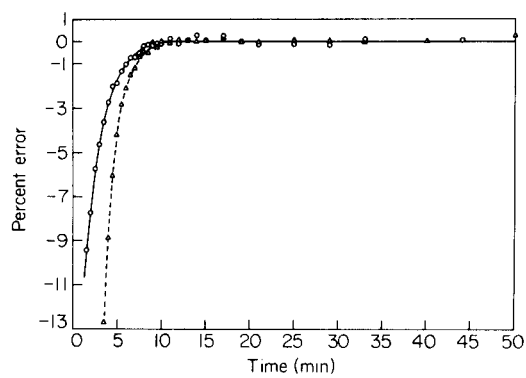

Fig. 2. Time—e.m.f. response curves for increasing fluoride concentrations.

Fig. 3. Typical per cent error in the fit of responses calculated from eqn. (6). Four data points were used to evaluate the parameters of the equation. (Δ) Electrode pre-equilibrated in blank solution (1 ng F^-g^{-1}) and then transferred to a solution containing 1.71 μg F^-g^{-1}. (○) In-situ addition of 17.5 μg F^-g^{-1} to a solution containing 4.9 ng F^-g^{-1}. Electrode not at equilibrium.

Empirical eqn. (6) has been applied successfully to hundreds of determinations of fluoride concentration and has proved valuable in the identification of other factors which affect the electrode response. Typical fits of the empirical eqn. (6) to experimental data are shown in Fig. 3. Four data points selected in the time range 10—50 min were used to derive the parameters e_i, e_∞ and λ in the equation. A good fit is not usually obtained until approximately 10 min after a concentration change has been made. The discrepancy, at early times, between the experimentally observed response and the response predicted by eqn. (6) is attributed to a diffusion mechanism, as concluded also by others [22—24] who used the equation of Müller [31]. The actual time required for attainment of diffusion equilibrium depends on the magnitude of the concentration change.

Essentially identical results are obtained with the Müller relationship (eqn. 5) when a reasonably fresh electrode is used. If the electrode has been aged in TISAB, the equilibrium values predicted by eqns. (5) and (6) show differences. Equation (5) predicts lower equilibrium values than eqn. (6) when the fluoride concentration in the solution is decreased. The converse applies when the fluoride concentration is increased.

It is of interest to note that the term $(1 - e^{-\lambda t})/\lambda t$ appearing in eqn. (6) is identical to the expression that relates the mean rate of change of a reactant, in a first-order reaction, to its instantaneous initial rate of change [35]. In terms of the model for the LaF_3 electrode depicted in Fig. 1, it is postulated that eqn. (6) relates the time—e.m.f. response to a reaction process controlled by the concentration change between the solution and the LaF_3—La complex interface. The reaction process is probably complicated and its specific details are not known. The mathematical model proposed by Buffle and Parthasarathy [23] appears to be a plausible description of this process.

The diffusion component, and its relation to reaction components in the electrode response

The discrepancy, at the earlier times, between the experimentally observed response and the response predicted by eqn. (5) or (6) can be attributed to a diffusion mechanism. In the Appendix, various elementary models of the electrode response, incorporating both reaction and diffusion processes, are examined. "Reaction" terms that were similar in form to those given by the empirical eqn. (6), or eqn. (5), were not obtained. However, the examination suggests that if "diffusion"-like components are to be included in the analysis of data, along with "reaction" terms of the type described by eqn. (6) or (5), it is plausible to assume equations of the form

$$e_t = e_\infty + P\frac{1 - e^{-\lambda t}}{\lambda t} + Qf(D/l^2, t); \quad e_i = e_\infty + P + Q, \tag{7}$$

for the empirical eqn. (6) plus diffusion analysis, and correspondingly

$$e_t = e_\infty \exp\left(\frac{\eta}{1 + Kt}\right) + Qf(D/l^2, t); \quad e_i = e_\infty \exp(\eta) + Q, \tag{8}$$

$$\equiv e_\infty + P(e^{\frac{\eta}{1 + Kt}} - 1)/(e^\eta - 1) + Qf(D/l^2, t); \quad P = e_\infty(e^\eta - 1), \tag{8'}$$

for the combined Müller and diffusion analysis. In these equations, $f(D/l^2, t)$ is the diffusion term defined in eqn. (A2), P and Q are constants that measure the relative importance of the reaction and diffusion components of the response. Equation (8') simply expresses eqn. (8) in a form analogous to eqn. (7).

Equations (7) and (8) were fitted to some of the experimental data by means of least-squares techniques on a CYBER 175/CDC 6600 computer system, without restraint on the parameters e_∞, P, λ, Q, D/l^2 for eqn. (7), or e_∞, η, K, Q, D/l^2 for eqn. (8). Usually very good fits were obtained (except perhaps for times $\leqslant 1$ min), indicating the presence of a diffusion-like process in the electrode response. Typical results of the fits, in the 1—50 min time range, are summarized in Table 1 for one set of data used in Fig. 3. The differences in the equilibrium concentration values, e_∞, calculated from two basic equations are typical of results of fits to data from an electrode aged in TISAB, and are attributed to a calibration drift process. This behaviour is discussed in detail later.

Dissolution component

If the electrode is run to equilibrium in a solution having a very low concentration of fluoride (< 1 ng g^{-1}), the apparent fluoride concentration will then increase at a rate which is proportional to time over many thousands of minutes (Fig. 4). This increase in concentration with time results from a number of factors, one of which is the rate at which the LaF_3 crystal dissolves. Others are the influx of fluoride with the saturated KCl from the salt bridge to the reference electrode, release of fluoride from the polypropylene stirrer through desorption and abrasion, adsorption to or desorption from the vessel used, diffusion of atmospheric HF through the polyethylene cover, and evaporation of the cell solution. The rate of increase for a fully aged LaF_3 electrode and polypropylene stirrer is about 4 pg F^- min^{-1}.

For measurements on very low level solutions (< 1 ng F^-g^{-1}), this source of contamination must be taken into account in the kinetic equation. Equations (7) and (8) should therefore be modified to the forms

$$e_t = e_\infty + P\frac{1 - e^{-\lambda t}}{\lambda t} + Qf(D/l^2, t) + kt \tag{9}$$

and

$$e_t = e_\infty \exp\left(\frac{\eta}{1 + Kt}\right) + Qf(D/l^2, t) + kt \tag{10}$$

with the initial values e_i as defined in eqns. (7) and (8).

TABLE 1

Least-squares fit of eqns. (7) and (8) to a typical small increase in fluoride concentration by in-situ addition of fluoride (The aged electrode was initially in 4.9 ng $F^- g^{-1}$ and not at equilibrium. Fluoride added = 17.5 ng $F^- g^{-1}$.)

Time (min)	e_t found (× 10^4)	Equation (7)		Equation (8)	
		e_t calc. (× 10^4)	Error (%)	e_t calc. (× 10^4)	Error (%)
(0.5)	0.8436	(0.8760)	(−3.85)	(0.8754)	(−3.77)
1.0	0.9555	0.9633	−0.82	0.9626	−0.74
1.5	1.0614	1.0523	0.85	1.0522	0.86
2.0	1.1384	1.1374	0.09	1.1378	0.06
2.5	1.2210	1.2181	0.24	1.2186	0.20
3.0	1.2944	1.2948	−0.03	1.2953	−0.07
3.5	1.3668	1.3680	−0.08	1.3684	−0.11
4.0	1.4379	1.4382	−0.02	1.4384	−0.04
4.5	1.5066	1.5056	0.06	1.5057	0.06
5.0	1.5664	1.5707	−0.28	1.5706	−0.27
5.5	1.6317	1.6337	−0.12	1.6334	−0.10
6.0	1.6932	1.6947	−0.09	1.6944	−0.06
6.5	1.7536	1.7540	−0.03	1.7536	−0.00
7.0	1.8090	1.8118	−0.15	1.8113	−0.12
7.5	1.8663	1.8680	−0.10	1.8676	−0.07
8.0	1.9253	1.9230	0.12	1.9225	0.14
8.5	1.9785	1.9767	0.09	1.9763	0.11
9.0	2.0292	2.0292	0.00	2.0289	0.01
9.5	2.0811	2.0806	0.02	2.0804	0.04
10.0	2.1303	2.1310	−0.03	2.1309	−0.03
11.0	2.2322	2.2289	0.15	2.2290	0.14
12.0	2.3208	2.3231	−0.10	2.3234	−0.11
13.0	2.4129	2.4140	−0.05	2.4145	−0.06
14.0	2.5087	2.5017	0.28	2.5025	0.25
15.0	2.5880	2.5865	0.06	2.5874	0.02
17.0	2.7543	2.7478	0.24	2.7487	0.20
19.0	2.8973	2.8988	−0.05	2.8996	−0.08
21.0	3.0358	3.0403	−0.15	3.0408	−0.17
25.0	3.2943	3.2980	−0.11	3.2975	−0.10
29.0	3.5197	3.5257	−0.17	3.5242	−0.13
33.0	3.7313	3.7275	0.10	3.7256	0.15
44.0	4.1772	4.1753	0.05	4.1769	0.01

Calculated parameters and statistics of fit

e_i	0.8040 × 10^{-4}	0.8068 × 10^{-4}
e_∞	6.2242 × 10^{-4}	6.9231 × 10^{-4}
A^a	0.9696	0.9678
λ	0.0525 min^{-1}	—
D/l^2	0.1542 min^{-1}	0.1594 min^{-1}
η	—	−1.929
K	—	0.06404 min^{-1}
Time span of fitted data	1—44 min	1—44 min

TABLE 1 (Continued)

	Equation (7)	Equation (8)
No. of points fitted	31	31
Mean % error	—0.0009	—0.0011
S.d. (%)	0.250	0.240
Error range (%)	1.67	1.60

[a] A is a measure of the relative importance of the reaction component in the response, i.e. $A = P/(P + Q)$. (See eqns. 7 and 8'.)

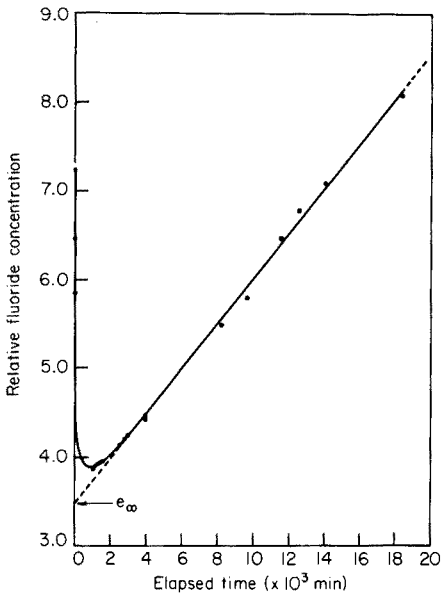

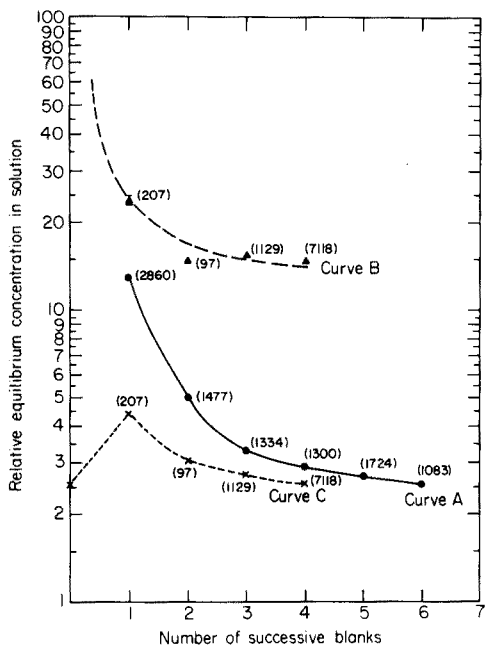

Fig. 4. Apparent dissolution rate for Orion Model 96-09 (Serial No. FS1) after a 126-h immersion in TISAB (= 4.35 pg F^-min^{-1}). The intercept of the extrapolated straight-line portion of the curve on the ordinate is the true equilibrium concentration value. Saturated KCl flow rate 3.00 mg h^{-1}. Solution in cell, 61.3 g. Initial [F^-] of solution 0.97 ng g^{-1}.

Fig. 5. Relative fluoride content of successive blank solutions as indicated by Orion Model 96-09 electrodes returning to equilibrium in a solution of lower fluoride content. Electrodes were not normalized. The numbers in parentheses beside each symbol give the exposure time, in minutes, in each fresh blank solution. (Curve A) Electrode Ser. No. FT-1 after exposure to fluoride concentrations to 14.58 $\mu g\ F^- g^{-1}$. (Curve B) Electrode Ser. No. EZ-1, immersed along with electrode Ser. No. FT-1 as a dual system, after equilibration of electrode Ser. No. EZ-1 in a blank spiked with 13.1 $\mu g\ F^- g^{-1}$. (Curve C) Electrode Ser. No. FT-1, immersed along with electrode Ser. No. EZ-1 as a dual system, after equilibration of electrode Ser. No. FT-1 in standard blanks.

Calibration drift process

Experimental data were obtained which either could not be fitted to the time—e.m.f. eqns. (9) and (10) over the full time range of the data, or when fitted showed a persistent drift in the calculated value for the equilibrium concentration term, e_∞, as the time range of the fitted data was varied. The effect is one of apparent drift in the value of E^0 in the Nernst equation. These perturbations all fit a consistent pattern which is the same for both eqns. (9) and (10). In view of the overall success of these equations, it was concluded that, more generally, additional terms are required to describe the complete kinetics of the electrode.

The drift process was found to be present at all stages in the life of LaF_3 electrodes in both TISAB-based and 0.1 M KNO_3 solutions [36]. In the case of electrodes in TISAB-based solutions, the effect becomes more prominent with increase in the accumulated time in solution. In general, the direction of drift is as follows. If a LaF_3 electrode, fully equilibrated at some fixed fluoride- or hydroxyl-ion concentration, is immersed in a solution of significantly lower fluoride-, or higher hydroxyl-ion concentration, the cell e.m.f. will drift slowly to higher values of E_t, and hence lower values of $\exp(-FE_t/RT)$, than predicted by fitting eqns. (9) or (10) to the data. The result is that the predicted value for the equilibrium concentration term, e_∞, will be higher than the value actually observed at equilibrium. The reverse effect is observed when the fully equilibrated electrode is exposed to a solution of higher fluoride-ion or lower hydroxyl-ion concentration. In this case a slow, but relatively much more rapid, drift of the cell e.m.f. is observed to a lower value of E_t, and hence a higher value of $\exp(-FE_t/RT)$, than predicted. The drift of an unequilibrated electrode, in response to concentration changes, was found to lie between the limits established for the transition between equilibrium states. A practical consequence of this drift process is that conventional calibration curves, prepared from measurements over a wide range of known fluoride concentrations, are variable and can lead to substantial errors.

The effect of drift on the response of an aged electrode to an increase in the fluoride concentration of the solution is shown in Table 2. As the time span of the data fitted to eqn. (9) is decreased, the value of the derived equilibrium concentration term, e_∞ (column 5), decreases significantly. Similar results are obtained with eqn. (10).

Drift in response to cyclic changes in concentration, typical of normal working conditions, is shown in Table 3 for a range of concentration changes. These data were taken with an Orion combination LaF_3 electrode, Model 96-09, with an accumulated exposure time of thirteen months in TISAB solutions with DCTA at low fluoride concentrations. Batches of blank solution, containing 0.688 ng $F^- g^{-1}$, were adjusted with standard fluoride solution to give solutions of 7.07, 68.9 and 679 ng $F^- g^{-1}$, respectively. A fresh aliquot was used for each run of ca. 40 minutes. The effect of drift, as indicated by the calculated values of e_∞, is seen to diminish as the fluoride

TABLE 2

Least-squares fit of eqn. (7) to different time spans of the data given in Table 1

Time span (min)	Derived values for constants					Statistics of fit		
	λ (min^{-1})	D/l^2 (min^{-1})	A[a]	e_∞ ($\times 10^4$)	e_i ($\times 10^5$)	Mean error (%)	S.d. (%)	Error range (%)
1.0—44	0.0525	0.154	0.970	6.224	8.040	—0.00087	0.250	1.671
1.0—29	0.0566	0.192	0.973	6.015	7.901	—0.00078	0.221	1.423
1.0—19	0.0608	0.241	0.975	5.808	7.759	—0.00053	0.209	1.216
1.0—14	0.0649	0.282	0.976	5.605	7.659	—0.00054	0.209	1.104
1.0—11	0.0789	0.536	0.970	5.031	7.096	—0.00041	0.175	0.868
1.0—44[b]	0.0488	0.151	0.961	6.353	8.129	—0.329	0.685	2.266

[a]See footnote, Table 1. [b]Fit from 8 points uniformly spaced in terms of successive response terms, e_{tn} and e_{tn+1}. An iterative procedure was used to solve for constants on a Hewlett-Packard 9830A with 4K memory.

TABLE 3

Best estimate of apparent equilibrium from kinetic data to 40 min for cyclic changes in fluoride ion concentration (e_∞ calculated from eqn. 6). The sequence of the changes made is shown in parentheses after each value of e_∞.

Electrode status at start of cycle	e_∞ (0.688 ng F^-g^{-1})	e_∞ (7.07 ng F^-g^{-1})	e_∞ (68.9 ng F^-g^{-1})	e_∞ (679 ng F^-g^{-1})
(1) Fully equilibrated in 0.688 ng F^-g^{-1}. Cycled between 0.688 ng F^-g^{-1} and 68.9 ng F^-g^{-1}.	1.62 E-5 (1)		1.77 E-3 (2)	
	2.40 E-5 (3)		1.72 E-3 (4)	
	3.04 E-5 (5)		1.82 E-3 (6)	
	3.50 E-5 (7)			
(2) Partially equilibrated in 0.688 ng F^-g^{-1}. Cycled between 0.688 ng F^-g^{-1} and 7.07 ng F^-g^{-1}.	1.95 E-5 (1)	1.62 E-4 (2)		
	2.47 E-5 (3)	1.57 E-4 (4)		
	2.86 E-5 (5)	1.54 E-4 (6)		
	3.12 E-5 (7)			
(3) Partially equilibrated in 0.688 ng F^-g^{-1}. Cycled between 7.07 ng F^-g^{-1} and 68.9 ng F^-g^{-1}.		1.62 E-4 (1)	1.82 E-3 (2)	
		1.64 E-4 (3)	1.82 E-3 (4)	
		1.76 E-4 (5)	1.82 E-3 (6)	
		1.91 E-4 (7)		
(4) Partially equilibrated in 7.07 ng F^-g^{-1}. Cycled between 68.9 ng F^-g^{-1} and 679 ng F^-g^{-1}.			1.91 E-3 (1)	2.03 E-2 (2)
			1.94 E-3 (3)	2.02 E-2 (4)
			2.00 E-3 (5)	2.05 E-2 (6)
			2.04 E-3 (7)	

concentration is increased. Since the rate of approach to equilibrium is faster at high fluoride concentrations than at low concentrations, the overall drift of the electrode, within the cycling time ranges used in the experiment, is towards the high concentration equilibrium.

In terms of the schematic representation shown in Fig. 1, it is postulated that the mechanism for drift in the cell e.m.f. is a variation in the thickness and the fluoride content of a dense La-complex layer on the surface of the LaF_3. With continued exposure to TISAB solutions of low fluoride content, the dissolution of LaF_3 results in an increasing thickness of this La-complex layer. Any change in the fluoride content of the solution relative to that of the complexing anions in the solution is presumed to induce a reversible change in the composition of this layer. This reaction may be represented by

$$La(X_a, F_{3-a}) + yF^- \underset{k_2}{\overset{k_1}{\rightleftharpoons}} La(X_{a-y}, F_{(3-a+y)}) + yX^- \qquad (11)$$

where X may be chloride, acetate, hydroxyl or DCTA anions, and the values for the rate constants, k_1 and k_2, are determined by the anion mixture.

The foregoing hypothesis is supported by the work of Anfält and Jagner [6] who showed that, in precipitation titrations of fluoride with lanthanum nitrate, acetate ions enter the solid phase, forming precipitates with the formula $LaF_{3-x}Ac_x$ $(0 < x < 1)$. They also noted that the presence of acetate causes the electrode to work sluggishly and to deviate from the Nernst law. Other carboxylic acids were shown [7] to behave in a similar manner. Janes and Margerum [37] observed that coordinated anions had a marked effect on the rate of dissociation of 1,2-diaminocyclohexanetetra-acetatomercurate(II). Balcombe and Wiseall [38] observed that acetate ions influence the rate of exchange of Ce(III)—polyaminocarboxylic acid chelates. In addition, the nature of the anion of the supporting electrolyte has a pronounced influence on the rate of exchange, with increases in the order $ClO_4^- < NO_3^- < Cl^-$. They assumed that mixed chelates of the type $CeLC^{2-}$ are formed and that these are more labile than the normal chelates.

The proposed drift mechanism predicts that an aged electrode equilibrated at a high fluoride content should release fluoride to the solution when returning to equilibrium in a solution of lower fluoride content. Such a release could be observed with the aid of a second LaF_3 electrode. Curve A in Fig. 5 shows the change in the calculated equilibrium concentration term, $\exp(-FE_\infty/RT)$, in the equilibration of electrode Ser. No. FT-1 by exposure to successive fresh aliquots of normal ($\approx$ 1 ng $F^- g^{-1}$) blank solutions. A second Orion Model 96-09 Electrode (Ser. No. EZ-1) was equilibrated at 13.1 μg $F^- g^{-1}$ of solution. Both electrodes were then transferred simultaneously, without rinsing, to the same fresh aliquot of normal blank solution. The change in the calculated equilibrium concentration term for the electrode returning to equilibrium (Ser. No. EZ-1) is shown as Curve B and the comparable response of the previously equilibrated electrode (Ser. No. FT-1)

as Curve C. Curve C clearly indicates a release of fluoride from the exposed electrode (Ser. EZ-1). Electrical interaction between electrodes was found, in a separate experiment, to result in an immediate and constant shift in potential of 0.5 mV for each electrode, one positive and the other negative, on immersion in the same solution. The high concentration of fluoride seen in the first blank of Curves B and C may be partially attributed to carry-over of adsorbed fluoride and droplets of solution with the unrinsed electrode (Ser. No. EZ-1). Drift effects in the unexposed electrode (Ser. No. FT-1) should be negligible with such a small change in fluoride concentration [28].

To obtain kinetic data for analytical study of the drift terms, a series of measurements was made with a well aged Orion Model 96-09 electrode. For each data set in this series, the electrode was first fully equilibrated in standard blank solution, transferred to a solution of higher fluoride concentration and then to two successive fresh blank solutions. The change in e.m.f. with time was followed until the electrode was deemed to be very close to equilibrium or until the response term, $e_t = \exp(-FE_t/RT)$, showed a linear increase with time.

In all, twelve experimental runs were made, the average duration of which was about 3.5 days, although one run required almost twelve days to complete. Three of the twelve runs were not amenable to data analysis because of experimental difficulties.

Analysis of data on the electrode response for an electrode returning to equilibrium in a blank solution ($\sim$ 1 ng $F^- g^{-1}$), after equilibration in solutions of much higher fluoride content indicated that a satisfactory resolution of the kinetic data is obtained with the addition of two terms of the exponential type, $A_1 \exp(-\alpha_1 t) + A_2 \exp(-\alpha_2 t)$, to eqns. (9) and (10). The complete kinetic equations for the response were therefore taken to be of the form

$$e_t = e_\infty + P\frac{1 - e^{-\lambda t}}{\lambda t} + Qf(D/l^2, t) + A_1 e^{-\alpha_1 t} + A_2 e^{-\alpha_2 t} + kt; \qquad (12)$$

$$e_i = e_\infty + P + Q + A_1 + A_2,$$

and

$$e_t = e_\infty \exp\left(\frac{\eta}{1 + Kt}\right) + Qf(D/l^2, t) + A_1 e^{-\alpha_1 t} + A_2 e^{-\alpha_2 t} + kt; \qquad (13)$$

$$e_i = e_\infty \exp(\eta) + Q + A_1 + A_2.$$

Note that, by analogy with eqns. (8) and (8′), eqn. (13) can be rewritten to correspond more exactly with the form of eqn. (12); $f(D/l^2, t)$ is defined in eqn. (A2).

Least-squares fits were then performed on the data with the dissolution component, kt, subtracted. The object was to determine the extent to which the introduction of the drift terms improved the fit, and, if possible, to

establish which of the two types of empirical equations best described the time—e.m.f. response over the time range $1-10^4$ minutes. Not all of the eqns. (5), (6), (7), (8), etc. were fitted for all runs. The choice of weights to be associated with the experimental points was an important consideration in the fitting. In the analysis it was assumed that the errors were proportional to the values of $e(t_i)$ at time t_i [39] so that the weights used were in effect proportional to $1/e^2(t_i)$. The weights $1/e^2(t_i)$ imply that the relative errors of each datum point are identical, which is close to the actual case for electrode response readings.

The results of the fits are summarized in Tables 4—6 for three of the runs. Table 4 gives the results for the condition involving the transfer of the electrode from a solution with a high fluoride concentration to the first blank solution. Table 5 gives the results of transfer of the electrode to a second fresh blank after exposure to equilibrium in a previous blank solution. Table 6 represents results obtained in response to transfer of an electrode, equilibrated in a blank solution, to a solution with high fluoride concentration.

The results presented in Tables 4—6 are typical of the results obtained from other runs. They confirm earlier observations that empirical eqns. (5) or (6) are equally effective in describing the basic electrode response, other perturbing factors being taken into account. They also indicate that the introduction of the exponential terms, as in eqns. (12) and (13), does not always result in improvements to the fit. This is consistent with the present hypothesis for the mechanism of the drift process. When the electrode is transferred from a solution with high fluoride concentration to one with a very low concentration of fluoride, the drift terms are expected to be highly significant. This is reflected in a very much better fit when the drift terms are introduced as shown in Table 4. When transferred to a second blank, following exposure to equilibrium in a previous blank, the electrode is expected to show a minor drift, and this is reflected in the results given in Table 5. When the electrode is transferred from a blank solution to one with a much higher fluoride concentration, the concentration of fluoride in the complex layer is expected to rise very rapidly by a reverse reaction. In this case the effect of drift is of short duration and may be masked by diffusion. Consequently, as illustrated in Table 6, the data are well fitted without the drift terms. In fact, in certain cases of this type, no least-squares fit seemed possible when the exponential terms were included.

The nature of the response of the LaF_3 electrode to hydroxyl has not yet been satisfactorily explained [33], although a significant contribution was made by the work of Cammann and Rechnitz [18]. The present drift hypothesis may be expected to apply to the time—e.m.f. response of a LaF_3 electrode to change in hydroxyl ion concentration, in an otherwise non-complexing medium such as 0.1 M KNO_3. This hypothesis predicts that, if a LaF_3 electrode is subjected to an increase in the pH of a solution in which it is immersed, with no change in fluoride ion concentration or ionic strength, a slow drift to higher e.m.f. values will be observed as the relative fluoride

TABLE 4

Least-squares fit to kinetic data, with the dissolution component subtracted, for electrode transferred to the first blank solution after immersion in a 0.016 $\mu g\ F^- g^{-1}$ spiked solution
(Time span of data, 1—4610 min. No. of data points used, 73. $k = 4.68 \times 10^{-10}\ min^{-1}$.)

Eqn. fitted (No.)	e_∞ ($\times 10^5$)	e_i ($\times 10^4$)	A[b]	Q ($\times 10^4$)	D/l^2 (min^{-1})	$\frac{\eta, \kappa}{\lambda}$	A_1 ($\times 10^5$)	α_1 ($min^{-1} \times 10^2$)	A_2 ($\times 10^5$)	α_2 ($min^{-1} \times 10^3$)	Mean error (%)	S.d. (%)	Error range (%)
5	3.132	2.735	1.000	—	—	2.167, 0.0203	—	—	—	—	0.391	6.29	28.21
7	3.051	3.075	0.463	1.487	0.0684	0.0296	—	—	—	—	0.0560	2.383	12.72
8	3.030	3.184	0.539	1.327	0.0827	1.813, 0.0113	—	—	—	—	0.0301	1.747	9.38
12[a]	3.130	3.628	0.560	0.8987	0.197	0.1518	3.593	1.232	2.006	1.977	0.0008	0.291	1.23
13[a]	3.121	3.721	0.652	0.7194	0.238	2.095, 0.0426	2.789	1.175	1.868	2.017	0.0007	0.266	1.23

[a] Less the dissolution term, kt. [b] A is a measure of the relative importance of the reaction component of the response. For eqns. (5) and (6), $A = 1$; for eqns. (7) and (8), $A = 1 - Q/(e_i - e_\infty)$; for eqns. (12) and (13), $A = 1 - (Q + A_1 + A_2)/(e_i - e_\infty)$.

TABLE 5

Least-squares fit to kinetic data, with dissolution component subtracted, for electrode transferred to the second blank solution after a 0.016 $\mu g\ F^- g^{-1}$ spike. Prior to transfer, the electrode was allowed to reach equilibrium in the first blank solution
(Time span of data, 1—2743 min. No. of data points used, 70. $k = 4.29 \times 10^{-10}\ min^{-1}$.)

Eqn. fitted (No.)	e_∞ ($\times 10^5$)	e_i ($\times 10^5$)	A[c]	Q ($\times 10^6$)	D/l^2 (min^{-1})	$\frac{\eta, \kappa}{\lambda}$	A_1 ($\times 10^6$)	α_1 ($min^{-1} \times 10^2$)	A_2 ($\times 10^6$)	α_2 ($min^{-1} \times 10^3$)	Mean error (%)	S.d. (%)	Error range (%)
7	2.629	3.288	0.759	1.588	0.0297	0.0112	—	—	—	—	0.0015	0.385	1.83
12[a]	2.641[b]	3.319	0.413	0.5336	0.1042	0.0301	1.384	2.528	2.056	2.136	0.0044	0.255	1.37
13[a]	2.636[b]	3.309	0.572	0.3940	0.0682	0.1362, 0.01910	0.8890	1.64	1.60	2.038	0.0371	0.273	1.43

[a] Less the dissolution term, kt. [b] A fully converged output not obtained. [c] See footnote, Table 4.

TABLE 6

Least-squares fit to kinetic data, with dissolution component subtracted, for electrode when a 1.149 $\mu g\ F^{-} g^{-1}$ spike is added to a standard blank solution
(Time span of data, 1—1717 min. No. of data points used = 62. $k = 3.0 \times 10^{-10}\ min^{-1}$.)

Eqn. fitted (No.)	e_∞ ($\times 10^2$)	e_i ($\times 10^4$)	A[c]	Q ($\times 10^2$)	D/l^2 (min^{-1})	$\frac{\eta, \kappa}{\lambda}$	A_1 ($\times 10^2$)	α_1 ($min^{-1} \times 10^2$)	A_2 ($\times 10^3$)	α_2 ($min^{-1} \times 10^3$)	Mean error (%)	S.d. (%)	Error range (%)
6	3.485	—39.59	1.000	—	—	0.5385	—	—	—	—	0.0247	1.584	5.26
5	3.514	0.0870	1.000	—	—	—8.304, 3.160	—	—	—	—	0.0074	0.869	4.03
7	3.530	7.962	0.378	—2.146	0.158	0.1215	—	—	—	—	0.0039	0.628	2.98
8	3.540[b]	0.1587	0.486	—1.820	0.164	—0.6645, 0.1687	—	—	—	—	—0.0032	0.567	3.39
12[a]	3.541[b]	6.864	0.007	—2.123	0.160	0.5352	—1.06	7.255	—2.661	5.18	0.0165	0.429	3.04
13[a]	3.555[b]	—26.51	0.641	—1.074	0.146	—1.1677, 0.5852	—0.1755	4.230	—1.215	2.876	0.0011	0.549	4.46

[a] Less the dissolution term, kt. [b] A fully converged output was not obtained. [c] See footnote, Table 4.

content of the surface layer of $La(OH_a^-, F_{3-a}^-)$ is reduced. By analogy with the behaviour of the LaF_3 electrode to change in the fluoride content of TISAB-based solutions, the drift effect should be most pronounced at low fluoride concentrations. Bock and Strecker [5] subjected a LaF_3 electrode to stepwise increases in solution pH at a number of different fluoride concentrations. Their results on a 10^{-5} M NaF solution show the predicted increase in cell e.m.f. (cf. Fig. 3 [5]). Again Veselý and Stulik [12] observed a hysteresis in the cell e.m.f. as the pH of the cell solution was cycled up and down. The drift hypothesis predicts that, with successive rapid increase in pH, the slow drift response will result in e.m.f. values below those corresponding to the equilibrium values. Conversely, with successive rapid decreases in pH, the slow drift response will introduce a lag such that the e.m.f. values observed will be higher than those corresponding to the equilibrium values. Such effects should become more pronounced as the fluoride content of the solution is reduced. The data shown by Veselý and Stulik (Fig. 1 [12]) are in accord with these predictions. Finally, it has been observed [36] that the response of the LaF_3 electrode to change in the pH of 0.1 M KNO_3 at constant low fluoride concentrations consists of two components. The first, a very fast response, is presumed to be a direct response to OH^-, analogous to that for fluoride ion. The second component is a rather slow response which cannot be fitted by the present empirical equations but which has many features in common with the drift response to change in fluoride concentration in TISAB solutions. This failure of the empirical equations to fit the data is attributed to the experimental difficulty in maintaining precise control of the pH over the time span of the measurements (1 day), compounded by the slow response of glass electrodes used to measure the pH.

CONCLUSIONS

The proposed empirical relationship between the diffusion, reaction, drift and combined dissolution—contamination processes appears to describe the response characteristic of LaF_3 electrodes. Other investigations have confirmed the presence of distinct diffusion [16, 22—25] and reaction [21—23, 31] processes. The exact nature of the reaction process has not yet been clearly defined, although Buffle and Parthasarathy [23] have formulated a plausible model based on second-order reaction kinetics.

The complete kinetic description of LaF_3 electrode response is very complex. Much of this complexity appears to arise from one aspect of the overall time-response relationship, here called the calibration drift process. The present investigations have shown that this process can be the controlling factor in the response under certain conditions of direction and magnitude of the concentration change. True equilibrium is a condition for Nernstian response [19]. The rate of approach to equilibrium increases with increase in, and absolute value of, fluoride concentration. The rate decreases with concentration decrease and becomes extremely slow at very low fluoride

concentrations. The lower limit for measurement of fluoride ion activity is determined only indirectly by dissolution of the LaF_3 membrane. In this respect, the LaF_3 electrode may indeed be an anionic analogue of the glass electrode as pointed out by Veselý [15].

The complexity of the LaF_3 electrode response imposes practical restrictions on its application to the measurement of low concentrations of fluoride. Failure to observe these restrictions can lead to very significant errors in the determination of fluoride. Although the time—e.m.f. response can be very well fitted overall by the proposed kinetic equations, in practice, on the basis of present knowledge, the equilibrium potential cannot always be calculated solely from measurements made during the first hour. This is particularly true when the electrode is exposed to a large decrease or a very low fluoride concentration. Until such time as the rate constants for the forward and reverse reactions involved in the drift process are more clearly defined, such a large extrapolation in fluoride concentration does not appear feasible. Nevertheless, with the aid of the equations for the diffusion and reaction processes — or even the reaction process alone when limited to an appropriate time interval — the electrode can be used successfully to determine low fluoride concentrations if the conditions are controlled to minimize the departure from drift equilibrium at the level of interest. This involves limiting the concentration of samples to be measured to a range close to the concentration of which the electrode has been equilibrated. This practical working range becomes narrower as the equilibrium concentration is reduced.

The authors gratefully acknowledge the assistance of many individuals for their co-operation in various phases of this investigation. We are particularly indebted to W. J. Edwards for many helpful discussions.

APPENDIX: A SUMMARY OF SOME ELEMENTARY MODELS FOR ELECTRODE RESPONSE

To provide some basis for incorporating diffusion-like or other components into the analysis of the kinetic data, the form of exact mathematical solutions to a few elementary models of electrode response involving material transfer and other processes was studied.

Diffusion models of electrode response have been discussed [17, 19, 21]. In the idealized one-dimensional situation depicted in Fig. 6(A), when the electrode in solution is considered as a semi-infinite crystal separated by a barrier of thickness l from the solution, the response is taken to be proportional to the concentration of ions at the crystal surface, $C(t)$, at time t. This concentration is known to be [40].

$$C(t) = C_\infty + (C_i - C_\infty) f(D/l^2, t) \tag{A1}$$

in which

$$f(D/l^2, t) = \frac{4}{\pi} \sum_{m=0}^{\infty} \frac{(-1)^m}{(2m+1)} \exp(-\pi^2 (2m+1)^2 Dt/4l^2) \tag{A2}$$

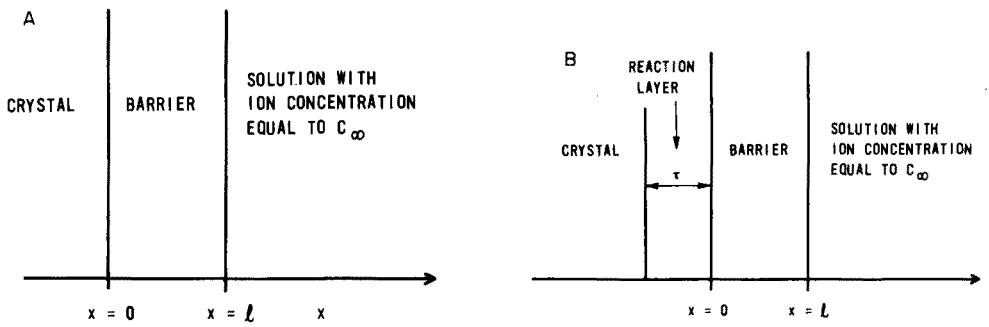

Fig. 6. (A) The electrode, with a single barrier, in idealized one-dimensional geometry. (B) The electrode with two barriers in idealized one-dimensional geometry.

where D is the ion diffusion coefficient in the barrier medium, C_i is the initial concentration of ions in the barrier at time $t = 0$, and C_∞ is the concentration of ions maintained in the solution.

A process analogous to diffusion is ion deposition-release. Consider again the one-dimensional situation depicted in Fig. 6A. If it is assumed that the concentration of ions in the barrier (of thickness τ) is at all times uniformly distributed, and if it is postulated that the release rate of the ions from the barrier to the solution is "r" and the flow of ions from the solution into the barrier, per unit surface area of barrier, is at a rate "uC_∞", then the concentration of ions in the barrier, $F(t)$, is described by

$$dF(t)/dt = -rF(t) + uC_\infty/\tau \qquad \text{(A3)}$$

If the electrode response e_t is proportional to $F(t)$, the response function is seen to be

$$e_t = e_\infty + (e_i - e_\infty)\, e^{-rt} \qquad \text{(A4)}$$

Such a model has been discussed by Lindner et al. [20].

If another fluoride concentration loss term is added to the right-hand side of eqn. (A3), i.e., a term of the type $-k_1F(t)$ representing losses of ions by a first-order reaction in the barrier medium, the form of the response function becomes identical with that of eqn. (A4). The only difference is that the time constant r is replaced by $r + k_1$. A more general case arises if, in addition to the term $-k_1F(t)$, it is assumed that reactions in the barrier lead also to the production of fluoride, the production rate being k_2X in which the generation of X is given by $k_1F(t)$. The equations are

$$dF(t)/dt = -F - k_1F + k_2X + uC_\infty/\tau \text{ and } dX(t)/dt = -k_2X + k_1F \qquad \text{(A5)}$$

It is readily established that the response function e_t, which is proportional to $F(t)$, in the above case is of the form

$$e_t = e_\infty + (e_i - e_\infty)\,[Ae^{-\mu_1 t} + (1 - A)e^{-\mu_2 t}] \qquad \text{(A6)}$$

in which μ_1 and μ_2 are time constants related to r, k_1, and k_2, and A is a constant related to the initial and final concentrations and the μ values. If $r \gg k_1 + k_2$, then $\mu_1 \approx k_2$, $\mu_2 \approx r$ so that the individual terms in eqn. (A6) describe the effects of the "reaction" and "diffusion" processes separately, A being a measure of the "fraction" of the response attributed to the reaction process. In general the constants μ_1 and μ_2 will be mixtures of diffusion and reaction rate constants, though one may correspond mainly to diffusion and the other to the reaction component.

Equations (A5) can be generalized by adding more species leading to more source and sink terms. Provided that the additional components are of a linear type, the mathematical solution of the generalized equations will be of the type given by eqn. (A6), but with more exponential type terms added. If non-linear reaction processes are included, the solutions become more complicated. As an example, consider a simple generalization of eqn. (A3), namely,

$$dF(t)/dt = -(r + k_1)F(t) - wF^2(t) + uC_\infty/\tau. \qquad (A7)$$

This is a Ricatti type equation [41] whose solution is of the form $F(t) = F_\infty + (F_i - F_\infty)\, e^{-\gamma t}/[1 + q(1 - e^{-\gamma t})]$, in which γ and q are constants related to r, k_1, etc.

The above examples of mathematical solutions pertain to processes taking place in a single layer bounding the electrode crystal. An alternative electrode structure has two layers bounding the crystal: a layer of thickness τ in which the ion concentration is assumed to be always uniformly distributed and in which reaction processes take place, and a layer of thickness l in which deposition—release, or diffusion processes take place (Fig. 6B).

For the case of simple deposition—release in the "diffusion" layer and a single reaction process in the "reaction" layer: if $G(t)$ and $F(t)$ represent the average ion concentrations in the respective regions, then in the "diffusion" layer, $dG(t)/dt = -rG + uC_\infty/l$, and in the "reaction" layer, $dF(t)/dt = -k_1F + f\,rG(t)l/\tau$, where f is the fraction of ions released from the diffusion layer that enter the reaction layer. The solution of these equations, written in terms of the response function e_t (e_t is proportional to $F(t)$), is

$$e_t = e_\infty + (e_i - e_\infty)[Ae^{-k_1 t} + (1 - A)e^{-rt}] \qquad (A8)$$

For this simplest two-region case, e_t contains two distinct components connected with "reaction" and "diffusion" processes, respectively.

Solutions for more complex models in this two-barrier case have been derived; e.g., models in which the concentration of ions as a function of position in the diffusion layer, $C(x, t)$, is governed by the diffusion equation $\partial C(x, t)/\partial t = D\,\partial^2 C(x, t)/\partial x^2$, while the concentration of the fluoride in the "reaction" layer is governed by $dF(t)/dt = -J(t)/\tau$ + other terms, in which the other terms are $-k_1F$ or $-k_1F + k_2X$ with the second part of eqn. (A5) defining X. Here the current, $J(t) = -D(\partial C(x, t)/\partial x)\big|_{x=0}$, provides the

coupling between the diffusion and reaction layers. A variety of initial and interface conditions were adopted.

These solutions are not presented in detail, but it can be indicated that the electrode response in these models can be formally expressed as

$$e_t = e_\infty + f_1(k, t) + f_2(D, t)$$

in which $f_2(D, t)$ is dominantly a "diffusion"-like solution while $f_1(k, t)$ contains whatever effects the reactions have on the response; the terms themselves are exponential in type. The solutions were obtained by a procedur similar to that described by Barrer [40], by ultimately expanding $J(t)$ in a series of the type

$$J(t) = \sum_{j=0}^{\infty} \theta_j \, e^{-\xi_j t}$$

in which θ_j and ξ_j are initially unknown parameters.

REFERENCES

1 M. S. Frant and J. W. Ross, Jr., Science, 154 (1966) 1533.
2 J. J. Lingane, Anal. Chem., 40 (1968) 935.
3 B. A. Raby and W. E. Sunderland, Anal. Chem., 39 (1967) 1304; 40 (1968) 439.
4 J. J. Lingane, Anal. Chem., 39 (1967) 981.
5 R. Bock and S. Strecker, Fresenius Z. Anal. Chem., 235 (1968) 322.
6 T. Anfält and D. Jagner, Anal. Chim. Acta, 47 (1969) 483.
7 T. Anfält and D. Jagner, Anal. Chim. Acta, 50 (1970) 23.
8 T. Ericksson and G. Johansson, Anal. Chim. Acta, 52 (1970) 465.
9 E. W. Baumann, Anal. Chim. Acta, 54 (1971) 189.
10 M. A. Peters and D. M. Ladd, Talanta, 18 (1971) 655.
11 I. Sekerka and J. F. Lechner, Talanta, 20 (1973) 1167.
12 J. Veselý and K. Stulik, Anal. Chim. Acta, 73 (1974) 157.
13 N. Parthasarathy, J. Buffle and D. Monnier, Anal. Chim. Acta, 68 (1974) 185.
14 J. Buffle, N. Parthasarathy and W. Haerdi, Anal. Chim. Acta, 68 (1974) 253.
15 J. Veselý, J. Electroanal. Chem., 41 (1973) 134.
16 R. Rangarajan and G. A. Rechnitz, Anal. Chem., 47 (1975) 324.
17 P. L. Markovic and J. O. Osburn, AIChE J., 19 (1973) 504.
18 K. Cammann and G. A. Rechnitz, Anal. Chem., 48 (1976) 856.
19 W. E. Morf, E. Lindner and W. Simon, Anal. Chem., 47 (1975) 1596.
20 E. Lindner, K. Tóth and E. Pungor, Anal. Chem., 48 (1976) 1071.
21 A. Shatkay, Anal. Chem., 48 (1976) 1039.
22 J. Mertens, P. Van den Winkel and D. L. Massart, Anal. Chem., 48 (1976) 272.
23 J. Buffle and N. Parthasarathy, Anal. Chim. Acta, 93 (1977) 111.
24 N. Parthasarathy, J. Buffle and W. Haerdi, Anal. Chim. Acta, 93 (1977) 121.
25 K. Tóth and E. Pungor, Anal. Chim. Acta, 64 (1973) 417.
26 J. S. Merritt and J. G. V. Taylor, Atomic Energy of Canada Limited Report No. AECL-2679 (1967), Chalk River Nuclear Laboratories, Chalk River, Ontario, Canada KOJ 1JO.
27 L. E. Negus and T. S. Light, Instrum. Technol., 19 (1972) 23.
28 R. C. Hawkings, L. P. V. Corriveau and D. M. Tennant, to be published.
29 G. A. Rechnitz and H. F. Hameka, Fresenius Z. Anal. Chem., 214 (1965) 252.

30 K. Tóth, I. Gavaller and E. Pungor, Anal. Chim. Acta, 57 (1971) 131.
31 R. H. Müller, Anal. Chem., 41 (1969) 113A.
32 Instruction Manual, Fluoride Electrodes, Model 94-09, Model 96-09, Orion Research, Cambridge, MA, Form IM96, 94-09/4721, 1974.
33 J. Koryta, Ion Selective Electrodes, Cambridge University Press, Cambridge, 1975.
34 M. J. D. Brand and G. A. Rechnitz, Anal. Chem., 42 (1970) 478.
35 R. C. Hawkings, W. J. Edwards and W. J. Olmstead, Can. J. Phys., 49 (1971) 785.
36 R. C. Hawkings and L. P. V. Corriveau, Unpublished data.
37 D. J. Janes and D. W. Margerum, Inorg. Chem., 7 (1966) 1135.
38 C. I. Balcombe and B. Wiseall, J. Inorg. Nucl. Chem., 36 (1974) 881.
39 J. R. Wolberg, Prediction Analysis, D. Van Nostrand, Princeton, N. J., 1967, p. 62.
40 R. M. Barrer in E. K. Rideal (Ed.), Diffusion In and Through Solids, The Cambridge Series on Physical Chemistry, Cambridge University Press, 1951.
41 E. L. Ince, Ordinary Differential Equations, Dover Publications, New York, 1944.

Analytica Chimica Acta, 102 (1978) 85—90

EFFECT OF pH ON THE RESPONSE OF A CYANIDE ION-SELECTIVE ELECTRODE

M. GRATZL, F. RAKIÁS, G. HORVAI, K. TÓTH and E. PUNGOR*

Institute for General and Analytical Chemistry, Technical University Budapest (Hungary)

(Received 11th May 1978)

SUMMARY

The influence of pH on the cyanide response of a silver iodide membrane electrode has been found to depend on the buffer system employed. A theoretical explanation of the results is attempted by assuming a pH-gradient in the vicinity of the electrode surface.

Ion-selective electrodes based on AgI or a mixture of AgI and Ag_2S have been widely used for the measurement of cyanide concentration [1, 2]. The operational model of this electrode has been discussed in a number of articles [3—12], and may be summarized as follows. In alkaline cyanide solutions, AgI is gradually dissolved from the membrane. Although there is a true thermodynamic equilibrium on the surface of the electrode, the dissolution process proceeds at finite rate because there is a diffusion barrier consisting of the Nernst layer, and in the case of mixed or heterogeneous membranes, of the porous matrix from which the AgI has been leached. The potential of the electrode is determined by the activity of iodide ions at the surface.

The same model was found earlier to be valid for Ag/AgI electrodes of the second kind by Jaenicke [13, 14]. The model was validated by dissolution measurements on Ag/AgI electrode [13] and by the good agreement between calculated and measured $K^{\mathrm{Pot}}_{\mathrm{CN},\mathrm{I}}$ values [9].

The behaviour of the cyanide electrode at pH values lower than 11 has also been discussed [5, 7, 8, 10], and an equation describing its potential response has been derived [5]. This equation was verified experimentally [7, 8], although it was in disagreement with previous experimental results [15]. This discrepancy motivated a re-examination of the relevant measurements described earlier [8, 15]. Since all these measurements could be reproduced, the investigation was extended to a number of different buffer systems, for the only significant difference between the contradictory experiments was the use of a phosphate buffer medium in one set of measurements [8], while no additional buffer (besides cyanide) was used in the other set [15].

EXPERIMENTAL

Apparatus and chemicals

A Radiometer Automatic Titrator TTT1c, SBR2c, ABU1b and a Radelkis Precision pH-meter OP-205 were used. The Radelkis OP-CN-7111 cyanide electrode, which incorporates a pressed AgI membrane, was connected to the titrator, while pH was measured by a Radelkis combined glass electrode (OP-9073). A Radiometer double-junction saturated calomel electrode (K 701) was used in combination with the cyanide electrode.

All reagents were of analytical grade.

Procedure

The buffered or unbuffered cyanide solution (10 ml) was made strongly alkaline by dissolution of a prewashed pellet of sodium hydroxide. The electrodes were placed into the solution, and the titration with hydrochloric acid was started. The potential of the cyanide electrode was recorded by the titrator, while pH was read on the pH-meter and marked on the titration graph.

RESULTS

The e.m.f. response of the electrode was plotted as a function of the measured pH for various buffers, and the concentrations of cyanide and buffer were varied. The results are shown in Figs. 1—6. Figure 1 confirms the results presented by Toth and Pungor [15], while Fig. 2 confirms those presented by Mascini [8]. Figures 3 and 4(a) show results obtained in other pH buffers.

All the curves obtained for buffered solutions show a break in the approximate range of maximum buffer capacity. In the case of Fig. 1, an additional pH buffer was not used and, in this case, the curves would be expected to

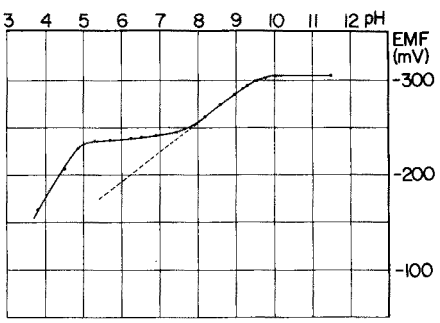

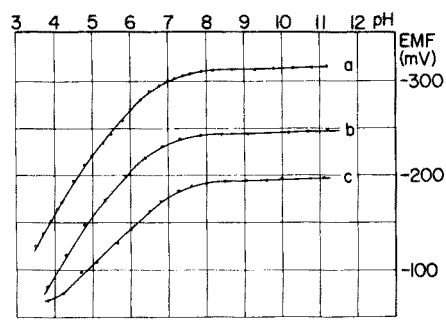

Fig. 1. E.m.f. as a function of pH when no additional buffer besides cyanide is used. (•) Experimental curve; total cyanide concentration, 10^{-2} M. (---) Expected curve (see text).

Fig. 2. E.m.f. as a function of pH when a 10^{-1} M phosphate buffer is used. (a) Total cyanide concentration, 10^{-2} M; (b) total cyanide concentration, 10^{-3} M; (c) total cyanide concentration, 10^{-4} M.

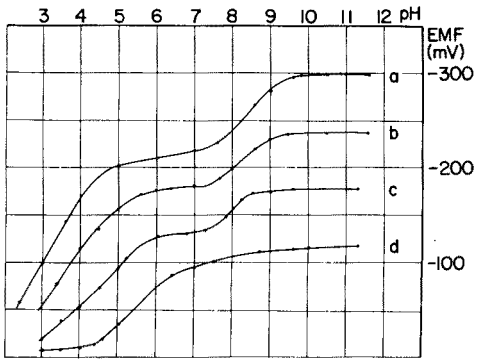

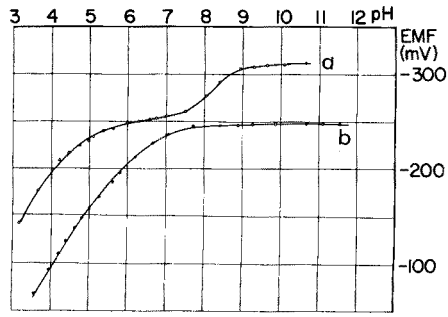

Fig. 3. E.m.f. as a function of pH when a 10^{-3} M acetate buffer is used. (a) Total cyanide concentration, 10^{-2} M; (b) total cyanide concentration, 10^{-3} M; (c) total cyanide concentration, 10^{-4} M; (d) total cyanide concentration, 10^{-5} M.

Fig. 4. (a) E.m.f. as a function of pH when a 10^{-1} M carbonate buffer is used. Total cyanide concentration, 10^{-2} M; (b) e.m.f. as a function of pH when a 2×10^{-2} M Britton—Robinson buffer is used. Total cyanide concentration, 10^{-3} M.

follow the dashed line (see below); the difference is attributed to the buffering action of the small carbonate content of the solution.

DISCUSSION

The most elaborate derivation of the expression describing the dependence of the potential of the cyanide electrode on the pH and total (analytical) cyanide concentration has been given by Koryta [5]. His derivation is based on the model given for alkaline solutions and outlined above. Equations between the diffusional mass fluxes in the boundary layer are set up on the basis of material and charge balances; and the heterogeneous equilibrium

$$AgI_{solid} + 2\ CN^- = Ag(CN)_2^- + I^-$$

is considered. The mass fluxes are expressed with the help of transport constants κ, and the concentration differences existing between the electrode surface and the bulk of the solution. This model is then modified for pH < 11 by introducing the equilibrium $HCN = H^+ + CN^-$, and by substituting the sum of CN^- and HCN concentrations in the flux equations. The equations thus obtained are used to express the iodide ion concentration at the surface of the electrode, for this governs the electrode response, i.e. the e.m.f. of the cell. Rearrangement of eqn. (122) in reference [5] yields for the iodide concentration at the surface of the electrode:

$$C_I(0) = C_Y \left(\frac{\kappa_{Ag(CN)_2}}{\kappa_I}\right)^{\frac{1}{2}} \frac{K^{\frac{1}{2}} K_{HCN}}{2(\kappa_I \kappa_{Ag(CN)_2}/\kappa_Y)^{1/2} K^{\frac{1}{2}} K_{HCN} + K_{HCN} + [H]} \qquad (1)$$

where the κ's are the transport constants of the indexed species, C is concentration, Y denotes the sum of CN^- and HCN, $K = C_{Ag(CN)_2}(0) \cdot C_I(0)/C^2_{CN}(0)$, and $K_{HCN} = [H]\,[CN]/[HCN]$; (0) denotes the concentration at zero distance from the electrode surface. The ionic charges have been omitted in the formulae.

Introducing eqn. (1) into the Nernst equation gives the potential of the electrode as a function of pH and total cyanide concentration. The graphical representation of this theoretical function is practically identical with that experimentally obtained in relatively concentrated Britton—Robinson buffer or phosphate buffer (Figs. 4(b) and 2). The experimental results shown in Figs. 1, 3 and 4(a), are inconsistent with the theoretical result.

It must be pointed out, however, that in the derivation of eqn. (1) the constancy of the pH across the diffusion barrier has been tacitly assumed. This assumption seems to be, in general, not justified. Rather, it should be assumed that hydrogen ion concentration changes with the distance measured from the surface, because at lower pH hydrogen ions are generated at the electrode surface in the dissolution reaction

$$AgI_{solid} + 2\,HCN = Ag(CN)_2^- + I^- + 2\,H^+ \qquad (2)$$

With this in mind, the derivation of eqn. (1) remains correct if [H](0) is inserted for [H].

The assumption of constant pH throughout the diffusion layer is, however, correct if the cyanide solution is effectively buffered in the pH range studied, for the buffering substance then levels out the differences in pH. Thus, if the sample is effectively buffered in the range between pH 11 and about pH 4, eqn. (1) is correct. This is shown by Fig. 4(b).

It is useful to consider, at least qualitatively, the general case when the sample is not buffered at all or is buffered only in a narrow pH range. In unbuffered pH regions below pH 11, reaction (2) must also be considered; hydrogen ions are generated at the surface, and consequently it can be assumed that the pH near the surface is lower than in the bulk solution. Accordingly, it is not unreasonable to expect that when pH in the bulk solution is, e.g., 9, the surface pH value will be about 7; thus the break in the e.m.f. vs. pH curve expected at about pH(0) 7 on the basis of eqn. (1) will occur at pH(bulk) 9 rather than 7. Such an effect can be seen in Figs. 1, 3 and 4(a). If the pH range of say 4—7 is buffered, then the difference between pH(0) and pH(bulk) observed near pH(bulk) 9, must gradually disappear by decreasing the pH(bulk), so that the e.m.f. vs. pH(bulk) curve changes from the type shown by the dashed line in Fig. 1 to the type shown in Fig. 4(b). This effect is demonstrated by Figs. 3 and 4. Below pH(bulk) 4, the evolution of HCN gas and the reversed direction of reaction (2) make the treatment difficult. It is evident from what has been said that a strong phosphate buffer has practically the same effect as the Britton—Robinson buffer (cf. Figs. 2 and 4(b)). This is also true for the results presented earlier [7, 8].

Figures 2, 3, 5 and 6 show the dependence of the e.m.f. vs. pH(bulk) curves on the concentration ratio of buffering substance and cyanide. Increasing the

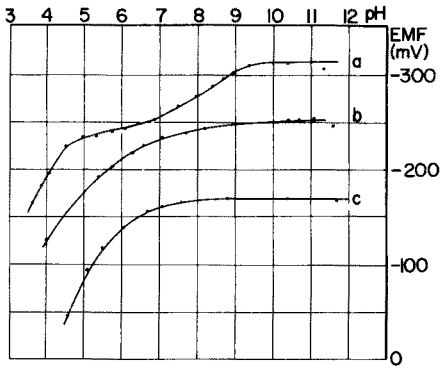

Fig. 5. E.m.f. as a function of pH when a 10^{-3} M phosphate buffer is used. (a) Total cyanide concentration, 10^{-2} M; (b) total cyanide concentration, 10^{-3} M; (c) total cyanide concentration, 10^{-4} M.

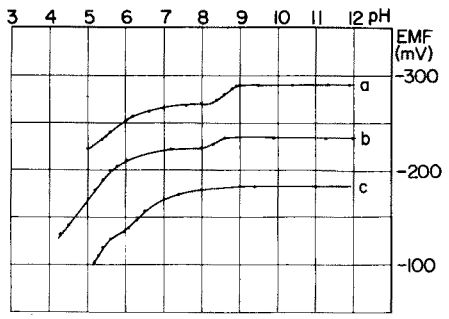

Fig. 6. E.m.f. as a function of pH when a 10^{-1} M acetate buffer is used. (a) Total cyanide concentration, 10^{-2} M; (b) total cyanide concentration, 10^{-3} M; (c) total cyanide concentration, 10^{-4} M.

concentration of a buffer substance broadens the range of effective buffering. Thus, an increase in the relative concentration of acetate to cyanide effectively buffers a broader pH(bulk) range so that the e.m.f. vs. pH(bulk) curve approaches the curve expected on the basis of eqn. (1) (Figs. 3 and 6). Conversely, decreasing the buffer concentration narrows the range of effective buffering, so that, e.g., in dilute phosphate buffer the e.m.f. vs. pH(bulk) curve (Fig. 5) approaches that obtained in unbuffered solution (Fig. 1). On extrapolating the results for phosphate and acetate buffers to the carbonate buffer, it becomes reasonable to assume that the difference between the dashed and solid curves in Fig. 1 is caused by the residual carbonate content of the solutions used.

It may be noted that the difference between the pH at the surface of the dropping mercury electrode and the pH in the bulk solution in poorly buffered systems has also been recognised in polarographic studies of substances participating in acid—base equilibria (see, e.g. [16]).

REFERENCES

1 E. Pungor and K. Tóth, Analyst, 95 (1970) 1132.
2 P. L. Bailey, Analysis with Ion-Selective Electrodes, Heyden, London, 1976.
3 J. W. Ross, in Proceedings on Ion-Selective Electrodes, Nat. Bur. Stand. (U.S.) Spec. Publ. 314, Washington, 1969, p. 84.
4 B. Fleet and H. von Storp, Anal. Chem., 43 (1971) 1575.
5 J. Koryta, Anal. Chim. Acta, 61 (1972) 329.
6 D. H. Evans, Anal. Chem., 44 (1972) 875.
7 G. A. Rechnitz and R. Llenado, Anal. Chem., 44 (1972) 468.
8 M. Mascini, Anal. Chem., 45 (1973) 615.
9 G. P. Bound, B. Fleet, H. von Storp and D. H. Evans, Anal. Chem., 45 (1973) 788.

10 M. Mascini and A. Napoli, Anal. Chem., 46 (1974) 447.
11 W. E. Morf, G. Kahr and W. Simon, Anal. Chem., 46 (1974) 1538.
12 A. Hulanicki and A. Lewenstam, Talanta, 24 (1977) 171.
13 W. Jaenicke, Z. Elektrochem., 55 (1951) 648.
14 W. Jaenicke and M. Haase, Z. Electrochem., 63 (1959) 521.
15 K. Tóth and E. Pungor, Anal. Chim. Acta, 51 (1970) 221.
16 I. M. Kolthoff and E. F. Orlemann, J. Am. Chem. Soc., 63 (1941) 664.

Analytica Chimica Acta, 102 (1978) 91—97

ANODIC STRIPPING VOLTAMMETRY AND CHRONOPOTENTIOMETRY OF COPPER AT A ROTATING CARBOSITAL DISK ELECTRODE

O. L. KABANOVA,* YU. A. GONCHAROV** and A. N. DORONIN

V. I. Vernadsky Institute of Geochemistry and Analytical Chemistry, U.S.S.R. Academy of Sciences, Vorobyevskoe shosse 47a, Moscow (U.S.S.R.)

(Received 29th March 1977)

SUMMARY

The use of a new carbon material — carbosital — for electrodes is reviewed. The behaviour of copper deposited on the carbosital electrode surface in anodic stripping voltammetry and chronopotentiometry is discussed. In anodic stripping voltammetry with a rotating carbosital disk electrode, the peak current and the number of coulombs involved in stripping copper are directly proportional to the square root of the electrode rotation rate during preelectrolysis; the peak current is directly proportional to the potential scan rate during stripping. For anodic stripping voltammetry and anodic stripping chronopotentiometry, linear calibration graphs are obtained in the range $1 \times 10^{-8} - 1 \times 10^{-6}$ M copper(II). The method is applicable to analysis of high-purity cadmium for copper.

Solid electrodes have become widely used in analyses for trace concentrations by anodic stripping methods. This paper reports the use of a rotating carbosital disk electrode for the determination of copper.

Carbosital was first synthesized in 1965 [1]. It has a low specific resistance ($12—18 \times 10^{-6}$ ohm m^{-1}), is almost impermeable to gases, and is resistant to atmospheric oxidation. It often contains ca. 4—5 wt.% boron, which is uniformly distributed throughout the bulk material, and considerably decreases (6—8 times) the chemical activity of graphite without addition of any other elements. Carbosital is isotropic [1, 2] and has been suggested for analytical use in electrodes [3]. In aqueous 0.1 M $NaClO_4$ solution at pH 2, the background currents observed with a rotating carbosital disk electrode in the range from 0.0 to —0.7 V (vs. s.c.e.) are of the same order as those observed with a glassy carbon electrode and decrease with decreasing potential scan rates [4]. In this supporting electrolyte, the voltammograms of scans towards positive potentials and back show hysteresis, because of the irreversibility of the adsorption processes on the electrode.

Well-defined reduction waves are obtained for lead(II) and the anodic stripping voltammograms for lead previously electrodeposited on the electrode show a peak current at —0.51 V (vs. s.c.e.). The amount of electricity required

**Present address: Tadjic State University, Dushanbe, U.S.S.R.

for stripping and the anodic peak current are directly proportional to the concentration of lead(II) ions down to 1×10^{-8} M [4, 5]. When lead is stripped the peak current and the number of coulombs expended in the process are directly proportional to the square root of the electrode rotation rate if the electrode rotates at the same rate during preelectrolysis and during stripping, and do not depend on the electrode rotation rate during stripping. The peak current increases in direct proportion to the potential scan rate, when other conditions are kept constant. The peak current is directly proportional to the number of coulombs used in stripping (in the range 13—1600 $\mu C\ cm^{-2}$), which is ca. 70% of that expended in the initial deposition of the lead [5]. Variations in the peak potential under different conditions have been described [6].

The use of a carbosital electrode (carbosital sealed into molybdenum glass) for the determination of cerium(III) by cathodic stripping voltammetry in the range 0.7—1.0 V (vs. s.c.e.) has been reported [7]. This method is also applicable for the determination of thallium in copper alloys [8]; $Tl(OH)_3$ is preconcentrated at + 1.1 V (vs. s.c.e.), and then Tl(III) is reduced. Studies on the anodic stripping chronopotentiometry of lead with the use of a rotating carbosital disk electrode have been described [9, 10]; the stripping time for lead with a constant direct current increases in direct proportion to the pre-electrolysis time and to the square root of the electrode rotation rate during pre-electrolysis. A change in the electrode rotation rate during stripping does not affect the stripping time, which is directly proportional to the lead(II) concentration in the range 1×10^{-9}—1×10^{-6} M. When a lead deposit is dissolved without current in a solution saturated with atmospheric oxygen, i.e. an oxygen concentration of 2.5×10^{-4} M, and the electrode rotation rate is decreased during dissolution, the stripping time increases quantitatively with the decrease in the amount of oxygen supplied to the electrode surface. The sensitivity of this method of determining lead in solution is 1×10^{-9} M, which is an order of magnitude better than can be achieved with anodic stripping voltammetry.

The use of a carbosital electrode for anodic stripping voltammetry of silver(I) has been described [11]. With the carbosital electrode in 0.1 M $HClO_4$ at a current density of 10^{-3} A cm^{-2} (calculated on the basis of the exposed electrode surface), the hydrogen overvoltage is 0.64—0.65 V, i.e. about 0.2 V higher than at a glassy carbon electrode [12]. The carbosital electrode can be used as the indicator electrode in the amperometric titration of rhenium(VII) [13], thallium [14], lead(IV) [15], iron(III), vanadium(IV) [16], silver [17], mercury and silver [18]. Some electrochemical characteristics of the ferrocene—ferricene couple at the carbosital electrode have been discussed [19].

The anodic stripping voltammetry and chronopotentiometry of copper are discussed in the present paper.

EXPERIMENTAL

Apparatus and reagents

The working electrode was a cylindrical carbosital rod pressed into a Teflon tube which had been expanded by heating. Carbosital is less brittle than glassy carbon and yields easily to mechanical treatment. The electrode surface was polished with a moist powder of carefully washed alumina on a filter paper, washed with water, immersed for 2—3 min in hot (ca. 60°C) concentrated sulphuric acid, and finally washed with water. After this treatment the electrode surface became shiny. During all these operations the electrode was rotated.

The exposed area of the electrode was 0.158 cm^2. The auxiliary electrode was a platinum wire spiral and the reference electrode was a Ag/AgCl (saturated KCl) electrode. All potentials mentioned below are relative to this electrode. All measurements were carried out in a thermostated hermetic three-electrode Pyrex cell at 25 ± 0.1°C. The anodic and cathodic chambers of the cell were separated by a stopcock. When not in use, the electrodes were stored dry.

The potential was kept constant by means of a potentiostat, which was also used in potential scanning. In chronopotentiometry, the potential was recorded on an a.c. oscillograph.

Sodium perchlorate was thrice recrystallized from water. After purification with ion-exchange resins, the water was distilled twice (first from alkaline or acidic $KMnO_4$ solution). Oxygen was removed from solutions by bubbling for 1.5—2 h with nitrogen or argon purified from traces of oxygen by means of a chromonickel catalyst. High-purity $CuSO_4$ was used in preparing the solutions. The working solutions were purified by electrolysis at a Specpure carbon cathode at −1.2 V for 6—8 h.

RESULTS AND DISCUSSION

Anodic stripping voltammetry

Figure 1 shows the voltammograms measured for an aqueous 0.1 M $NaClO_4$ solution at pH 2, with scanning from +0.4 V to −0.8 V (curve 1′) and back (curve 1). As in the case of more negative potentials [4], there was hysteresis, which indicates irreversible processes at the carbosital electrode. The background current was of the order of 10—15 $\mu A\ cm^{-2}$. When copper was stripped by scanning from −0.3 V to +0.6 V, the voltammogram (Fig. 1, curve 2) showed a sharp peak at −0.02 to +0.04 V. On some voltammograms obtained for 1×10^{-8} M copper(II) or less, the anodic current peak was slightly split. The peak current, i_p, was measured as indicated in Fig. 1; the amount of electricity involved, Q_a, was estimated from the hatched area.

Figure 2 shows that the peak current and the number of coulombs expended in stripping do not depend on the deposition potential for values below −0.3 V. At a deposition potential of −0.15 V, i_p and Q_a were zero. For the further experiments, a deposition potential of −0.4 V was selected.

The values of Q_a and i_p found experimentally vary in direct proportion with

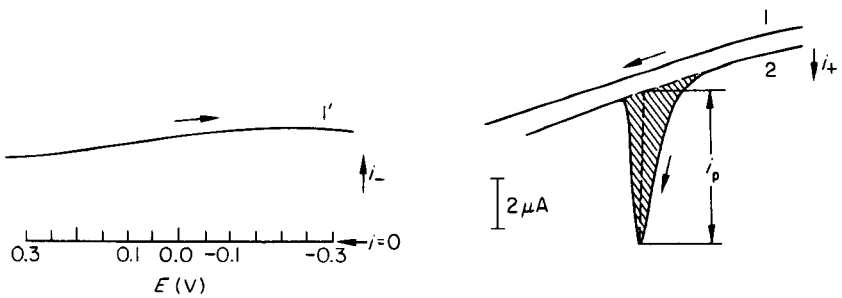

Fig. 1. Anodic stripping voltammograms for blank solutions and 10^{-7} M copper(II) solution at the carbosital electrode. Electrode rotation speed, 75 rev/s; scan rate, 0.020 V s^{-1}; pre-electrolysis time, 600 s.

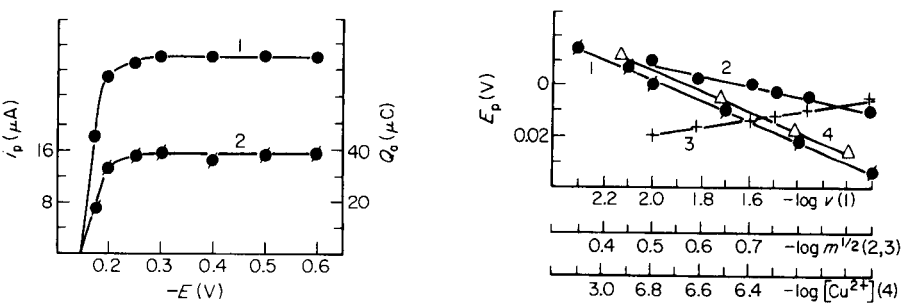

Fig. 2. Dependence of Q_a (curve 1) and i_p (curve 2) on the deposition potential for a 5×10^{-7} M copper(II) solution. Electrode rotation speed, 75 rev/s; pre-electrolysis time, 600 s; scan rate 0.010 V s^{-1}.

Fig. 3. Dependence of peak potential on log v (1), log $m^{\frac{1}{2}}$ (2), log $m_a^{\frac{1}{2}}$ (3) and log [Cu(II)] (4). Copper(II) concentration, 1×10^{-7} M for curves 1—3; t_e, 600 s; for curves 1—4, electrode rotation speed was 75 rev/s; for curves 2—4, the scan rate was 0.020 V s^{-1}; for curve 3, m_e = 75 rev/s.

the square root of the electrode rotation speed if the speeds during deposition (m_e) and stripping (m_a) are the same. For different m_a rates, with constant m_e rates, the values of Q_a and i_p remain constant. These results agree with those of Kopanika and Vydra [20] for a glassy carbon electrode. As with the glassy carbon electrode [20], i_p increases in direct proportion with the potential scan rate v, whereas Q_a remains unchanged.

The relationship of Q_a or i_p to the copper(II) concentration is directly proportional over the range 1×10^{-8}—1×10^{-6} M. With further decrease of the copper(II) concentration the current peak does not disappear, but the values

of Q_a and i_p no longer fall on the straight line obtained. The reproducibility of the measurements is characterized by the standard deviation 4×10^{-9} M for a copper(II) concentration of 6×10^{-8} M. The correlation coefficient for the dependence of Q_a/t_e and i_p/t_e (t_e is the preelectrolysis time) on copper(II) concentration is 0.97. With a rotating glassy carbon disk electrode, the sensitivity is about the same [20].

The peak current is directly proportional to the number of coulombs used in stripping the copper deposited. Table 1 lists the data for $\delta i_p/\delta Q_a v$; the mean value is 21.7 V^{-1} (σ = 0.3). Table 2 lists the data for $\delta i_p/\delta Q_a v$ obtained for different Cu(II) concentrations in solution; the mean value is 23 V^{-1} (σ = 2).

The experimental values of Q_a (4—90 μC) for copper are ca. 80% of the calculated values, assuming that copper electrodeposition occurs at the limiting diffusion current and $D_{Cu(II)} = 6.6 \times 10^{-6}$ $cm^2 s^{-1}$ [21]. These low values can be explained by inaccuracies in the estimation of Q_a caused by distortions of the stripping voltammograms by foreign processes, and by the fact that the number of electrons involved in the process is not two.

Figure 3 shows the experimental dependences of the peak potential on the logarithm of the potential scan rate (curve 1), the square root of the

TABLE 1

Values of $\delta i_p/\delta Q_a v$ at various v values for 1×10^{-7} M copper(II) (t_e = 600 s; m = 75 rev/s)

v ($V\ s^{-1}$)	0.005	0.008	0.010	0.020	0.040	0.080
$\delta I_{max}/\delta Q_a$ (s^{-1})	0.11	0.18	0.22	0.43	0.86	1.70
$\delta I_{max}/\delta Q_a v$ (V^{-1})	22.0	22.5	22.0	21.5	21.5	21.0

TABLE 2

Values of $\delta i_p/\delta Q_a v$ at various concentrations of copper(II) (m_e = 75 rev/s; v = 0.020 V s^{-1})

Cu(II) ($\times 10^{-8}$ M)	100	60	30	12.5	10	6	3	2
$\delta Q_a/\delta t_e$ ($\times 10^{-2}$ C s^{-1})	25.0	14.4	6.8	3.0	2.5	1.4	0.8	0.6
$\delta i_p/\delta t_e$ ($\times 10^{-2}$ A s^{-1})	12.2	7.2	3.2	1.5	1.0	0.6	0.32	0.25
$\delta i_p/\delta Q_a v$ (V^{-1})	22.4	25.0	23.5	25.0	20.0	21.4	20.0	20.5

electrode rotation rate for $m_e = m_a$ (curve 2), the square root of the electrode rotation rate during stripping for constant m_e (curve 3), and on the copper(II) concentration (curve 4); the slopes are 40, 38, 38, —2, and 40 mV, respectively. The dependence of the peak potential on the electrode rotation rate during stripping indicates a diffusion-controlled step [6]. The slope of the concentration plot differs from that for a reversible 2e process, which indicates that the stripping process for copper is limited not only by diffusion but also by kinetics.

Anodic stripping chronopotentiometry

A 0.1 M $NaClO_4$ solution at pH 2 was used as the supporting electrolyte. The copper deposited by electrolysis during 1200 s was stripped at 100 μA; the electrode rotation rate was 75 rev/s. A typical anodic stripping chronopotentiogram (E—t curve) for copper is given in Fig. 4 (curve 1). Stripping was observed at ca. 0.05 V (at Q_k ca. 30 μC). The stripping time τ is directly proportional to the copper(II) concentration (Fig. 4, curve 2) over the range 1×10^{-8}—1×10^{-6} M, with a correlation coefficient of 0.97. The reproducibility is indicated by the standard deviation 8×10^{-10} M for a copper concentration of 5×10^{-8} M.

The experimental Q_a values were virtually the same as the calculated values in the range 4—90 μC. Thus the stripping of a copper deposit is a quantitative process involving two electrons without any complicating phenomena such as copper adsorption.

Analytical uses

The anodic stripping voltammetric method was used to determine the copper content in analytically pure cadmium. A 0.01 M $Cd(NO_3)_2$ solution was prepared by dissolving metallic cadmium in several drops of nitric acid (1 + 1). The solution was diluted with water, enough $NaClO_4$ was added to give 0.1 M, and then the solution was acidified with perchloric acid to ca. pH 2. After oxygen had been removed, and after preelectrolysis at —0.2 V (m = 75 rev/s, t_e = 900 s), the anodic stripping voltammogram for copper

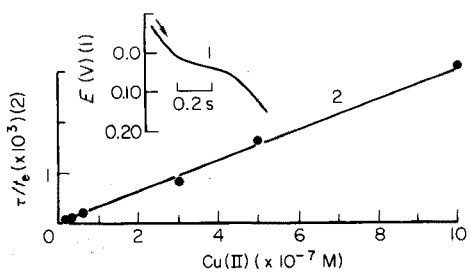

Fig. 4. The potential—time relationship for copper stripping (curve 1) and the dependence of τ/t_e on the copper(II) concentration. i = 100 μA; m = 75 rev/s.

was recorded at a scan rate of 0.02 V s^{-1} from −0.2 to 0.4 V. In this case the preelectrolysis potential was −0.2 V instead of −0.4 V, to prevent interference from lead which was present in the sample in amounts comparable with those of copper. The concentration of copper(II) in solution was determined from i_p measurements by the method of standard additions. The pure cadmium was found to contain 7.0×10^{-3}% copper, with a relative standard deviation of 7%. The results of this analysis agreed with the data obtained by activation analysis [22].

REFERENCES

1 G. M. Volkov, V. I. Kalugin and K. I. Syskov, Dokl. Akad. Nauk S.S.S.R., 183 (1965) 396.
2 G. M. Volkov, Ya. A. Leontyev, Yu. S. Lopatto, D. K. Khakimova and L. G. Khromenkov, Izv. Akad. Nauk S.S.S.R., Ser. Neorgan. Mater., 9 (1973) 140.
3 O. L. Kabanova and S. M. Beniaminova, Zh. Anal. Khim., 26 (1971) 111.
4 O. L. Kabanova and Yu. A. Goncharov, Zh. Anal. Khim., 28 (1973) 1665.
5 O. L. Kabanova and Yu. A. Goncharov, Zh. Anal. Khim., 31 (1976) 902.
6 O. L. Kabanova, Yu. A. Goncharov and S. M. Beniaminova, Elektrokhimia, 13 (1977) 1448.
7 B. A. Anokhin and V. I. Ignatov, Zh. Anal. Khim., 29 (1974) 1221.
8 E. Ya. Neiman and V. I. Ignatov, Zavod. Lab., 41 (1975) 937.
9 A. N. Doronin and Yu. A. Goncharov, Zh. Anal. Khim., 31 (1976) 309.
10 Yu. A. Goncharov and A. N. Doronin, Zh. Anal. Khim., 31 (1976) 897.
11 S. M. Beniaminova and O. L. Kabanova, II Vses. Sov. Po Analysu Prirodn. Stochn. Vod, Moskwa, Nauka, 1977, p. 73. S. M. Beniaminova and O. L. Kabanova, Proc. Anal. Div. Chem. Soc., 15 (1978) 180.
12 O. L. Kabanova, Yu. A. Goncharov and A. N. Doronin, Fifth All-Union Conference on Electrochemistry, Summaries of Reports, Moscow, 1974, Vol. II, p. 399.
13 V. T. Solomatin, S. P. Rzhavichev, Zavod. Lab., 42 (1976) 529.
14 V. T. Solomatin and S. P. Rzhavichev, Zh. Anal. Khim., 31 (1976) 2345.
15 V. T. Solomatin, V. A. Balusov, S. P. Rzhavichev and V. G. Klochkova, Izv. Visch. Uch. Zaved., Khim. Khim. Technol., 20 (1977) 1472.
16 T. N. Artemova, V. T. Solomatin and E. I. Vasilyeva, Zavod. Lab., 43 (1977) 1313.
17 V. T. Solomatin, V. I. Ignatov and S. P. Rzhavichev, Zh. Anal. Khim., 32 (1977) 948.
18 V. G. Klochkova, V. T. Solomatin, S. P. Rzhavichev and V. I. Ignatov, Izv. Vysh. Uch. Zaved., Khim. Khim. Technol., 20 (1977) 677.
19 V. I. Ignatov and V. T. Solomatin, Zh. Anal. Khim., 32 (1977) 56.
20 M. Kopanika and F. Vydra, J. Electroanal. Chem., 31 (1971) 175.
21 Yu. V. Pleskov and V. Yu. Filinovsky, Rotating Disk Electrode, Nauka, Moscow, 1972, p. 51.
22 B. Savel'yev, personal communication.

Analytica Chimica Acta, 102 (1978) 99—112

A FLOW DETECTOR BASED ON SQUARE-WAVE POLAROGRAPHY AT THE DROPPING MERCURY ELECTRODE

J. WANG[‡], E. OUZIEL, CH. YARNITZKY, and M. ARIEL*
Department of Chemistry, Technion - I.I.T., Haifa (Israel)
(Received 17th May 1978)

SUMMARY

Square-wave polarography (s.w.p.) at the DME has been adapted for detection in various analytical flow systems. The combination of high sensitivity with rapid potential scan rates results in detector characteristics significantly superior to those previously reported for techniques involving constant applied potential. In an automated flow system for the analysis of discrete samples, s.w.p. allows sensitive and reproducible multi-component sample analysis, at a sampling rate of 22.5 samples per hour (at a 1:1 sample/wash ratio and with relatively low sample volumes). The electrochemical selectivity of the detector may be exploited for monitoring chromatographic column effluents, in cases where the chromatographic separation is incomplete: species eluted simultaneously but having different reduction potentials can be determined with satisfactory sensitivity. The in-situ monitoring system based on s.w.p. allows rapid simultaneous determinations (~ 300 per hour) of a number of contaminants present at the sub-ppm level; because of its long-term stability and reproducibility, it seems well suited for continuous contaminant control.

Analytical flow systems have lately been applied to the monitoring of chromatographic column effluents [1], the monitoring of environmental contaminants and various industrial processes in situ [2] and to the analysis of discrete samples according to the AutoAnalyzer principle [3]. Electrochemical detectors, with a constant potential imposed on the working electrode, and the resulting current proportional to the concentration of the monitored species in the detector, are becoming increasingly common [4]. The potential chosen depends on that required for the electrode reaction (oxidation or reduction, as the case may be) of the species; in detectors monitoring chromatographic column effluents, it is usually made sufficiently high to ensure the reaction of all sample components; these react in the order of their elution [5]. The constantly renewed electrode surface, extended cathodic potential range and excellent reproducibility make DME-equipped polarographic flow cells well suited to the demands of prolonged use; accordingly they are the preferred electrochemical detectors for flow systems.

Pulse polarographic techniques, a routine tool for the sensitive determination of organic, inorganic and biological substances [6], have been recently adapted

[‡]Present address: Department of Chemistry, University of Wisconsin, Madison, U.S.A.

to flow systems by tuning the potential pulse to a specific wave of one component in the mixture [7, 8].

The selectivity inherent in employing a rapid potential scan on a hanging mercury drop electrode (HMDE) allows the determination of sample components which are not separated by the chromatographic column; rapid potential scans, carried out at different intervals during the elution, allow the determination of sample components which are not efficiently separated by the column and which have similar half-wave potentials [8]. In DME-equipped flow detectors, no potential scans have hitherto been used for the simultaneous determination of several sample components. The unsuitability of polarographic techniques for this purpose stems from the slow potential scan, dictated, in turn, by the relatively long drop life. In automated systems for the analysis of discrete samples this requires large sample volumes and a low sampling rate; in chromatographic column monitors slow potential scans may make it impossible to detect the species eluting last but reacting electrochemically at potentials corresponding to the beginning of the scan. In flow systems designed for the monitoring of contaminants and industrial processes in situ, slow scan rates preclude the perfection of a "rapid warning system" indicating sudden changes in the concentration level of the monitored species.

Various complex systems have been proposed for the identification of sample components in a flow system: a bi-electrode amperometric detector, with each working electrode held at a different potential [9]; the cyclic application of successive potential steps, each adjusted according to the potential required for the electrochemical reaction of one of the species to be determined [1]; intermittent flow stoppage accompanied by a potential scan of the solution trapped in the detector [10]. Anodic stripping voltammetry has recently been adapted for the simultaneous monitoring of a number of heavy metals, at trace level concentrations, both in an in-situ warning system [11] and in an automated flow system for discrete samples [12]. This approach is applicable to amalgam-forming metals only, and is limited in the rate of sample throughput by the time required for the pre-electrolysis step.

Square-wave polarography (s.w.p.) at the DME [13] allows the simultaneous determination of electroactive species at ppm and sub-ppm levels, with relatively rapid potential scan rates (100—200 mV s^{-1}). In the work described here, rapid-scan s.w.p. was adapted for detection in a variety of flow systems and the detector response was characterized and optimized.

EXPERIMENTAL

Flow-through cell

The flow-through cell and nebulizer employed for detection and removal of dissolved oxygen in experiments tailored for the monitoring of chromatographic column effluents have been described [14]. The flow-through cell serving as detector for the automated analysis of discrete samples and for a continuous (in situ) monitoring system, shown in Fig. 1, consists of a

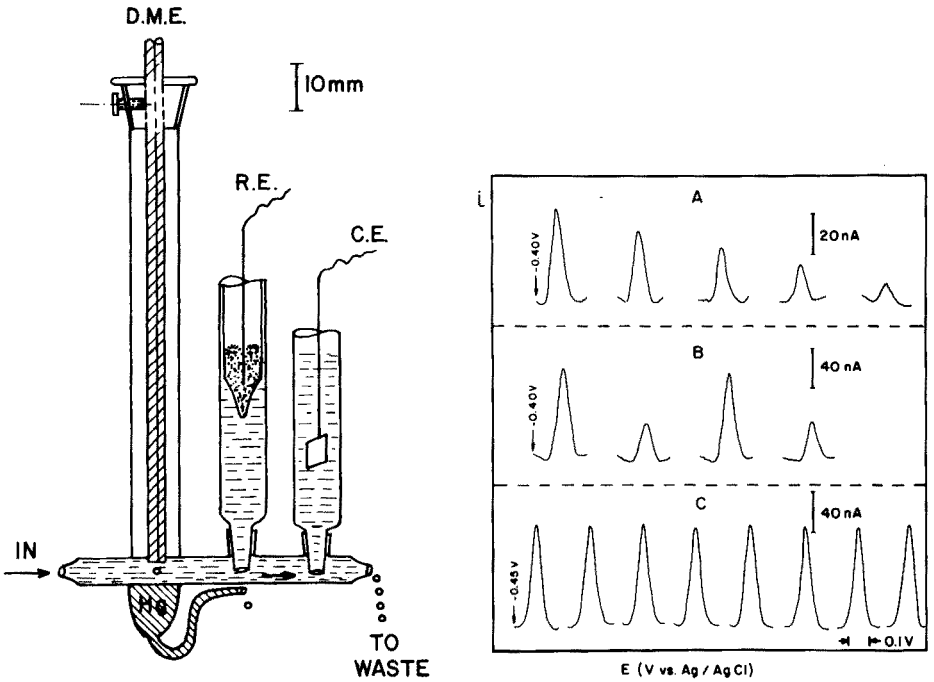

Fig. 1. Polarographic flow-through cell for the automated analysis of discrete samples and continuous (in-situ) monitoring systems.

Fig. 2. Continuous flow studies with the AutoAnalyzer set-up. (A) Cd^{2+} calibration with sequential "descending concentration" samples: 10, 8, 6, 4 and 2×10^{-7} M, 0.1 M KCl solution. (B) Carry-over between sequential samples: 2.0, 0.8, 2.0 and 0.8×10^{-7} M Cd^{2+}, 0.1 M KCl solution. (C) Precision of replicate sampling for 2.2×10^{-6} M Cd^{2+}, 0.1 M KCl solution. Solution flow rate, 4.6 ml min^{-1}; drop life, 20 s; delay time, 6 s; square-wave amplitude, 25 mV; potential scan rate, 125 mV s^{-1}; (staircase amplitude, 5 mV). All sample tubes were alternated with wash tubes (0.1 M KCl); polarograms for those are not shown.

horizontal pyrex glass tube, through which the solution flows. About 15 mm past the tube inlet is placed a vertical glass tube in which the DME is held in position by a Teflon stopper with a screw. The space around the DME capillary acts as debubbler, allowing the gas segments separating discrete samples to escape via the space between the capillary and the stopper. The mercury drops collect in a small Hg pool connected to a voiding tube, which also serves for mercury levelling. Further along the horizontal tube, ground joints allow the introduction of salt bridges leading to the reference electrode (Ag/AgCl, saturated KCl, with the supporting electrolyte in the bridge) and the auxiliary electrode (a Pt foil dipping into the supporting electrolyte solution). In the analysis of discrete samples, the solutions leaving the cell are discarded to waste; in the continuous monitoring system, a three-way stop-cock

at the cell outlet allows the choice of either discarding or recycling the solution as required. Adjustment of a clamp on the outlet Tygon tubing ensures the maintenance of a constant solution level in the cell, regardless of the solution flow rate employed.

Set-up for the automated analysis of discrete samples

Various components of the automated system, such as the sampler (consisting of a test-tube tray and sampling-deaeration probe) were modified to allow the simultaneous sparging of 4 adjacent test tubes (including that being sampled). The diameter of the sampling tube clamped to the first deaerating tube was diminished to 0.7 mm, thus decreasing the "dead volume" (from the tip of the sampling tube to the DME) to 1.3 ml. To minimize mechanical noise, the pump, flow cell and recorder were placed on three separate marble blocks.

Liquid chromatography set-up

A polarographic spray cell, placed at the outlet of the chromatographic column serves as detector. The cell contains two glass nebulizers, capable of being activated either simultaneously or separately, as required [14]. The nitrogen pressure at the nebulizer inlet is controlled, by adjusting the cylinder pressure and a Teflon stopcock between it and the nebulizer, according to the flow rate in the column, to effect rapid atomization of the effluent and the complete and immediate removal of dissolved oxygen. When two nebulizers are employed to mix the column effluent with the supporting electrolyte solution, the desired mixing ratio is determined by the pressure of the nitrogen at each nebulizer inlet. The mixing ratio is monitored by continuous measurement of the cell resistance. The system may be used in the 2- or 3-electrode mode; in the former the ohmic potential drop is compensated with the dynamic compensator [15].

In the 3-electrode mode, the mercury pool below the DME (0.6 mm i.d.) serves as auxiliary electrode; the reference is an Ag/AgCl, KCl (sat.) electrode. The chromatographic eluent was stored in a sealed container and passed through a silica-gel pre-column onto a Vydac ODS reversed-phase column (25 cm long, i.d. 5 mm; Spectra-Physics), with a constant-volume piston pump (LEWA-Herbert Ott Versuchsgruppe - Endabnahme). The samples were injected with a 10-μl Hamilton microsyringe. The column effluent was passed through a length of Tygon tubing (0.7 mm i.d.) to the nebulizer, sprayed into a collecting—separation cell and mixed, in a controlled ratio, with supporting electrolyte solution (the latter was usually 5% of the effluent volume).

The nebulizer efficiently smoothed out any pulsations remaining after passage through a 0.5-m damping coil placed between the pump and the column inlet.

Set-up for continuous (in-situ) monitoring system.

The system is nearly identical to that described for a.s.v. detection [11]; obviously, the mercury solution container is omitted and the polarographic flow cell substituted as detector. A locally built square-wave polarograph and

drop detector [16, 17] were used in conjunction with the various flow systems; polarograms were recorded on a Yokogawa 3077 X-Y recorder.

Reagents and solutions

Reagents and metal ion stock solutions were prepared as described [11]. A 10^{-3} M As(III) solution was prepared by dissolving As_2O_3 in water and ammonia. The solutions were stored in polyethylene containers. Sea-water samples (subsequently spiked to bring up their metal ion content to the sub-ppm level and used to illustrate continuous monitoring) were taken, unfiltered from surface water near the Oceanographic Institute, Haifa.

The chromatographic eluent was a 60:40 water—methanol mixture. The supporting electrolyte solution sprayed into the cell was 0.2 M KNO_3 in 60:40 water—methanol.

The chromatographic system was tested for the separation of three diketones: benzil and camphorquinone (synthesized and purified in the photochemical laboratory of this Department) and 1,4-naphthoquinone (puriss., Fluka). The sample mixtures were prepared by weighing the diketones, dissolving in 1 ml of dimethylformamide and making up to volume with 60:40 water—methanol.

Liquid chromatographic procedure

The eluent is pumped from the storage container to the silica-gel pre-column, for solvent cleaning, and then to the chromatographic column. The effluent at the column outlet is atomized, with the immediate removal of dissolved oxygen, and collects in the collection—separation cell [14]. The gas separates from the aerosol and is removed through the upper cell outlet; the deaerated effluent flows on towards the DME-equipped detector. Before entering the detector, the effluent is mixed with the supporting electrolyte solution (0.2 M KNO_3), which is sprayed into the cell at a controlled rate, so that its contribution to the final sample volume is 5%, i.e. a constant (0.01 M) KNO_3 concentration is maintained in the detector. The mixing ratio is monitored by continuous measurement of the cell resistance.

The range of the potential scan imposed on the DME is determined by the half-wave potentials of the compounds to be separated. Drop life and the delay between the beginning of drop growth and the start of the potential scan are synchronized with the rate of potential scan and the retention time of the sample components in the column. The potential scan is started, with the injection of sample, in order to record the baseline, and is continued until the last component has been eluted. Two rates of potential scan were used: 50 mV s^{-1} and 125 mV s^{-1}. The staircase width and the square-wave amplitude employed throughout were 40 ms and 25 mV, respectively. At the lower scan rate, longer drop lives (> 20 s) and short delay times were mandatory to allow the scanning of the extensive potential range required for the reduction of the three α-diketones (+0.2 to −1.2 V vs. Ag/AgCl). At the faster scan rate, shorter drop lives and longer delay times may be used.

Procedure for the continuous (in-situ) monitoring system

Spiked sea-water samples were introduced into the sample container and sparged with pure nitrogen (passage of nitrogen through the sample is maintained throughout the procedure). The deaerated sample is streamed (at a rate of 8 ml min^{-1}) towards the flow cell. The initial potential, range of potential scan and delay time between the beginning of the drop growth and the start of the potential scan were chosen and synchronized according to the species to be determined and the drop life employed. Drop lives of 12 s and potential scan rates of 125 mV s^{-1} were used in most of these experiments. Successive potential scans were performed every 12 s and the resulting polarograms recorded.

Automated analysis of discrete samples

The sampling and deaeration procedure, based on that proposed by Lund and Opheim [4] and described in detail in a previous paper [12], was modified for combination with the s.w.p. detector. Sample and wash solution (blank) test tubes, each containing 8 ml, were alternated on the tray; 4 deaeration tubes and the sampling probe were dipped into the 4 leading test tubes so that 3 solutions were sparged before sampling (compared with 1 or 2 in previous studies [4, 12]), and sparging was prolonged to 4 min. This ensured the degree of deareation required by the high sensitivity of the subsequent determinations; 0.1% residual oxygen is equivalent to a 10^{-7} M concentration which is of the order of concentration of the test species. As the sampling time is shortened to 80 s (including sample shift), the simultaneous deaeration of 3 preceding tubes is mandatory.

The sample and wash solutions are pumped alternately at the rate of 4.6 ml min^{-1} for 75 s per solution. The transfer of the sampling–deaeration probe by one notch takes another 5 s; this sample shift is performed by raising the probe in two steps [12] without interrupting the pumping and is also exploited for segmenting the pumped solutions with nitrogen bubbled through the orifice of the deaeration tube clamped to the sampling probe. Sampling time consists of 17 s "dead time" (the time required for the sample to reach the detector = dead volume/solution flow rate), plus the 45-s response time required for attainment of the steady state of the sample in the detector (see Table 1), plus 13 s consisting of the delay time and the measurement. Drop life was synchronized with the remaining stages of the procedure, to achieve maximum sensitivity, minimum carry-over effects, simplicity of operation and fastest sampling rate. The long drop life chosen (20 s) ensures high sensitivity and is adjusted so that the duration of the sampling (80 s) is exactly equal to 4 drop lives. The beginning of the growth of the first drop is synchronized with the start of the sample shift, so that within the lifetime of the first 3 drops drops (encompassing the 45-s period needed for attainment of steady state), no potential scans are imposed; measurement is effected on the 4th drop only, after a delay of 10 s at the very least (depending on the potential range to be scanned). As a result, measurement takes place 65 s (or more) after the steady

TABLE 1

Response time studies
(2.0×10^{-6} M Cd^{2+} in 0.1 M KCl; drop life, 8 s; delay time, 2 s; potential scan rate, 125 mV s^{-1}; solution flow rate 4.6 ml min^{-1}.)

Time from start of sampling to measurement (s)	Time from sample arrival in detector to measurement (s)	i_p (nA)	i_p/i_p (steady state)
6	—	0	0
14	—	0	0
22	5	30	0.19
30	13	104	0.67
38	21	132	0.85
46	29	143	0.92
54	37	149	0.96
62	45	155	1.00
70	53	155	1.00
78	71	155	1.00
86	79	154	0.99
94	87	155	1.00

state in the detector has been attained. With the fall of the 4th drop line sampling—deaeration probe is shifted by one notch, to sample the next solution on the tray and deaerate the 3 solutions behind it. A sampling rate of 22.5 samples per hour (with a 1:1 ratio between sample and wash solutions) is thus obtained. The above procedure, carried out manually, lends itself easily to full automation with commercially available units.

RESULTS AND DISCUSSION

Carry-over studies and analytical exploitation

The continuous flow data obtained with sequential Cd^{2+} solutions differing in concentration (Fig. 2A and B) illustrate the absence of carry-over effects. The linear correlation between peak height and concentration (Fig. 2A) is the basis of quantification by comparison to peak heights obtained with a set of calibrating solutions placed in the end positions of each test tube tray. The concentration range employed was 1.0×10^{-6}—2.0×10^{-7} M (110—22 ppb). The replicate peaks shown in Fig. 2C were obtained with a series of sample test tubes, all filled with 2.2×10^{-6} M Cd^{2+}, separated by tubes containing an appropriate wash solution; the relative standard deviation for this series was 1.4%.

Figure 3 illustrates the application of the system to the automated analysis of multiple discrete multicomponent samples at the sub-ppm level. Well defined and separated peaks were obtained, with no observable carry-over between the sample and wash solutions. Procedures developed for the simultaneous determination of a number of electroactive species in a single sample may be easily adapted for this multi-sample flow system.

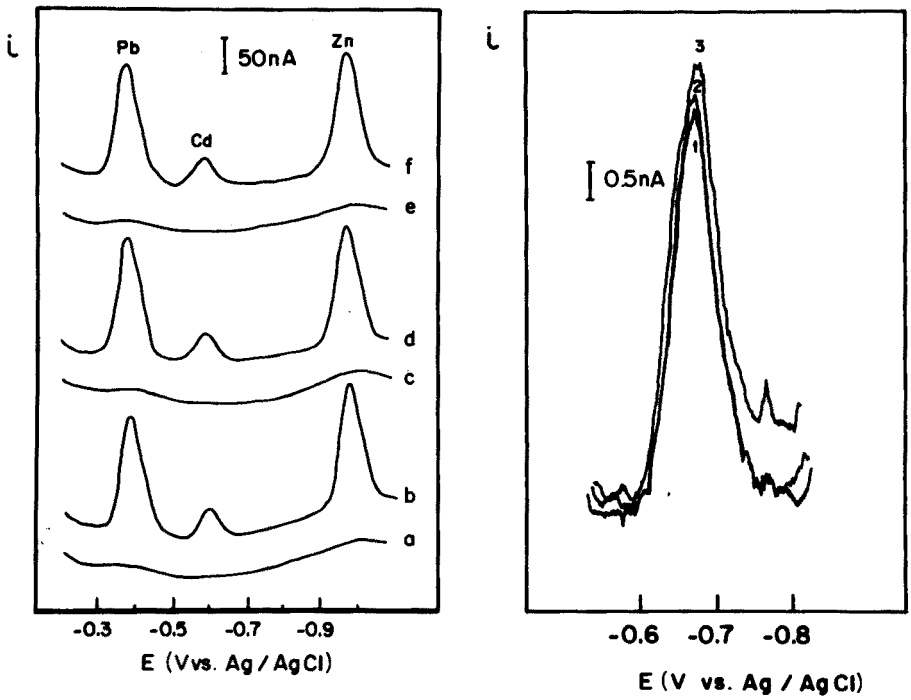

Fig. 3. Continuous flow studies with the AutoAnalyzer set-up: multi-component solution. (a), (c), (e), Wash solution blank (0.1 M KCl); (b), (d), (f), 2.4×10^{-6} M Pb^{2+}, 6.4×10^{-7} M Cd^{2+} and 2.5×10^{-6} M Zn^{2+} in 0.1 M KCl solution. Solution flow rate and measuring conditions as for Fig. 2. 22.5 samples per hour (1:1 sample/wash).

Fig. 4. Three successive polarograms recorded during the direct nebulization of a 2.0×10^{-7} M benzil solution into the detector cell. Solvent, 60:40 water—methanol; supporting electrolyte, 0.1 M KNO_3; solution flow rate, 2.7 ml min^{-1}; square-wave amplitude, 25 mV; potential scan rate, 50 mV s^{-1} (staircase amplitude, 2 mV); drop life, 12 s; delay time, 2 s.

Liquid chromatography studies

Polarographic pulse methods, applied in a liquid chromatography detector, improve the limit of detection and are also often selective with regard to certain components, or discriminate between components which have identical retention times. This combination allows the detection of components in complex matrices, without requiring a multiplicity of chromatographic column eluents or detectors, which is the usual approach to the analysis of samples difficult to separate.

In electrochemical, DME-equipped, h.p.l.c. detectors employing short drop times, drop reproducibility, cell volume constancy and low noise level are hard to achieve [1, 8]. The rapid-pulse s.w.p. method offers high sensitivity and avoids the problem of the different capillary noise accompanying successive drops.

Results obtained with the polarographic spray cell [14] operated in the s.w.p. mode are shown in Fig. 4. Apart from serving for monitoring of column effluents, the detector can also be easily adapted to the system for the automated analysis of discrete samples. Its low dead time and response time ensure a high sampling rate, while small sample volumes suffice. The high sampling rate also allows the recording of several successive polarograms during the elution of each sample component (Fig. 5). The third peak corresponding to the maximum concentration of benzil in the effluent was recorded 2.75 min after injection. Faster potential scans, e.g. 125 mV s^{-1}, further improve sensitivity, because a faster scan permits the delay time to be increased beyond 0.2 s, so that the benzil reaction occurs when the area of the mercury drop is larger.

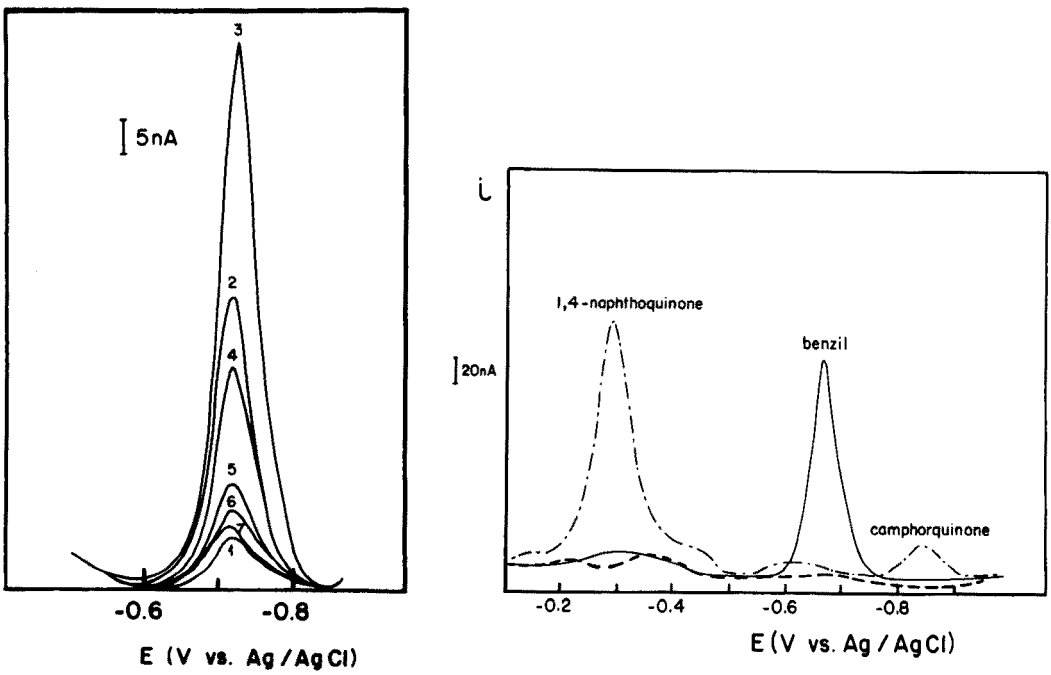

Fig. 5. Elution of 10 μl of a 2.76 x 10^{-4} M benzil solution from a Vydac ODS (C-18) column with 60:40 water—methanol. Composition of solution entering detector, 0.0075 M KNO_3 in 60:40 water—methanol; solution flow rate, 3,7 ml min^{-1}; square-wave amplitude, 25 mV; potential scan rate, 50 mV s^{-1} (staircase amplitude, 2 mV); drop life, 8 s; delay time, 0.2 s.

Fig. 6. Elution of 10 μl of a solution containing 0.83 μg of 1,4-naphthoquinone, 0.72 μg of camphorquinone and 1.00 μg of benzil in 60:40 water—methanol. Composition of solution entering detector, 0.01 M KNO_3 in 60:40 water—methanol; solution flow rate 3.7 ml min^{-1}; square-wave amplitude, 25 mV; potential scan rate, 50 mV s^{-1} (staircase amplitude: 2 mV); drop life, 24 s; delay time, 4 s (---) t_0 = 0.75 min; (·--) t_0 = 1.25 min; (—) t_0 = 2 min.

Selectivity

In h.p.l.c. no special effort was made to achieve complete resolution betweer overlapping peaks. The selectivity of the detector was exploited to improve resolution [1]: when overlapping peaks are related to compounds with different polarographic half-wave potentials, each can be determined separately by imposing the appropriate constant potential on the DME and by performing repetitive runs equal to the number of overlapping peaks.

Rapid-scan single drop s.w.p. applied to column effluents fully exploits the selectivity inherent in electroanalytical methods. Compounds with different reduction potentials but overlapping elution peaks are recorded as separate peaks; those with similar reduction potentials but separated by the column, are recorded as peaks at the same potential, but at different times. For example in the separation of a mixture of benzil, camphorquinone and 1,4-naphthoquinone on a Vydac ODS (C-18) column, with a 60:40 water—methanol eluent at 3.7 ml min^{-1}, camphorquinone and 1,4-naphthoquinone elute as a single peak, followed by benzil. The difference in their reduction potentials allows the first two to be determined in one rapid potential scan; continued scanning of successive drops allows detection of the separated benzil. Figure 6 shows the separated peaks: the potential scan initiated 0.75 min after sample injectior gives the base line; a further scan, 1.25 min after injection, shows the camphorquinone and 1,4-naphthoquinone peaks (compounds which are not separated by the column); 2 min after injection a third potential scan detects the benzil peak. The camphorquinone peak is lower than expected, because at the potential scan rate employed (50 mV s^{-1}), part of the compound has left the detector before the potential at the DME reaches the required reduction potential; a decrease in the delay will remedy this, but will decrease the sensitivity for 1,4-naphthoquinone.

The same sample separation was also performed with the same detector but with the application of two different operating modes: direct current polarography (d.c.p.) and differential pulse polarography (d.p.p.) (Fig. 7). With d.c.p. three identical runs were made with a negative potential so that 1,4-naphthoquinone and camphorquinone were recorded as a single peak and benzil as a separate one; at less negative potentials, only 1,4-naphthoquinone and benzil were reduced and were recorded as separate peaks. The difference in the areas of the first peak, as obtained at these different potentials, allows the determination of both 1,4-naphthoquinone and camphorquinone. With d.p.p. high sensitivity and selectivity were achieved; tuning to the appropriate potentials allowed the separate determination of each component. A Radiometer PO4 polarograph and electromagnetic drop timer (drop time, 1.5 s) were employed for d.c.p.; d.p.p. was done with a PAR-174, the pertinent drop timer being synchronized with pulse initiation. Drop lifetimes of 2 s, pulse durations of 57 ms and sampling times of 17 ms were used. Different capillaries were employed in d.p.p. and d.c.p., so that the drop areas differed. The low peaks obtained with d.p.p. for benzil and naphthoquinone result from the difference in drop area at the sampling time.

Rapid pulse techniques, such as s.w.p. and d.p.p., applied to the monitoring

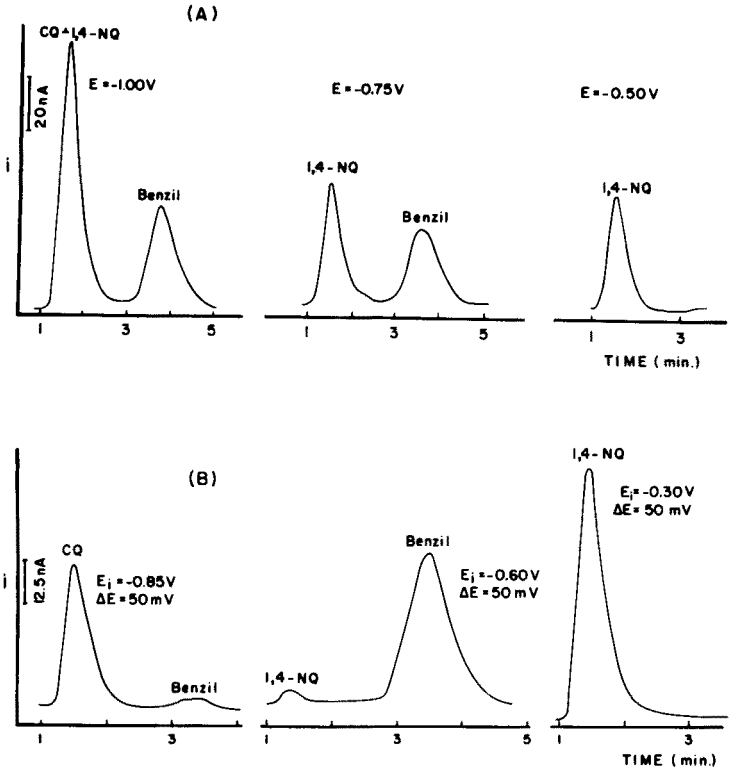

Fig. 7. (A) D.c.p. and (B) d.p.p. chromato-polarograms optimized for the selective detection of camphorquinone (24 μg) benzil (28 μg) and 1,4-naphthoquinone (29 μg) in methanol. Column, Vydac ODS. Eluent, 55:45 water—methanol. Composition of solution entering detector, 0.005 M KNO_3 in 55:45 water—methanol.

of h.p.l.c. effluents are insensitive to changes in the effluent flow rate (which affects signal height in electrochemical detectors employing a fixed electrode with a constant imposed potential). The insignificant depletion of the diffusion layer resulting from the pulse minimizes the influence of changes in the thickness of the layer caused by variations in the effluent flow rate. The rapid potential scans employed in s.w.p. contribute to the charging of the double layer; however, the compensation of charging currents and the increased sensitivity make up for this.

Continuous monitoring studies

The demand for in-situ, continuous monitoring devices for the control of various contaminants at the ppm and sub-ppm level in the environment, in the course of industrial processes, in industrial effluents and in sewage processing has been widely discussed (see, e.g. [2]). Whenever available, the use of a sensor capable of monitoring several parameters is preferable to a combination

of individual sensors. Polarographic pulse methods allow the simultaneous determination of several species at this concentration level and are well suited to in-situ performance [19].

Rapid warning in case of sharp changes in the level of the monitored parameters is often required; it is, therefore, crucially important to make the measurements approach the ideal of continuity. The slow potential scans employed in regular pulse polarography unduly prolong the time taken to traverse the potential working range (3—15 min); in contrast, rapid-scan s.w.p. dramatically shortens this time. The system was tested under conditions requiring a rapid repetition of analytical scans performed on a flowing sample stream. A sea-water sample, spiked with 0.23 ppm Cu^{2+}, 0.64 ppm Pb^{2+}, 0.21 ppm Cd^{2+} and 0.27 ppm Zn^{2+}, was recycled through the flow cell and 95 successive analytical runs were performed on it, at 12-s intervals; the polarograph settings were as shown for Fig. 2. The 12-s drop life, with a delay time of 2 s was chosen as a compromise between the demand for increased sensitivity (i.e. longer drop life) and rapid successive scans (shorter drop life). Under these conditions, 300 analytical scans per hour were possible and an adequate assurance of "rapid warning" was thus achieved.

In contrast to a.s.v. detection, which is limited to amalgam-forming metals, the s.w.p. detector may be employed to monitor a wide range of inorganic and organic contaminants. Cr(VI), Mn^{2+}, NTA, As(III), S^{2-}, IO_3^- and many others which are determined today by slow-scan pulse polarography [19], by taking discrete samples to the laboratory, may be determined in situ. As an illustration the d.p.p. determination of traces of As(III) [20] was adapted for the system; the simultaneous analysis of Cu^{2+}, Cd^{2+}, Pb^{2+} and As(III) in a spiked sea-water sample acidified with HCl is shown in Fig. 8. At the 10^{-6} M concentration

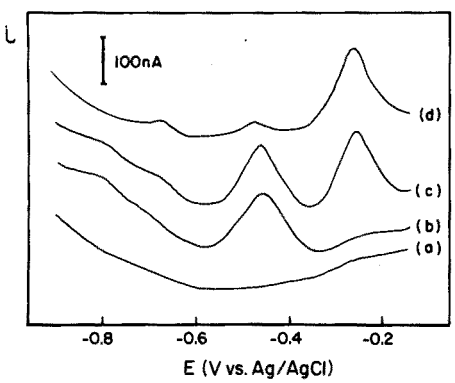

Fig. 8. Determination of As(III) in the presence of Pb^{2+}, Cd^{2+} and Cu^{2+}. (a) Blank solution (acidified sea water, 1 M HCl); (b) after spiking with 5.6×10^{-6} M As(III); (c) after further spiking with 4.0×10^{-7} M Pb^{2+}, 2.6×10^{-7} M Cd^{2+} and 2.6×10^{-6} M Cu^{2+}; (d) after the addition of excess Ce^{4+} (to oxidize completely As(III)) to (c). Drop life 12 s; delay time, 2 s; sample solution flow rate, 19 ml min^{-1}; Ce^{4+} (10^{-3} M) solution flow rate, 0.36 ml min^{-1} square-wave amplitude, 25 mV; potential scan rate, 125 mV s^{-1}.

level the main reduction peak of As(III) in this medium appears at —0.46 V and is accompanied by a second smaller peak at —0.80 V; the maximum reported earlier [20] is nearly obliterated, possibly by surfactants present in the sea water. Pb^{2+} and Cd^{2+}, present at a lower concentration level — 15 or 20 times lower than that of As(III) — cannot be determined, because they are dwarfed by the arsenic peak, their stripping peak potentials in this medium being —0.48 and —0.67 V respectively (Fig. 8, curve c). The solution , proposed for the batch process, of adding excess of Ce^{4+} to oxidize As(III) to the electrochemically inert As(V) [20] was applied to the flow system by connecting two identical flow cells in series. In the first, the total peak current corresponding to the sum of all sample components was measured; the solution leaving this cell was mixed with a constant stream of Ce^{4+}, at a rate and concentration ensuring an excess of Ce^{4+}, without appreciably diluting the sample. After passage through a suitable reaction coil, the sample was analyzed in the second cell (Fig. 8, curve d); Pb^{2+} and Cd^{2+} could then be easily determined. As(III) was determined by subtracting the Pb^{2+} peak height obtained in the second cell (curve d) from the common peak (curve c). The Cd^{2+} peak became clearly visible after the removal of the As(III) interference. The determination of Cu^{2+} is not affected.

At the ppm and sub-ppm levels, rapid-scan s.w.p. has certain advantages over a.s.v. in flow systems [e.g. 11]. The sampling rate in both methods is similar; however, the constant renewal of the DME surface allows its use under conditions which would cause deterioration of thin film electrodes [21]; this, and its freedom from interferences by the formation of intermetallic compounds, makes it the preferred detector for automated systems. S.w.p. is applicable to a far wider range of electroactive species than a.s.v. However, at the ppb and sub-ppb levels, only a.s.v. offers the required sensitivity.

Thanks are due to Prof. M. Rubin for making his h.p.l.c. available for this work.

REFERENCES

1 P. T. Kissinger, Anal. Chem., 49 (1977) 447A.
2 K. H. Mancy and W. J. Weber in I. M. Kolthoff and P. J. Elving (Eds.), Treatise on Analytical Chemistry, Part III, Vol. 2, Wiley, New York, 1971, p. 413.
3 L. Snyder, J. Levine, R. Stoy and A. Conneta, Anal. Chem., 48 (1976) 942A.
4 See, e.g. W. Lund and L.-N. Opheim, Anal. Chim. Acta, 79 (1975) 35.
5 W. Kemula, Rocz. Chem., 26 (1952) 281.
6 A. M. Bond and D. R. Canterford, Anal. Chem., 44 (1972) 721.
7 D. G. Swartzfager, Anal. Chem., 48 (1976) 2189.
8 E. Ouziel, Ph. D. thesis, Technion, Haifa (1977).
9 C. L. Blank, J. Chromatogr., 117 (1976) 35.
10 R. C. Buchta and I. J. Papa, J. Chromatogr. Sci., 14 (1976) 213.
11 See, e.g. J. Wang and M. Ariel, J. Electronal. Chem., 83 (1977) 217.
12 J. Wang and M. Ariel, Anal. Chim. Acta, 101 (1978) 1.
13 J. H. Christie, J. H. Turner and R. A. Osteryoung, Anal. Chem., 49 (1977) 1899, 1904.
14 Ch. Yarnitzky and E. Ouziel, Anal. Chem., 48 (1976) 2024.
15 Ch. Yarnitzky and Y. Friedman, Anal. Chem., 47 (1975) 876.

16 Ch. Yarnitzky and R. A. Osteryoung, to be published.
17 Ch. Yarnitzky, C. A. Wijnhorst, B. Van De Laar, H. Reyn and J. H. Sluyters, J. Electroanal. Chem., 77 (1977) 391.
18 I. H. Suffet, J. V. Radziul and D. R. Goff in J. W. Scales (Ed.), Water Quality Instrumentation, Vol. 1, Instrument Society of America, Pittsburg, 1972, p. 11.
19 W. Davison and M. Whitfield, J. Electroanal. Chem., 75 (1977) 763.
20 D. J. Meyers and J. Osteryoung, Anal. Chem., 45 (1973) 267.
21 P. L. Brezonic, P. A. Brauner and W. Stumm, Water Res., 10 (1976) 605.

Analytica Chimica Acta, 102 (1978) 113—119

DETERMINATION OF GERMANIUM(IV) IN PERCHLORIC ACID SOLUTION BY A.C. POLAROGRAPHY AND DIFFERENTIAL PULSE POLAROGRAPHY IN THE PRESENCE OF 3,4-DIHYDROXYBENZALDEHYDE

A. M. SHAFIQUL ALAM, O. VITTORI and M. PORTHAULT*

Laboratoire de Chimie Analytique III, (Equipe de Recherche associée au CNRS (E.R.A. 070474), 43 Bd du 11 Novembre 1918, 69621 (Villeurbanne (France)

(Received 17th April 1978)

SUMMARY

Germanium(IV) at trace levels can be determined in perchloric acid solution containing 3,4-dihydroxybenzaldehyde by alternating current and differential pulse polarography with dropping mercury and hanging mercury drop electrodes. The results are comparable by the two methods. The possible interferences of some elements are discussed. The serious interference of lead(II) can be prevented by addition of EDTA in hydrochloric acid medium. Interference of selenium can be avoided by precipitation with potassium iodide. The method is applied to silver—germanium alloys.

Germanium is frequently used in the semiconductor industry, in special alloys with Fe, Au, Mo, and in some optical glasses. Since germanium is a dispersed element, it is also found in natural waters and rocks. The concentrations to be determined are always very low, so that sensitive analytical methods are required. Many different analytical techniques, especially gravimetric, spectroscopic and electrochemical methods, are available for germanium [1]. The more sensitive of them are spectrophotometry with phenylfluorone [2], atomic absorption with a graphite furnace [3, 4], and neutron activation analysis [5]; detection limits are usually in the range 0.1—1 μg ml^{-1}.

Polarography has long been used to determine divalent and tetravalent germanium at trace levels [6, 7]. Das Gupta and Nair [8, 9] indicated that the reduction of germanium in acidic solutions is possible only with complex-forming agents. At pH values above 5, complexing agents are not necessary and germanium(IV) is reduced irreversibly to Ge(0) in a four-electron process [10]. At pH values below 1, reduction takes place in the presence of oxalic, tartaric, and salicylic acids [11], and with *o*-diphenols such as pyrocatechol and pyrogallol [12—16]. Structures of these complexes vary with pH, and their study is a special part of germanium chemistry [1]. A 1:1 complex is present in very acidic medium, and the reduction step is a kinetic process [12]:

$$Ge + L \rightleftharpoons GeL + ne \rightleftharpoons Ge(0)$$

This paper describes the determination of germanium(IV) in 1 M perchloric acid solution in the presence of an excess of 3,4-dihydroxybenzaldehyde (DHB). This reagent is more soluble (up to 5×10^{-2} M) in acidic medium than in water. Stock solutions of such a concentration are not stable with time and a brown precipitate is rapidly formed. More dilute solutions (10^{-3} — 5×10^{-3} M) are quite stable for a week.

EXPERIMENTAL

All polarograms were recorded with Solea-Tacussel PRG 3 (a.c. polarography and PRG 4 (pulse polarography) instruments. An electromagnetic hammer drop timer (MPO 3) was used, and the usual drop times were 2.5 or 3 s. The flow rate of mercury was selected between 0.5 and 0.6 mg s^{-1}. A Metrohm E410 hanging mercury drop electrode was used. A saturated calomel reference electrode was used with a NaCl salt bridge to prevent $KClO_4$ precipitation in the porous glass junction.

All solutions were prepared from analytical-grade products (Merck or Prolabo Suprapur). Water was deionized with mixed ion exchangers and then twice-distilled. The mercury used had been distilled 6 times (Rhone Alpes Mercure), and was conditioned under nitrogen. Stock solutions (10^{-2} M) of germanium(IV) were prepared by dissolving a measured quantity of germanium dioxide in the minimum quantity of sodium hydroxide, the solutions being diluted with water to give the required concentrations. All additions were made by 10-, 50- and 100-μl Eppendorf micropipettes. All other precautions normally required in polarography were taken.

RESULTS AND DISCUSSIONS

Germanium(IV) is reduced in 1 M $HClO_4$ when an excess of DHB is added. This reduction step is characterized by a half-wave potential of —0.43 V vs. SCE. The wave is well developed in classical polarography and the slope of the log $(i_d/i_d - i)$ vs. potential plot is 30 mV per log unit.

In a.c. and differential pulse polarography, the recorded peaks are symmetrical and have a width at half-height of about 45—50 mV. These and other observations indicate a reversible 2e transfer step [17, 18]. This conclusion does not agree with previous studies related to other complexing agents [1, 12], where a 4e exchange was assumed. However, the results of classical, a.c., and pulse polarography on the one hand, and cyclic voltammetry on the other, do not agree reasonably with such an assumption (Fig. 1). For example, the peak intensities are much too high compared to the limiting current obtained in classical polarography [17, 18]. Fortunately for analytical purposes an exact knowledge of the electron transfer step is not required, provided that the recorded intensity varies linearly with concentration, which is the case for germanium. Peaks are narrow and symmetrical which are the important practical points in analyses for low concentration of germanium, such as occur in residues of zinc ores and coal ashes.

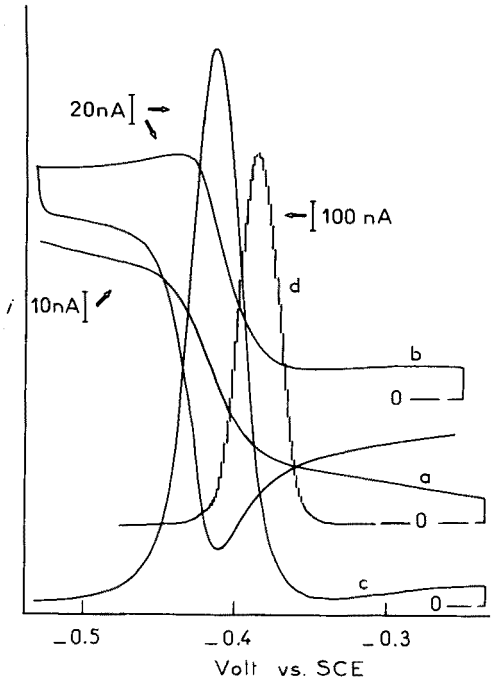

Fig. 1. Comparative polarograms of 10^{-4} M Ge(IV) in perchloric medium with DHB. (a) Classical polarography, [DHB] = 10^{-3} M; (b) linear sweep voltammetry, 20 mV s^{-1} scan rate, [DHB] = 10^{-3} M; (c) a.c. polarography, N = 70 Hz, t = 3 s, θ = 0°, [DHB] = 10^{-3} M; (d) differential pulse polarography, ΔE = 50 mV, t_m = 0.03 s, [DHB] = 2×10^{-2} M.

Optimum conditions for analysis

As mineralization of samples often leads to strongly acidic solutions, all the determinations reported here were run in 1 M $HClO_4$. The concentration of DHB was generally fixed at 10^{-3} M, but sometimes 10^{-2} M was used; because of the low stability of concentrated stock solutions, the 10^{-3} M solution was usually preferred, and it provides an adequate excess for germanium traces.

The linearity of the current vs. germanium concentration plots was studied with the dropping mercury electrode (DME) and the hanging mercury drop electrode (HMDE). As the surface area of the HMDE is greater than that of the DME, the sensitivity is increased. However, perhaps because of adsorption of DHB on the mercury, differential pulse polarography gives much the same sensitivity as a.c. polarography and an uncertain linearity of response [17]. Some results are shown in Table 1.

Electrical parameters were chosen in the usual ranges. For a.c. polarography, the parameters were 10-mV signal amplitude, 60-Hz frequency, 0° phase angle and 3-s drop time. For d.p.p., a constant pulse of 50 mV amplitude is

TABLE 1

Linearity and detection limits for germanium with a.c. and differential pulse (d.p.) polarography

DHB (M)	Method	Electrode	Detection limit (M)	Linear range (M)
10^{-3}	A.c.	DME	$6-7 \times 10^{-7}$	$10^{-6} \rightarrow 10^{-4}$
10^{-3}	A.c.	HMDE	$3-4 \times 10^{-8}$	$6 \times 10^{-8} \rightarrow 10^{-5}$
5×10^{-3}	A.c.	HMDE	$8-9 \times 10^{-9}$	$2 \times 10^{-8} \rightarrow 10^{-6}$
10^{-3}	D.p.p.	DME	$\sim 10^{-6}$	$\sim 10^{-6} \rightarrow 10^{-4}$
5×10^{-3}	D.p.p.	DME	$3-4 \times 10^{-7}$	$4 \times 10^{-7} \rightarrow 5 \times 10^{-}$
10^{-3}	D.p.p.	HMDE	$1-2 \times 10^{-7}$	Non-linear

convenient and gives satisfactory peak width; drop time was fixed at 3 s and the current sampling time was 35 ms.

The estimation of detection limits is not a simple problem, as there is no exact definition of this term in electrochemistry. Currents are in the nanoampere range and the base line is often high; thus the limits tend to depend on the possible compensation and/or the stability of the instrument itself. In the present work, the detection limit was taken as the concentration for which the peak had a measurable width and the peak potential could be determined accurately; and not the arbitrary measurement of the difference from base line of three standard deviations as applied in spectrometry. Results given in Table 1 show that germanium may be estimated at the $\mu g\ l^{-1}$ (1 ppb) with high-purity reagents and in the absence of lead.

Possible interferences

Many elements may interfere with the determination of germanium. Zinc, which is present in ores, gives a reduction wave at —1.0 V vs. SCE but this does not interfere in the acidic medium used. Other elements such as lead(II), copper(II), cadmium(II), arsenic(III), antimony(III), selenium(IV) and tellurium(IV) were investigated. Lead(II) is reduced at about —0.4 V vs. SCE, close to the reduction potential for germanium. In this particular case, 0.01 M HCl—4×10^{-2} M EDTA—10^{-3} M DHB was selected as the medium for germanium determination; EDTA is just sufficiently soluble in 0.01 M HCl and masks lead up to 10^{-5} M, so that germanium can be determined without prior separation or extraction.

Selenium is reduced in perchloric acid solution at about —0.45 V vs. SCE, which corresponds to the second step leading to selenide formation [19, 20]. The first step is an irreversible 4e transfer in which HgSe is formed at the mercur surface. This adsorbed compound is present when germanium reduction occu [21]. Selenium(IV) can be precipitated with potassium iodide, by the reactio $SeO_3^{2-} + 4I^- + 6H^+ \rightarrow Se^0 + 3H_2O + 2I_2$. The solution becomes coloured with triiodide and excess of KI is required to avoid precipitation of iodine. Germanium can then be determined without any other separation.

Like selenium(IV), tellurium(IV) is reduced in two steps: first Te(IV) gives Te(0) at —0.2 V vs. SCE and is adsorbed on mercury. At —0.65 V vs. SCE, Te(0) forms telluride [22]. Germanium is reduced between these two steps, but there is no apparent interference. However, the base line is greatly enhanced in presence of tellurium and even with the a.c. and d.p.p. techniques, detection limits are poorer than for germanium alone.

Arsenic, antimony, cadmium and copper do not interfere in the range 10^{-5}—10^{-4} M. Copper gives a complex with DHB, and the base line is increased slightly. As shown in Table 2, a.c. and d.p.p. often give the same results, probably because of weak adsorption of DHB, as pointed out earlier. The phase angle plays an important rôle as its value may be adjusted with precision near zero to eliminate capacitive currents; consequently, the base line can be reduced to a minimum, and d.p.p. is no better than a.c. polarography.

Application to silver alloys

Silver does not interfere. The method was therefore applied to the analysis of some germanium—silver alloys, which were prepared by fusion of known quantities of each metal for physical measurement purposes. The samples received for analysis were grey powders obtained by shaving the alloys. Mineralization of 10—20-mg samples was done by adding 5 ml of 18 M H_2SO_4 and boiling for 15 min [23]; with more than 25 mg of alloy, the solution became black. A large excess of acid was avoided in order to achieve a suitable

TABLE 2

Interferences of Pb, Cu, Cd, Sb, As, Se and Te in 1 M $HClO_4$ containing 10^{-3} M DHB

Interfering elements	Method	Detection limit (M)	Linear range (M)	Slope
10^{-5} M Cu(II)	A.c. DME	10^{-6}	$10^{-6} \rightarrow 10^{-4}$	1.00
10^{-4} M Cu(II)	A.c. DME	10^{-6}	$10^{-6} \rightarrow 10^{-4}$	1.00
10^{-4} M Cd(II)	A.c. DME	5×10^{-7}	$5 \times 10^{-7} \rightarrow 10^{-4}$	1.00
10^{-5} M As(III)	A.c. DME	2.5×10^{-7}	$2.5 \times 10^{-7} \rightarrow 10^{-4}$	1.00
10^{-4} M As(III)	A.c. DME	1.8×10^{-6}	$1.8 \times 10^{-6} \rightarrow 10^{-4}$	1.00
10^{-5} M Te(IV)	A.c. DME	5×10^{-7}	$5 \times 10^{-7} \rightarrow 10^{-4}$	1.00
5×10^{-5} M Te(IV)	A.c. DME	8×10^{-7}	$8 \times 10^{-7} \rightarrow 10^{-4}$	1.00
10^{-4} M Cu(II)	A.c. HMDE	6×10^{-8}	Average	0.70
10^{-5} M Se(IV)	A.c. DME	10^{-5}	Average	1.10
10^{-5} M Se(IV)[a]	D.p.p. DME	10^{-6}	Average	0.90
10^{-5} M Se(IV)	D.p.p. DME	3×10^{-6}	Average	$\sim$1.00
10^{-5} M Cu(II)	D.p.p. DME	10^{-6}	$10^{-6} \rightarrow 10^{-5}$	0.80
10^{-5} M As(III)	D.p.p. DME	3×10^{-6}	$3 \times 10^{-6} \rightarrow 10^{-4}$	1.00
5×10^{-5} M Sb(III)	D.p.p. DME	10^{-6}	$10^{-6} \rightarrow 10^{-4}$	1.10
10^{-5} M Pb(II)[b]	A.c. DME	10^{-6}	$10^{-6} \rightarrow 5.10^{-5}$	1.05
10^{-5} M Pb(II)[b]	D.p.p. DME	3×10^{-8}	$3 \times 10^{-8} \rightarrow 10^{-5}$	1.00

[a] 0.1 M HCl. [b] 0.01 M HCl and 4×10^{-2} M EDTA.

TABLE 3

Application to Ag—Ge alloys of various composition

Sample	Weight taken (mg)	Ge[a] theor. (mg)	Ge found (mg)	Ag by difference (mg)	Ag [a] theor. (mg)	Ag found (mg)	Ge by difference (mg)
1	23.65	3.08	3.18	20.57	20.57	20.90	2.75
2	23.20 + 8.88 Ge	11.90	11.49	20.60	20.18	20.40	11.68
3	20.30	2.00	2.00	18.30	18.30	18.33	1.97
4	15.70	1.55	1.67	14.03	14.15	13.76	1.94
5	12.30	1.60	1.84	10.46	10.70	10.86	1.44
6	11.50	1.50	1.54	9.96	10.00	10.14	1.36

[a]Calculated from the initial weights of Ag and Ge before fusion.

working medium after dilution. In mixed concentrated nitric—perchloric—sulfuric acid medium, dissolution was not complete and a white precipitate appeared. After dilution with water, germanium was determined by comparison with standard solutions of germanium dioxide. For this purpose, to a solution of 20 ml of 10^{-3} M DHB in 1 M $HClO_4$, 10 to 50 μl of known and unknown solutions were added alternately. This was necessary because excessive amounts of sulphate interfered and the germanium peak disappeared. Silver was determined by a classical potentiometric titration (Ag electrode). Results (Table 3) showed good agreement between the theoretical and found values.

In conclusion, polarography allows detection limits down to a few ppb without special instrumentation and can be useful for determinations of germanium at trace levels in aqueous solutions.

REFERENCES

1 V. A. Nazarenko, Analytical Chemistry of Germanium, J. Wiley, New York, 1974.
2 W. A. Schneider and E. B. Sandell, Mikrochim. Acta, (1954) 262.
3 D. J. Johnson, T. S. West and R. M. Dagnall, Anal. Chim. Acta, 67 (1973) 79.
4 P. Hocquellet and N. Labeyrie, Analusis, 3 (1975) 505.
5 H. P. Yule, Anal. Chem., 38 (1966) 818.
6 I. P. Alimarin and B. N. Ivanov-Emin, Zh. Prikl. Khim., 17 (1944) 204.
7 M. Prytz and T. Osterud, Chem. Zentralbl., 2 (1942) 1885.
8 A. K. Das Gupta and C. K. Nair, J. Sci. Ind. Res. Sect. B, 10 (1951) 322.
9 A. K. Das Gupta and C. K. Nair, Anal. Chim. Acta, 9 (1953) 287.
10 J. Bognar and K. Toth, Mikrochim. Acta, (1966) 526.
11 M. L. Borlera, Ric, Sci., 29 (1959) 100.
12 R. G. Canham, D. A. Aikens, N. Winograd and G. Mazepa, J. Phys. Chem., 74 (1970) 1082.
13 N. Konopik, Fresenius Z. Anal. Chem., 186 (1962) 127.
14 I. A. Tserkovnitskaya and V. N. Epimakhov, Zh. Anal. Khim., 20 (1965) 688.

15 V. Stejskal and M. Bartusek, Collect. Czech. Chem. Commun., 38 (1973) 3103.
16 H. Vandebroek and F. Verbeek, Anal. Lett., 5 (1972) 317.
17 A. M. Shafiqul Alam, Thèse Doctorat ès-Sciences, Lyon n° 77-30, 1977.
18 A. M. Shafiqul Alam, O. Vittori and M. Porthault, to be published.
19 A. M. Shafiqul Alam, O. Vittori and M. Porthault, J. Electroanal. Chem., 61 (1975) 191.
20 J. J. Lingane and L. W. Niedrach, J. Am. Chem. Soc., 70 (1948) 1997, 4115.
21 G. D. Christian, E. C. Knoblock and W. C. Purdy, Anal. Chem., 35 (1963) 1128.
22 M. Volaire, O. Vittori and M. Porthault, Bull. Soc. Chim. Fr., (1974) 2415; Anal. Chim. Acta, 71 (1974) 185.
23 P. R. Falkner, Mikrochim. Acta, (1968) 1273.

Analytica Chimica Acta, 102 (1978) 121—131

POLAROGRAPHIC STUDY OF AN ALKYL BENZIMIDAZOLYL SULFOXIDE AND THE CORRESPONDING SULFIDE AND SULFONE

BO-LENNART JOHANSSON and BJÖRN PERSSON*

Department of Analytical Chemistry, University of Uppsala, P.O.B. 531, S-751 21 Uppsala 1 (Sweden)

(Received 22nd May 1978)

SUMMARY

2-(5-Methylbenzimidazolyl) 1-(2-pyridyl)ethyl sulfide, 2-(5-methylbenzimidazolyl) 1-(2-pyridyl)ethyl sulfoxide and 2-(5-methylbenzimidazolyl) 1-(2-pyridyl-1-oxide)ethyl sulfone are reduced at a dropping mercury electrode in aqueous ethanol. Coulometric experiments at a mercury pool prove that 2-ethylpyridine and 2-mercapto-5-methylbenzimidazole are formed in the reduction process of the sulfide and the sulfoxide. Coulometric reduction of the sulfone results in some conversion of the pyridine-1-oxide group together with a reductive fission of the ethyl—sulfonyl bond. One of these fission products undergoes secondary reactions. The concentration of 2-benzimidazolyl 2-pyridyl methyl sulfoxide in a pharmaceutical formulation has been determined by differential pulse polarography.

Recently, 2-(5-methylbenzimidazolyl) 1-(2-pyridyl)ethyl sulfoxide (II) and 2-benzimidazolyl 2-pyridylmethyl sulfoxide (III) have been tested as gastric secretion inhibitors. The synthesis of the sulfoxides by chemical oxidation of the corresponding sulfides (e.g. 2-(5-methylbenzimidazolyl) 1-(2-pyridyl)-ethyl sulfide (I)) implies that the related sulfones (e.g. 2-(5-methylbenzimidazolyl) 1-(2-pyridyl-1-oxide)ethyl sulfone (IV)) appear in the raw products of the sulfoxides. Presently, liquid chromatography is applied for the assay of alkyl benzimidazolyl sulfoxides in pharmaceutical formulations. In order to find a reference method for the determination of this type of sulfoxide and the related sulfides and sulfones it was of interest to investigate the polarographic behaviour of compounds I—IV.

I

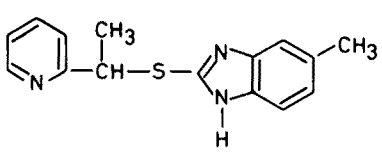

II

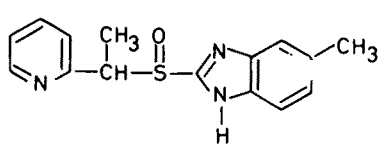

* Present address: Analytical Chemistry and Biochemistry, AB Hässe, Fack, S-43120 Möhndal (Sweden).

III

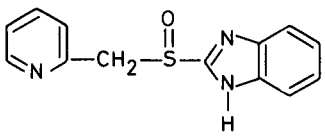

IV

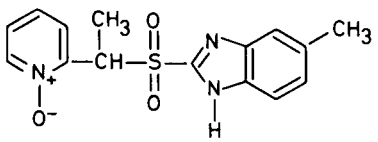

V

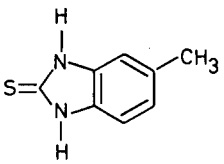

The polarographic half-wave potentials of diaryl or alkyl aryl sulfides, sulfoxides and sulfones range from —2 V vs. SCE to even more negative potentials. A sulfinate anion and a hydrocarbon are formed in the reduction of a sulfone, which consumes 2 electrons per molecule [1]. Sulfoxides are reduced by 2 electrons to the corresponding sulfides [2]. The electrode process for the sulfide involves 2 electrons per molecule and results in fission of one of the carbon—sulfur bonds [3]. Generally, the very negative half-wave potentials render polarography an unattractive method for the determination of diaryl or alkyl aryl sulfur compounds. However, a strong interaction betwee the sulfur-containing group and groups attached to the sulfur atom may result in more positive reduction potentials for certain classes of sulfur compounds [4]. In molecules of types I—IV, the sulfur-containing group and the benzimidazolyl ring system interact through resonance. Apart from the protor tautomerism of the benzimidazolyl group, where the proton may be bound to either of the two nitrogen atoms, 2-mercapto-5-methylbenzimidazole, like thiourea and 2-mercaptoimidazole, may exist as a thiol as well as a thione (e.g., V).

EXPERIMENTAL

Chemicals

The 2-(5-methylbenzimidazolyl) 1-(2-pyridyl)ethyl sulfide used (m.p. 140°C) gave the following elemental analysis: 66.7% C, 5.7% H, 15.6% N. The 2-(5-methylbenzimidazolyl) 1-(2-pyridyl)ethyl sulfoxide (m.p. 156°C) gave 63.0% C, 5.4% H, 14.7% N and the 2-benzimidazolyl 2-pyridyl methyl sulfoxide (m.p. 156°C) gave 60.6% C, 4.2% H, 16.2% N. The 2-(5-methylbenzimidazolyl) 1-(2-pyridyl-1-oxide)ethyl sulfone (m.p. 218°C) gave 56.9% C, 5.0% H and 13.1% N. Mass spectra, n.m.r. spectra and i.r. spectra of the sulfide (I), sulfoxide (II) and sulfone (IV) were consistent with the presumed

chemical structures. Formic acid and 1,2-diamino-4-methylbenzene were used as starting materials in the synthesis of 5-methylbenzimidazole [5]. The 2-ethylpyridine-1-oxide was prepared by oxidation of 2-ethylpyridine with hydrogen peroxide in acetic acid [6].

The aqueous alcoholic buffer solutions contained 40% (v/v) ethanol. The following acids and buffers were used: perchloric acid, pH 1.8 and 2.4; acetate, pH 5.5; phosphate, pH 7.7; and borate, pH 10.7. The pH readings were taken in the aqueous alcoholic buffer solutions with a pH meter standardized against aqueous buffer solutions.

Apparatus and general procedure

A PAR Model 170 was used for the electrochemical measurements. The experiments were performed at 21.0 ± 0.1°C; all potentials refer to the saturated calomel electrode. The drop time of the dropping mercury electrode at pH 7.7 was 4.18 s at open circuit with a mercury flow rate of 2.00 mg s^{-1} and 486 torr. In d.c. polarography the influence of the mercury pressure on the wave height was tested between 280 and 880 torr. Differential pulse polarography, normal pulse polarography, phase-sensitive a.c. polarography and sampled d.c. polarography were applied, at a controlled drop time of 2 s and a potential scan rate of 2 mV s^{-1}. In differential pulse polarography, the pulse amplitude was 25 mV. The voltage amplitude in a.c. polarography was 5 mV. All polarograms were recorded in the presence of 0.001% Triton X-100 in the test solutions.

During the coulometric experiments, which were carried out at controlled potential in a volume of 5—20 ml over a mercury pool (8 cm^2), the current as well as the current integral were recorded as a function of time.

Procedure for the polarographic determination of 2-benzimidazolyl 2-pyridylmethyl sulfoxide (III) in a pharmaceutical formulation

The tablets (50 mg) were extracted with 25 ml of ethanol for at least 5 min, after which the alcoholic solution was centrifuged. The centrifugate (0.5 ml) was added to the polarographic cell, containing 5 ml of aqueous 40% ethanolic phosphate buffer (pH 7.7). The differential pulse polarogram was recorded between −0.6 and −1.4 V. The concentration of (III) was evaluated from a calibration graph, in which the peak currents of the sulfoxide standard solutions (concentration of sulfoxide < 0.3 mM) were plotted against the corresponding concentrations of sulfoxide.

Procedures for product analysis in the coulometric experiments

In the coulometric experiments with the sulfide (I) and the sulfoxide (II), u.v. spectroscopy and thin-layer chromatography (t.l.c.) were applied to the identification of 2-ethylpyridine and 2-mercapto-5-methylbenzimidazole. For the u.v. measurements, 2-ethylpyridine and 2-mercapto-5-methylbenzimidazole were separated from each other by extraction of the catholyte with diethyl ether at pH 13. The t.l.c. was carried out on silica gel plates with chloroform/ethanol (9:1) as eluant. The concentration of 2-ethylpyridine was determined by gas chromatography (g.c.) on a QF-1 column (solid

support coated with sodium hydroxide) at 72°C with 2,4,6-trimethylpyridine as internal standard.

Quantitative analysis for 2-mercapto-5-methylbenzimidazole was done by coulometry at E = 0.1 V. During the coulometric experiments with the sulfoxide (II), formation of the sulfide (I) was tested by g.c. on a SE-30 column at 240°C. The sulfoxide was reduced at potentials corresponding to the beginning as well as the top of the d.c. polarographic wave recorded for the sulfoxide. The sample of sulfoxide used in these experiments, contained 0.1% of sulfide; during the coulometric experiments the concentration of sulfide in the catholyte did not exceed the concentration which corresponded to this degree of impurity.

When 2-(5-methylbenzimidazolyl) 1-(2-pyridyl-1-oxide)ethyl sulfone (IV) was reduced, the following compounds were identified in the catholyte by t.l.c. on silica gel plates with chloroform/ethanol (4:1) as eluant: 2-ethylpyridine, 2-ethylpyridine-1-oxide and 5-methylbenzimidazole. The identity of 2-ethylpyridine-1-oxide and 5-methylbenzimidazole was also proved by gas chromatography—mass spectrometry and the concentrations of these two compounds in the catholyte were determined by g.c. on a Carbowax 20 M column (solid support coated with sodium hydroxide) at 220°C. The determination of 2-ethylpyridine by g.c. was done as described above.

In the catholyte from the coulometric reduction of the sulfone, the total amount of sulfur was determined as methylene blue [7]. The catholyte was extracted with chloroform to remove most of the reduction products which did not contain sulfur. The aqueous phase was first treated with hydrogen peroxide to oxidize sulfur compounds. The sensitivity of the method towards sulfur in the various organic compounds undoubtedly differs, hence the results of the sulfur determination must be regarded as minimal values of the total sulfur content. The presence of sulfite in the catholyte (reduction of sulfone at pH 7.7) was tested by differential pulse polarography (peak potential, —0.05 V) and by the sodium nitroprusside—zinc sulfate colour reaction. Under the experimental conditions the detection limits for sulfite were 0.5 mM by differential pulse polarography and 1.5 mM by the nitroprusside test. The initial concentration of sulfone was 3 mM and the concentration of sulfite in the reduction product was below these detection limits.

RESULTS

Polarographic behavior of the sulfide, sulfoxide and sulfone

One peak appeared in the differential pulse polarograms of the sulfide (I) and sulfoxide (II), but the polarograms of the sulfone (IV) showed two peaks. For the sulfone the peak potential (E_p) of the peak at the more negative potential coincided with E_p of 2-ethylpyridine-1-oxide. Since E_p of the sulfoxide was 0.2 V more positive than that of the sulfone (the more positive peak) it was possible to detect the sulfone in presence of the sulfoxide by differential pulse polarography, provided that the amount of sulfone was >3% of the amount of sulfoxide (Fig. 1). The peak potentials, peak currents

(i_p) and peak half-widths ($w_{1/2}$ = width of the peak at half the peak height) were dependent on pH (Table 1). The ratio $\Delta E_p/\Delta$pH was 100 mV for the sulfide in the pH interval 2—11, 80 mV for the sulfoxide at pH 6—11 and 90 mV for the sulfone (more positive peak) at pH 2—8. Polarographic studies of the sulfoxide in an acidic medium were impossible because of decomposition reactions. At pH 10.7, comparatively small polarographic currents were obtained for the sulfide and the sulfoxide (Table 1). Although the sulfone was stable in borate solutions, it did not give rise to any polarographic currents at pH 10.7.

The differential pulse polarographic peaks were broadened and E_p became more negative with increasing concentration of depolarizer (Table 2). The ratio between i_p and concentration decreased with increasing concentration (Fig.2 and Table 2). However, in sampled d.c. polarography the limiting currents were proportional to the concentration (Fig. 2). Polarographic n-values (Table 2) were estimated from the wave heights in sampled d.c. polarography, assuming n = 2 electrons per molecule for the sulfide and equal diffusion coefficients of the three substances. The n-value of the sulfone was calculated for the wave at the more positive potential.

For the sulfide (I), sulfoxide (II) and sulfone (IV) (more positive wave), the influence of the mercury pressure on the d.c. polarographic wave heights proved that these were diffusion-controlled.

In the normal pulse polarograms a peak appeared on top of the wave (Fig. 3, curve a). Besides a small faradaic peak at −1 V the a.c. polarograms of the three compounds showed a tensammetric peak at 0 V (Fig. 3, curves b and c).

TABLE 1

Influence of pH on the differential pulse polarographic peak potential, peak current, and peak half-width and on the limiting current in sampled d.c. polarography for compounds (I), (II) and (IV) in aqueous 40% ethanol

Compound	Concn. (mM)	pH	E_p (V vs. SCE)	$i_p c^{-1}$ (mA l mol^{-1})	$w_{1/2}$ (mV)	$i_d c^{-1}$ (mA l mol^{-1})
Sulfide	0.27	10.7	−1.33	9.4	118	3.0
		7.7	−1.04	11.4	160	3.6
		5.5	−0.81	18.3	95	3.4
		1.8	−0.45	12.4	125	3.1
Sulfoxide	0.21	10.7	−1.24	0.8	195	1.1
		7.7	−0.99	31.8	115	7.3
		5.5	−0.85	31.9	115	7.3
Sulfone	0.20	7.7	−1.21, a	20.0, a	121, a	5.5, a
		5.5	−1.07, −1.35	20.4, 2.0	125, 90	6.0, 0.6
		1.8	−0.70, −1.04	17.8, 9.5	106, 120	3.7, 4.0

[a]Incomplete resolution from background.

TABLE 2

Dependence of differential pulse polarographic peak potential, peak half-width and peak current on the concentration of compounds (I), (II) and (IV) in aqueous 40% ethanol (pH 7.7).

Compound	Concn. (mM)	E_p (V vs. SCE)	$w_{1/2}$ (mV)	$i_p c^{-1}$ (mA l mol^{-1})	n^b (F mol^{-1})
Sulfide	0.028	−1.02	145	13.2	2.0
	0.27	−1.04	160	11.4	2.0
Sulfoxide	0.032	−0.99	117	32.6	4.0
	0.92	−1.06	142	21.9	4.0
Sulfone	0.045	−1.20, a	108, a	24.7, a	3.1
	0.65	−1.29, −1.52	146, 140	14.7, 1.7	2.8

[a]Incomplete resolution from background. [b]Number of electrons measured by sampled d.c. polarography.

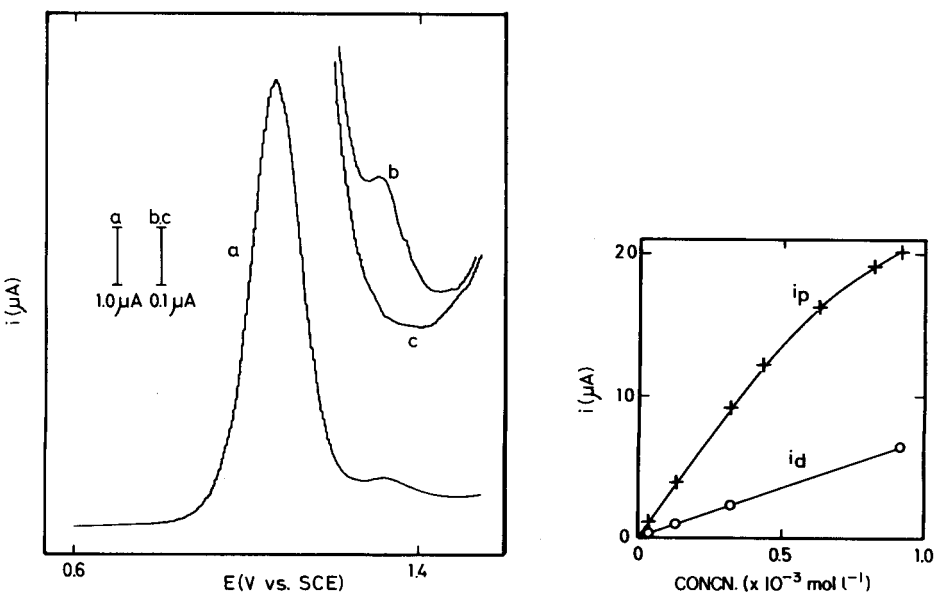

Fig. 1. Differential pulse polarograms: (a) and (b) of the mixture 0.28 mM (II) and 0.011 mM (IV) in aqueous 40% ethanol (pH 7.7); (c) of 0.28 mM (II) in the absence of (IV).

Fig. 2. Dependence of peak current in differential pulse polarography (i_p) and limiting current in sampled d.c. polarography (i_d) on the concentration of (II) in aqueous 40% ethanol at pH 7.7.

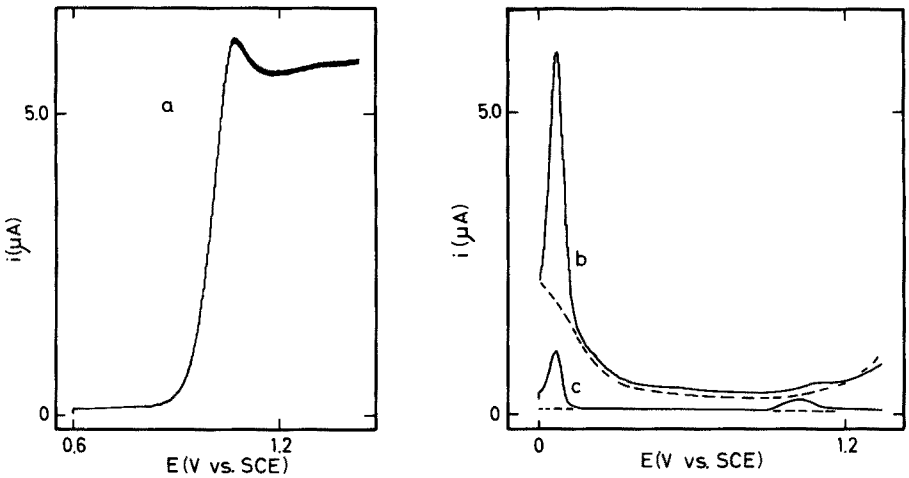

Fig. 3. Polarograms of 0.22 mM (II) in aqueous 40% ethanol at pH 7.7: (a) normal pulse polarogram with initial potential —0.6 V; (b) and (c) a.c. polarograms with phase-sensitive detection and current sampling of (II) (—) and the supporting electrolyte (- -). Frequency, 65 Hz; a.c. measured (b) 90° out of phase, (c) in phase with the applied alternating voltage.

Determination of the sulfoxide in a pharmaceutical formulation

Since 2-(5-methylbenzimidazolyl) 1-(2-pyridyl)ethyl sulfoxide (II) and 2-benzimidazolyl 2-pyridylmethyl sulfoxide (III) showed the same polarographic behavior, it was possible to apply differential pulse polarography to the determination of (III) in a pharmaceutical formulation. Tablet A (based on a mixture of lactose and starch with povidone as dispersing agent) was found to contain 14.9 ± 0.1% sulfoxide. The percentage of (III) in tablet B (which besides having a coating of a poly(methacrylic acid) derivative, Eudragit L, was of the same composition as tablet A) was 16.3 ± 0.2%. The sulfoxide contents were also determined by liquid chromatography; the results were 15.5 ± 0.5% (tablet A) and 16.5 ± 0.5% (tablet B).

Coulometric reduction of the sulfide, sulfoxide and sulfone

In the coulometric experiments on the sulfide (I) and sulfoxide (II), the amount of 2-ethylpyridine and 2-mercapto-5-methylbenzimidazole in the reduction product corresponded to >90% of the amount of starting material (Table 3). The sulfide consumed 2 electrons and the sulfoxide 4 electrons per molecule in the reduction process.

Coulometric reduction of the sulfone (IV) at —1.3 V and pH 7.7 resulted in the formation of 2-ethylpyridine, 2-ethylpyridine-1-oxide and 5-methylbenzimidazole (Table 3). The same substances were obtained when the sulfone was electrolyzed at —0.9 V in an acidic medium. When the reduction potential was —1.1 V at pH 2.4, 2-ethylpyridine-1-oxide was reduced quantitatively to 2-ethylpyridine (Table 3). (The half-wave potential of 2-ethyl-

TABLE 3

Coulometric reduction at controlled potential of compounds (I), (II) and (IV), with analysis of the reduction products.

Compound	Quantity (μmol)	pH	*E* (V vs. SCE)	*n* (F mol^{-1})	2-Ethylpyridine (μmol)	2-Ethylpyridine-1-oxide (μmol)	2-Mercapto-5-methylbenzimidazole (μmol)	5-Methylbenzimidazole (μmol)
Sulfide	2.54	7.7	−1.25	2.0	2.50		2.39	
	3.99	7.7	−1.25	2.0	3.68		3.97	
Sulfoxide	2.50	7.7	−1.25	4.0	2.28		2.26	
	3.48	7.7	−1.25	4.0	3.35		3.43	
Sulfone	30.8	7.7	−1.30	2.9	18	8		23
	15.3	2.4	−0.90	2.6	3	10		14
	15.3	2.4	−1.10	5.0	16	<0.1		14

pyridine-1-oxide was —1.1 V in the acidic medium.) As the sulfone was reduced at pH 7.7 the total sulfur in the catholyte amounted to 55% of the starting amount of sulfone.

DISCUSSION

The coulometric experiments prove that the electrochemical reduction of compounds (I) and (II) consumes 2 and 4 electrons per molecule, respectively, and leads to fission of a carbon—sulfur bond (Table 3). In these respects, the electrochemical properties of the sulfide and sulfoxide are in accordance with the general reduction pattern of sulfides and sulfoxides [2, 3]. Since the ratio between the diffusion currents of the sulfide and sulfoxide is 1:2, the same overall equations are proposed for the coulometric and polarographic reduction processes:

$$RSR' + 2H^+ + 2e^- \rightarrow R'SH + RH \quad (1)$$

$$RS(O)R' + 4H^+ + 4e^- \rightarrow R'SH + RH + H_2O \quad (2)$$

where R = 1-(2-pyridyl)ethyl- and R′ = 2-(5-methylbenzimidazolyl)-. As a rule, the reduction potentials of sulfides and sulfoxides are more negative than the polarographic peak potentials of the sulfide (I) and sulfoxide (II). The more positive reduction potentials of compounds (I) and (II), which are almost coincident, reflect the interaction between the sulfur atom and the benzimidazolyl ring system. Unlike an alkyl aryl sulfoxide or a diaryl sulfoxide, 2-(5-methylbenzimidazolyl) 1-(2-pyridyl)ethyl sulfoxide is reduced to the thiol in one main step. A similar reduction pathway has been described for the β-ketosulfoxides [8].

As confirmed by reduction at controlled potential at pH 2.4 (Table 3), compound (IV) contains two electroactive groups, the sulfonyl group and the *N*-oxide function. In the differential pulse polarograms (Tables 1 and 2) the peak at more positive potentials involves reduction of the sulfonyl group and the peak at more negative potentials involves reduction of the *N*-oxide group. Pyridine-1-oxides are reduced by 2 electrons per molecule to the corresponding pyridines [9]. Such a reduction scheme also applies to the *N*-oxide function of the sulfone (IV). The decrease in the polarographic current of the pyridine-1-oxides with increasing pH (caused by the finite rate of a preprotonation reaction [9]) is observed for the *N*-oxide group of the sulfone as well.

The characteristic polarographic potentials for the reduction of the sulfonyl group in the sulfone (IV) are more positive than the potentials reported for simple alkyl aryl sulfones. The presence of 2-ethylpyridine and 2-ethylpyridine-1-oxide together with 5-methylbenzimidazole in the catholyte (Table 3) verifies the cleavage of two carbon—sulfur bonds in the coulometric reduction of the sulfone. Coulometric and polarographic *n*-values for the sulfonyl reduction are significantly larger than the 2 electrons per molecule expected for a sulfone (Tables 2 and 3), but are still not large enough to

account for a reductive fission of two bonds, requiring at least 4 electrons. Considering the general reduction mechanism for a sulfone [1], the following scheme is proposed for the electrochemical reduction of the sulfonyl group of substance (IV)

$$R''SO_2R' + H^+ + 2e^- \rightarrow R'SO_2^- + R''H \quad (3)$$

$$R'SO_2^- \rightarrow R'H + \text{products} \quad (4)$$

where R′ = 2-(5-methylbenzimidazolyl)- and R″ = 1-(2-pyridyl-1-oxide)ethyl-. The suggested intermediate, the 2-(5-methylbenzimidazole) sulfinate ion, could not be identified during the coulometric experiments, nor was it possible to establish the form (probably inorganic) in which sulfur existed in the catholyte. Structurally related sulfinate anions, like 2-imidazolesulfinate [10] and aminoiminomethanesulfinate [11], are unstable and the carbon—sulfur bond is cleaved in the disintegration reactions. Under polarographic conditions the disintegration of 2-(5-methylbenzimidazole)sulfinate must involve an electrochemical step to account for an apparent *n*-value of about 3 electrons per molecule (Table 2).

Polarographic behavior of the sulfide, sulfoxide and sulfone

The influence of pH on the polarographic currents (Table 1) can be related to the acid-base properties of the compounds (I), (II) and (IV). In alkaline medium the hydrogen-nitrogen bond of the benzimidazolyl ring system dissociates with formation of a proton and an anion. As proved by titration with 0.01 M sodium hydroxide in aqueous 40% ethanol, the dissociation constant (K_A) of this reaction decreases in the order sulfone ($K_A = 3 \times 10^{-9}$ M) > sulfoxide (10^{-10} M) > sulfide ($<10^{-11}$ M). The anion, which for the sulfoxide and sulfone predominates in alkaline media, seems to be electroinactive. At pH 10.7 the polarographic currents of the sulfoxide and the sulfone are determined by the rate of the recombination reaction [12] to give the neutral benzimidazole derivative, which *is* electroactive.

In differential pulse polarography an increase in concentration of sulfide, sulfoxide or sulfone is connected with a shift of the peak potential towards more negative potentials, a peak broadening and a decrease in $i_p c^{-1}$ (Table 2). With fast electron-transfer reactions, these effects can arise from coupling between an electron-transfer process and adsorption of the reactant at the mercury—solution interface [13]. In normal pulse polarograms a peak on top of the polarographic wave (Fig. 3, curve a) is typical of a fast charge-transfer reaction coupled with reactant adsorption [14, 15]. Adsorption of compounds (I), (II) and (IV) at the mercury—solution interface is confirmed by the large capacitive peak at 0 V in the a.c. polarograms of these substances (Fig. 3, curve b). The small a.c. polarographic peak at —1 V (Fig. 3, curve c) reflects the small rate constant of the electrode process. Thus, the influence of reactant adsorption on the shape of differential pulse polarographic peaks and also on the shape of normal pulse polarographic waves can be of the

same character for slow charge-transfer reactions as for fast electron-transfer processes.

Polarographic determination of sulfoxide (III)

Differential pulse polarography offers a convenient method for the determination of 2-benzimidazolyl 2-pyridylmethyl sulfoxide in pharmaceutical formulations. For tablets A and B the base constituents did not interfere in the polarographic measurement. The following substances would interfere in polarographic analysis for the sulfoxide: 2-benzimidazolyl 2-pyridylmethyl sulfide and an unidentified product from acid-catalyzed cleavage of the sulfoxide. Because of the non-linearity of the calibration curve, constructed for the interval $10^{-7}-10^{-3}$ M, the concentration of sulfoxide in standards and test solutions should not exceed 0.3 mM. The relative standard deviation of four measurements of the peak current was 0.5%, when different test solutions were used from the same centrifugate. In three independent determinations of the sulfoxide concentration in the tablets the relative standard deviation was $< 1\%$. The sulfoxide concentrations measured by differential pulse polarography were in accordance with the results obtained by liquid chromatography.

A grant from AB Hässle is gratefully acknowledged. The compounds (I)—(V) and the results of the liquid chromatographic analysis were generously furnished by AB Hässle.

REFERENCES

1 L. Horner, in M. M. Baizer (Ed.), Organic Electrochemistry, M. Dekker, New York, 1973, p. 746.
2 R. C. Bowers and H. D. Russell, Anal. Chem., 32 (1960) 405.
3 R. Gerdil, J. Chem. Soc. B, (1966) 1071.
4 B. Lamm and B. Samuelsson, Acta Chem. Scand., 24 (1970) 561.
5 E. C. Wagner and W. H. Millett, Org. Synth. Coll. Vol. II, (1943) 65.
6 E. Ochiai, J. Org. Chem., 18 (1953) 534.
7 L. Gustafsson, Talanta, 4 (1960) 227.
8 B. Lamm and B. Samuelsson, Acta Chem. Scand., 23 (1969) 691.
9 T. Kubota and H. Miyazaki, Bull. Chem. Soc. Jpn., 39 (1966) 2057.
10 R. A. F. Bullerwell, J. Polarogr. Soc., 9 (1963) 7.
11 J. E. McGill and F. Lindstrom, Anal. Chem., 49 (1977) 26.
12 J. Heyrovský and J. Kůta, Principles of Polarography, Academic Press, New York, 1966, p. 360.
13 J. B. Flanagan, K. Takahashi and F. C. Anson, J. Electroanal. Chem., 81 (1977) 261.
14 G. C. Barker and J. A. Bolzan, Fresenius Z. Anal. Chem., 216 (1966) 215.
15 J. B. Flanagan, K. Takahashi and F. C. Anson, J. Electroanal. Chem., 85 (1977) 257.

Analytica Chimica Acta, 102 (1978) 133—140

PULSE POLAROGRAPHIC DETERMINATIONS OF NITROSAMINES
Part I. Determination of *N*-Nitrosodiethanolamines in Grinding Fluids

ROBERT SAMUELSSON

Department of Analytical Chemistry, University of Umeå, S-901 87 Umeå (Sweden)

(Received 17th May 1978)

SUMMARY

Differential pulse polarography is assessed as a method for the determination of *N*-nitrosodiethanolamine (NDEA) in aqueous media. Optimum conditions with respect to pH and supporting electrolyte are found with simple mineral acid solutions (H_2SO_4) at pH 1—2. Detection limits in this medium are of the order 5×10^{-8} M NDEA. The procedure is applied to the direct determination of NDEA in commercially available grinding fluids which contain, on manufacture, precursors for nitrosamine formation. High concentrations of NDEA were found (75 μM) with an estimated accuracy better than 92% and a precision of ±8%.

The family of chemicals known as nitrosamines is among the most potent cancer-causing substances so far discovered. Since Magee and Barnes [1] discovered that dimethylnitrosamine caused malignant tumours in the rat, more than 120 *N*-nitroso compounds have been tested for carcinogenicity in animals and about 80% of them induced tumours of one kind or another [2]. Epidemiological studies on the possible role of nitrosamines in causing human cancer have so far been inconclusive. Nevertheless there are strong indications that nitrosamines may contribute significantly to the worldwide occurrence of human cancer [3].

N-Nitroso compounds are readily formed by the reaction of secondary or tertiary amines with nitrosating agents, the commonest of which in aqueous systems is the nitrite ion. Nitrite is formed by bacterial reduction of nitrate, for example, in the mouth, and is often present in preserved food. Usual sources of secondary and tertiary amines are food, drugs, medicines and agricultural chemicals [3]. Although the optimum pH for the reaction is about pH 3, nitrosamines can be formed in strongly acidic or neutral conditions, or even in alkaline solutions, e.g. in the presence of certain carbonyl compounds [4]. Thus nitrosoamines may be formed in almost any system containing the precursors, e.g. fried bacon [5, 6], smoked fish [6, 7], grinding fluids [8] and even in the human stomach [9].

Studies of the prevalence, toxicity and significance to public health of nitrosamines require analyses at the 1—10 $\mu g\ kg^{-1}$ level [10]. The most widely used technique is gas chromatography combined with various detectors,

such as the nitrogen-specific Coulson electrolytic conductivity detector [6], the alkali flame ionization detector [6], the mass spectrometric (m.s.) detector [11] and the thermal energy analyzer (t.e.a.) detector [12]. Of these techniques only the g.c.—m.s. and g.c.—t.e.a. systems now provide both qualitative and quantitative information sufficiently reliable for routine analytical operation, but the g.c.—m.s. analysis is time-consuming and expensive. Both can be applied only to volatile compounds.

Polarography can be used for the determination of nitrosamines [10, 13—17], and has the advantage that it can be applied to both volatile and involatile compounds. Although the direct-current (d.c.) technique lacks sensitivity, the development of pulse techniques during recent years has made analysis in the 1—10 $\mu g\ kg^{-1}$ range possible.

This paper describes a pulse polarographic method for the direct determination of *N*-nitrosodiethanolamine (NDEA) in grinding fluids. Some grinding fluids contain relatively high levels of diethanolamine (DEA) and nitrite. One would expect NDEA to be formed in such fluids, and as NDEA is carcinogenic [18] these liquids constitute hazards for people handling them.

EXPERIMENTAL

Materials

All chemicals used were of analytical grade. The tetraalkylammonium salts were purified as described earlier [19]. *N*-Nitrosodiethanolamine was synthesized as described earlier [10]. Diethanolamine (16.4 mg; Merck zur Synthese) was dissolved in 80 ml of 0.1 M HCl, and 0.69 g $NaNO_3$ (Merck p.a.) was added slowly with cooling in a cold water bath. After reacting for 1 day, the solution was purged from nitrite with a gas stream of N_2 [10] and diluted to 100 ml with 0.1 M HCl. The stock solutions, 1.56×10^{-3} M and 1.56×10^{-4} M, were prepared in 0.1 M HCl and 0.01 M HCl, respectively. They were stable for over 6 months.

The concentrated grinding fluids which were examined have the following main composition: 12—20% triethanolamine (TEA) (technical grade), 20% nitrite, 0.02% fluorescein and water. Technical triethanolamine consists of 85% triethanolamine with 15% mono- and diethanolamine. Before use in industry, these concentrations are diluted with water to a final concentration of about 1—2%. The fluids had been stored over a period of four years before analysis.

Instrumentation

The model 174 polarographic analyzer used (Princeton Applied Research Corp., Princeton, N.J.) was equipped with a model 174/70 drop timer, and was connected to an Omnigraph model 2000 *X*—*Y* recorder (Houston Instrument Co., Austin, Texas). The capillary used had a mercury flow rate (m) of

2.42 mg s^{-1} and a natural drop time (t_d) of 3.40 s in 0.1 M potassium chloride at open circuit and at a mercury height (h_{uncorr}) of 57 cm.

The potential was measured against a saturated calomel reference electrode (SCE) and a carbon rod was used as counter electrode. Except as noted, the following instrumental parameters were used in all experiments: scan rate, 2 mV s^{-1}; modulation amplitude, −50 mV; drop time, 2 s; h_{uncorr}, 57 cm. Presaturated nitrogen was used to deoxygenate the solutions. pH was measured with a Metrohm EA 147X combined glass electrode and Orion model 701 digital pH meter. The temperature during the experiments was 22 ± 1°C. All pH measurements above pH 2.5 were made in Britton-Robinson buffers. Below pH 2.5, HCl was used to adjust pH.

RESULTS

Optimization of method for determining NDEA

Effects of pH. The effect of pH on the nitrosamine reduction peak potentials, E_p, is shown in Fig. 1A. Reduction occurred over the whole pH interval 0—13, but the wave was not well separated from the background at pH 5.25—6.75. The curve can be divided into four pH intervals. In the first interval between pH 0 and 2.5 the slope is 101 ± 7.3 mV/pH; between pH 2.5 and 4.25 the slope is 79 ± 1.3 mV/pH; in the third between pH 4.25 and 5.5 the slope is 152 ± 3.0 mV/pH; and in the fourth interval above pH 6.5, E_p is independent of pH. The pH dependence was determined twice with different pH electrodes. Similar results were obtained in both cases.

The effect of pH on the reduction peak current is shown in Fig. 1B. The curve consists of two intervals. The first covers the range pH 0—5.5, which has a maximum at ca. pH 2.5 and a minimum value of the half-peak width (ca. 100 mV) at the same pH. The second interval lies above pH 6.5; the maximum current is obtained at ca. pH 7.75 and the half-peak width is about 150 mV throughout the pH interval.

Effect of various electrolytes. The reduction of nitrosodiethanolamine was examined in various electrolytes; the results are summarized in Table 1.

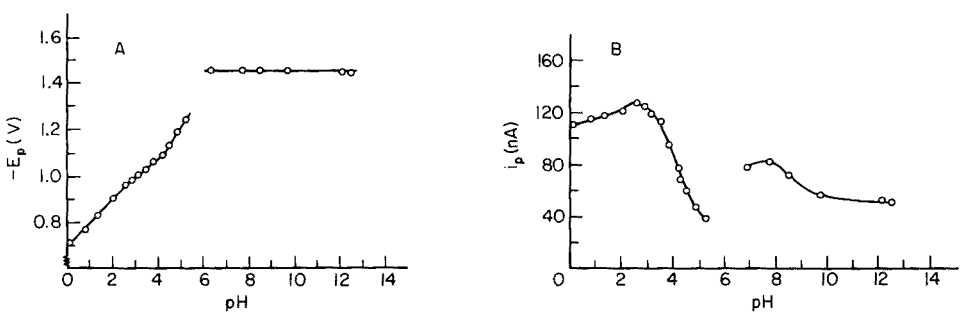

Fig. 1. Effect of pH on (A) peak potentials and (B) peak currents for *N*-nitrosodiethanolamine. Conditions: 1.56 × 10^{-5} M NDEA; h_{uncorr}, 42 cm; drop time, 1 s.

TABLE 1

Effect of various supporting electrolytes on the determination of *N*-nitrosodiethanolamine in aqueous media

Electrolyte	pH	E_p (mV)	Sensitivity (nA μM^{-1})	S (nA)	Detection limit (μM)
0.1 M H_2SO_4[a]	0.91	−785	11.55	0.2196	0.073
0.01 M H_2SO_4[a]	1.45	−839	11.56	0.1466	0.045
0.1 M HCl[a]	1.07	−799	11.18	0.4866	0.147
Tartrate buffer[b]	1.79	−862	11.21	0.1264	0.046
B—R buffer + 0.1 M LiCl[b]	2.61	−970	11.31	0.2691	0.096
HCl, KCl buffer[b]	1.78	−873	10.76	0.1629	0.061
Citrate buffer[b]	1.84	−875	9.85	0.7071	0.241
0.1 M H_2SO_4 + 0.5 mM TEAP[b]	0.91	−813	10.05	0.2822	0.113
0.1 M H_2SO_4 + 0.5 mM TPAP[b]	0.91	−875	9.15	0.2251	0.099
0.1 M H_2SO_4 + 0.5 mM TBAP[b,c]	0.91	—	—	—	—
0.1 M H_2SO_4 + 0.25 mM TBAP[b,d]	0.91	−1050	6.05	0.0689	0.046
0.1 M H_2SO_4 + 0.1 mM TBAP[b]	0.91	−845	8.56	0.0832	0.039

[a]Mean of duplicates. [b]Single determinations. [c]Not separated from background. [d]Not well separated from background.

Significant decreases in sensitivity were observed for the HCl—KCl buffer and the citrate buffer. A successive decrease in sensitivity was found for the various tetraalkylammonium salts, as well as changes in the peak potentials. The background current for 0.1 M H_2SO_4 + 0.1 mM TBAP was lowered by a factor of 4 compared with 0.1 M H_2SO_4 alone. Detection limits (*dl*) were calculated by the procedure of Skogerboe and Grant [20], i.e. $dl = t \cdot s/m$, where t is the t statistic at the 99% confidence level, s the standard deviation of the calibration curve and m the slope of the curve. Typical differential pulse polarograms with a mineral acid and a buffer as supporting electrolyte are shown in Figs. 2 and 3, respectively. The calibration graph pertaining to Fig. 2 was linear over the whole range. The difference in slope of the base lines in Figs. 2 and 3 should be noted. Investigation of the effect of Triton X-100 showed a small decrease in sensitivity at a concentration of 10^{-3}%, and the E_p value was shifted cathodically by about 10 mV. At a concentration of 10^{-2}% Triton X-100, the reduction was fully inhibited.

Linearity was examined with 0.01 M H_2SO_4 and 0.1 M HCl. In both cases linearity extended beyond an upper concentration limit of 1.5×10^{-5} M.

Determination of NDEA in synthetic and real samples

Synthetic samples. To solutions containing 0.17% TEA (p.a.), 0.03% DEA (p.a.), 2×10^{-4}% fluorescein and 5% ammonium sulphamate in 0.1 M H_2SO_4 (pH 1.5), enough NDEA was added to give 0.31 μM, 1.6 μM and 7.8 μM solutions. A polarogram was recorded for 20.0 ml of each sample solution and the concentration was determined by precise additions of nitrosamine

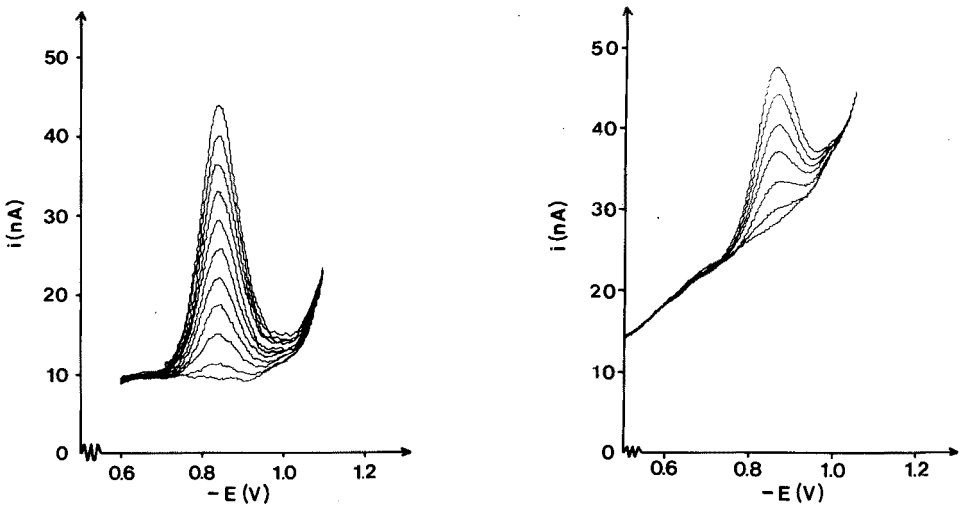

Fig. 2. Differential pulse polarograms of *N*-nitrosodiethanolamine in 0.01 M H_2SO_4 (pH 1.45). The curves correspond to (1.56—29.1) x 10^{-7} M NDEA.

Fig. 3. Differential pulse polarograms of *N*-nitrosodiethanolamine in tartrate buffer (pH 1.79). The curves correspond to (1.56—17.2) x 10^{-7} M NDEA.

standards (samples 1—3, Table 2). These determinations were also carried out in synthetic solutions with 10 times less TEA, DEA and fluorescein (samples 4—6, Table 2).

Grinding fluid samples. The blank solution used was the synthetic solution prepared above to which nitrite was added slowly to a final concentration of 0.2%. Stirred solutions were used to obtain maximum reaction rate and to remove nitrogen from the solution. The fluid samples were prepared as follows: 1 ml of grinding fluid concentrate was added slowly to a solution of ammonium sulphamate (5%, v/v) and H_2SO_4 (0.1 M). Stirred solutions were

TABLE 2

Estimation of the validity of the base-line approximation

Sample	NDEA added (μM)	NDEA found (μM)	Recovery (%)	Sensitivity (nA μM^{-1})	$-E_p$ (mV) (mV)
1[a]	0.31	0.33 ± 0.015	106	6.2 ± 0.19	900
2[a]	1.56	1.4 ± 0.11	92	6.5 ± 0.36	880
3[a]	7.76	7.3 ± 0.13	94	7.33 ± 0.072	880
4[b]	0.31	0.26 ± 0.021	84	6.9 ± 0.23	815
5[b]	1.56	1.45 ± 0.035	93	7.27 ± 0.067	810
6[b]	7.76	7.54 ± 0.098	97	7.7 ± 0.11	810

[a]Mean of 5 measurements. [b]Mean of 3 measurements.

used as above. When the reaction had finished, the samples were diluted to exactly 100.0 ml. Owing to the high levels of NDEA the samples were diluted another 10 times to obtain a suitable concentration for analysis. The pH was adjusted to ca. 1.1 with H_2SO_4.

Two samples from each grinding fluid were prepared and three measurements were carried out on each sample. The polarograms were recorded as usual.

DISCUSSION

The results of the pH investigation are in general accord with earlier studies of nitrosamines. In acidic solution the protonated nitrosamine is reduced and the variation of peak potential with pH between 0 and 6 probably reflects differences in reaction mechanisms. These mechanisms have not been examined in detail.

In alkaline medium the neutral nitrosamine is reduced according to $2\ \text{=N—N—NO} + 3\ H_2O + 4\ e^- \rightarrow 2\text{-N—H} + N_2O + 4\ OH^-$, and this reaction is completely independent of pH.

The maximum in peak current at about pH 2.5 depends on kinetic effects, i.e. the reaction is most reversible at this pH. This is verified by the minimum value of the half-peak width at the same pH.

The peak current in alkaline solution is approximately half the peak current in acidic solution. This is as expected because the reaction involves two electrons per molecule in alkaline medium, whereas the acidic reaction involves four electrons per molecule.

The sensitivity values observed for the different electrolytes remain reasonably constant. A possible explanation for the decrease in sensitivity with the HCl/KCl and citrate buffers is that the higher viscosities of these media lower the diffusion coefficient of the nitrosamine. The lower sensitivities with the various tetraalkylammonium salts are most probably caused by adsorption of the salts on the electrode surface. This makes it more difficult for the nitrosamine to reach the electrode and the electron transfer is complicated, as indicated by the shift in E_p. Adsorption increases with increased chain length [21], and this agrees with the present results.

Detection limits are of the order of 10 ppb for most of the electrolytes. The best results were obtained for 0.01 M H_2SO_4 (see Fig. 2) and 0.1 M H_2SO_4 plus 0.1 mM TBAP. The low detection limit for the latter electrolyte is due to greater stability of the background current. As can be seen in Fig. 3, the large slope of the baseline makes it impossible to increase the gain to allow more sensitive measurement of the peak current. Therefore the detection limit listed for the tartrate buffer is rather unrealistic.

On the basis of the above observations it can be concluded that optimum conditions for nitrosamine measurements are obtained in simple mineral acid solutions at pH 1—2. Such conditions were therefore chosen for the analyses of grinding fluids.

To obtain a successful analysis of grinding fluids, the nitrite must be destroyed prior to measurement. This is easily carried out with ammonium sulphamate [13]. Ascorbic acid also destroys the nitrite [22] but the unfavourable background current makes subsequent analysis impossible.

Because the background currents of the pulse polarograms for the determination of NDEA in grinding fluids are unknown, the baseline was approximated by a straight line between the background on each side of the peak. However, the validity of this approximation is rather dependent on the appearance of the real baseline. To test the approximation, a synthetic grinding fluid with a composition similar to the commercial one was prepared and known amounts of NDEA were added and determined. The accuracy of these determinations was taken as a measure of the baseline validity. In the case of the grinding fluids shown in Table 2, the relative error of the approximation is less than 8% except for sample 4. The precision is better than 8% in all cases. These results are fully acceptable, as the purpose of the determinations does not require better accuracy.

The sensitivity is lowered by a factor of almost 2 and the peak potential is shifted cathodically by about 100 mV for the undiluted solutions (samples 1—3, Table 2) and by about 25 mV for the diluted solutions (samples 4—6, Table 2). This indicates that adsorption effects from the matrix complicate the reduction as is expected from the preliminary investigations.

Table 3 summarizes the determinations of NDEA in grinding fluids. In order to check that NDEA was not formed during the treatment of the grinding fluid samples, blank solutions were handled in exactly the same manner. The blank solutions showed that no or very little nitrosamine was formed during

TABLE 3

Determination of *N*-nitrosodiethanolamine in diluted (1% v/v) grinding fluids. (The samples were diluted 10 times before analysis.)

Sample	Grinding fluid	pH of the concentrated grinding fluid	NDEA found in 1% grinding fluid (μM)	Sensitivity (nA μM^{-1})
1	Blank	—	0.11 ± 0.034	5.9 ± 0.22
2	A (12% TEA, technical grade)	10.6	74 ± 3.4	7.2 ± 0.21
3	A (12% TEA, technical grade)	10.6	73 ± 1.8	7.36 ± 0.092
4	B (20% TEA, technical grade)	11.4	36.9 ± 0.29	6.9 ± 0.21
5	B (20% TEA, technical grade)	11.4	38 ± 2.5	6.7 ± 0.14
6	C (20% TEA, 98—100%)	10.8	30.3 ± 0.61	7.7 ± 0.12
7	C (20% TEA, 98—100%)	10.8	30.7 ± 0.31	7.66 ± 0.069

the sample treatment. High levels of NDEA were found in the grinding fluids investigated. The determinations were carried out with a precision of better than 7% and the relative error is of the order of 7% (samples 5—6, Table 3). Adsorption occurred with the same effect as above. The results agree well with earlier investigations on similar fluids [8]. Longer storage time explains the somewhat higher nitrosamine concentrations. The lower pH value of A, which favours nitrosamine formation, together with the long storage time, appear to have raised the NDEA concentration above that for B.

The major conclusions which can be drawn from this investigation are: (i) that differential pulse polarography is a particularly suitable technique for the direct determination of NDEA in grinding fluids, offering good sensitivity and acceptable accuracy and precision; (ii) that significant nitrosamine formation [8] takes place in grinding fluids which contain ethanolamines and nitrite even at pH values as high as 10—11 and that these fluids constitute a source of exposure to carcinogenic agents.

The author thanks Dr. M. Sharp for valuable discussions and for linguistic revision of the manuscript. This work was supported by the Swedish Work Environment Fund.

REFERENCES

1 P. N. Magee and J. M. Barnes, Brit. J. Cancer, 10 (1956) 114.
2 W. Lijinsky, New Scientist, 73 (1977) 216.
3 P. N. Magee, Ambio, 6 (1977) 123.
4 L. K. Keefer and P. P. Roller, Science, 181 (1973) 1245.
5 N. P. Sen, B. Donaldson, J. R. Jyengar and T. Panalaks, Nature, 241 (1973) 473.
6 N. T. Crosby, J. K. Foreman, J. F. Palframan and R. Sawyer, Nature, 238 (1972) 342.
7 T. Fazio, J. N. Damico, J. W. Howard, R. H. White and J. O. Watts, J. Agric. Food Chem., 19 (1971) 250.
8 P. A. Zingmark and C. Rappe, Ambio, 6 (1977) 237.
9 W. Lijinsky and S. S. Epstein, Nature, 225 (1970) 21.
10 K. Hasebe and J. Osteryoung, Anal. Chem., 47 (1975) 2412.
11 T. A. Gough and K. S. Webb, J. Chromatogr., 79 (1973) 57.
12 D. H. Fine, D. P. Rounbehler and P. E. Oeltinger, Anal. Chim. Acta, 78 (1975) 383.
13 H. Lund, Acta Chem. Scand., 11 (1957) 990.
14 C. L. Walters, E. M. Johnson and N. Ray, Analyst, 95 (1970) 485.
15 W. F. Smyth, P. Watkiss, J. S. Burmicz and H. O. Hanley, Anal. Chim. Acta, 78 (1975) 81.
16 S. K. Chang and G. W. Harrington, Anal. Chem., 47 (1975) 1857.
17 R. Vilvala and J. Halmekoski, Farm. Aikak, 84 (1975) 171.
18 J. Hilfrich, I. Schmeltz and D. Hoffmann, Cancer Lett., (1978) in press.
19 C. K. Mann in A. J. Bard (Ed.), Electroanal. Chem., Vol. 3., M. Dekker, New York, 1969, p. 132.
20 R. K. Skogerboe and C. L. Grant, Spectrosc. Lett., 3 (1970) 215.
21 E. Bou Karam, R. Bennes and D. Bellostas, J. Electroanal. Chem., 84 (1977) 21.
22 S. S. Mirvish, L. Wallcave, M. Eagen and F. Shubik, Science, 177 (1972) 65.

Analytica Chimica Acta, 102 (1978) 141—155

POLAROGRAPHIC ANALYSIS FOR CORTICOSTEROIDS
Part 1. The Electroanalytical Properties of Corticosteroids

H. S. DE BOER, J. DEN HARTIGH, H. H. J. L. PLOEGMAKERS and W. J. VAN OORT*

Department of Analytical Pharmacy, Faculty of Pharmacy, State University of Utrecht, Catharijnesingel 60, Utrecht (The Netherlands)

(Received 10th March 1978)

SUMMARY

The electroanalytical behaviour of corticosteroids has been studied in different supporting electrolytes. The reduction patterns are established by examining pH profiles, by constant-potential coulometry, fast-sweep voltammetry, potentiometry with ion-selective electrodes and differential pulse polarography. Dimerization and alcohol formation take place with the reduction of the C-3 keto group resulting in one or two peaks, depending on the number of double bonds in the A-ring and the pH. The C-20 keto group is reduced to an alcohol. Both reduction steps can be used for analytical purposes. The differential pulse peak height is linear with the concentration down to 10^{-6} M steroid.

Corticosteroids are produced by the adrenal cortex and have important physiological activities, such as anti-inflammatory action, and effects on carbohydrate, water and electrolyte metabolism. The natural corticosteroids — hydrocortisone and cortisone — are used therapeutically, mainly because of their anti-inflammatory action. However, increased corticosteroid activity in the blood stream gives rise to unwanted side effects such as increased serum sodium content or inhibition of antibody production. With some synthetic compounds such as prednisone and prednisolone, certain side effects are decreased. The introduction of a halogen atom (particularly fluorine) at certain places in the ring system yields a considerable intensification of the anti-inflammatory action so that the therapeutic dosage can be lowered and side effects decreased proportionally. Corticosteroids can be administered as tablets, solutions, injections, suppositories, ointments and creams. Figure 1 shows the general formula of corticosteroids with anti-inflammatory effects. Steroids with an alcohol group at C-21 like prednisolone are used in tablets. Aqueous solutions (injections) are based on the water-soluble esters with polybasic acids (prednisolone, disodium phosphate) whereas lipophilic media (ointments, creams) require the oil-soluble esters with monobasic acids such as acetic acid and butyric acid. Esterification usually takes place at C-21, and in a few cases at C-17 and at C-16 with C-17 (acetonides, e.g. triamcinolone acetonide).

Many different methods of analysis have been described: ultraviolet

spectrophotometry [1], colorimetry with tetrazolium blue [2], fluorimetry [3], radio-immunoassay [4], h.p.l.c. [5] and polarography [6]. The polarographic analysis makes use of the reducibility of the conjugated carbonyl group at C-3. Ekwall et al. [7] utilized d.c. polarography for the determination of deoxycorticosterone acetate in 83% ethanol containing lithium chloride as the supporting electrolyte. Kabasakalian et al. [6] demonstrated the applicability of polarography for the determination of corticosteroids with the analysis of mixtures of prednisone and cortisone in 50% methanol and acetic acid buffer of pH 5.5. Kabasakalian and McGlotten studied the polarographic reduction of prednisone, prednisolone, cortisone and hydrocortisone by means of constant-potential coulometry and u.v. spectrophotometry [8]; halogenated steroids were studied in 96% alcoholic medium [9]. Zuman et al. studied the behaviour of deoxycorticosterone and structurally related compounds such as testosterone [10] and described the polarographic reduction of aldehydes and ketones [11—13], deducing the mechanism at several pH values in alcoholic media. All authors have proposed a reduction mechanism involving dimerization.

Corticosteroids are often used in multicomponent preparations, mostly in low concentrations. In that case or when the sample is diluted by a clean-up procedure, d.c. polarography is not sensitive enough. Differential pulse polarography is a suitable method of analysis for these mixtures because of its sensitivity and its selectivity [14—17]. If differential pulse polarography is to be applied, the electroanalytical behaviour of the compounds in different solutions and supporting electrolytes at different pH values must be known. Accordingly, in the work reported here, the following analytical properties of corticosteroids were examined: $E_{\frac{1}{2}}$—structure relations, pH profiles, the reduction mechanism, the reversibility of the reactions, and the linearity of the diffusion current with the concentration.

EXPERIMENTAL

Apparatus

The polarographic and voltammetric curves were recorded on a Bruker E310 modular electrochemical system and a PAR model 174 polarograph both of which were equipped with a drop timer and a Houston Model 2200-3-3 X—Y recorder. Kalousek polarographic curves were obtained by using a Metrohm Polarecord E506, equipped with a drop timer E505. A water-jacketed 10-ml polarographic cell (Metrohm EA880-T-5) was employed with a dropping mercury electrode, an Ingold 373-90 Ag/AgCl reference electrode and a platinum wire auxiliary electrode. The cell was kept at a temperature of 20 ± 0.2°C. The "salt bridge" of the reference electrode was filled with the supporting electrolyte; the potential of this electrode filled with 0.03 M tetramethylammonium hydroxide in methanol versus a saturated calomel electrode was −32 mV. The pH values were measured with a Radiometer PHM 64 and an Ingold combined glass electrode (type LOT-401) calibrated

in aqueous buffer solutions. For potentiostatic coulometry, a home-made potentiostat [18] and integrator were used. During a coulometric analysis (30—60 min) potassium ions diffused via the salt bridge into the cell and caused an increased base signal. The pathway for potassium ions was therefore lengthened by using a reference electrode type Metrohm EA432; the potential of this electrode filled with 0.03 M tetramethylammonium hydroxide in methanol versus a saturated calomel electrode was —52 mV. A piston microburette (Metrohm E457) was used for standard additions of small volumes of sample. An Orion fluoride-selective electrode, model 94-09A, was used for fluoride determinations.

Chemicals

The steroids used were: progesterone, hydrocortisone, cortisone, prednisolone, prednisone, dexamethasone, hydrocortisone acetate, hydrocortisone hemisuccinate, dexamethasone disodium phosphate (Nogepha); hydroxyprogesterone, corticosterone, testosterone (Merck); fluprednisolone, hydrocortisone cypionate (Upjohn); betamethasone, hydrocortisone disodium phosphate (Glaxo); deoxycorticosterone (Fluka); Triamcinolone (Lederle); hydrocortisone butyrate (Mycofarm); hydrocortisone sodium succinate (Lark); dexamethasone acetate (Organon). The solvents and materials for the supporting electrolytes were: methanol (Nanograde, Mallinckrodt), dimethylformamide (DMF; Uvasol), acetic acid (99% reinst), phosphoric acid (99% reinst), tetramethylammonium hydroxide (TMAH; 10% zur Polarographie), lead nitrate (p.a.), sodium nitrate (p.a.) (Merck) and boric acid (Baker). The other reagents were of analytical-reagent grade or reagent grade and were used without further purification unless otherwise stated.

Procedures

Polarography. Because of the variety of dosage forms of corticosteroids, three analysing procedures were developed with different lipophilic properties of the solutions: a mixture of Britton—Robinson buffer in methanol (50% v/v) at pH 10, 0.03 M TMAH in methanol and 0.02 M TMAH in a mixture of DMF (87% v/v) and water. When pure corticosteroids are determined in a mixture of methanol and Britton—Robinson buffer, the steroid has to be dissolved in pure methanol before being mixed with the buffer. The addition of some water to DMF results in a decrease of its lipophilic properties but prevents premature mercury drop fall. At the optimum water content, the potential limit in DMF is —2300 mV versus the Ag/AgCl electrode. For solutions with low quantities of corticosteroids, the usual period of oxygen removal of 10 min was not enough: particularly in methanol and DMF, bubbling of oxygen-free nitrogen [19] through the solution for 20—30 min was necessary. After each addition of standard solution nitrogen bubbling for another 5 min was sufficient. The polarograms were recorded at a scan rate of 2 mV s^{-1} for a pulse amplitude of 100 mV; a drop time of 2 s was used in methanol/BR buffer or methanol/TMAH, and a drop time of 1 s in DMF.

TABLE 1

Dependence of the peak potentials on the structure of the steroids at concentrations of 10^{-4} M in 0.03 M TMAH in methanol, in Britton–Robinson buffer pH 10 (50% v/v in methanol) and in 0.02 M TMAH in DMF (87% v/v).
(The reduction of the C-3 keto group is represented by Δ (enones) or by Φ (dienones), and the reduction of the C-20 keto group by Ψ. See text for other symbols. This table should be read in combination with Fig. 1.)

Compound	C_1=C_2	R_1	R_2	R_3	R_4	R_5	R_6	In methanol (10 ml)/10% TMAH in water (0.03 ml)
I	Single	(1[a]	OH	H	H	H	H	
II	Single	H	H	H	H	H	H	
III	Single	H	OH	H	H	H	H	
IV	Single	OH	H	H	H	H	H	
V	Single	OH	H	H	OH	H	H	
VI	Single	OH	OH	H	OH	H	H	
VII								
VIII								
IX								
X								
XI								
XII								
XIII	Single	OH	OH	H	O	H	H	
XIV	Double	OH	OH	H	OH	H	H	
XV	Double	OH	OH	H	O	H	H	
XVI	Double	OH	OH	H	OH	H	F	
XVII	Double	OH	OH	CH_3	OH	F	H	
XVIII	Double	OH	OH	CH_3	OH	F	H	
XIX								
XX								
XXI								
XXII	Double	(1	O	CH_3	OH	F	H	
XXIII	Double	OH	OH	OH	OH	F	H	
XXIV								

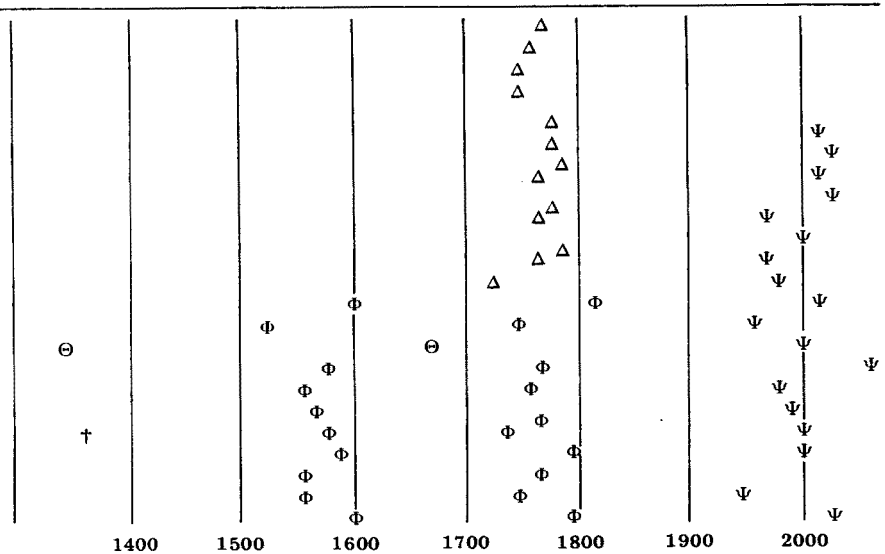

Key to compounds: I = Testosterone; II = Progesterone; III = Hydroxyprogesterone; IV = Deoxycorticosterone; V = Corticosterone; VI = Hydrocortisone; VII = Hydrocortisone-21-acetate; VIII = Hydrocortisone-17-butyrate; IX = Hydrocortisone-21-cypionate; X = Hydrocortisone-21-sodiumphosphate; XI = Hydrocortisone-21-succinate; XII = Hydrocortisone-21-sodiumsuccinate; XIII = Cortisone; XIV = Prednisolone; XV = Prednisone; XVI = Fluprednisolone; XVII = Betamethasone; XVIII = Dexamethasone; XIX = Dexamethasone-21-acetate; XX = Dexamethasone-21-isonicotinate; XXI = Dexamethasone-21-sodiumphosphate; XXII = 9α-fluoro-11β-hydroxy-16α-methylandrost-1,4-diene-3,17-dione; XXIII = Triamcinolone; XXIV = Triamcinolone acetonide.

TABLE 1 (continued)

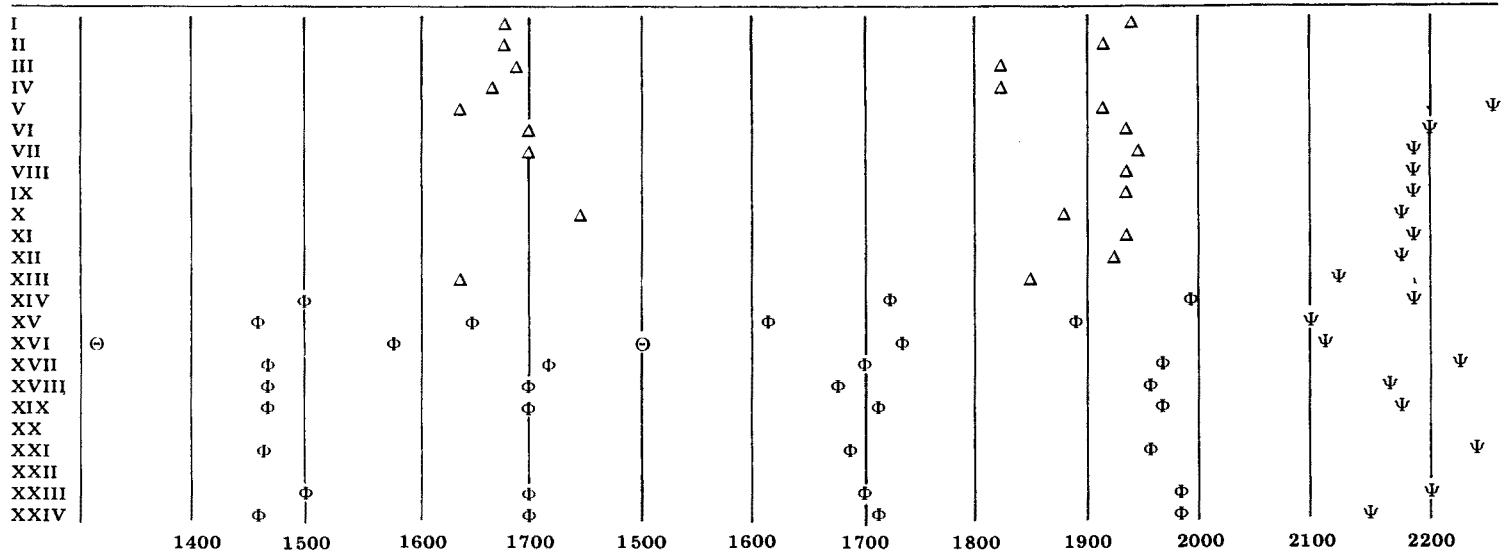

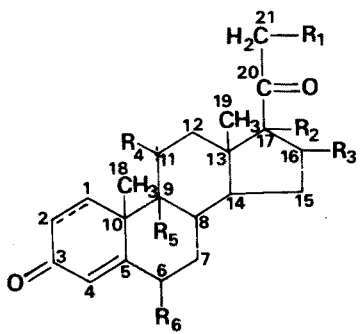

R_1 = — H or — OH

R_2 = — H or — OH

R_3 = — H, — OH or — CH_3

R_4 = — H, — OH or = O

R_5 = — H or — F

R_6 = — H or — F

Fig. 1. General formula of corticosteroids.

Constant-potential coulometry. Constant-potential analyses were carried out with a volume of 10 ml. A mercury pool electrode was used for the determination of the number of electrons involved in the reaction. The concentration of the steroid was 10^{-3} M. Before and during the analysis, oxygen-free nitrogen was bubbled through the solution. Two procedures were applied. In the first method, the blank current of the supporting electrolyte was measured, after becoming constant, during a certain period. The average value was subtracted from the value obtained over the same period with a solution of a steroid. In the second method, the constant blank current of the supporting electrolyte was measured. A sample of steroid in a small cup was then added to the same solution. After the value of the original blank current had been reached the total number of coulombs was corrected for this value. The second method proved to be the more reliable (e.g. with standard lead(II) solutions and calibration).

RESULTS AND DISCUSSION

In the literature, most attention has been paid to the reduction of the C-3 carbonyl group, but there is another electroactive site in the molecule: the carbonyl group at C-20. This group is unconjugated but the reduction is activated by the neighbouring hydroxyl group(s). To obtain a better understanding of the reducibility/structure relation numerous (cortico-)steroids were examined for their half-wave potentials and other polarographic properties. In anticipation of analysis in different pharmaceutical preparations, this qualitative study was done in three different solutions: 0.03 M TMAH in methanol, 0.02 M TMAH in DMF (87% v/v), and methanol/Britton—Robinson buffer of pH 10 (50% v/v). These solutions can be used (without further purification) for the analysis of samples with concentrations down to 10^{-6} M.

Wave pattern of (cortico)steroids in methanol

The peak potentials (vs. Ag/AgCl) of the steroids determined by differential pulse polarography are presented in Table 1. With the Brucker E 310 polarograph, the measured values are corrected automatically for the pulse amplitude. The list is completed with some esters of an enone (hydrocortisone) and of a dienone (dexamethasone).

The following conclusions can be reached from these results.

The Δ^4-3 keto group is reduced at −1.75 to −1.77 V. Kabasakalian and McGlotten [20] found that the half-wave potential for the reduction of an unconjugated C-3 carbonyl group to a carbinol lies at about −2.5 V (vs. SCE).

The $\Delta^{1,4}$-3 keto group is reduced at −1.60 V. The extra C=C bond between C-1 and C-2 results in a positive $E_{\frac{1}{2}}$ shift of 170 mV. The dienone steroids show an extra (small) peak at −1.76 V; this peak appears with a change in the first ring (dienone) independent of the reduction of the C-20 carbonyl group (Table 1) This was proved by constant-potential coulometry

(see below), and by the reduction of a dienone in which the aliphatic side chain was replaced by a non-conjugated C-17 carbonyl group [21]: only the third peak disappeared (Fig. 2). The pattern of the C-17 carbonyl derivative of dexamethasone (9α-fluoro-11β-hydroxy-16α-methylandrost-1,4-diene-3,17-dione) is similar to the testosterone pattern with a positive shift.

The reduction of the C-20 carbonyl group in methanol/TMAH can be seen only if hydroxyl groups are present at C-17 and C-21 (electron-withdrawing properties). If one or both groups are absent, the reduction proceeds with greater difficulty and the peak is overlapped by the reduction of the supporting electrolyte. The difference in the $E_{\frac{1}{2}}$ values of dexamethasone and betamethasone for the C-20 carbonyl reduction (—1.97 V and —2.07 V) is remarkable. The value for dexamethasone agrees with those of other corticosteroids, whereas the value for betamethasone is more negative. A possible explanation is the steric hindrance caused by the methyl group at C-16: in the β-position in betamethasone, this group hinders the reduction more than in in the α-position in dexamethasone.

The introduction of a carbonyl group instead of a hydroxyl group at C-11 results in a positive shift of the peak potential of about 50 mV for the C-3 carbonyl reduction, as can be seen with hydrocortisone/cortisone and prednisolone/prednisone. The small intermediate peak shows the same behaviour.

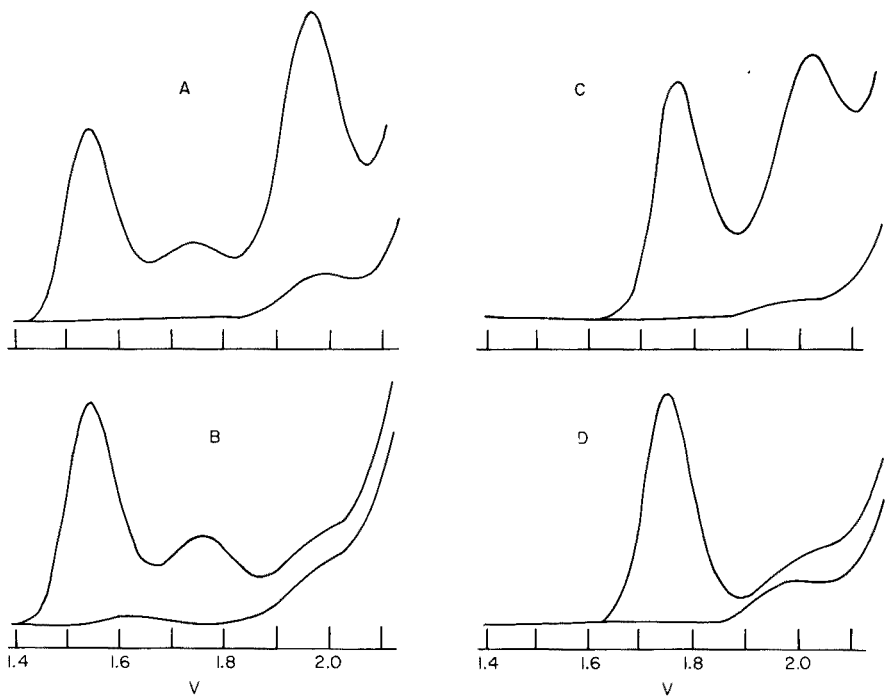

Fig. 2. Differential pulse polarograms of (A) 10^{-4} M dexamethasone, (B) 10^{-4} M 17-keto derivative of dexamethasone, (C) 10^{-4} M hydrocortisone, and (D) 10^{-4} M testosterone in methanol—TMAH.

The peak potential of steroids with a fluorine atom at C-6 (fluprednisolone) shifts 200 mV in the positive direction (shown in Table 1 by Θ). Kabasakalian and McGlotten [9] studied the reduction of halogenated steroids and concluded that the halogen atom can be eliminated in the potential range studied here, only when neighbouring electron-withdrawing groups are present. The conjugated system of C-4 and the double bond make the reduction possible. This was proved by monitoring the fluoride concentration with a fluoride-selective electrode during constant-potential coulometric analysis at the peak potential of the first peak in the polarogram of fluprednisolone. The resulting fluoride concentration equalled the original fluprednisolone concentration. No fluoride was set free in similar experiments with dexamethasone and betamethasone: the fluoride atom at C-9 is too isolated to be reduced in this potential range.

Esterification of the hydroxyl group at C-21 does not affect the $E_{\frac{1}{2}}$ value for the reduction of the C-3 carbonyl group and the C-20 carbonyl group. Sometimes the height of the intermediate peak increases with esterification. Dexamethasone isonicotinate shows an extra peak at −1.36 V (shown in Table 1 by †) caused by reduction of isonicotinic acid.

Quantitative analysis showed that the reduction of the C-3 carbonyl group (first peak) and of the C-20 carbonyl group obey the Ilkovič equation; there is a linear relationship between the d.p.p peak current and concentration in the range 10^{-3}—10^{-6} M. The calibration curves show a correlation coefficient of at least 0.99 in the lower range and 0.999 in the higher range. The calibration curve for the intermediate peak shows a parabolic behaviour with a small linear part in the lowest concentration range.

Wave pattern of (cortico)steroids in DMF

The half-wave potentials of a number of (cortico)steroids in DMF are presented in Table 1. The reduction in DMF is similar to that in methanol, but the individual values are less reproducible. Other differences are: the potential range in DMF is larger; the C-20 carbonyl reduction can be used for analytical purposes even when only one neighbouring hydroxyl group is present; and the sensitivity in DMF is smaller, mainly because of the shorter drop time of 1 s (which is necessary because of the premature drop fall at longer drop times).

Wave pattern of (cortico)steroids in methanol—buffer mixtures

The behaviour of (cortico)steroids was studied in methanol—buffer mixtures at different pH values. In the acidic range, adsorption processes interfere with the reduction, resulting in nonlinearity and asymmetric d.p.p. peaks. In the medium pH range, enones showed wave splitting [10, 22]. For analytical application, only the basic range (pH 10) is suitable (see below). The peak potentials of a number of (cortico)steroids in a methanol—buffer mixture at pH 10 are presented in Table 1. The wave patterns in this mixture have roughly the same shape as those in methanol and DMF. The main

difference is the overlap of the C-20 carbonyl reduction peak by the wave of the supporting electrolyte. The potential range is smaller.

Study of the reduction mechanism

Kabasakalian and McGlotten [8] investigated the reduction mechanism of prednisone, prednisolone, cortisone and hydrocortisone in 50% ethanol at pH 5.5. They proposed the formation of a pinacol, the dimerization product of a radical after reduction of a carbonyl group. They measured the number of electrons involved in the reaction (*n* values) by constant-potential coulometry; additional evidence was obtained by u.v. spectrophotometry. In a more general way Zuman et al. [11] studied the reduction of aldehydes and ketones and established different reduction mechanisms depending on pH, medium and supporting electrolyte. Holleck and Mahapatra [23] reported the reduction of conjugated carbonyl compounds to a pinacol in DMF, in methanol—buffer mixtures and in methanol. The active group in the compounds studied resembles the A-ring system in some of the corticosteroids. Elving and Leone [24] studied the electrochemical reduction of phenylketones by polarography and by coulometry and found a divalent reduction to a pinacol and an alcohol depending on the pH; pinacol formation occurred only in strongly acidic and strongly basic solutions while alcohol was formed in the medium pH range. Savéant et al. [25—27] studied the dimerization step in the reduction process; fast-sweep voltammetry was used to distinguish between several dimerization paths: coupling of unprotonated, partly protonated and completely protonated radicals. Diagnostic criteria were given for recognition of the dimerization mechanism by measuring the shift in peak potential at different scan rates. Zuman et al. [10] ascribed splitting of the reduction wave of the Δ^4-3 keto group, depending on pH, to a protonated and an unprotonated form. The half-wave potential of the protonated form is pH-dependent; that of the unprotonated is not. Kabasakalian and McGlotten [22], using an organic buffer system, did not notice this behaviour, but other workers [28—30] have mentioned wave splitting with similar compounds. The literature on corticosteroids is particularly incomplete in this respect and contains many contradictions. A more exhaustive study was therefore undertaken.

pH profiles

The above study of wave patterns indicates that further examination of the electrochemical behaviour can be confined to a small number of representative (cortico)steroids: testosterone, hydrocortisone, prednisolone and dexamethasone. The pH profiles were measured in Britton—Robinson buffer (50% v/v methanol). The pH was measured after mixing of buffer and methanol and is therefore the apparent pH. The pH dependence of the reduction wave for the C-3 carbonyl group is shown in Fig. 3. The profile for testosterone is similar to that determined by Zuman et al. [10]. The profile of hydrocortisone (an enone) is very similar to that of the enone testosterone (the

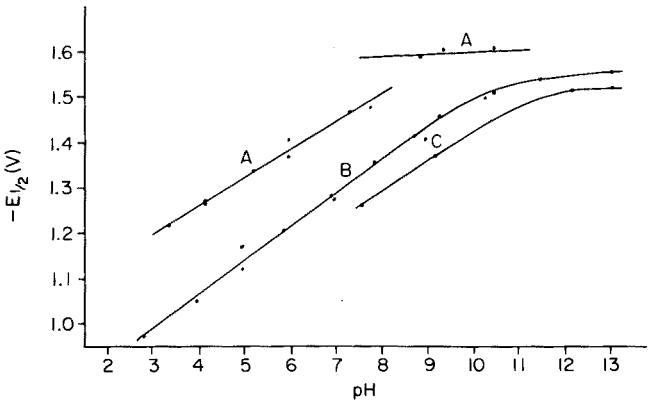

Fig. 3. Dependence of the peak potentials on the apparent pH in methanol—buffer mixtures of hydrocortisone (A), prednisolone (B) and dexamethasone (C).

only structural difference is the aliphatic side-chain at C-17). The slope of the $E_{\frac{1}{2}}$—pH relationship for hydrocortisone is 61 mV, which is close to the value 58 mV found for testosterone at pH 3—9 by Zuman et al. All the enones measured showed wave splitting, which is in agreement with Zuman et al. [10] but not with Kabasakalian and McGlotten [22]. The second peak which appears above pH 8 shows little pH-dependence. However, the dienones prednisolone and dexamethasone do not show peak splitting between pH 3 and 13. At about pH 10 the slope of the $E_{\frac{1}{2}}$—pH relation decreases from 68 mV for dexamethasone and 73 mV for prednisolone to almost zero. Probably the peaks of the reduction of the protonated and unprotonated form for these compounds lie close together and are not recorded separately.

Constant-potential coulometry

In the reduction of a solution of steroids or other carbonyl compounds, the transference of one electron per molecule indicates the formation of a radical which can dimerize to a pinacol. For alcohol formation this n value must be 2. Table 2 shows the n values obtained for two enones and two dienones. The steroids were electrolysed at different potentials as indicated.

In accordance with Chatten et al. [16] and Kabasakalian and McGlotten [8] who investigated related steroids, n values of about 1 were found for the reduction of the Δ^4-3 keto group and the $\Delta^{1,4}$-3 keto group at the potential of the most positive peak: a radical is formed and dimerization must occur. Electrolysis at the $E_{\frac{1}{2}}$ value of the first peak of the dienones results in the disappearance of the first wave as well as of the intermediate wave in the polarogram recorded afterwards. It has already been concluded that both waves are related to reduction of the $\Delta^{1,4}$-3 keto group. Electrolysis at the $E_{\frac{1}{2}}$ value of the intermediate wave gives n values between 1 and 2; this indicates that the $\Delta^{1,4}$-3 keto group is partly reduced to an alcohol at potentials higher than that of radical formation [11]. After pre-electrolysis at potentials corresponding to the first two peaks, electrolysis at —2.0 V indicated n values

TABLE 2

Values of n determined at different potentials by constant-potential coulometry of two enones (testosterone and hydrocortisone) and two dienones (prednisolone and dexamethasone) in 0.03 M TMAH in methanol (Column A gives the n values obtained by electrolysis at the potential corresponding to the most positive peaks (cf. Fig. 2, curves A and C), for the appropriate compound. Column B gives the sum for electrolysis at the potentials corresponding to the intermediate peak (if present). Column C gives the n values for electrolysis at the potentials corresponding to the most negative peak after complete pre-electrolysis at the potential of the first peak (and possibly the intermediate peak).
(The last column gives the n values obtained by electrolysis at the potential of the most negative peak without pre-electrolysis of more positive peaks.)

	A	B	C	Sum
Testosterone	1.02 (−1.74 V)			1.15 (−2.00 V)
Hydrocortisone	0.96 (−1.74 V)		2.10 (−2.00 V)	3.68 (−2.00 V)
Prednisolone	0.98 (−1.60 V)	1.59 (−1.74 V)	2.07 (−2.00 V)	3.70 (−2.00 V)
Dexamethasone	0.96 (−1.55 V)	1.59 (−1.75 V)	2.15 (−2.00 V)	3.51 (−2.00 V)

of about 2, which suggests that the C-20 keto group in the aliphatic side-chain is reduced to an alcohol. Electrolysis at −2.0 V without pre-electrolysis at more positive potentials resulted in n values of about 3.6, corresponding to the total reduction process. There is remarkable agreement in the n values for the total reduction at −2.0 V between hydrocortisone, prednisolone and dexamethasone despite the absence of the intermediate peak in the polarogram of hydrocortisone. In the case of hydrocortisone, this small peak is overlapped by the large final wave. Electrolysis of testosterone at −2.0 V gave slightly higher results than at −1.75 V, but obviously hardly any alcohol was formed, probably because of the absence of the aliphatic side chain at C-17.

The dependence of the n value of the intermediate peak on apparent pH is presented in Fig. 4, which shows that in acidic and very basic (aqueous) media, the alcohol is not formed, because of the excess and the total absence of protons, respectively. In the medium pH range (including methanol—TMAH), a mixed reduction takes place. Elving and Leone [24] reported a similar behaviour for phenylketones.

Fast-sweep voltammetry

To gain a better understanding of the main reduction path (pinacol formation), fast-sweep voltammetry [25—27] was applied. Savéant et al. [25—27] mentioned three possible dimerization mechanisms:

DIM I: coupling of two radicals each formed by the uptake of one electron;

DIM II: radical/substrate coupling in which a radical is coupled to an unreduced molecule after which the dimer takes up a second electron;

DIM III: ion/substrate coupling in which the product of a 2-e transfer reacts with the unreacted molecule (not very likely).

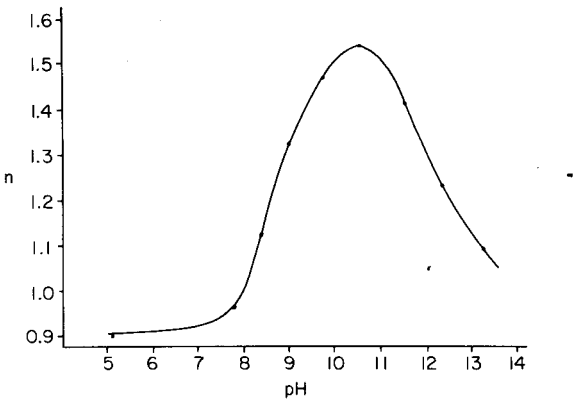

Fig. 4. Variation of the n value with apparent pH of prednisolone in methanol—buffer mixtures.

They distinguished between these possibilities by determining the relation between the peak potential of a fast-sweep voltammogram and the logarithm of the scan rate. A slope of about 20 mV/decade indicates a DIM I mechanism, a slope of about 30 mV/decade a DIM II mechanism and a slope of about 15 mV/decade a DIM III mechanism, if protonation is neglected [25, 26]. The shift of the peak potential ($\approx E_{\frac{1}{2}}$) with the logarithm of the scan rate, the logarithm of the initial concentration and the pH can also be used for diagnosis. However, recent experimental verification of the reduction obtained with benzaldehydes [27] gives a value of 43.6 mV/decade (E_p / log v) caused by the coupling of two protonated radicals. The results for prednisolone and hydrocortisone are presented in Fig. 5. In the acidic range, values are high. In the medium pH range, the DIM II mechanism is the most likely for prednisolone (dE_p /d log v of about 30 mV/decade). In the basic range the values approach 20 mV/decade probably because of a DIM I mechanism. In methanol—TMAH, the values were about 25 mV/decade for hydrocortisone and for prednisolone.

Reduction mechanism

Combining the methods of Zuman and Savéant, the following reduction pattern in the different media was deduced.

In acidic media, only a 1-e wave related to the reduction of a protonated steroid molecule (S) to a radical was observed:

$$S + H^+ \leftrightarrows SH^+;\ SH^+ + e \xrightarrow{E_1} S^{\cdot}H;\ 2S^{\cdot}H \rightarrow H{-}S{-}S{-}H$$

The half-wave potential of E_1 depends on the pH, protonation being the potential-determining step. From the results of cyclic voltammetry and Kalousek polarography, reaction E_1 appears to be slightly reversible. The results of fast-sweep voltammetry suggest the final coupling of two protonated radicals. Despite the results of Zuman and Turcsanyi [30] who investi-

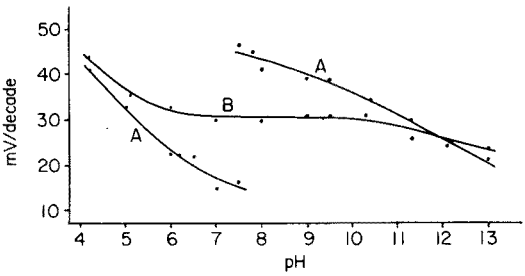

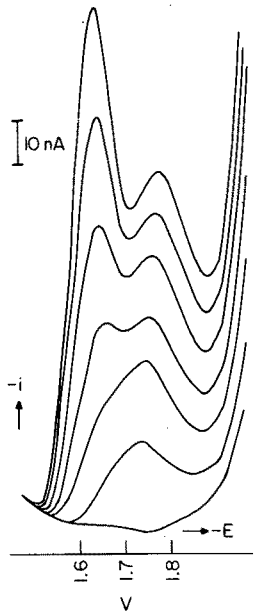

Fig. 5. Dependence of the slope of the peak potential—scan rate relation in fast-sweep voltammetry on the apparent pH for 10^{-4} M hydrocortisone (A) and of 10^{-4} M prednisolone (B) in methanol—BR buffer.

Fig. 6. Differential pulse polarograms of dexamethasone in 0.03 M TMAH in methanol (0.5, 1.0, 1.5, ... × 10^{-5} M dexamethasone).

gated this mechanism with aryl—alkyl ketones, a second wave corresponding to further reduction to an alcohol in the acidic range was not observed.

In the medium pH range, the steroid molecule is reduced before protonation, and two waves appear, in agreement with Zuman [11]. The sequence of reduction and protonation is e, H^+, e, H^+. The first wave (E_2) is independent of the pH.

$$S + e \xrightarrow{E_2} S^{\cdot(-)}$$

$$S^{\cdot(-)} + H^+ \leftrightarrows S^{\cdot}H$$

$$S^{\cdot}H + e \xrightarrow{E_3} HS^{\cdot\cdot(-)}$$

$$HS^{\cdot\cdot(-)} + H^+ \leftrightarrows SH_2$$

$$S + S^{\cdot}H \rightarrow H{-}S{-}S^{\cdot}$$

$$H{-}S{-}S^{\cdot} + e \xrightarrow{E_4} H{-}S{-}S^{\cdot\cdot(-)}$$

$$H{-}S{-}S^{\cdot\cdot(-)} + H^+ \leftrightarrows H{-}S{-}S{-}H$$

After the protonation of the radical $S^{\cdot(-)}$, two reaction patterns are possible: the protonated radical is reduced to an alcohol resulting in the second (intermediate) wave (E_3) or the radical couples with the substrate to form a dimer which can be reduced further to an anion radical followed by protonation.

In the medium pH range, both patterns occur. Constant-potential coulometry proved that the second wave is (partly) caused by the formation of alcohol. Fast-sweep voltammetry proved that the dimerization involves a DIM II mechanism (slope of 30 mV/decade). Probably the waves of E_3 and of E_4 overlap. The percentage of dimerized radical is unknown. The half-wave potentials of the reduction of the protonated (E_1) and of the unprotonated (E_2) steroids are close together with dienones (no wave splitting) but differ with enones (wave splitting).

In basic media, Zuman deduced an (e, e, H^+, H^+) reduction pattern. However, a second wave corresponding to alcohol formation was not observed. The radical is not protonated, and the anion radical cannot produce an anion at the negative electrode. Only dimerization occurs, according to the *n* value found (see Fig. 4). Dimerization proceeds via the DIM I mechanism:

$$S + e \overset{E_2}{\rightarrow} S^{\cdot(-)};\ S^{\cdot(-)} + H^+ \leftrightarrows HS^{\cdot}$$

$$HS^{\cdot} + S^{\cdot(-)} \rightarrow H{-}S{-}S^{\cdot\cdot(-)};\ H{-}S{-}S^{\cdot\cdot(-)} + H^+ \leftrightarrows H{-}S{-}S{-}H$$

The dimerization of two unprotonated radicals is unlikely; methanol—0.03 M TMAH is rather an aprotic medium. The behaviour of the steroid in this medium resembles that in aqueous solutions of about pH 12: a small alcohol wave can be seen. Figure 6 shows a series of standard additions of dexamethasone in methanol—0.03 M TMAH. The peak height corresponding to the alcohol formation is fairly constant; the peak height corresponding to dimerization varies linearily with concentration and can be used, like the 21-keto reduction wave, for the determination of corticosteroids in pharmaceutical preparations. The ratio of dimerization to alcohol formation decreases at lower concentrations, probably because of the second-order character of the dimerization reaction.

The authors express their gratitude to Prof. Dr. P. Zuman (Potsdam, N.Y.) for his encouraging advice and Mr. K. R. Kooistra for experimental help.

REFERENCES

1 R. E. Graham, P. A. Williams and C. T. Kenner, J. Pharm. Sci., 59 (1970) 1152.
2 R. E. Graham, P. A. Williams and C. T. Kenner, J. Pharm. Sci., 59 (1970) 1472.
3 C. E. White and A. Weissler, Anal. Chem., 44 (1972) 182 R.
4 V. K. Ganjam, Steroids, 28 (1976) 631.
5 N. W. Tymes, J. Chromatogr. Sci., 16 (1977) 151.
6 P. Kabasakalian, S. DeLorenzo and J. McGlotten, Anal. Chem., 28 (1956) 1669.
7 P. Ekwall, T. Lundsten and L. Sjöblom, Acta Chem. Scand., 5 (1951) 1383.
8 P. Kabasakalian and J. McGlotten, J. Am. Chem. Soc., 78 (1956) 5032.
9 P. Kabasakalian and J. McGlotten, Anal. Chem., 34 (1962) 1440.
10 P. Zuman, J. Tenygl and M. Březina, Collect. Czech. Chem. Commun., 19 (1954) 46.
11 P. Zuman, Collect. Czech. Chem. Commun., 33 (1968) 2548.
12 P. Zuman and B. Turcsanyi, Collect. Czech. Chem. Commun., 33 (1968) 3090.
13 A Ryvolová-Kejharová and P. Zuman, J. Electroanal. Chem. 21 (1969) 197.

14 D. Cantin, J. Alary and A. Coeur, J. Pharm. Belg., 32 (1977) 255.
15 L. G. Chatten, R. Narayan Yadav and D. R. Madan, Pharm. Acta Helv., 12 (1976) 381.
16 L. G. Chatten, R. Narayan Yadav, S. Binnington and R. E. Moskalyk, Analyst, 102 (1977) 323.
17 L.-N. Opheim, Anal. Chim. Acta, 91 (1977) 331.
18 J. A. Von Fraunhofer and C. H. Banks, The Potentiostat and its Applications, Butterworth, London, 1972.
19 L. Meites, Polarographic Techniques, 2nd edn., Interscience., New York, 1965, p. 87.
20 P. Kabasakalian and J. McGlotten, Anal. Chem., 3 (1959) 1091.
21 C. J. W. Brooks and J. K. Norymberski, Biochem. J., 55 (1953) 371.
22 P. Kabasakalian and J. McGlotten, J. Electrochem. Soc., 105 (1958) 261.
23 L. Holleck and S. Mahapatra, J. Electroanal. Chem., 35 (1972) 381.
24 P. J. Elving and J. T. Leone, J. Am. Chem. Soc., 80 (1958) 1021.
25 C. P. Andrieux, L. Nadjo and J. M. Savéant, J. Electroanal. Chem., 26 (1970) 147.
26 L. Nadjo and J. M. Savéant, J. Electroanal. Chem., 44 (1973) 327; 33 (1971) 419.
27 F. Ammar, L. Nadjo and J. M. Savéant, J. Electroanal. Chem., 47 (1973) 146.
28 M. Suzuki and P. J. Elving, J. Phys. Chem., 65 (1961) 391.
29 M. Okmori and M. Takagi, Bull. Chem. Soc. Jpn., 50 (1977) 773.
30 P. Zuman and B. Turcsanyi, Collect. Czech. Chem. Commun., 33 (1968) 3090.

Analytica Chimica Acta, 102 (1978) 157—166

THE DETERMINATION OF ALL THE PLATINUM GROUP ELEMENTS AND GOLD IN ROCKS AND ORE BY NEUTRON ACTIVATION ANALYSIS AFTER PRECONCENTRATION BY A NICKEL SULPHIDE FIRE-ASSAY TECHNIQUE ON LARGE SAMPLES

E. L. HOFFMAN*, A. J. NALDRETT and J. C. VAN LOON,

Department of Geology, University of Toronto, Toronto, Ontario (Canada)

R. G. V. HANCOCK

SLOWPOKE II Reactor, University of Toronto, Toronto, Ontario (Canada)

and A. MANSON

INCO Metals Company Ltd., J. Roy Gordon Research Centre, Mississauga, Ontario (Canada)

(Received 10th April 1978)

SUMMARY

The noble metals are inhomogeneously distributed in sulphide ores and their host rocks. It is therefore necessary to analyse large sample sizes to obtain representative analyses. A nickel sulphide fire assay technique has been adapted to extract the noble metals from a large sample size (50 g) into a nickel sulphide button. Subsequently the fire assay button is dissolved in hydrochloric acid and the solution is filtered. The noble metal residue retained on the filter paper is analysed quantitatively by i.n.a.a. techniques. This method is rapid, relatively inexpensive and has better sensitivities for all the noble metals than other analytical techniques.

The noble metals are inhomogeneously distributed [1—6] in rocks and ores, forming discrete noble metal minerals and possibly occurring in solid solution in rock-forming minerals, chromites and sulphides. The levels (ppb) at which the noble metals occur in most rocks and ores are generally well below the detection limits of most analytical techniques [4]; neutron activation with γ-spectrometry gives sensitivities under ideal conditions that are several orders of magnitude better than those obtainable by other approaches. The limiting factors in n.a.a. are the small sample size (typically less than 500 mg) and the complexity and cost of isolating the individual elements from the interfering matrix so that the best sensitivities may be realized. N.a.a. provides a powerful analytical method at relatively low cost if large sample sizes can be treated rapidly.

A nickel sulphide fire-assay technique quantitatively collects all the platinum group metals (PGM) and gold from a large sized sample. The bead is dissolved in 12 M HCl; the residue is collected on filter paper and irradiated. The noble metals on the filter paper can be determined by instrumental neutron activation analysis (i.n.a.a.).

---

*Present address: X-ray Assay Laboratories Ltd., 45 Lesmill Rd., Don Mills, Ontario, Canada.

Previous noble metal analyses by n.a.a.

It has rarely been possible to determine the noble metals by i.n.a.a. at the sub-μg levels at which they occur in rocks and ores. Crocket [7] stated that radiochemical neutron activation analysis (r.n.a.a.) methods were necessary for terrestrial rocks; however, some elements, particularly Au and Ir, could be determined instrumentally in some meteorites and ores.

Various r.n.a.a. procedures have been developed for the determination of most of the noble metals (excluding Rh) in rocks and ores. Crocket et al. [8] developed a procedure for Ru, Pd, Os, Ir, Pt and Au by fusion of a small (100—200 mg) irradiated sample with non-radioactive carriers of those elements; Nadkarni and Morrison [9] determined Au, Ru, Pd, Os, Ir and Pt in geological materials by r.n.a.a. procedures on 300—500 mg samples with Strafion NMR (Polycycle-NBL-17) ion-exchange resin; Caramella-Crespi et al. [10] determined Pd, Pt, Ir, Au and Ag by r.n.a.a. techniques after selective adsorption of these metals on molybdenum dibromide; and Millard and Bartel [2] used a mini-lead fire-assay procedure after sample irradiation (0.5—1-g sample) to separate Pd, Pt, Au, Ru, Os and Ir from their matrix.

Turkstra et al. [11] determined Rh, Pd, Pt, Au, Ir and Ag in ores, mattes and lead assay beads by i.n.a.a. procedures. Only Ir, Pt and Au could be determined directly in South African platinum ores, whereas Rh, Pd, Ag, Ir, Pt, and Au could possibly be determined in mattes containing very high PGM contents (15—500 ppm). Lead fire-assay beads prepared from South African platinum-bearing ores could be used to determine Rh, Pd, Ag, Ir, Pt and Au if these samples contained very high PGM concentrations. Ru and Os were not detectable by any of these methods.

Fire-assay procedures

The classical fire-assay technique uses lead as the collector for the noble metals. Beamish [12] found that there was "non-quantitative collection of the more insoluble platinum metals in the classical fire-assay". The insoluble noble metals were iridium, osmium and ruthenium. Robert et al. [13] reported that the lead fire-assay procedure did collect the noble metals quantitatively; however, subsequent cupellation for the separation of the lead resulted in large losses of osmium, ruthenium and iridium. Samples which contained sulphur had to be roasted and if more than 0.5% nickel was present it had to be removed with an HCl leach. For nickel sulphide ores these preliminary processes were necessary but undesirable as possible losses of the noble metal could occur.

Robert et al. [13] found that for all the noble metals a nickel sulphide fire-assay procedure was equal or superior to collection of the noble metals by the lead method; with the nickel sulphide procedure samples containing any amounts of nickel and sulphur do not require any pretreatment and a lower fusion temperature (1000°C in comparison with 1000—1200°C) reduces the possibility of losses of some of the more volatile PGM, particularly osmium. (High purity nickel produced through a carbonyl process

was supplied by Inco Metals Company Ltd. This material contains only 0.1 ppb Au and Ir; < 1 ppb Pt, Pd, Os, Ru and Rh.)

Subsequent to the fire-assay procedure, Robert et al. [13] dissolved the nickel sulphide fire-assay bead in 12 M HCl, filtered the solution and dissolved the noble metal residue in hydrochloric acid and peroxide. Robert et al. [14] studied the effects of sample matrix elements on the efficiency of the fire-assay procedure. The noble metals were determined colorimetrically or by atomic absorption spectroscopy. The preparation of three fire-assay beads (if Os < 10 ppm) was necessary and the sensitivities realized were poorer than those possible by n.a.a. techniques.

EXPERIMENTAL

Apparatus

During the fusion procedure a large home-made muffle furnace capable of reaching 1000°C was used. For the filtration procedure a Gelman Instrument Company vacuum filter apparatus (cat. no. xx1004720) was used.

Irradiations were performed (SLOWPOKE II reactor, University of Toronto) with a thermal neutron flux of 1.0×10^{11} n cm^{-2} s^{-1}. Pd and Rh were counted on a horizontally mounted Ge(Li) detector which has a resolution of 1.93 keV (FWHM), a peak-to-compton ratio of 32:1 for the 1332-keV peak of ^{60}Co, and a relative efficiency of 6.7%. The detector was connected to a Canberra Instruments 8180 4096-channel analyser. Pd, Pt, Ir, Os, Ru and Au radioisotopes were counted with a Princeton Gamma-Tech Ge(Li) detector with an active crystal volume of 65 cm^3, connected to a Tracor Northern TN-1700, 4096-channel analyser. This system has a resolution of 1.75 keV (FWHM), a peak-to-compton ratio of 43.1:1 for the 1332-keV peak of ^{60}Co, and a relative efficiency of 12.4%.

Reagents

All reagents must be tested to make sure that they are free of noble metals. Commercially available nickel products may contain substantial amounts of noble metals. Blank fire-assay charges were analysed whenever new reagent batches were introduced to ensure absence of noble metals. The following reagents were used in the fusion procedure: fused, ground sodium borate (Fisher Scientific S-252); calcined dry, purified sodium carbonate (Fisher Scientific S-261); silica floated powder, ca. 240 mesh (Fisher Scientific S-153); sublimed sulphur (J. T. Baker Chemical Co., 5-4088); nickel carbonyl powder (Inco Metals Co. Ltd.); 30-g fire-assay crucible (Canlab 8522-30C). During the dissolution stage 12 M HCl (J. T. Baker Chemical Co., 3-9535) and Metricel GA-1 (pore size 5.0 μm, 47 mm) filter papers (Gelman Filtration Products, #60003) were used.

Sample preparation

Fusion. Nickel sulphide fire-assay buttons were prepared from 30—50-g

samples, according to the fusion procedure of Robert et al. [13] with slight modifications. Instead of mixing the reagents and sample on glazed paper it was more satisfactory and convenient to mix them directly in the crucible; nickel powder, prepared by the nickel carbonyl process, was used instead of nickel oxide; after fusion the crucible contents were allowed to solidify in situ instead of pouring the crucible contents into an iron mold.

Dissolution and filtering. The bead was crushed in a hardened steel piston-type device to obtain a particle size of ca. 1 mm. The crushed pellet was heated with 400 ml of 12 M HCl in a covered beaker on a hotplate until the sample dissolved completely. When cooled, the solution was filtered under vacuum and washed with ca. 400 ml of distilled water. The black residue on the filter paper was folded into a triangular shape and sealed in plastic ready for the irradiation and counting procedure.

I.n.a.a.

The noble metal content was determined by a procedure involving two to three countings. Rhodium and palladium were determined during the first count, palladium if required (low levels, below ca. 50 ppb are not detected in the first count) during a second counting and the balance of the noble metals in a third count.

Rhodium and palladium. The samples were irradiated serially for 5 min and then allowed to decay for 60 s so that very short-lived radioisotopes, e.g. $^{77\,m}$Se ($t_{\frac{1}{2}}$ = 17.5 s), could decay. Samples and standards were counted for 200 s for the ^{109m}Pd and ^{104m}Rh γ-rays. Nuclear data for the radioisotopes are given in Table 1. Peak areas, corrected for background, were compared for samples and standards.

Palladium, platinum, osmium, ruthenium, iridium and gold. Up to forty

TABLE 1

Nuclear data (Data from Bureau of Radiological Health and the Training Institute Environmental Control Administration [18])

Element	Induced nuclear reaction	Isotope counted	% Isotopic abundance target isotope (θ)	Cross-section (barn)	Half-life of nuclide produced ($t_{\frac{1}{2}}$)	γ-ray used (keV)
Rhodium	^{103}Rh (n, γ) ^{104m}Rh	^{104m}Rh	100.0	800	4.41 min	51
Palladium	^{108}Pd (n, γ) ^{109}Pd	^{109}Pd	26.7	12	13.5 h	88
	^{108}Pd (n, γ) ^{109m}Pd	^{109m}Pd	26.7	0.2	4.69 min	186
Platinum	^{198}Pt (n, γ) ^{199}Pt (β^-) ^{199}Au	^{199}Au	7.2	4	3.15 d	158
Iridium	^{191}Ir (n, γ) ^{192}Ir	^{192}Ir	38.5	750	74.2 d	317 468
Osmium	^{190}Os (n, γ) ^{191}Os	^{191}Os	26.4	3.9	14.6 d	129
Ruthenium	^{102}Ru (n, γ) ^{103}Ru	^{103}Ru	31.5	1.4	38.9 d	497
Gold	^{197}Au (n, γ) ^{198}Au	^{198}Au	100.0	98.8	64.8 h	412

samples, ore standard, internal standard and flux monitors were sealed in a 27-cm^3 plastic irradiation container which was irradiated for 16 h. Samples were allowed to decay for ca. 4 h from the end of the irradiation and were counted for ^{109}Pd for 500—2500 s depending on the palladium content.

The samples were allowed to decay for a further 7—9 d depending on the rhenium content of the sample. The 155-keV ^{185}Re γ-peak interfered with the 158-keV ^{199}Au photopeak. The samples were recounted for ^{199}Au (for platinum content), ^{191}Os, ^{103}Ru, ^{192}Ir and ^{198}Au. Integrated peak areas, corrected for background, were entered into a computer program, which took into account sample weights, yield through the crushing procedure, irradiation time, counting time, and duration of count. Radioisotopes were corrected for decay and the activity was compared with standards of known concentration.

Various problems have been encountered [8, 15, 16] in neutron activation techniques for the noble metals, e.g. the fission production of ^{103}Ru and ^{109}Pd by the reactions ^{235}U (n, f) ^{103}Ru and ^{235}U (n, f) ^{109}Pd, particularly in rocks containing uranium at levels in excess of the noble metals. Gijbels [16] found that this problem was not serious in rocks with low uranium contents, as would be found in basic to ultrabasic rocks and nickel sulphide ores.

Millard and Bartel [2] reported that 75-keV lead x-rays produced by γ-rays from the sample, bombarding the shielding surrounding their Ge(Li) detector, interfered with the 77-keV ^{197}Pt peak. The ^{197}Pt isotope was not used in this work, but it was noted that the 88-keV ^{109}Pd peak suffered from interference from 88-keV lead x-rays. This problem was effectively eliminated by lining the interior of the counting chamber with copper and cadmium sheeting to absorb the lead x-rays; similar results were then obtained for palladium from the 88-keV ^{109}Pd and the 186-keV ^{109m}Pd peaks.

Platinum was counted by means of the 158-keV ^{199}Au γ-ray produced by the reaction ^{198}Pt (n, γ) ^{199}Pt (β^-) ^{199}Au. However, ^{199}Au may theoretically be produced by the reaction ^{197}Au (n, γ) ^{198}Au (n, γ) ^{199}Au.

Filter papers, impregnated with various amounts of gold, were irradiated under the conditions used for samples and standards to test that ^{199}Au was not produced from ^{197}Au by the latter reaction. After a decay period similar to that used for the samples, the test filter papers were counted. Production of 158-keV ^{199}Au from ^{197}Au was negligible.

RESULTS AND DISCUSSION

The proposed procedure was followed for the internal ore standard L.S. 4 [1]; the results presented in Table 2 show better than 13% reproducibility for the 11 individual fire-assay pellets analysed. Certain pellets were split into two portions prior to the dissolution stage and were analysed separately; the reproducibility for different portions of the pellet (e.g., Pt value of H1-18 and H2-18) is poorer, signifying that the fire-assay beads may not be completely homogeneous.

TABLE 2

Reproducibility of analytical data for noble metals in the internal standard L.S. 4

Run	Found (ppb)						
	Rh	Pd	Pt	Ir	Os	Ru	Au
A-4	115	272	285	71	35	132	30
B-2	128	300	339	74	35	125	42
C1-9	134	323	267	80	32	155	43
C2-9	135	320	277	83	32	175	44
(Av.	135 ± 1	322 ± 2	272 ± 7	82 ± 2	32 ± 0	170 ± 10	43 ± 1)
D-10	134	338	312	82	33	173	44
E1-13	130	285	300	76	33	150	41
E2-13	135	275	279	78	31	156	42
(Av.	133 ± 4	280 ± 7	290 ± 20	77 ± 1	32 ± 4	153 ± 4	41 ± 1)
F1-15	130	283	282	74	32	158	42
F2-15	139	291	298	73	34	148	43
(Av.	135 ± 6	288 ± 7	290 ± 10	74 ± 1	33 ± 1	153 ± 7	43 ± 1)
H1-18	143	337	341	80	31	169	37
H2-18	146	331	234	65	31	141	31
(Av.	145 ± 2	334 ± 4	290 ± 80	70 ± 10	31 ± 0	150 ± 20	34 ± 4)
I1-16	132	366	307	76	29	136	46
I2-16	136	332	280	75	28	126	46
(Av.	134 ± 3	350 ± 20	290 ± 20	75 ± 1	29 ± 1	131 ± 7	46 ± 0)
J1-17	141	376	275	76	30	147	46
J2-17	135	327	236	68	26	135	37
(Av.	138 ± 4	350 ± 40	260 ±30	72 ± 6	28 ± 3	141 ± 8	42 ± 6)
SN-1	141	321	248	—	—	—	36
SN-2	—	—	270	75	—	152	57
Averages	135 ± 7	320 ± 40	290 ± 30	75 ± 5	30 ± 3	150 ± 20	42 ± 6

The accuracy of the method was tested on PTC, the Canadian certified noble metal ore standard; the results are presented in Table 3. For Rh, Pd, Pt, and Au the average values are well within the 95% confidence limits of the recommended values specified by McAdam et al. [17] and the values for Os, Ru, Ir are within the 95% confidence limits of the estimated mean.

The accuracy and precision shown are superior to those reported for most analytical procedures for the noble metals. The detection limits obtained by this method (Table 4) are superior to analytical procedures that do not utilize n.a.a.

The recovery of the noble metals was tested by adding irradiated noble metals to a variety of sample types and carrying out the fusion and dissolution procedures. Loss of the noble metals through these procedures occurs mainly during the fusion procedure in which the average total losses were less than 6% for Pd, Pt, Ir, Os, Ru, and Au. Individual losses for Au did run as high as 8%. These results are summarized in Table 5. Losses of Rh through the procedure could not be tested by radiotracer techniques because of the short half-life of ^{104m}Rh (4.41 min). The experimentally determined and recommended values for Rh are very similar (Table 3).

TABLE 3

Analyses of noble metals-bearing concentrate, PTC, and comparison with the recommended values for Rh, Pd, Pt and Au, and the estimated mean values for Os, Ru and Ir

Run	Found (ppm)						
	Rh	Pd	Pt	Au	Os	Ru	Ir
1a	0.62	13.2	3.1	0.55	0.35	0.63	0.21
1b	0.58	12.9	2.8	0.55	0.31	0.54	0.19
(Av.	0.60	13.0	2.9	0.55	0.33	0.59	0.20)
2a	0.62	12.9	3.3	0.57	0.32	0.58	0.21
2b	0.61	12.1	2.8	0.57	0.31	0.49	0.19
2c	0.64	13.0	3.4	0.64	0.34	0.62	0.21
(Av.	0.62	12.7	3.1	0.59	0.32	0.56	0.20)
3a	0.62	12.6	3.1	0.57	0.37	0.60	0.21
3b	0.59	13.3	3.3	0.58	0.38	0.63	0.20
3c	0.63	12.1	2.8	0.58	0.39	0.59	0.21
(Av.	0.61	12.7	3.0	0.58	0.38	0.61	0.20)
5a	0.64	12.6	2.6	0.58	0.31	nd	0.20
5b	0.64	13.0	2.9	0.61	0.37	nd	0.20
5c	0.62	12.7	2.7	0.78	0.35	nd	0.20
5d	0.64	12.6	2.2	0.60	0.28	nd	0.16
(Av.	0.64	12.7	2.6	0.64	0.33		0.19)
Averages (this study)							
	0.62	12.8	2.9	0.59	0.34	0.59	0.20
Earlier values [17]							
	0.62[a]	12.7[a]	3.0[a]	0.65[a]	0.24[b]	0.65[b]	0.17[b]
95% confidence intervals [17]							
Low	0.55	12.0	2.8	0.55	—	0.34	0.00
High	0.69	13.0	3.2	0.72	—	0.93	0.34
Number of labs. reporting results					1	3	3

[a]Recommended values [17]. [b]Estimated mean [17].

Detection limits by n.a.a. are superior to other methods with the possible exception of electrothermal a.a.s. which is, however, still very much unproven for the real analysis of the noble metals at present. In any case, a fire assay, followed by more lengthy chemical treatments than necessary for the above procedure would be essential for these types of samples prior to a.a.s.

The determination of all the noble metals in rocks and ores by n.a.a. has not been reported previously. Although preconcentration of the noble metals by lead fire-assay techniques prior to activation was tried by Turkstra et al. [11], the analyses did not include Os or Ru and the data were poor for Pt, Pd, and Rh.

TABLE 4

Noble metal detection limits and counting details (Ge(Li) detector number 1 at the SLOWPOKE II reactor facility, University of Toronto, was used for Rh and Pd. All other elements were analysed with the Ge(Li) detector at the Erindale College, neutron activation laboratory)

Element	Detection limits[a] (ppb)	Time counted (s)
Rh	1	200
Pd	50	200
	5	500—2500
Pt	5	700—5000
Ir	0.1	700—5000
Ru	3	700—5000
Os	2	700—5000
Au	0.1	700—5000

[a]Detection limits achieved at the maximum time counted. (Detection limit is defined as the smallest concentration which gives a net peak count of twice the standard deviation of the background.)

One of us (E.L.H.) is grateful to the National Research Council of Canada for support in the form of NRC postgraduate scholarships. Financial assistance was given by the Canada Department of Energy, Mines and Resources, and by the NRC operating grant of A.J.N. Sample collection was supervised by R. A. Alcock (INCO Metals Company, J. Roy Gordon Research Centre) who also helped to improve the manuscript by critical appraisal. Thanks are also due to the staff of INCO Metals Company who aided in various aspects of this study and to S. Naldrett for providing some PGM analyses. C.-L. Chou provided the neutron activation facilities at which a portion of the counting was done.

TABLE 5

Recovery of the noble metals from the nickel sulphide fire-assay fusion and dissolution procedures

Sample	Type	Loss (%)[a]						Fusion or dissolution[b]
		Pd	Pt	Ir	Os	Ru	Au	
L.S. 4	Massive sul.	3	3	2	1	1	4	(1)
		—	—	—	—	—	1	(2)
		3	3	2	1	1	5	Total
L.S. 17	Diss. Sul.	4	5	2	2	1	7	(1)
		—	—	—	—	—	1	(2)
		4	5	2	2	1	8	Total
L.S. 35	Host rock (gabbroic)	1	6	1	5	3	5	(1)
		—	—	—	—	—	1	(2)
		1	6	1	5	3	6	Total
L.S. 40	Stringer ore	6	2	2	4	4	6	(1)
		—	—	tr	—	—	1	(2)
		6	2	2	4	4	7	Total
F417917	Host rock (ultramafic)	4	4	—	3	5	4	(1)
		—	—	—	—	—	1	(2)
		4	4	—	3	5	5	Total
F418355	Massive Sul.	5	5	1	3	5	6	(1)
		—	—	—	—	—	1	(2)
		5	5	1	3	5	7	Total
F418341	Vein ore	3	5	2	3	—	4	(1)
		—	—	—	—	—	1	(2)
		3	5	2	3	—	5	Total
L.S. 1	Diss. Sul.	2	2	4	2	—	4	(1)
		—	—	—	—	—	—	(2)
		2	2	4	2	—	4	Total
Average total losses		<4	<4	<2	<3	<3	<6	

[a]— Indicates not detected; tr indicates only traces detected; [b]Fusion stage loss (1); dissolution stage loss (2).

REFERENCES

1 E. L. Hoffman, The Platinum Group Element and Gold content of Some Nickel Sulfide Ores, Ph.D. Thesis (in preparation), University of Toronto, 1978.
2 T. Millard, Jr. and A. J. Bartel, in A. O. Brunfelt and E. Steinnes (Eds.), Activation Analysis in Geochemistry and Cosmochemistry, Universitetsforlaget, 1971, 353.
3 T. L. Wright and M. Fleischer, U.S. Geol. Survey Bull., 1214-A (1965) 24.
4 J. C. Van Loon, Pure Appl. Chem., 49 (1977) 1495.
5 I. S. Rozhkov, Dokl. Akad. Nauk SSSR, 191 (1970) 927.
6 L. J. Cabri and J. H. G. Laflamme, Econ. Geol., 71 (1976) 1159.

7 J. H. Crocket, in A. O. Brunfelt and E. Steinnes (Eds.), Activation analysis in Geochemistry and Cosmochemistry, Universitetforlaget, 1971, 339.
8 J. Crocket, R. Keays and S. Hsieh, J. Radioanal. Chem., 1 (1968) 487.
9 R. A. Nadkarni and G. H. Morrison, Anal. Chem., 46 (1974) 232.
10 V. Caramella-Crespi, U. Pisani, M. T. Ganzerli-Valentini, S. Meloni and V. Maxia, J. Radioanal. Chem., 23 (1974) 23.
11 J. Turkstra, P. J. Pretorius and W. J. DeWet, Anal. Chem., 42 (1970) 835.
12 F. E. Beamish, The Analytical Chemistry of the Noble Metals, Pergamon, Oxford, 1966, p. 609.
13 R. V. D. Robert, E. Van Wyk and R. Palmer, N.I.M. report 1371, 1971.
14 R. V. D. Robert, E. Van Wyk and T. W. Steele, N.I.M. report 1705, 1975.
15 J. Crocket and G. Skippen, Geochim. Cosmochim. Acta, 30 (1966) 129.
16 R. Gijbels, Talanta, 18 (1971) 587.
17 R. C. McAdam, Sutarno and P. E. Moloughney, Dept. Energy, Mines and Resources, Mines Branch, Ottawa, Report TB176, 1973, p. 25.
18 Bureau of Radiological Health and the Training Institute Environmental Control Administration, Radiological Health Handbook, U.S. Public Health Service, 1970, p. 552.

Analytica Chimica Acta, 102 (1978) 167—176

INFLUENCE DES SOLVANTS ORGANIQUES SUR LES EQUILIBRES D'ECHANGE D'IONS ENTRE UNE RESINE A GROUPEMENTS SULFONIQUES
I. Partage d'éléments métalliques monovalents et divalents

A. R. RODRIGUEZ et C. POITRENAUD*

Institut National des Sciences et Techniques Nucléaires de Saclay, B.P. n° 6, 91190 Gif-sur-Yvette (France)

(Reçu le 10 Mai 1978)

RESUME

Les coefficients de partage des cations monovalents du sodium, du césium et de l'argent et des cations divalents du cobalt, du nickel et du cuivre, entre une résine échangeuse de cations Bio-Rad AG 50W-X8 et des mélanges de l'eau avec un solvant organique (méthanol, éthanol, n-propanol, acétone, dioxane, tétrahydrofuranne ou l'acide acétique) ont été déterminés en fonction de la composition du mélange hydro—organique. Les constantes d'échange, K_{nH}^{M} (n = 1 ou 2), en ont été déduites.

SUMMARY

Effect of organic solvents on exchange equilibria with a sulphonic acid resin. Part 1. Distribution of monovalent and divalent metal ions.

The distribution coefficients of the monovalent cations sodium, cesium and silver and the divalent cations cobalt, nickel and copper between Bio-Rad AG 50W-X8 cation-exchange resin and mixtures of water with organic solvents (methanol, ethanol, n-propanol, acetone, dioxane, tetrahydrofuran, acetic acid) have been determined as a function of the composition of the aqueous—organic mixtures. The equilibrium constants K_{nH}^{M} (n = 1 or 2) are reported.

De nombreuses publications concernant le comportement des échangeurs d'ions dans des mélanges de l'eau avec des solvants organiques variés ont été regroupées dans plusieurs mises au point bibliographiques [1—10]. Ces études ont permis de mettre en évidence certains facteurs dont dépendent les constantes d'échange d'ions en milieu hydro—organique: nature du solvant, constante diélectrique de ces mélanges avec l'eau, nature des ions échangés, etc. Toutefois, les résultats rapportés par ces publications sont difficilement comparables car les mesures ont été effectuées dans des conditions différentes. En effet, les taux de saturation des résines étudiées sont très différents; les constantes d'échange ont été déterminées ou bien au voisinage de la demi-saturation de la résine en chacun des ions qui s'échangent ou bien à saturation de l'échangeur en l'un d'eux, l'autre se trouvant à l'état de traces. De plus, le milieu et la force ionique dans lesquels les mesures ont été réalisées sont

quelquefois mal précisés. Les résultats expérimentaux sont présentés sous forme de variations du coefficient de partage ou des constantes d'échange d'ions en fonction de la composition du mélange hydro—organique, mais souvent les constantes d'échange indiquées représentent des constantes conditionnelles non corrigées des effets des réactions de formation de complexes en solution. En outre, ces mesures ont été le plus souvent effectuées dans des domaines de teneurs en solvant comprises entre 0 et 70—80%, les mélanges très pauvres en eau étant beaucoup moins étudiés. Enfin, les résultats dont on dispose concernent surtout l'échange des cations alcalins et de l'ion hydrogène, en particulier l'échange Na^+—H^+ dans des mélanges de l'eau avec des solvants peu variés, surtout méthanol et éthanol.

Pour toutes ces raisons, il semble difficile de faire une étude comparative des résultats que l'on trouve dans la littérature relatifs à l'échange d'ions en milieu hydro—organique.

Pour permettre de dégager plus nettement l'influence de différents paramètres sur l'équilibre d'échange d'ions en milieu hydro—organique, nous avons réalisé des mesures des coefficients de partage de cations monovalents et divalents entre une résine échangeuse de cations et une solution acide de leurs sels dans des mélanges hydro—organiques de compositions variées; nous en avons ensuite déduit les constantes d'échange de ces ions dans les mélanges étudiés. Les mesures ont été effectuées dans des mélanges hydro—organiques couvrant une gamme étendue de pourcentages d'eau (4—100%). En outre, afin de pouvoir réaliser des études comparatives, nous avons choisi des ions de taille différente dans des mélanges de l'eau avec divers solvants organiques. En particulier, nous avons cherché à utiliser des solvants de propriétés, telles que la constante diélectrique, la polarité et le pouvoir solvatant, très différentes.

PARTIE EXPERIMENTALE

L'échangeur d'ions était la résine Bio-Rad AG 50W-X8, 50—100 mesh, mise sous forme H^+ après plusieurs cycles d'échange H^+—Na^+.

L'acide acétique, le méthanol, l'éthanol, le n-propanol, l'acétone, le dioxanne, le tétrahydrofuranne, l'acide perchlorique et l'acide nitrique étaient des produits R. P. Prolabo. Les mélanges hydro—organiques ont été préparés par pesées. Le perchlorate de sodium (Fluka), le perchlorate d'argent (Touzart et Matignon), l'acétate de césium (Merck), le chlorure de cobalt, le nitrate de nickel et le nitrate de cuivre (R. P. Prolabo) étaient utilisées.

L'argent a été dosé par volumétrie à l'aide d'une solution titrée d'iodure de potassium avec détermination potentiométrique du point équivalent (pH-mètre Beckman de recherche). Le sodium, le césium, le cobalt et le cuivre ont été dosés par la mesure de la radioactivité des traceurs ^{22}Na, ^{137}Cs, ^{57}Co, ^{60}Co et ^{64}Cu, réalisée par spectrométrie-γ, à l'aide d'un scintillateur NaI(Tl) relié à un sélecteur multicanaux. Le nickel a été dosé par la mesure de la radioactivité β des traceurs ^{63}Ni, à l'aide d'un compteur à scintillation liquide

(spectromètre à scintillation liquide ABAC SL40, liquide scintillant Insta-Gel, Packard).

Les expériences effectuées par simple équilibre en flacon consistent à mettre en présence une solution d'un sel d'un titre connu dans un mélange hydro—organique et un échantillon de résine (1 g environ) sous forme acide préalablement mis en équilibre avec le même mélange. Le coefficient de partage a été déduit de la variation de la concentration du cation en solution avant et après équilibre. Dans le cas où les éléments métalliques ont été dosés à l'aide de traceurs radioactifs, nous avons ajouté une quantité d'élément métallique non actif pour avoir une concentration d'élément d'environ 10^{-3} M dans la solution en contact avec la résine. La quantité totale d'élément métallique représente 0,5% de la capacité de l'échangeur.

Dans le cas de partage d'éléments divalents, les activités des solutions, avant et après l'équilibre, étaient très différentes à cause de la forte fixation des éléments étudiés sur l'échangeur. Nous avons donc vérifié que le nombre d'impulsions mesurées (c'est-à-dire la surface du pic photoélectrique du radioisotope, déduction faite du bruit de fond) était proportionnel à la concentration du radioisotope dans la gamme de concentrations utilisées dans nos mesures de coefficient de partage.

La vitesse d'établissement de l'équilibre d'échange d'ions peut être faible dans le cas des mélanges hydro—organiques qui gonflent peu la résine, tels que les mélanges eau—acide acétique, eau—tétrahydrofuranne et eau—dioxanne riches en solvant organique, où la quantité de liquide qui imbibe la résine représente 50% environ du liquide de gonflement dans l'eau [11]. Afin de vérifier que l'équilibre d'échange dans ces mélanges riches en solvant est atteint dans un temps suffisamment court, nous avons effectué une étude cinétique dans le cas de la fixation de l'ion Na^+ dans les mélanges eau—tétrahydrofuranne—acide perchlorique 0,1 M à 5,0% d'eau et eau—dioxanne—acide perchlorique 0,1 M à 4,5% d'eau. L'équilibre d'échange est atteint au bout de 30 et de 60 min dans les mélanges eau—tétrahydrofuranne et eau—dioxanne, respectivement. Le coefficient de partage du sodium a été mesuré après des temps d'agitation de 15, 30, 60, 90, 150, 1440 et 2820 min. Dans la plupart de nos expériences nous avons agité l'échantillon de résine et la solution pendant 18 h (1080 min) environ.

Pour chaque mélange hydro—organique, nous avons fait deux essais parallèles sur deux échantillons de résine et nous avons adopté comme résultat la moyenne de deux valeurs qui, en général, ne diffèraient pas de plus de 3%. Toutes les expériences ont été effectuées à la température ambiante (20—25°C).

RESULTATS

Nous avons déterminé les coefficients de partage de trois cations monovalents et de trois cations divalents entre une résine échangeuse d'ions et des mélanges hydro—organiques. Sur les Figs. 1 et 2 sont représentées les courbes de variation de coefficients de partage du sodium, du césium, de l'argent, du cobalt, du

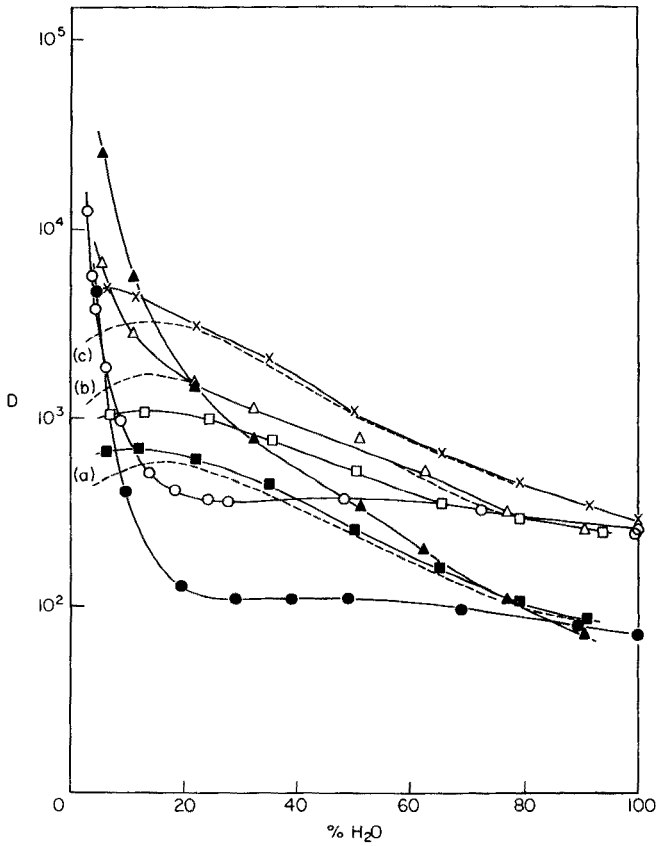

Fig. 1. Variation de D_M en fonction du pourcentage d'eau des mélanges hydro—organiques. (—) Milieu acide nitrique 0,1 M: eau—méthanol (■) Na, (□) Ag, (×) Cs; eau—acide acétique (●) Na, (○) Ag; eau—tétrahydrofuranne (△) Na, (▲) Ag. (---) Milieu acide perchlorique 0,1 M: eau—méthanol (a) Na, (b) Ag, (c) Cs.

nickel et du cuivre, entre la résine acide sulfonique et différents mélanges eau—solvant organique—acide minéral 0,1 M; le solvant pouvant être le méthanol, l'éthanol, le n-propanol, l'acétone, le dioxanne, le tétrahydrofuranne ou l'acide acétique et l'acide minéral étant l'acide perchlorique ou l'acide nitrique. Sur tous ces graphiques la variable portée en abscisse est le pourcentage (en poids) d'eau dans les mélanges extérieurs à la résine.

La répartition des résultats expérimentaux entre ces graphiques a été faite de façon que soient possibles les comparaisons; à cet effet, dans certains cas des courbes figurant sur un autre graphique ont été reproduites en tireté.

Dans les mélanges riches en eau toutes les courbes de variation du coefficient de partage tendent vers une même valeur pour chaque cation, quel que soit l'acide minéral présent et le solvant. Cette valeur représente le coefficient

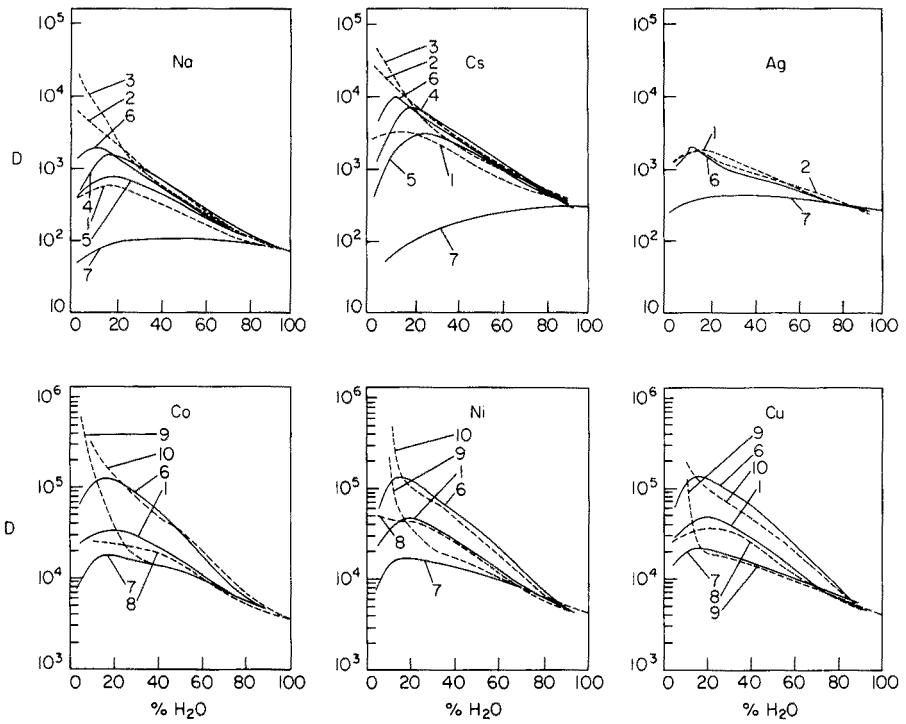

Fig. 2. Variation de D_M en fonction du pourcentage d'eau des mélanges hydro—organiques. Milieu acide perchlorique 0,1 M: (1) eau—méthanol; (2) eau—éthanol; (3) eau—n-propanol; (4) eau—acétone; (5) eau—dioxanne; (6) eau—tétrahydrofuranne; (7) eau—acide acétique. Milieu acide nitrique 0,1 M: (8) eau—méthanol: (9) eau—acide acétique; (10) eau—tétrahydrofuranne.

limite de partage de chaque élément dans une solution aqueuse d'acide fort 0,1 M.

Dans les mélanges pauvres en eau les coefficients de partage, D_M, des cations sont beaucoup plus grands en milieu nitrique qu'en milieu perchlorique dans les mélanges eau—acide acétique et eau—tétrahydrofuranne (Figs. 1 et 2). Ces valeurs élevées de D_M résultent de la faible concentration de l'ion échangeable H^+ due à la faible dissociation de l'acide nitrique dans ces mélanges peu dissociants [12]. Par contre, dans les mélanges eau—méthanol, les courbes présentent la même allure et sont assez voisines en milieu nitrique et en milieu perchlorique, pour un cation donné (Figs. 1 et 2). En effet, dans ces mélanges de constantes diélectriques élevées, les deux acides et leurs sels sont complètement dissociés et les coefficients de partage des éléments ne dépendent pas de la nature de l'acide minéral présent.

Dans les mélanges eau—solvant organique—acide perchlorique, on peut distinguer deux types de courbes $D_M = f(\%\ H_2O)$: (a) celles qui présentent, pour tous les pourcentages d'eau étudiés, une variation continuellement

croissante lorsque la teneur en eau du mélange diminue (D_{Na} et D_{Cs} dans les mélanges eau—éthanol et eau—n-propanol); (b) celles qui présentent un maximum dans la zone de pourcentage d'eau étudiée.

Cette distinction est peut-être arbitraire car rien ne permet d'affirmer que les courbes du premier groupe ne présentent pas un maximum dans la zone du pourcentage d'eau très faible (< 4%) que nous n'avons pas étudiée. Contrairement à nos résultats, Fessler et Strobel [13] ont trouvé un maximum dans le cas du sodium dans les mélanges eau—éthanol, mais leurs expériences n'ont pas été réalisées dans les mêmes conditions que les nôtres; en particulier, le taux de saturation de la résine en ion Na^+ était de 50%, alors que nous avons étudié des coefficients limites de partage.

Exploitation des résultats

Pour pouvoir connaître l'influence d'un solvant organique sur l'équilibre d'échange d'ions il faudrait corriger les valeurs expérimentales des coefficients de partage des effets des réactions en solution afin de pouvoir atteindre les valeurs des constantes d'échange des ions simples. En effet, le coefficient de partage d'un élément monovalent, M, entre une résine échangeuse de cations sous forme H^+ et une solution acide de ses sels dépend de la constante d'échange des ions M^+ et H^+, mais aussi des constantes de dissociation de l'acide et du sel mis en jeu [12]. Les variations des coefficients de partage avec la composition d'un mélange hydro—organique peuvent être très différentes de celles des constantes d'échange lorsque les constantes de dissociation de l'acide et du sel sont très différentes. C'est le cas de l'échange Ag^+—H^+ dans les mélanges eau—acide acétique—acide nitrique, comme nous l'avons déjà montré [12]. Par contre, si les constantes de dissociation de l'acide et du sel sont voisines, la constante d'échange d'ions est directement proportionnelle au coefficient de partage. Nous avons également montré que dans les mélanges eau—acide acétique—acide perchlorique, les constantes de dissociation de l'acide chlorique et des perchlorates d'argent, de sodium et de césium étaient voisines et que la variation des coefficients de partage avec la composition du mélange avait la même allure que celle de la constante d'échange d'ions [12, 14]. Dans ce cas particulier, la constante d'échange, K_H^M, peut être déduite du coefficient de partage, D, par l'expression

$$K_H^M = D\, C_o/C_E \qquad (1)$$

où C_o est la concentration de l'acide en solution et C_E la capacité d'échange de la résine.

Dans les mélanges hydro—organiques dissociants, comme les mélanges eau—alcool, il est logique de supposer que cette expression est valable. En outre, nous avons admis qu'il en était de même dans tous les mélanges eau—solvant organique—acide perchlorique étudiés, même dans le cas de solvants peu dissociants. Cette hypothèse a été d'ailleurs vérifiée dans le cas de l'échange Na^+—H^+ dans les mélanges eau—dioxanne et eau—tétrahydrofuranne. En effet, pour un mélange de teneur en eau constante et faible, nous avons trouvé

expérimentalement une variation linéaire de D_{Na} en fonction de l'inverse de la concentration d'acide perchlorique en solution, comme le prévoit l'expression (1). Ceci laisse supposer que, dans ces milieux, les réactions en solution ont un effet négligeable ou que les constantes de dissociation de l'acide et du sel présents sont voisines.

Par ailleurs, les valeurs des constantes d'échange des ions Na^+ et H^+ calculées à l'aide de l'expression (1) dans les mélanges eau—dioxanne— acide perchlorique sont en très bon accord avec celles déterminées dans ces mêmes mélanges par Boni et Strobel [15] par dosage des éléments dans les deux phases.

En ce qui concerne les éléments divalents, il paraît difficile de refaire une étude semblable à celle réalisée dans le cas des éléments monovalents [12], car les agrégats des ions possibles entre le cation divalent et les anions de la solution conduisent à de nombreuses espèces et l'expression de D deviendrait très complexe et inexploitable.

Par contre, si l'on admet que, comme dans le cas des ions monovalents, les constantes de dissociation des agrégats d'ions en milieu perchlorique sont grandes ou voisines, on peut supposer que dans ce milieu, la constante d'échange des ions divalents et des ions hydrogène est directement proportionnelle au coefficient de partage de ces éléments.

DISCUSSION

L'ensemble de nos résultats expérimentaux peut nous permettre de dégager l'influence de certains facteurs sur les constantes d'échange des éléments étudiés.

Les théories les plus simples pour décrire l'équilibre d'échange d'ions en fonction des propriétés d'un milieu hydro—organique prévoient une variation linéaire du logarithme de la constante d'échange avec l'inverse de la constante diélectrique du mélange [16—18]. Nous avons donc représenté sur la Fig. 3 le logarithme de la constante d'échange des ions Na^+—H^+, calculée à l'aide de l'expression (1) en fonction de l'inverse de la constante diélectrique des mélanges hydro—organiques extérieurs à la résine. Des courbes d'allure analogue ont été obtenues dans le cas du césium, de l'argent, du cobalt, du nickel et du cuivre. On observe que, dans les milieux riches en eau, $\log K$ est une fonction linéaire de $1/\epsilon$. La pente de la droite est une caractéristique des ions échangés mais semble indépendante du solvant. La loi linéaire n'est suivie que pour des valeurs de $1/\epsilon$ inférieures à une valeur limite qui dépend des ions échangés et du solvant organique. Le domaine de linéarité peut être très étendu (cas des alcools) ou très réduit (cas de l'acide acétique).

Dans les milieux pauvres en eau la loi linéaire simple n'est plus suivie. L'écart à la droite dépend des ions échangés et du solvant organique. Il semble d'autant plus important que la différence de composition entre le liquide qui imbibe la résine et la solution extérieure est plus grande, que la tendance à être solvaté des ions mis en jeu est plus différente et que la différence entre les pouvoirs solvatants du solvant organique et de l'eau est plus grande.

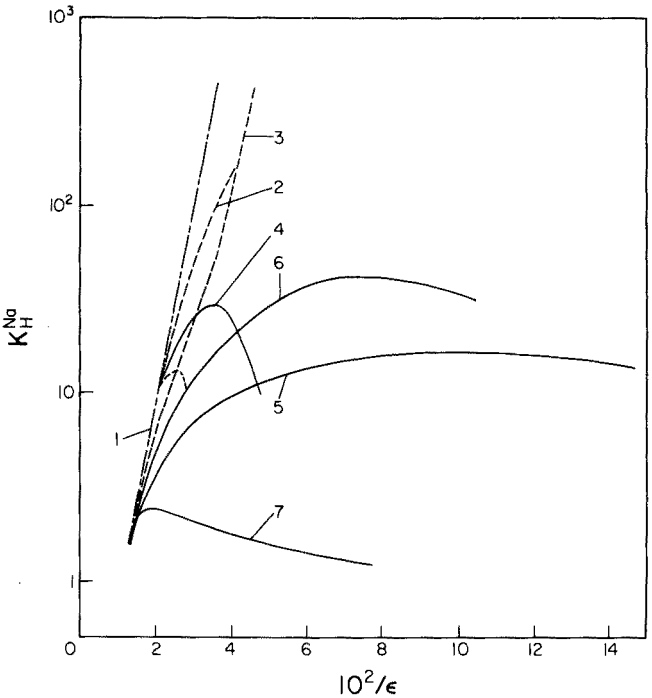

Fig. 3. Variation de la constante d'échange des ions Na^+ et H^+ en fonction de l'inverse de la constante diélectrique des mélanges hydro—organiques. (1) Eau—méthanol; (2) eau—éthanol; (3) eau—n-propanol; (4) eau—acétone; (5) eau—dioxanne; (6) eau—tétrahydrofuranne; (7) eau—acide acétique. Valeurs des constantes diélectriques d'après [19—22].

D'autre part, en ce qui concerne la séparation des éléments métalliques étudiés à l'aide des résines échangeuses de cations, des mélanges de l'eau avec des solvants organiques variés ont été souvent étudiés. Nous avons voulu savoir si les mélanges que nous avons étudiés étaient plus sélectifs que l'eau vis-à-vis des ces éléments. Pour cela nous avons calculé les coefficients de sélectivité de ces cations (rapport de coefficients de partage) en fonction de la teneur en eau des mélanges hydro—organiques en milieu nitrique et perchlorique. Les résultats concernant le partage des éléments divalents sont représentés sur la Fig. 4. On remarque que l'addition d'un solvant organique modifie l'affinité relative de la résine vis-à-vis des cations étudiés. On observe aussi que ces coefficients dépendent de la nature de l'acide minéral en solution; ils sont sensiblement les mêmes dans les mélanges eau—solvant organique—acide perchlorique, où les constantes de dissociation des espèces sont voisines, que dans l'eau. Par contre, les coefficients de sélectivité deviennent différents de ceux trouvés dans l'eau lorsque l'on ajoute un acide minéral dont l'anion est capable de donner des paires d'ions avec les cations considérés tel que l'acide nitrique. Ceci montre que dans le cas d'ions de propriétés voisines, l'addition d'un solvant organique modifie la sélectivité apparente de la résine vis-à-vis

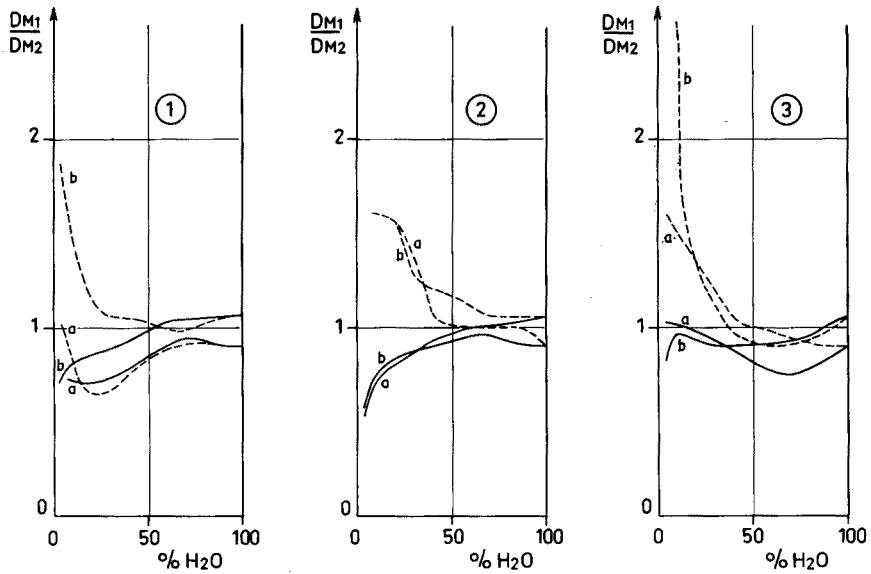

Fig. 4. Variation du coefficient de sélectivité, D_{M_1}/D_{M_2}, en fonction du pourcentage d'eau des solutions. (a) D_{Co}/D_{Cu}; (b) D_{Ni}/D_{Cu}. Mélanges: (1) eau—méthanol; (2) eau—acide acétique; (3) eau—tétrahydrofuranne. (—) Milieu perchlorique; (---) milieu nitrique.

des ions mis en jeu non pas par une action sur la constante d'échange d'ions, mais par l'apparition de réactions secondaires que déplacent l'équilibre d'echange. Des séparations difficiles à réaliser dans l'eau ne peuvent donc être améliorées par l'utilisation d'un solvant organique qu'en présence d'acides minéraux, autres que l'acide perchlorique, capables de former des paires d'ions avec les cations présents.

Ce travail a été réalisé grâce à l'aide matérielle du Commissariat à l'Energie Atomique et à l'aide scientifique de M. le Professeur B. Trémillon (Université Pierre et Marie Curie) que les auteurs tiennent à remercier. Ils sont aussi reconnaissants à M. J. L. Barret de l'aide qu'il leur a apportée au cours du travail expérimental.

BIBLIOGRAPHIE

1 B. Trémillon, Les séparations par les résines, échangeuses d'ions, Gauthier-Villars, Paris, 1965, chap. II, pp. 120—142.
2 J. Korkisch, Ion Exchange in Mixed and Non-aqueous Media, dans D. C. Stewart et H. A. Elion (Eds.), Progress in Nuclear Energy, Series IX, Analytical Chemistry, vol. 6, Pergamon Press, New York, 1966, pp. 3—94.
3 M. Fojtik et V. Koprda, Chem. Zvesti, 22 (1968) 983.
4 G. J. Moody et J. D. R. Thomas, Analyst, 93 (1968) 557.
5 G. J. Moody et J. D. R. Thomas, Lab. Pract., 19 (1970) 284, 378 et 487.
6 Y. Marcus et A. S. Kertes, Ion Exchange and Solvent Extraction of Metal Complexes, J. Wiley, New York, 1969, Chap. 4, pp. 239—321.

7 W. R. Heumann, C. R. C. Crit. Rev. Anal. Chem., 2 (1971) 425.
8 Y. Marcus, Ion Exchange in Non-aqueous and Mixed Solvents dans J. A. Marinsky et Y. Marcus (Eds.), Ion Exchange and Solvent Extraction, vol. 4, M. Dekker, New York, 1973, pp. 1—119.
9 H. F. Walton, Anal. Chem., 46 (1974) 398 R; 48 (1976) 52 R.
10 D. J. Pietrzyk, C. R. C. Crit. Rev. Anal. Chem., 6 (1976) 131.
11 A. R. Rodriguez et C. Poitrenaud, J. Chromatogr., 127 (1976) 29.
12 A. R. Rodriguez et C. Poitrenaud, Anal. Chim. Acta, 87 (1976) 125.
13 R. G. Fessler et H. A. Strobel, J. Phys. Chem., 64 (1963) 2562.
14 A. R. Rodriguez et C. Poitrenaud, Anal. Chim. Acta, 87 (1976) 141.
15 K. A. Boni et H. A. Strobel, Z. Phys. Chem. (Frankfurt am Main), 87 (1973) 169.
16 T. Sakaki, Bull. Chem. Soc. Jpn., 28 (1955) 217 et 220.
17 N. A. Izmailov, Elektrokhimiya Rastvorov (Electrochemistry of Solutions), Izd. Khar' kovsk. Gos. Univ. Kharkov, 1959, p. 684.
18 T. Sakaki et H. Kakihana, Kagaku, 23 (1953) 471.
19 G. Charlot et B. Trémillon, Les Réactions Chimiques dans les Solvants et les Sels Fondus, Gauthier-Villars, Paris, 1963, pp. 304, 391 et 433.
20 F. E. Critchfield, J. A. Gibson, Jr., et J. L. Hall, J. Am. Chem. Soc., 75 (1953) 6044.
21 A. N. Campbell et J. M. T. M. Gieskes, Can. J. Chem., 42 (1964) 1379.
22 Yu. Ya. Borovikov et Yu. Ya. Fialkov, Electrokhimiya, 1 (1965) 1106.

Analytica Chimica Acta, 102 (1978) 177—180

Short Communication

A GENERAL X-RAY FLUORESCENCE SPECTROMETRIC TECHNIQUE BASED ON SIMPLE CORRECTIONS FOR MATRIX EFFECTS

H. KRUIDHOF

Twente University of Technology, Department of Chemical Engineering, Laboratory for Inorganic Chemistry and Materials Science, Enschede (The Netherlands)

(Received 14th February 1978)

X-ray fluorescence spectrometry is highly selective but, as is well known, problems arise when the x-rays are absorbed in different ways by the samples and standards. When the composition of the samples is approximately known, these matrix effects can be prevented by preparing standards and samples in the same way, e.g. by a borax fusion technique [1—5]. This procedure, when it is used correctly, ensures sufficient compensation of matrix effects. If, however, almost nothing is known about the composition of the samples, this method is not applicable. Even when it is applied, much work is involved in the preparation of new standards. Accordingly, several methods of correcting for matrix effects have been suggested [6—11]; some of them give good results but are rather complicated, while others may be restricted to certain wavelengths.

The method reported here, which is relatively simple and generally applicable for most materials, involves a combination of borax fusion with matrix effect corrections. The latter are done with algorithms, which are derived from the intensity formulae, together with empirical coefficients.

Experimental

Sample preparation. Accurately weigh two different amounts of the same sample (S_1 g and S_2 g on an ignited base) into Pt—5% Au crucibles, and add 6.000 g (dry weight) of borax. Mix well and fuse in a furnace at about 1000°C. Cast the melt into Pt—5% Au moulds, maintained at about 800°C, to produce glass discs of 30-mm diameter. For the determination of an element j, measure the intensities at a certain wavelength (λ_j) and correct for the background and dead-time; the corrected intensities are I_{jS_1}, and I_{jS_2}, respectively.

Standard preparation. If possible, use only the anhydrous oxides of the required elements, although other inorganic anhydrous compounds may be used at need. For element j, weigh two different amounts of its compound (m_1 g and m_2 g on an ignited base) and prepare glass discs as described above. The respective corrected measured intensities are I_{jm_1} and I_{jm_2}.

Matrix absorption corrections

Excitation by the total primary spectrum of an x-ray tube can be replaced by excitation by a hypothetical effective wavelength (λ_e). The absorption coefficients for this wavelength, $\mu_i(\lambda_e)$, are then used to calculate the primary absorption of the sample. The total sample absorption for element j is given by: $\Sigma_i W_i\,[\mu_i(\lambda_{je}) + A\mu_i(\lambda_j)]$, where the first term indicates the absorption for the effective wavelength of element j, and the second term the absorption for the characteristic wavelength.

Let the absorption coefficients for the borax be K_j' for the effective wavelength and K_j'' for the characteristic wavelength of element j, and let the absorption coefficients for the sample be a_j' and a_j'' for the effective wavelength and characteristic wavelength of element j, respectively. The absorption for the glass disc with S_1 g of sample (see sample preparation) can then be described by

$$\frac{6}{(6+S_1)}(K_j' + AK_j'') + \frac{S_1}{(6+S_1)}(a_j' + Aa_j'')$$

The terms $(K_j' + AK_j'')$ and $(a_j' + Aa_j'')$ depend on the wavelength, but are constants for element j measured under fixed conditions. A is an apparatus constant. Thus new combined absorption coefficients for primary and secondary radiation can be introduced.

If $(K_j' + AK_j'') = K_j$ and $(a_j' + Aa_j'') = A_j$, the expression becomes $(6K_j + S_1A_j)/(6 + S_1)$. Analogously, the absorption of the glass disc with S_2 g of sample can be described by $(6K_j + S_2A_j)/(6 + S_2)$, and the absorptions of the standard discs (see standard preparation) by $(6K_j + m_1B_j)/(6 + m_1)$ and $(6K_j + m_2B_j)/(6 + m_2)$, respectively. Here, B_j is the so-called combined absorption coefficient for primary and secondary absorption of the compound used for making standard discs of element j.

Calculations of absorption coefficients. For the sample the following expression now holds:

$$S_2I_{jS_1}(6+S_1)\frac{6K_j + S_1A_j}{(6+S_1)} = S_1I_{jS_2}(6+S_2)\frac{6K_j + S_2A_j}{(6+S_2)}$$

Thus A_j can be calculated in terms of K_j; and the real value of K_j is not important, because all the absorption coefficients are in terms of K_j. If K_j is taken as a constant parameter of 1 for every wavelength, rearrangement gives for A_j (and analogously for B_j):

$$A_j = 6(S_1I_{jS_2} - S_2I_{jS_1})/S_1S_2\,(I_{jS_2} - I_{jS_1})$$

$$B_j = 6(m_1I_{jm_2} - m_2I_{jm_1})/m_1m_2\,(I_{jm_2} - I_{jm_1})$$

The amount of element j in the disc with S_1 g sample is then given by

$$C_j = bm_1\frac{I_{jS_1}}{I_{jm_1}}\frac{(6+S_1A_j)}{(6+S_1)}\frac{(6+m_1)}{(6+m_1B_j)}\frac{(6+S_1)}{(6+m_1)} = bm_1\frac{I_{jS_1}}{I_{jS_2}}\frac{(6+S_1A_j)}{(6+m_1B_j)}$$

where b is a conversion factor for the compound of element j which is used for making standards. The concentration of element j in the sample can then be easily calculated.

Results and discussion

Several ceramic materials were analysed as described above. The amounts weighed for the sample (S_1 g and S_2 g, respectively), were about 0.5 g and 0.3 g, while the weights (m_1 g and m_2 g) of the oxides used for making the standard discs were about 0.12 g and 0.07 g, respectively. To prevent loss of lead, samples and standards containing lead were fused first at 800°C and then at 1000°C. The results are shown in Table 1.

Some B.C.S. alloys were also analysed (Table 2). These alloys were dissolved in acid, and two different aliquots of the same solution were transferred to platinum crucibles, evaporated to dryness and ignited. Glass discs were prepared from the ignited materials. A synthetic mixture of Fe, Cr and Ni solutions was also analysed (Table 3).

TABLE 1

Results (in %) for some ceramic samples

	Sample 1		Sample 2		Sample 3	
	Present	Found	Present	Found	Present	Found
Pb	57.6	57.7	57.6	57.4	—	—
Ti	17.08	17.02	17.16	17.20	—	—
Sm	8.02	7.95	8.03	7.97	48.38	48.50
Zr	—	—	—	—	32.52	32.63

TABLE 2

Results (in %) for some B.C.S. alloys

Alloy	B.C.S. 218/2		B.C.S. 263/1		B.C.S. 330		B.C.S. 235/2	
	Present	Found	Present	Found	Present	Found	Present	Found
Fe	—	—	0.35	0.36	—	—	—	—
Cr	0.10	0.11	0.24	0.26	—	—	18.60	18.57
Ni	0.18	0.18	—	—	—	—	9.38	9.58
Mn	0.63	0.63	0.36	0.36	0.45	0.46	—	—

TABLE 3

Results (in mg) for a synthetic Fe—Cr—Ni solution

	Fe	Cr	Ni
Present	886	102.8	609.7
Found	885	102.5	607.2

The influence of possible enhancement on this technique is not known exactly, but in practice good results are obtained, where enhancement could be expected, so that probably only slight interference will occur. It is clear that, for every wavelength measured, the discs must be infinitely thick.

It can be concluded that the method described is reliable with an acceptable accuracy for most materials. The applicability of the technique to specific materials is under investigation and will be reported later.

The author thanks Dr. K. J. de Vries and Professor A. J. Burggraaf for their stimulating interest and valuable discussions.

REFERENCES

1 K. G. Carr-Brion, Analyst, 89 (1964) 556.
2 R. Jenkins and J. L. de Vries, Practical X-ray Spectrometry, Philips Technical Library, 1968, p. 150.
3 A. Strasheim and M. P. Brandt, Spectrochim. Acta, Part B, 23 (1967) 183.
4 F. F. Rinaldi and P. E. Aguzzi, Spectrochim. Acta, Part B, 23 (1967) 15.
5 J. H. H. G. van Willigen, H. Kruidhof and E. A. M. F. Dahmen, Talanta, 18 (1971) 450.
6 M. L. Salmon and J. P. Blackledge, Norelco Rept., 3 (1956) 68.
7 K. Norrish and R. M. Taylor, Clay Miner. Bull., 5 (1962) 98.
8 G. Anderman and J. W. Kemp, Anal. Chem., 30 (1958) 1306.
9 D. A. Stephenson, Anal. Chem., 43 (1971) 310.
10 J. H. H. G. van Willigen, H. Kruidhof and E. A. M. F. Dahmen, Anal. Chim. Acta, 62 (1972) 279.
11 W. K. de Jong, X-ray Spectrom., 2 (1973) 151.

Analytica Chimica Acta, 102 (1978) 181—184

Short Communication

EFFECT OF ACIDS ON THE DETERMINATION OF NICKEL BY ATOMIC ABSORPTION SPECTROMETRY

MOSTAFA M. EMARA*, MONIR M. ALI** and ABDL EL-AZIZ GHARIB***

Department of Chemistry, Faculty of Science, Al-Azhar University, Nasr City, Cairo (Egypt)

(Received 10th June 1977)

There have been few reported interferences in the determination of nickel by atomic absorption spectrophotometry. Billings [1] reported molecular absorption by calcium at the nickel line (232.0 nm) in an air—acetylene flame; correction could be made with use of the 232.57-nm Ni line. Rayland [2] found molecular absorption interference by calcium and iron in the analysis of granites. Billings et al. [3, 4] showed that the determination of nickel in silicates is relatively interference-free, provided that the calcium or iron content is insufficient to cause molecular absorption. Fletcher [5] and Foster [6] used a hydrogen lamp continuum to correct for the non-atomic absorption.

Terashima [7] showed that background absorption in the determination of nickel increases linearly with concentration up to 4000 ppm for each of Na, K, Mg, Co, Fe and Al, in silicate analysis. This could be overcome by addition to the standard solutions of an amount of calcium equivalent to the total quantity of Na, K, Mg, Ca, Fe and Al in the sample. No other interfering effects of metals have been reported, although this aspect has been extensively investigated.

The effects of acids on the determination of nickel by atomic absorption spectrometry, however, have received relatively little attention. This communication, therefore, describes a detailed study of the interference effect of acids on nickel absorptions, especially those acids used in digestion techniques for geological materials.

Experimental

All chemicals used were of analytical-reagent grade. HCl (*d*, 1.18), H_2SO_4 (*d*, 1.84), HNO_3 (*d*, 1.42) and $HClO_4$ (*d*, 1.299) were used. Nickel solutions (1 mg Ni ml^{-1}) were prepared by dissolving 0.5 g of nickel in 50 ml of 5 M nitric acid with heating, and diluting to 500 ml with deionized distilled water when cool.

**Present address: Geology Department, Atomic Energy Commission of Egypt.
***Present address: Geological Survey of Egypt.

A Perkin-Elmer Model 303 atomic absorption spectrometer was used under the following conditions: flame path length, 10 cm; lamp current (Perkin-Elmer hollow-cathode) 25 mA; wavelength, 342.6 nm; slit setting, 3; air pressure, 30 psi; acetylene pressure, 8 psi. The acetylene flows used for the single-slot burner were settings 32 (optimum), 25 (oxidizing) and 42 (reducing) with air at 55. When a 3-slot burner was used, the acetylene flows were 36 (optimum), 32 (oxidizing) and 42 (reducing), with the air flow at 60. The burner heights used were 1 and 3 cm, measured from the top of the burner to the centre of the light beam.

Results and discussion

The effects of 0—50% hydrochloric, nitric, sulphuric and perchloric acids on the absorbance of 1, 5 and 20 ppm Ni solutions was investigated, under different conditions of acidity and nickel concentrations and instrumental parameters.

Hydrochloric acid ($\leqslant$ 25%, v/v) had no effect on the absorbance of 1 ppm of nickel in any of the flames used, when a single slot burner was used, but there was suppression of larger concentrations of nickel. The results obtained with the optimal flame conditions are illustrated in Fig. 1. Similar results were obtained with a three-slot burner, but some suppression of the absorption of 1 ppm nickel was also observed. Results similar to those shown in Fig. 1a were obtained with a reducing flame and a single-slot burner at a height of 3 cm.

Nitric acid had effects similar to those of hydrochloric acid. The effects of up to 10% (v/v) on a 1 ppm Ni solution were small, but there was significant depression at higher acidities and at larger nickel concentrations. The results obtained under optimal conditions are shown in Fig. 2.

Sulphuric acid severely depressed nickel absorption at concentrations above 4% (v/v). The effects were similar in the three flame types investigated, at both burner heights, and with single- and three-slot burners. Figure 3 shows some typical results obtained under "optimal" flame conditions.

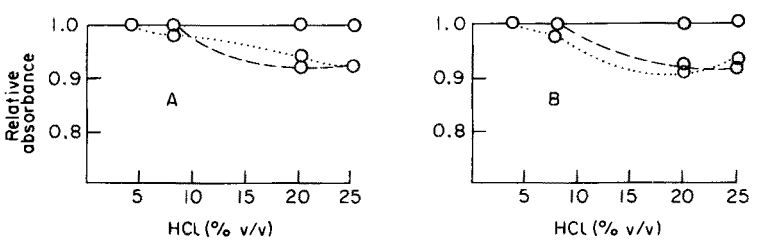

Fig. 1. Absorption of nickel in the presence of hydrochloric acid under "optimal" flame conditions. (—) 1 ppm nickel; (.....) 20 ppm nickel; (- - -) 5 ppm nickel. (A) Single-slot burner; 1-cm burner height. (B) Single-slot burner; 3-cm burner height.

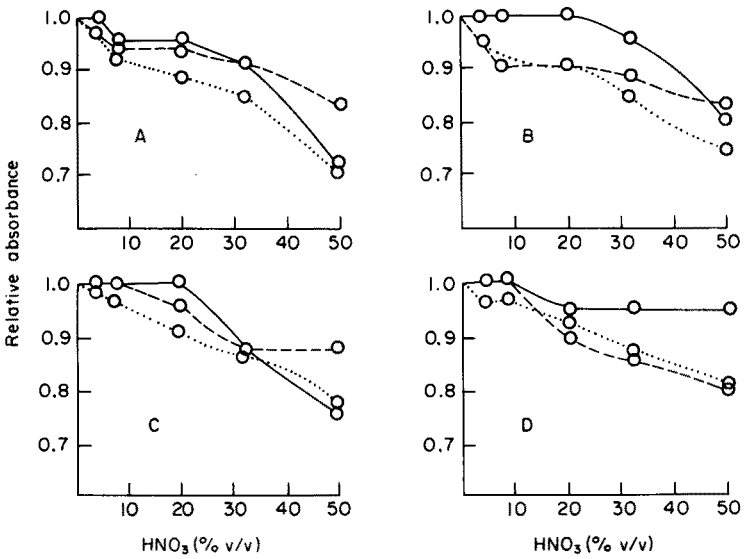

Fig. 2. Absorption of nickel in the presence of nitric acid under "optimal" flame conditions. (—) 1 ppm nickel; (....) 20 ppm nickel; (- - -) 5 ppm nickel. (A) 3-slot burner at 1-cm height; (B) 3-slot burner at 3-cm height; (C) 1-slot burner at 1-cm height; (D) 1-slot burner at 3-cm height.

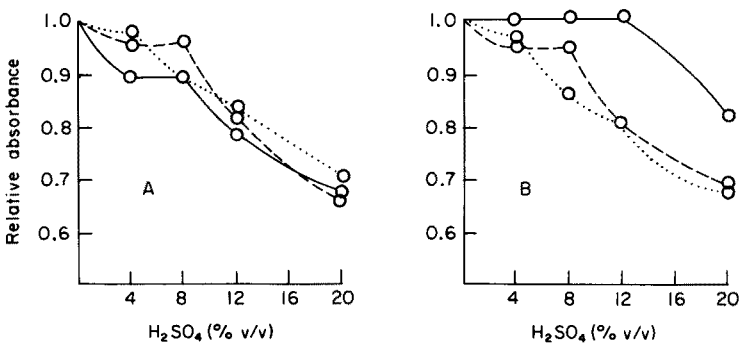

Fig. 3. Absorption of nickel in the presence of sulphuric acid under "optimal" flame conditions. (—) 1 ppm nickel; (....) 20 ppm nickel; (- - -) 5 ppm nickel. (A) 1-slot burner at 1-cm height; (B) 3-slot burner at 3-cm height.

Perchloric acid (12%) had no effect on the absorption of nickel at a burner height of 1 cm whether a single- or three-slot burner was used under oxidizing or "optimal conditions"; slight suppression was observed at higher acidities and higher nickel concentrations. With a reducing flame, some enhancement was obtained as illustrated in Fig. 4.

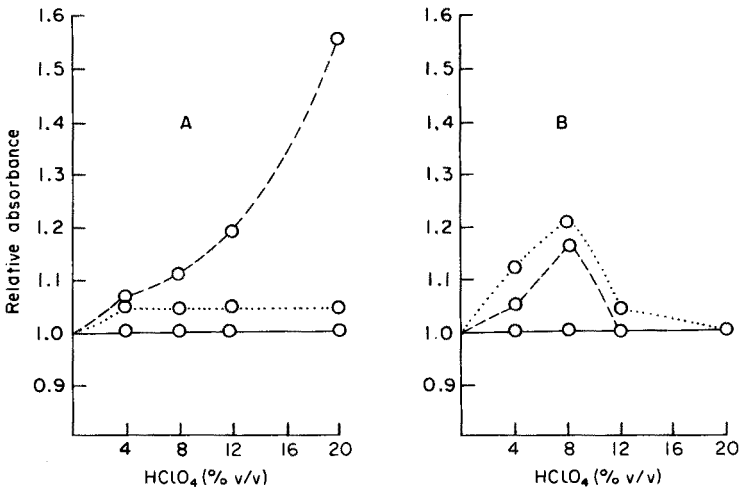

Fig. 4. Absorption of nickel in the presence of perchloric acid under reducing flame conditions. (—) 1 ppm nickel; (....) 20 ppm nickel; (- - -) 5 ppm nickel. (A) 3-slot burner at 3-cm height; (B) 1-slot burner at 1-cm height.

If hydrochloric acid has to be used, the results indicate that the best instrumental conditions are a one-slot burner at 3-cm height with a reducing flame or at 1-cm height with an "optimal" flame. However, it is obvious from Fig. 1 that care is necessary. Clearly, nitric acid should be removed by evaporation in any applied analysis. The overall results indicate that if solutions of high but variable acidity have to be analyzed, solutions in perchloric acid are likely to give the least chance of error in the determination of nickel. They also emphasize, again, the effect of large concentrations of chemicals on atomic absorption signals,which arise, at least in part, from changes in nebulization efficiency.

REFERENCES

1 G. K. Billings, At. Absorpt. Newsl., 4 (1965) 357.
2 P. C. Rayland, Atomic Absorption Spectrometry in Geology, Elsevier, Amsterdam, 1967.
3 G. K. Billings and J. A. S. Adams, At. Absorpt. Newsl., 23 (1964) 1.
4 P. C. Ragland and G. K. Billings, Southeast. Geol., 6 (1965) 87.
5 K. Fletcher, Econ. Geol., 65 (1970) 588.
6 J. R. Foster, Can. Inst. Min. Metal, 11 (1971) 554.
7 S. Terashima, Bull. Geol. Surv. Jpn., 22 (1971) 19.

Analytica Chimica Acta, 102 (1978) 185—188

Short Communication

ELIMINATION OF IONIC INTERFERENCE EFFECTS IN THE ATOMIC ABSORPTION SPECTROMETRIC DETERMINATION OF RUTHENIUM

MOHAMED M. M. EL-DEFRAWY**, J. POSTA and M. T. BECK*

Department of Physical Chemistry, Kossuth Lajos University, H-4010 Debrecen (Hungary)

(Received 30th March 1978)

In connection with work on the catalytic effect of ruthenium complexes, new compounds were prepared. Atomic absorption spectrometry (a.a.s.) was to be used for their analysis. The literature on the a.a.s. of ruthenium is surprisingly meagre; the data indicate that many other metal ions and complex forming substances interfere greatly. Scarborough [1] has found that the interfering effect of molybdenum, palladium and rhodium can be eliminated by the presence of a large amount of uranium. According to Montford and Cribbs [2], uranium can be used to eliminate the interfering effect of many other metal ions and complex forming substances. Rowston and Ottaway [3] have applied copper and cadmium sulphates to eliminate the interfering effects of different metal ions and ligands, and Harrington [4] showed that the presence of titanium could serve the same purpose.

These methods could not be applied to the complexes studied therefore the effect of cyanide ions for elimination of interfering effects has been studied, because of the great stability of cyanide complexes [5].

Experimental

Apparatus. The analyses were carried out with a Unicam SP 1900 double-beam atomic absorption spectrometer, and a Beckman hollow-cathode lamp. The samples were nebulized into an air—acetylene flame, on a 10-cm slot burner. The optimum parameters were as follows: wavelength, 349.9 nm; lamp current, 12 mA; slit-width, 0.2 mm; burner height, 6 mm; air flow rate, 5 l min^{-1}.

The absorbances were increased by a 2.5× scale expansion. After integrating for 4 s, the data were printed out by a Weyfringe DR 10 digital printer.

Reagents. The stock ruthenium solution was prepared from ruthenium(III) chloride hydrate (Fluka) by dissolving it in 0.3 M hydrochloric acid. The nominal concentration of ruthenium in the stock solution was 1000 $\mu g\ ml^{-1}$.

All other reagents were of analytical reagent grade.

Procedure. For the experiments with interfering substances, the following procedure was used, and is recommended for the determination of ruthenium:

**On leave from the University of El-Mansoura (Egypt).

To the solution of ruthenium (15 ml) add 0.5 ml of 1 M potassium cyanide solution, 5 ml of 37% hydrochloric acid and finally 1 ml of 2 M sulphuric acid. Dilute in a volumetric flask to 25 ml with distilled water. Determine the ruthenium content by a.a.s. under the recommended conditions.

Results and discussion

The effect of potassium cyanide and of mineral acids on the absorbance of ruthenium is shown in Fig. 1. Cyanide ions considerably increase the absorbance in the presence of both hydrochloric acid and sulphuric acid, but have much less effect when only hydrochloric acid is used. Greatest absorbance is obtained when the final concentrations are 2 M hydrochloric acid and 0.08 M sulphuric acid. Under these conditions the absorbance is independent of the concentration of cyanide over a broad range of concentration, and the absorbance is nearly three times the value found in the absence of cyanide. Typical linear calibration graphs are given in Fig. 2.

Although numerous species are reported to influence the ruthenium absorbance, Tables 1 and 2 show that under the recommended conditions (i.e. with cyanide masking in hydrochloric and sulphuric acids) most of the interfering effects are eliminated. Since the determination is not influenced by EDTA or the triphenylphosphine derivative, this method appears particularly useful for the analysis of ruthenium complexes. Among the platinum metals, only iridium seriously interferes; rhodium and palladium can be present in a 50-fold excess.

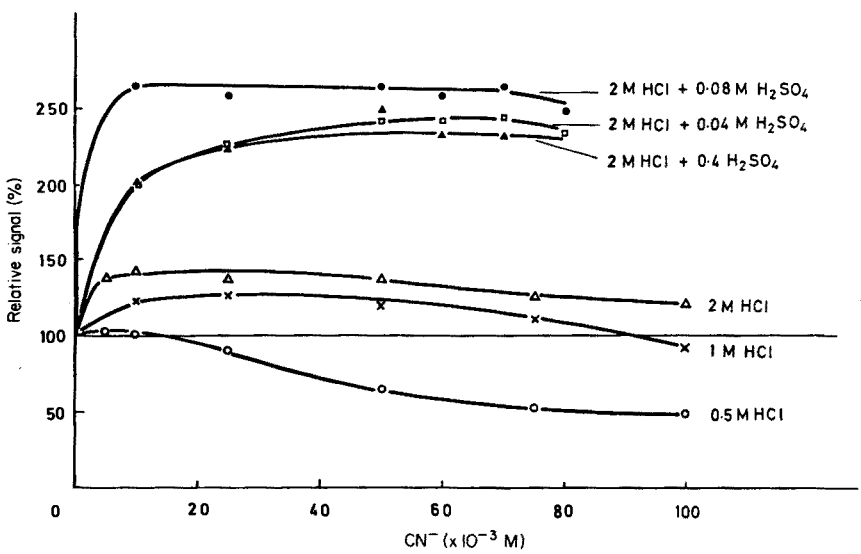

Fig. 1. The effect of cyanide ion, hydrochloric acid and sulphuric acid on the absorbance of ruthenium (20 μg ml^{-1}). The 100% line indicates the signal in the absence of cyanide.

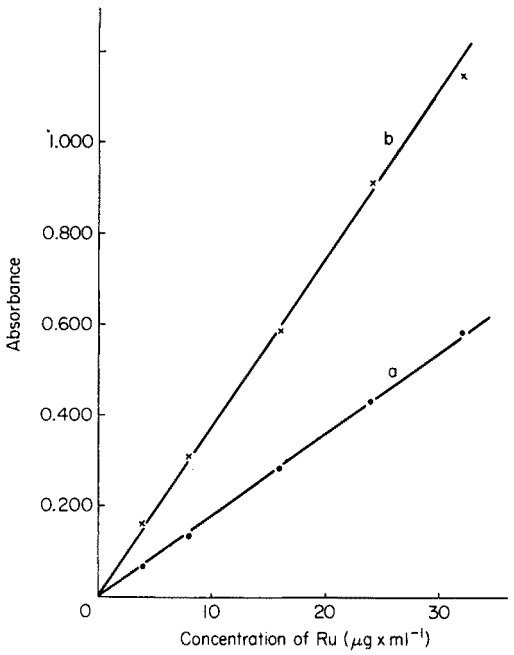

Fig. 2. Calibration graphs for ruthenium: (a) obtained by simple dilution of the stock ruthenium solution; (b) obtained by the recommended procedure.

TABLE 1

Effect of different ions with and without the masking procedure (The anions were introduced as the corresponding acid, the cations (unless indicated otherwise) as chlorides. The concentrations of these ions were 200 μg ml^{-1}; that of DPM (sodium salt of diphenylphosphinobenzene-*m*-sulphonic acid) was 100 μg ml^{-1}. Ruthenium concentration, 20 μg ml^{-1}.)

Other species	Ru recovery (%)		Other species	Ru recovery (%)	
	Without masking	With masking		Without masking	With masking
None	100	100	Cu^{2+}	204.6	90.5
NO_3^-	40.2	103.2	Al^{3+}	25.3	100
K_2SO_4	100.4	100	Fe^{3+}	83.1	97.3
Na^+	95.4	97.3	Rh^{3+}	236.0	98.9
K^+	89.7	100	$K_2Pd\ Cl_4$	202.7	100
Cs^+	146.0	97.3	OsO_4	207.5	97.9
Ca^{2+}	109.0	98.7	$H_2Ir\ Cl_6$	266.0	44.7
Mn^{2+}	101.0	100	$(NH_4)_2PtCl_4$	183.0	98.7
Co^{2+}	75.7	97.3	$UO_2(NO_3)_2$	180.0	100
Ni^{2+}	56.1	97.3	EDTA	0	100
Mg^{2+}	106.0	100	DPM	13.4	100
Ba^{2+}	95.4	97.3	Maleic acid	22.4	97.3
			Oxalic acid	36.5	98.7

TABLE 2

Joint effect of several metals with and without the masking procedure (The concentration of each metal was 200 $\mu g\ ml^{-1}$, except Fe, Rh, Pd and Pt (100 $\mu g\ ml^{-1}$ of each). Ruthenium concentration, 20 $\mu g\ ml^{-1}$.)

Added metals	Ru recovery (%)	
	Without masking	With masking
None	100	100
Al, Ca, Mg	129	100
Al, Ca, Co	116	101
Al, Ca, Rh	89	99
Al, Ca, Fe	65	98
Fe, Rh, Pd, K	154	100
U, Pd, Pt, Rh, K, NH_3	207	88
Rh, Ni, Ca	174	100
Mg, U, Pd, K	203	101
Fe, U	48	100
Mg, Rh, Pd, K	188	93
U[a], Pd, Pt, Rh, K	179	100
U, Pt, Rh	203	102
Ir, Rh, Pd, Os, Pt	208	38

[a]Uranium concentration, 400 $\mu g\ ml^{-1}$.

It is suggested that the elimination of the interfering effects by the suggested procedure is mainly due to the high stability of the cyanocomplexes of ruthenium. The complexation makes the immediate environment of ruthenium, both in the solution and in the flame, independent of the composition of the solution. The advantageous effect of sulphuric acid cannot be explained at present. It is unlikely that under the experimental conditions a mixed cyanide sulphate complex is formed. However, the value of the application of sulphuric acid has been established. Experiments are in progress to apply cyanide to eliminate interfering effects in the atomic absorption spectrometric determination of the other transition metal ions.

REFERENCES

1 J. M. Scarborough, Anal. Chem., 41 (1969) 250.
2 B. Montford and S. C. Cribbs, Anal. Chim. Acta, 53 (1971) 101.
3 W. B. Rowston and J. M. Ottaway, Anal. Lett., 3 (1970) 411.
4 D. E. Harrington, At. Abs. Newsl., 11 (1972) 107; D. E. Harrington and W. R. Bramstedt, Talanta, 22 (1975) 411.
5 A. G. Sharpe, The Chemistry of Cyano Complexes of Transition Metals, Academic Press, London, 1976.

Analytica Chimica Acta, 102 (1978) 189—194

Short Communication

DETERMINATION OF METHYLMERCURY IN THE MUSCLE OF MARINE FISH BY COLD-VAPOUR ATOMIC ABSORPTION SPECTROMETRY

I. M. DAVIES

DAFS Marine Laboratory, PO Box 101, Victoria Road, Torry, Aberdeen (Great Britain)

(Received 5th May 1978)

Because of the possible injurious effects of the ingestion of foodstuffs containing methylmercury, and the potential significance of the methylmercury content of certain fish in the diet [1], this laboratory has undertaken the analysis of marine fish muscle for methylmercury. Commonly, 80—100% of the total mercury in marine fish muscle is in monomethylated forms [2]. The volatility of dimethylated mercury limits its occurence, whilst other alkyl and aryl mercurial compounds are common only in areas where they have been introduced in significant quantities by man [3]. The method of analysis for methylmercury used previously was essentially that of Westöö [4] involving the extraction of methylmercury as its chloride, followed by a clean-up procedure, and determination of the methylmercury in the final organic solvent by gas chromatography. Whilst the method is specific for the sum of mono- and dimethylmercury, the main disadvantages encountered were the poor extraction efficiency (usually 60—70%), and the poor overall sensitivity in that only a very small proportion of the final extract which contains only ca. 25% of the methylmercury present in the sample is injected into the chromatograph. The detection limit for the whole procedure with a 10-g sample is 0.01—0.02 $\mu g\ g^{-1}$. Unless the method is in daily use, considerable time is necessary to re-establish the gas chromatographic stage.

As the routine measurement of total mercury in this laboratory employs cold-vapour atomic absorption spectrometry (a.a.s.), a method combining the solvent extraction procedure of Westöö [4] with determination by cold-vapour a.a.s. has considerable attraction. In a similar approach Bisogni and Lawrence [5] extracted methylmercury from marine organic material into benzene and then into cysteine acetate solution. The methylmercury in cysteine solution was oxidized with potassium permanganate and potassium persulphate, and inorganic mercury in the digest was determined by cold-vapour a.a.s. This communication describes a modification of the oxidation stage and subsequent treatment of the digest. The sample is homogenized in distilled water, sodium chloride is added, and the methylmercury is converted to its chloride by addition of hydrochloric acid. Methylmercury

chloride is extracted into toluene, and back-extracted into cysteine acetate solution. This is oxidized by $KMnO_4$—H_2SO_4 solution and, following reduction with tin(II) chloride, the mercury is collected in a $KMnO_4$—H_2SO_4 trap. Total mercury in the trap is then determined by the method of Topping and Pirie [6].

Experimental

Homogenize by Ultra-Turrax (Jauke and Kunkel KG., 7813 Staufen i Br., Germany) homogenizer (or equivalent) a weighed portion of up to 10 g of wet fish muscle with ca. 20 cm^3 of distilled water in a 200-cm^3 glass centrifuge tube. Bring the volume to 50 cm^3 with distilled water and add 10 g of sodium chloride and 14 cm^3 of 12 M HCl. The sample should contain less than 4 μg of methylmercury. Add 70 cm^3 of toluene, shake mechanically for 15 min, and then allow to settle. It is frequently necessary to centrifuge after this stage to effect a good phase separation.

Pipette 50 cm^3 of the toluene layer into a 100-cm^3 separatory flask. Add 6 cm^3 of cysteine acetate reagent, prepared by dissolving 1.0 g of cysteine hydrochloride, 0.755 g of sodium acetate trihydrate and 12.5 g of anhydrous sodium sulphate sequentially in distilled water to a final volume of 100 cm^3. Shake the flask vigorously for 2 min and allow the phases to separate. Run off most of the aqueous layer into a glass tube. It is necessary occasionally to centrifuge this aqueous layer briefly to bring about complete separation.

Pipette 4 cm^3 of the cysteine extract into a 80-cm^3 Pyrex boiling tube. Add 10 cm^3 of 2% (w/v) potassium permanganate, and 10 cm^3 of (1 + 1) H_2SO_4, mix, and heat in a water bath at 90°C for 1 h to oxidize the organic mercury to the mercury(II) form.

Cool the tube, and position a Leurquin head, so that air may be passed through the sample, and through another Leurquin head, into a trap containing a solution of 10 cm^3 of 2% potassium permanganate plus 10 cm^3 of (1 + 1) H_2SO_4 in a boiling tube. Add to the digest 10 cm^3 of 20% (w/v) tin(II) chloride in (1 + 1) HCl, quickly replace the Leurquin head, and pass air (cleaned previously by passage through a mixture of 2% potassium permanganate and (1 + 1) H_2SO_4) through the sample at 1—1.5 dm^3 min^{-1} for 30 min.

Determine the methylmercury, now present as an inorganic mercury salt in the trap, by cold-vapour a.a.s. Transfer the solution to a Dreschel bottle, make up to 50 cm^3 with distilled water, add 10 cm^3 of 20% (w/v) tin(II) chloride solution, and sweep the mercury into the instrument by an air flow of 2 dm^3 min^{-1} [6]. Measure the peak heights on a potentiometric strip-chart recorder. Prepare standards by addition of microlitre quantities of 10 mg dm^{-3} inorganic mercury stock solution to 2% $KMnO_4$—(1 + 1)H_2SO_4 mixtures as used in the trap.

All apparatus should be cleaned thoroughly by soaking overnight in distilled water containing 20 cm^3 of 2% potassium permanganate and 20 cm^3 of (1 + 1) H_2SO_4 per litre. Any brown stains can be removed by rinsing with $SnCl_2$ solution, followed by thorough rinsing in tap water (Aberdeen tap

water contains very little mercury, but distilled water may be necessary elsewhere). All chemicals were of analytical grade, with the exception of the cysteine hydrochloride. Possible mercury contamination from the tin(II) chloride can be removed by bubbling air vigorously through the solution for 2—3 h before use.

Discussion

The method is based on two established methods: the extraction [4] and the determination [6]. Two stages were introduced between these procedures: the oxidation, and transfer of mercury to the trapping solution; the success of the method depends on the efficiency of these stages.

The oxidation of methylmercury by acidic permanganate is retarded by the presence of cysteine acetate solution; for 4 cm^3 of solution the oxidation is complete under these conditions after ca. 30 min. In 2 cm^3 of cysteine acetate solution the oxidation requires only 10 min but in volumes greater than 8 cm^3 the oxidation takes several hours and losses of mercury can occur by volatilization after the permanganate has been decolourized completely. Whilst this problem could probably be solved by the addition of larger quantities of permanganate, no advantage is gained, as the extraction of methylmercury from 50 cm^3 of toluene into cysteine is very efficient (Table 1).

Transfer to the solution in the trap removes any traces of toluene or chlorine which may interfere with the determination stage, a problem which Bisogni and Lawrence [5] overcame by bubbling oxygen or nitrogen through the oxidized sample for 10—15 min. It also ensures that the matrix from which the mercury is volatilized into the instrument is identical for all samples and standards. It is closely analogous to the final volatilization step, and is therefore probably complete in less than 5 min; the time allowed (30 min) is thus more than adequate. The final trap solutions are stable for several days; although oxides of manganese may be deposited on the glass during storage, they do not carry significant quantities of mercury.

The method is not specific for monomethylmercury, but will measure any mercury species extracted into the cysteine acetate solution, e.g. other organomercurial compounds, dimethylmercury (which is decomposed to monomethylmercury under the strongly acidic conditions of the initial extraction) and possibly small amounts of inorganic mercury compounds carried over during the extraction. Interference by other organomercurial

TABLE 1

Recovery of 1 μg of methylmercury in solution in toluene added to 50 cm^3 of toluene and extracted into cysteine acetate reagent

Total cysteine acetate reagent (cm^3)	4	4	6	6
Aliquot digested (cm^3)	3	3	4	4
Recovery (%)	98	97	100	102

compounds should be very small in marine fish muscle, but there is a suggestion of slight interference from inorganic mercury when present in 1000-fold excess (Table 2). It is necessary [4] to add large amounts (100 mg/10 g sample) of mercury(II) chloride to materials such as egg yolk, liver, and some sediments to release methylmercury from them; under these conditions, several micrograms of inorganic mercury are carried over into the cysteine acetate reagent.

Table 2 shows that recovery is 75—80% efficient in pure solutions, i.e. somewhat higher than that obtained from Westöö's [4] complete method (60—70%). As the toluene—cysteine extraction is complete, the losses must occur through an unfavourable partition coefficient for the initial extraction into toluene. Some improvement may be made by extraction with two aliquots of toluene, or, for small samples, by reducing the volume of the aqueous phase.

It is necessary, however, to determine the extraction efficiency by the addition of small volumes of an aqueous methylmercury solution to samples before homogenization as a variation of between 75 and 80% can occur with change of matrix (Table 3).

The method has been applied to the wet muscle of common ling and halibut, and to freeze-dried muscle of cod. The results may be compared (Table 4) with measurements of total mercury made by a combustion technique [7]. Previous work in this laboratory has shown that 90—100% of the total mercury in ling and halibut is present as methylmercury.

There is a small reagent blank associated with the cysteine acetate solution added. The mean of six determinations, spread over 4 days, was 0.019 μg ($\sigma = \pm 0.003$). The detection limit of the method is estimated to be 0.01—0.02 μg, i.e. 0.001—0.002 $\mu g\ g^{-1}$ for a 10-g sample, and offers, therefore, a 10-fold improvement in sensitivity over Westöö's [4] method. The method requires little equipment additional to that used routinely for total mercury determination and an experienced analyst can perform ca. 60 analyses per week.

TABLE 2

Interference of inorganic mercury (added as mercury(II) nitrate) on the recovery[a] of 1 μg of methylmercury in 50 cm^3 of distilled water

Inorganic Hg added (μg)	Methylmercury Recovered (μg)	Recovery (%)
0	0.77	77
1	0.77	77
1	0.77	77
10	0.77	77
100	0.80	80
100	0.73	73
1000	0.82	82

[a] All recoveries in Tables 2 and 3 are expressed after mathematical allowance has been made for incomplete utilization of the toluene and cysteine extracts.

TABLE 3

Recovery[a] of methylmercury added to fish muscle[b]

Species	Sample No.	Sample wt. (g)	MeHg added (μg)	Recovery[c] (%)	Mean recovery (%)
Ling (wet muscle)	56 77 LG	2.0	1.0	79	79
	57 77 LG	2.0	1.0	79	
Halibut (wet muscle)	33 77 H	1.0	0.5	79	79
			0.5	79	
			1.0	80	
			1.0	79	
Cod (powdered freeze-dried muscle)	FDC—1	0.5	0.4	81	75
			0.4	74	
			0.8	70	
			0.8	76	

[a] See Table 2.
[b] Natural content of methylmercury shown in Table 4.
[c] Recoveries are calculated from the difference between samples with and without added methylmercury.

TABLE 4

Determination of methylmercury in fish muscle

Species	Sample No.	Sample wt. (g) extracted for MeHg	Total Hg[a] (μg g^{-1})	MeHg (μg g^{-1})
Ling (wet muscle)	55 77 LG	2.0	0.43	0.42
	56 77 LG	2.0	0.25	0.26
	57 77 LG	2.0	0.15	0.15
	58 77 LG	2.0	0.28	0.31
Halibut (wet muscle)	33 77 H	1.0	0.34	0.31
				0.34
				0.32
				Mean 0.32
Cod (powdered freeze-dried muscle)	FDC—1	0.5	0.80	0.84
			0.85	0.90
			0.88	0.84
			0.90	
			0.90	
			0.91	
			Mean 0.87	Mean 0.86

[a] Determined by a combustion technique.

REFERENCES

1 H.M.S.O., Pollution Paper No. 10., Dept. of the Environment, Central Unit of Environmental Pollution, 1976.
2 A. V. Holden, J. Food Technol., 8 (1973) 1.
3 J. Vostal, in, Mercury in the Environment, CRC Press, Cleveland, Ohio, 1972, p. 15.
4 G. Westöö, Acta Chem. Scand., 22 (1968) 2277.
5 J. J. Bisogni and A. W. Lawrence, Environ. Sci. Technol., 8 (1974) 850.
6 G. Topping and J. M. Pirie, Anal. Chim. Acta, 62 (1972) 200.
7 G. Topping, J. M. Pirie, W. C. Graham and R. J. Shepherd, I.C.E.S., C.M.1975, Fisheries Improvement Ctte., E: 37.

Analytica Chimica Acta, 102 (1978) 195—199

Short Communication

IMPROVED PRECISION BY SERVOMECHANICAL STABILIZATION OF CYANOGEN BAND EMISSION IN A NITROUS OXIDE—ACETYLENE FLAME

A. A. VERBEEK[‡] and A. M. URE*

Department of Spectrochemistry, The Macaulay Institute for Soil Research, Craigiebuckler, Aberdeen (Great Britain)

(Received 30th May 1978)

In the course of an investigation into the use of a nitrous oxide—acetylene flame for the determination of elements such as molybdenum, aluminium and barium, it soon became clear that the sensitivity and precision of the determination was critically dependent on the flow rates of the fuel and oxidant gases. Fluctuations occurring in the flow rate of nitrous oxide as a result of condensation produced by expansion cooling at the cylinder regulator were minimized by wrapping the regulator with electrically heated tape. However, short-term fluctuations and long-term drift in the acetylene flow rate also occurred, especially at the high consumption required for a fuel-rich nitrous oxide—acetylene flame. While the use of conventionally regulated gas supplies was adequate for the determination of some elements such as calcium and magnesium, for other elements the emission or absorption signal was so highly dependent on the relative proportion of fuel and oxidant that an improvement in gas supply stability was desirable if reasonable precision was to be obtained at low levels of concentration.

It has been suggested [1] that, because of a correlation between the molybdenum line and cyanogen band intensities in a nitrous oxide flame, the use of a cyanogen (CN) band-head as a form of internal standard for the determination of molybdenum by atomic emission spectrometry (a.e.s.) might offer improved precision. This approach was examined for an Instrumentation Laboratory Inc. model IL751 atomic absorption/emission spectrometer in which one of the two channels was used to measure the emission of the barium line at 553.5 nm while the other channel simultaneously measured the emission of the CN band-head at 387.2 nm. Preliminary experiments demonstrated that while both emissions were strongly dependent on gas flow rates, the CN emission was much more sensitive to flow rates than that of barium, and hence the ratio of Ba to CN emission was seriously affected by flame conditions. It was felt, therefore, that it might be more fruitful to

[‡] On leave from: Department of Chemistry, University of Natal at Pietermaritzburg, South Africa.

attempt to control the fuel-gas flow rate in order to achieve more constant flame conditions, and thus more stable emission by Ba (and other elements), rather than attempt to apply the internal standard technique. In the experiments described below, the CN band-head emission was monitored by one channel of the IL751 and the signal from the recorder output socket was used in a closed-loop feed-back system to control the acetylene flow rate in such a way as to keep the CN emission constant. This provided a stabilized CN-band emission intensity and might be expected to maintain more constant flame conditions for the measurement of, for example, the barium or aluminium line emission on the other channel of the IL751 instrument.

Experimental

A simple apparatus was devised to estimate the usefulness of stabilizing the CN band emission by servomechanically controlling the acetylene flow. The arrangement is shown diagrammatically in Fig. 1. Channel M_1 of the IL751 and its digital readout R_1 were used to measure the intensity of the emission of the Ba 553.5-nm line (or the Al 396.2-nm line). The second channel, M_2, was set to measure the CN band-head at 387.2 nm and the recorder output from readout R_2 was connected to the input terminals of a 100-mV Beckman 6-inch laboratory pen-recorder (Cat. No. 93507). The shaft of the servo-motor, S, driving the recorder pen, P, was fitted with a pulley wheel (35-mm diameter) which was used to drive, by means of a belt, a corresponding pulley wheel (30-mm diameter) fitted to the shaft of the acetylene needle valve, NV, controlling the acetylene flow rate in the IL751 instrument. The direction of the CN signal connection was such that

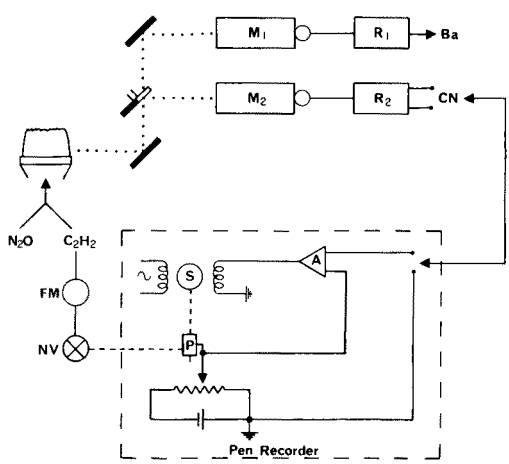

Fig. 1. Schematic diagram of apparatus for regulating CN-band emission, showing the two-channel, $M_1 M_2$, spectrometer, with twin readouts, R_1 R_2, and pen recorder with servo-amplifier, A, and motor, S, driving pen, P, and needle valve control, NV, for the acetylene supply monitored by flow meter, FM.

an increase in CN band emission produced an error signal with respect to the slide wire reference voltage. This caused the amplifier A to drive the servo-motor, S, and the pen, P, in a direction which turned the needle-valve, NV, to reduce the acetylene flow. A decrease in CN band emission operated in the reverse direction, i.e. to increase the acetylene flow. In consequence, CN band emission was stabilized, and this resulted in a much improved long-term stability of the acetylene flow rate as measured by the flow meter, FM.
The arrangement for recorder servo-control of the acetylene needle valve is shown in Fig. 2. The initial recorder pen position could be set by the recorder zero control while the overall loop gain could be altered by a small amount by means of the recorder span control. If the gain was set too high, oscillation of the servo-motor occurred and the flame alternated between fuel-rich and lean conditions with a period of about 1 s. For operation the gain was set to a point just below the onset of oscillation.

In obtaining the results presented here, the best gas flow rates and burner height were first selected for the element being determined in channel M_1 of the spectrometer, and then the channel M_2 gain was adjusted so that, under the given conditions, a suitable recorder output was obtained. The recorder pen was positioned at some convenient point along its scale and then the pen drive and acetylene valve pulleys were linked by the belt while the recorder was on "stand by". A solution (2 ppm Ba or 70 ppm Al) of the element of interest was then nebulized, the spectrometer measuring system activated, and the recorder pen brought immediately into operation by pressing the "Record" button. A series of ten or more digital readings, each integrated over a period of one or four seconds was then collected from read-outs R_1 and R_2, and the recorder was again switched to "stand by" while the spectrometer microprocessor was used to calculate and print the mean concentration of the element in solution (Channel M_1), and the mean emission from

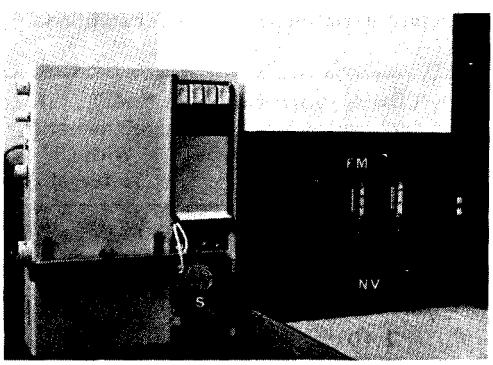

Fig. 2. Photograph of apparatus showing the pulley and belt drive connecting the servo-motor S and the needle valve control, NV, of the flow meter, FM.

the CN band (Channel M_2), together with the standard deviations of each set of readings and the relative standard deviation (r.s.d.). To obtain a comparison with no servo-control in operation, a set of values was immediately taken by again activating the spectrometer measuring circuit while the recorder was on "stand by". The whole procedure was repeated a number of times with barium and aluminium as the test elements.

Results and discussion

The results in the first two columns of Table 1 were obtained in the direct determination of aluminium and barium by a.e.s. with the regulated and unregulated CN emission modes. The results in the last column of the table were obtained by using the CN band-head emission in channel M_2 as an internal standard to correct the measured emission of aluminium in channel M_1.

It is clear that in each case the average value of the relative standard deviation for a set of results is significantly lower for the experiments with the regulated CN emission mode than for those without such regulation. Similar results were obtained when integration times, number of readings per set and number of sets of results were different from those listed in the Table. In every case, the mean r.s.d. was lower when CN regulation was used. In one case, this difference was not significant at the 95% level of confidence. The reason for the lower level (92%) of confidence in this case is to be found in three exceptionally stable periods of operation in the unregulated mode, which resulted in three of the ten values of r.s.d. having exceptionally low values. The variance of the set of results was thus large and while the calculated value of F [2] for the regulated and unregulated sets was 8.4, the calculated value of t [2] was only 1.93. It is apparent that unusually stable periods of gas

TABLE 1

Effect of CN emission regulation on relative standard deviation of results for solutions containing 70 ppm Al and 2 ppm Ba.

Channel M_1, signal from	Al	Ba	CN	Al
Type of measurement	Direct	Direct	Direct	With CN internal std.
Integration time per reading (s)	4	4	1	1
No. of readings per set	10	20	10	10
No. of sets of results	4	6	10	10
Mean r.s.d. (%):				
(i) regulated CN	0.45	1.40	2.89	2.71
(ii) unregulated CN	0.71	1.83	5.21	4.56
Level of significance of difference in (r.s.d.) values (%)	>95	>95	>95	>95

flow do occur from time to time; but it is important to realise that these do not seem to occur very often and to note that even in the one such case observed the average value of the r.s.d. for the unregulated set of results was again higher.

It was also noted that the improvement in precision obtained by using the regulated conditions tended to be greater when longer integration times for each reading were used. This would be expected on the basis of greater long-term stability of the flame resulting from the absence of drift in flow rates under regulated conditions.

It is also clear from Table 1 that the r.s.d. for determinations of aluminium with the CN band-head as an internal standard was greater than that obtained in the direct determination of aluminium, regardless of whether regulation of the CN emission had been in operation or not. The principal reason for the failure of the CN emission as an internal standard can be attributed to the fact that it was affected by gas flow rates to a much greater degree than was the emission of an atomic line of aluminium or barium. It can be concluded that using the CN band-head emission to control flame conditions is more fruitful than using it as an internal standard. Such an approach leads to an increase in the precision of measurement over either the direct, but unregulated, method or the internal standard approach. Such improvements in precision can be of importance and could be achieved with any twin monochromator emission spectrometer. The use of a more sophisticated control system than the simple and relatively crude one reported here might be expected to lead to greater improvements in precision of measurement. Although the application of flame regulation in this fashion could not be tested for a.a.s. with the instrumentation available, an improvement in precision would again be expected, because the sensitivity of determination for the elements in question is critically dependent, in both emission and absorption, on the gas mixture used, as is the production of CN species.

REFERENCE

1 A. M. Ure, Int. Atomic Absorption Conf., Sheffield, 1969, Paper B7.
2 R. C. Weast and S. M. Selby (Eds.), Handbook of Chemistry and Physics, The Chemical Rubber Co., 48th edn., 1967, p. 160.

Analytica Chimica Acta, 102 (1978) 201—204

Short Communication

DETERMINATION OF COPPER IN GASOLINE BY ATOMIC ABSORPTION SPECTROMETRY WITH ELECTROTHERMAL ATOMIZATION

N. M. POTTER

Analytical Chemistry Department, General Motors Research Laboratories, Warren, Michigan 48090 (USA)

(Received 3rd May 1978)

The presence of low concentrations of copper in gasoline is undesirable because copper promotes the formation of gums and lacquers during heating or storage of the gasoline. Methods for the accurate determination of copper in gasoline are often lengthy, requiring chemical separations followed by colorimetric reactions, e.g., the Institute of Petroleum Method 225/71 [1].

Few rapid methods are available for the direct determination of copper in gasoline. Cotton and Jenkins [2] employed an atomic fluorescence technique for the direct determination of copper, but few data were given to support the method. Atomic absorption spectrometry (a.a.s.) offers an attractive approach for the direct determination of copper. However, direct comparisons of sample and standard signals yield inaccurate results, because signal responses are affected by sample matrices. Moore et al. [3] used an a.a.s. method involving the standard addition technique and dilution with acetone to minimize matrix effects.

Experience in this laboratory has shown that a hydrogen—nitrous oxide flame can be used for the direct determination of copper in gasoline, although an empirical correction factor must be applied to all results. A few samples have given erroneous results because this factor did not apply. A method involving evaporation of the gasoline followed by ashing the residue and measuring the copper concentration by a.a.s. has also been tested, although contamination levels limit its usefulness. Because the evaporation and ashing procedures are analogous to the sample treatment when a heated graphite furnace atomizer is used, flameless a.a.s. was selected to provide a rapid method for the determination of copper in gasoline. Runnels et al. [4] have successfully used flameless a.a.s. to determine trace metals in petroleum products. In this report, the results obtained by the flameless method developed are compared with those obtained by a standard photometric method [1].

Experimental

Apparatus and operating parameters. A Perkin-Elmer Model 403 atomic absorption spectrometer was used with a deuterium background corrector and

a Perkin-Elmer HGA-2100 graphite tube furnace equipped with a ramp programmer. Absorbance measurements were recorded with a Leeds and Northrup Speedomax XL recorder, operated at a chart speed of 2.5 cm min^{-1}. Peak heights were measured, and data were processed on a PDP-8 computer. The light source was a Westinghouse Model WL 22603 copper hollow-cathode lamp operated at 10 mA. The copper resonance line at 324.8 nm was used, and the slit width was set so that the spectral band pass was approximately 0.7 nm.

A 25-μl sample was injected into the furnace, brought to 50°C in 10 s, and dried at 50°C for 5 s. The temperature was then increased to 100°C in 15 s and held at 100°C for another 5 s. Copper was then atomized at 2500°C for 9 s. A continuous flow of argon was maintained in the graphite furnace at all times.

Photometric measurements were made with a Beckman Model B spectrophotometer.

Standards and reagents. ASTM isooctane (2,2,4-trimethylpentane) was used as the solvent for standard preparation and sample dilution. Calibration solutions containing 0.00—0.25 μg Cu ml^{-1} were prepared by dissolving weighed portions of a 500-ppm copper metal-organic oil standard (Conostan, C-20) and making appropriate dilutions.

Reagents for the photometric procedure were as recommended [1]. Johnson and Matthey Specpure copper was used to prepare calibration solutions.

Determination of copper — flameless method. Each fuel sample (5 ml) was diluted with 10 ml of isooctane before injection into the furnace. Samples containing more than 0.75 μg Cu ml^{-1} were further diluted with isooctane to obtain a final concentration between 0.10 and 0.25 μg ml^{-1}. The copper absorbance was measured after injecting 25 μl from each solution into the graphite furnace. Each calibration solution was measured four times and each sample solution twice.

Determination of copper — photometric method. Suitable aliquots from each fuel sample were processed according to the Institute of Petroleum Method No. 225/71 for copper [1].

Results and discussion

Standard selection and calibration solutions. A Conostan C-20 metal—organic oil standard (500-ppm Cu) was selected to prepare calibration solutions. To verify the accuracy of the standard, weighted portions of the oil were ashed with HNO_3 and $HClO_4$ and analyzed by conventional a.a.s. Results from seven determinations gave a value of 496 μg Cu ml^{-1} of oil (relative standard deviation, 2%). All glassware used to prepare calibration and sample solutions was cleaned with HNO_3 before use. The ASTM isooctane used for dilutions was found to have a copper concentration of less than 0.002 μg ml^{-1}. Calibration solutions were stable for two weeks.

Sample measurement. All samples were diluted with at least two parts of isooctane to one part of gasoline to facilitate sample injection into the graphite furnace. Gasoline alone was not injected because its low surface

tension caused leakage from the micropipets. However, it was later found that gasoline could be directly injected if the pipet tips were pre-conditioned by rinsing five times with the sample just before injection.

The conditions used for the graphite furnace were established to minimize sample treatment. Because most gasoline samples in this study contained between 0.1 and 1.0 μg Cu ml^{-1}, conditions were set to encompass this range rather than to maximize sensitivity. Sample and calibration solutions were dried successively at 50°C and 100°C to remove volatile organic components. A high-temperature char (> 100°C) of the samples was not required, because little smoke was emitted during atomization. In addition, a high temperature char could vaporize any low-boiling copper compounds. If copper compounds which volatilize below 100°C are suspected, the copper concentrations of at least a few samples should be verified by an independent method. The ramp programmer was used during the drying of the specimens to eliminate spattering within the graphite tube. The copper was atomized without use of the ramp programmer to minimize peak broadening. The background corrector cancelled any extraneous interferences, and a constant flow of argon was maintained during the entire cycle to remove volatilized sample components. Recorded peak heights were found to be suitable for concentration calculations.

Method evaluation. A series of gasoline samples containing varying amounts of copper was analyzed by flameless a.a.s. and by the Institute of Petroleum method. Gasolines containing residues were not examined because injections of such samples into the furnace led to erratic data. Sample aliquots taken within three days of one another were processed by each method. Changes in concentration from copper depositing on the sample bottle were not found within this time period. However, copper can be deposited on storage container walls; thus, samples should be analyzed as soon as feasible. A comparison of the results obtained is presented in Table 1. A "*t*" test [5] applied to the

TABLE 1

Comparison of results obtained for copper (in μg ml^{-1}) by the photometric and flameless a.a.s. methods

Sample No.	Photometric method	Flameless a.a.s. method
1	0.04	0.03
2	0.05	0.05
3	0.19	0.17
4	0.20	0.20
5	0.30	0.30
6	0.50	0.53
7	0.55	0.52
8	0.73	0.74
9	0.86	0.84
10	1.47	1.45
11	1.62	1.62
12	2.50	2.49

data at the 0.05 confidence level showed that there was no significant difference between the two methods. The relative standard deviation calculated from 8 results on sample 3 was 1.9%.

Finally, this flameless a.a.s. method offers an attractive alternative to wet chemical methods, because samples can be processed rapidly. Experience has shown that three to four times as many samples can be processed within a given time period as is possible with the standard method [1].

REFERENCES

1 Institute of Petroleum Standards for Petroleum and Products, Pt. I, Section II, Applied Science Publishers, Barking, 1974, p. 964.
2 D. H. Cotton and D. R. Jenkins, Spectrochim. Acta, Part B, 25 (1970) 283.
3 E. J. Moore, O. I. Milner, and J. R. Glass, Microchem. J., 10 (1966) 148.
4 J. H. Runnels, R. Merryfield, and H. B. Fisher, Anal. Chem., 47 (1975) 1258.
5 W. Volk, Applied Statistics for Engineers, McGraw Hill, New York, 1958, p. 112.

Analytica Chimica Acta, 102 (1978) 205—210

Short Communication

DIFFERENTIAL PULSE POLAROGRAPHIC DETERMINATION OF DISODIUM CROMOGLYCATE IN URINE

A. G. FOGG* and N. FAYAD

Chemistry Department, Loughborough University of Technology, Loughborough, Leics. (Gt. Britain)

(Received 22nd May 1978)

Disodium cromoglycate (DSCG; the disodium salt of 1,3-di(2-carboxy-4-oxychromen-5-yloxy)propan-2-ol) is used in the treatment of bronchial asthma, and is administered as a fine powder by means of a special inhalation device. Methods developed for its determination in absorption and metabolic studies include a fluorimetric procedure for its determination in plasma [1], and a colorimetric procedure for its determination in urine [1,2]; interferences have so far precluded the use of the fluorimetric method for urine analysis. DSCG, which is excreted unchanged in urine, is separated from urine by an ion-exchange procedure before it is determined colorimetrically. The colorimetric procedure involves alkaline hydrolysis of the DSCG to the bis-hydroxyacetophenone which is then derivatized with diazotized *p*-nitroaniline.

In the present work the polarography of DSCG has been studied, and a differential pulse polarographic (d.p.p.) method has been developed for the determination of DSCG in urine. Separation of DSCG from urine can be effected either by extraction of cromoglycic acid from acidic solution into ethyl acetate or by extraction of di(tri-n-butylbenzylphosphonium) cromoglycate from aqueous solutions over a wide pH range into chloroform. In either case the organic solvent is evaporated and the cromoglycate is dissolved in a suitable supporting electrolyte for polarography. Although the solvent extraction step limits interference, nevertheless polar natural constituents of the urine produce a substantial background current so that, whereas 0.05 μg DSCG ml^{-1} can be determined in standard aqueous solutions, the lowest level that can be determined in urine is about 0.5 μg ml^{-1}.

Preliminary tests

Pure DSCG was examined in Britton—Robinson buffers as supporting electrolyte; buffers which also contained glycine and citric acid gave an adsorption peak between the two peaks obtained for DSCG in the pH range 2—5. The potentials and heights of the d.p.p. peaks obtained for a 10^{-4} M solution of DSCG in Britton—Robinson buffer at various pH values

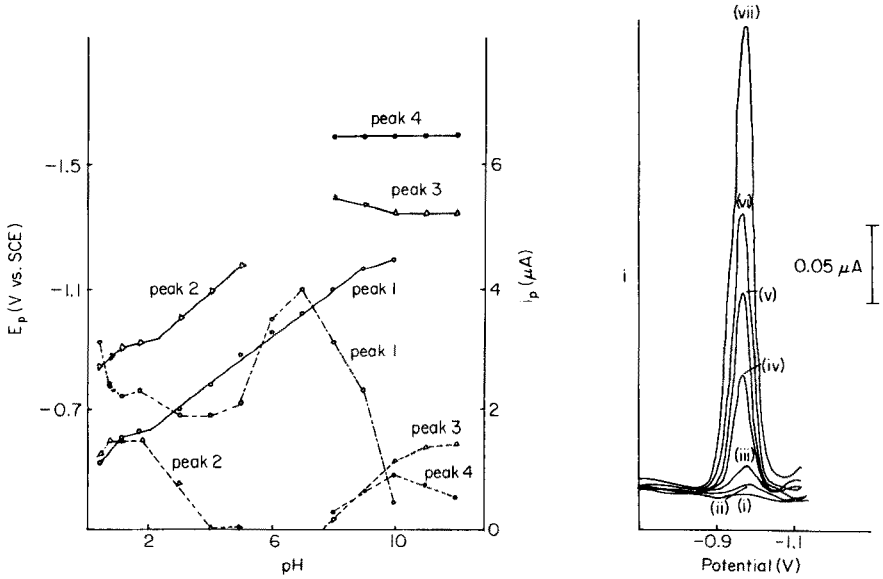

Fig. 1. Effect of pH on the peak potentials and peak currents of the d.p.p. peaks obtained for a 10^{-4} M solution of DSCG in Britton—Robinson buffer. Full lines, peak potential vs. pH; broken lines, peak current vs. pH.

Fig. 2. Typical d.p. polarograms obtained in Britton—Robinson buffer pH 5.8 with 10% methanol. DSCG concentration: (i) 0, (ii) 0.04, (iii) 0.14, (iv) 0.53, (v) 0.92, (vi) 1.31, (vii) 2.14 μg ml^{-1}.

are shown in Fig 1. The half-wave potential ($E_{p/2}$) of the main (first) peak is (—0.47 — 0.078 pH) V in the pH range 2—9; the change of $E_{p/2}$ with pH is consistent with an irreversible electrode reaction. The size of the main peak is clearly dependent on pH and is at a maximum at pH 7. In contrast, the height of the d.c. wave was not affected markedly by changes of pH. Above pH 8, two small peaks appeared at more negative potentials. The main peak became indistinct above pH 10.

Analysis of d.c. polarograms of the main wave with respect to changes in the limiting current with height of the mercury reservoir indicated diffusion control. Typical d.p. polarograms obtained for DSCG in Britton—Robinson buffer pH 5.8 are shown in Fig. 2.

Polarography of DSCG in urine

As was expected, it was necessary to separate DSCG from the urine before the polarographic determination. Ion-pair extraction of the cromoglycate into an organic solvent was considered first, and tri-n-butylbenzylphosphonium chloride (Maybridge Chemical Co. Ltd.) was found to extract cromoglycate effectively from aqueous solutions (pH 2—9) into chloroform. The cromoglycate was recovered in two ways from the chloroform. In the

first approach, the chloroform was evaporated and the cromoglycate was taken up in a small volume of methanol before the supporting electrolyte was added for polarography. In the second approach, the cromoglycate was back-extracted from the chloroform into an aqueous 0.4 M sodium perchlorate solution, the cromoglycate exchanging with perchlorate which is more readily extracted into chloroform as its tri-n-butylbenzylphosphonium salt than is cromoglycate. Both methods worked well, but the evaporation method was adopted because of its simplicity. Several other phosphonium salts were also tried, but tri-n-butylbenzylphosphonium chloride was readily soluble in water and gave low polarographic blanks. Extraction of cromoglycate as the free acid (pK_{a1} = pK_{a2} = 2) from 2 M hydrochloric acid solution into ethyl acetate also proved to be satisfactory.

Both the phosphonium extraction into chloroform and the extraction of the free acid into ethyl acetate were readily adapted to determinations on urine samples spiked with DSCG. In the case of the free acid extraction, interferents in the urine were extracted with ethyl acetate before cromoglycic acid was extracted at higher acidities. The polarograms obtained when the phosphonium extraction was used seemed to be slightly superior. Even so, interferents in the urine produced a fairly steep baseline and restricted the determination of DSCG to 0.5 μg ml^{-1} in the urine, compared with 0.05 μg ml^{-1} in aqueous standards.

Attempts were made to extract interferents from the urine into chloroform before cromoglycate was extracted with the phosphonium salt. Good recovery of cromoglycate was obtained but the baseline was no better: a considerable improvement was observed, however, when pre-extraction of impurities was done with n-butanol. Other extractive clean-up procedures with iso-amyl alcohol and hexane were tried unsuccessfully. The recommended procedures for the determination of DSCG in urine are as follows.

Experimental

Equipment. Polarographic measurements were made with a PAR 174 polarographic analyser (Princeton Applied Research). For differential pulse operation, the forced drop time was 0.5 s, the pulse height 50 mV and the scan rate 5 mV s^{-1}, except where otherwise indicated. Three-electrode operation was used with a platinum counter electrode and a saturated calomel reference electrode.

Chemicals. A pure sample of disodium cromoglycate (Fisons Pharmaceuticals Ltd.) was dried at 100°C in a vacuum oven before use. Aqueous standard solutions were prepared freshly.

For Britton—Robinson buffer pH 1.9, prepare a solution 0.04 M in boric acid, orthophosphoric acid and acetic acid. For buffers pH 3.4 and 5.8, adjust the pH of some of the above buffer to the required value with 0.2 M sodium hydroxide solution.

Procedure with phosphonium extraction. Into a clean, dry 35-ml glass-stoppered centrifuge tube, place 2 ml of urine sample and 5 ml of n-butanol.

Shake the tube gently for 30 s and then centrifuge for 3 min at 2000 rpm. Carefully remove the (upper) organic layer with a syringe and discard it. To the aqueous layer in the centrifuge tube, add 1 ml of buffer pH 1.9, 2 ml of aqueous 0.2 M tri-n-butylbenzylphosphonium chloride solution and 5 ml of chloroform. Shake the tube gently for 30 s and centrifuge for 4 min at 4000 rpm. Carefully transfer the (lower) chloroform layer by means of a syringe to a container suitable for evaporating the chloroform. (To ensure that only chloroform is drawn into the syringe, draw a small amount of air into the syringe before passing the cannula through the aqueous layer; expel this air when the tip is in the chloroform, thus discharging any aqueous phase.) Re-extract the aqueous layer with a second 5-ml portion of chloroform in the same way. Evaporate the combined chloroform extracts to dryness in a water bath with a stream of nitrogen. Dissolve the residue in 0.5 ml of methanol and then add 4.5 ml of buffer pH 5.8. Transfer the solution to a suitable polarographic cell, deoxygenate it with nitrogen for 10 min, and obtain a differential pulse polarogram between −0.6 and −1.0 V. Compare the height of the peak with those obtained after extracting normal urine samples spiked with known amounts of DSCG.

Typical d.p. polarograms obtained from urine samples by this procedure are shown in Fig. 3a. Polarograms obtained after extraction of aqueous standards are shown in Fig. 3b. Comparison of the heights of these peaks with those obtained with aqueous DSCG standards without extraction indicated that the recoveries of DSCG from aqueous standards and from urine samples were 95% and 73%, respectively. The relative standard deviation obtained for the determination of DSCG at the 1 μg ml^{-1} level in urine (10 determinations) was 4%.

The concentration of tri-n-butylbenzylphosphonium chloride in the polarographed solution affected the height of the d.p.p. peak of DSCG. Previous workers [3] have shown that surface-active materials have this effect. Addition of an equimolar amount of tri-n-butylbenzylphosphonium chloride to DSCG at the 10^{-5} M level (pH 5.8) increased the height of the DSCG d.p. peak by 30%; much larger concentrations of the phosphonium salt, however, depressed the height of the peak. U. v. spectrophotometry showed that about 90% of the tri-n-butylbenzylphosphonium chloride added in the extraction procedure given above is extracted into the chloroform and is present in the polarographed solution. The amount of tri-n-butylbenzylphosphonium chloride used in the procedure leaves the height of the cromoglycate peak unchanged, but if the amount used is increased by 20%, the peak height is depressed by 10%. For this reason the amount of tri-n-butylbenzylphosphonium chloride used in the extraction of standards and samples should be controlled fairly closely.

Procedure with ethyl acetate extraction. Place 2 ml of urine sample and 5 ml of ethyl acetate in a clean, dry 35-ml centrifuge tube. Shake the mixture gently for 30 s, carefully remove (by syringe) the (upper) ethyl acetate layer and discard it. Extract the urine with a second 5-ml portion of ethyl acetate and again discard the organic layer.

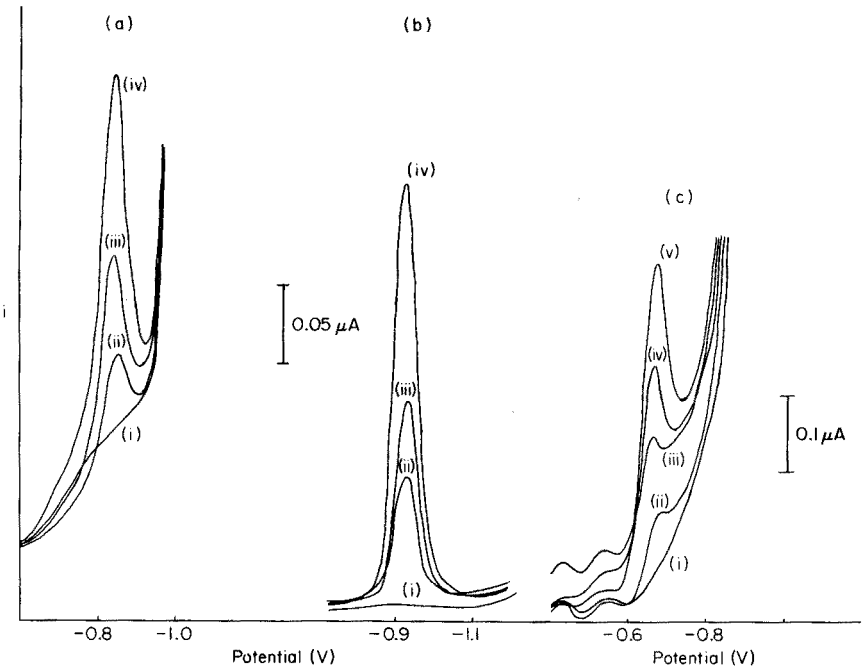

Fig. 3. Typical d.p. polarograms obtained for cromoglycate: (a) and (b) after extraction with tri-n-butylbenzylphosphonium chloride from (a) urine and (b) aqueous standards, for DSCG concentrations of (i) 0, (ii) 1.75, (iii) 2.5, (iv) 5 μg ml^{-1} ; (c) after extraction of cromoglycic acid into ethyl acetate from urine for DSCG concentrations (i) 0, (ii) 0.5, (iii) 1, (iv) 2.5, and (v) 5 μg ml^{-1} . Scan rate, 2 mV s^{-1}; drop time, 1 s.

To the urine add 2 ml of 2 M hydrochloric acid solution. Extract with two 5-ml portions of ethyl acetate and evaporate off the ethyl acetate as described above for chloroform. Dissolve the residue in 0.5 ml of methanol and 4.5 ml of Britton—Robinson buffer pH 3.4, and record the polarogram as indicated above. (Alternatively, in the case of extractions into ethyl acetate from aqueous standards, the cromoglycate may be back-extracted into 2 ml of 2 M sodium hydroxide solution. In this case, add 3 ml of Britton—Robinson buffer pH 1.9, deoxygenate and record the polarogram. This procedure does not work well with urine samples.)

Typical polarograms obtained by this procedure are shown in Fig. 3c. The recovery of DSCG exceeded 95% and the relative standard deviation (10 determinations) at the 1 μg ml^{-1} level was 5%.

Discussion

The d.p. procedure for the determination of DSCG in urine samples covers approximately the same concentration range as the colorimetric procedure [1, 2]. The clean-up procedure recommended for use with the polarographic method, however, is simpler and quicker than that used with the colorimetric

method, and avoids the use of ion-exchange resins and concentrated formic acid solutions. Further, Curry and Mills [2], to obtain sufficient precision when formate-treated resins were used, found it necessary to use a radioactive internal standard to determine the DSCG recovery; in contrast, the precision of the polarographic method is good.

The concentration of electroactive constituents in urine is affected by the sampling time and by the physiological state of the individual at the time of sampling. In the present work, a higher concentration of electroactive interferences — indicated by a steeper baseline — was observed in early morning samples, so that samples taken later in the day are to be preferred.

Previous authors [4, 5] have commented on the fact that half-wave and peak potentials of organic compounds in, or after extraction from, biological fluids, can differ from the potentials of the same compounds measured directly in aqueous supporting electrolyte. This was true in the present work, the peak potential of cromoglycate extracted from urine being some 60 mV more positive than that obtained directly in aqueous buffer at the same pH. The mechanism of the polarographic reduction of chromones has been discussed by Knobloch [6].

The polarographic method should be readily adaptable to the determination of DSCG in formulations, and should be particularly valuable in stability testing as the drug can be determined without derivatization.

The authors thank Fisons Pharmaceuticals Ltd., for providing a sample of DSCG, and Mr. J. E. Tillman and colleagues for helpful discussion.

REFERENCES

1 G. G. Moss, K. M. Jones, J. T. Ritchie and J. S. G. Cox, Toxicol. Appl. Pharmacol., 20 (1971) 147.
2 S. H. Curry and G. G. Mills, J. Pharm. Pharmacol., 25 (1973) 678.
3 E. Jacobsen and H. Lindseth, Anal. Chim. Acta, 86 (1976) 123.
4 J. A. F. de Silva, I. Bekersky, M. A. Brooks, R. E. Weinfeld, W. Glover and C. V. Puglisi, J. Pharm. Sci., 63 (1974) 1440.
5 W. F. Smyth and B. Leo, Anal. Chim. Acta., 76 (1975) 289.
6 E. Knobloch, Adv. Polarogr., 3 (1960) 875.

Analytica Chimica Acta, 102 (1978) 211—214

Short Communication

THE DETERMINATION OF SMALL AMOUNTS OF STRONG ACID IN PRESENCE OF AN EXCESS OF WEAK ACID

PER ASBJØRN OVERVOLL and WALTER LUND*

Department of Chemistry, University of Oslo, Boks 1033 Blindern, Oslo 3 (Norway)

(Received 17th February 1978)

Mixtures of strong and weak acids can often be analyzed successfully by potentiometric titrations with alkali. However, if the dissociation constant of the weak acid is greater than ca. 10^{-5}, or the concentrations of the acids are low, the inflection point corresponding to the strong acid content of the sample will be poorly defined, and the determination of this acid will be difficult. Furthermore, even if an inflection point can be distinguished, this point may differ from the equivalence point of the titration [1, 2]. Occasionally, the determination of the end-point is also complicated by kinetic effects and precipitation reactions. In some of these cases, the use of Gran plots [3, 4] will facilitate the detection of the end-point of the titration. However, when a small amount of strong acid is to be determined in presence of an excess of a weak acid, this procedure cannot be used [4].

The situation is improved considerably if the dissociation of the weak acid is suppressed by the addition of a relatively large amount of an indifferent strong acid, prior to the analysis. This will improve the accuracy of the Gran plot procedure [4], and it also makes possible alternative approaches to the determination of the strong acid content of the sample. Thus, Ahrland et al. [5] determined the amount of strong acid in such samples directly from the difference between the total amount of strong acid, obtained from the pH value of the acidified sample, and the known amount of acid added.

In this communication a more accurate method, based on titration with a strong acid, is decribed. The method is applied to the determination of the content of strong acid in a uranyl salt; the uranyl ion behaves as a moderately weak acid in aqueous solutions, owing to marked hydrolysis.

Experimental

The pH titrations were carried out in a thermostatted (25.0°C) glass cell, in an argon atmosphere, with a Metrohm E485 (10-ml) multi-burette. The Beckman Research pH meter, equipped with Orion glass and single-junction reference electrodes, was standardized against 0.05 m potassium hydrogenphthalate and 0.01 m borax buffers.

A 0.05 M solution of UO_2^{2+} was prepared by dissolving 12.5 g of uranyl nitrate in 0.5 l of 0.1 M potassium nitrate. The solution was standardized

gravimetrically by precipitation as ammonium diuranate and ignition to U_3O_8 [6]. The 0.2 M nitric acid was made by dilution of the concentrated acid. The 0.1 M potassium nitrate was neutralized with sodium hydroxide to pH 6.9—7.1 in an argon atmosphere.

Results and discussion

The principle of the new method is as follows. A known amount v_s of a strong acid is added to the sample to suppress the dissociation of the weak acid, and the pH of the acidified sample is then measured. A reference solution is then made by mixing the same strong acid with a suitable salt solution, in such a way as to give a final solution with exactly the same pH, total volume and ionic strength as the acidified sample. Assuming that the amount of strong acid needed to make up the reference solution is v_r, the original amount of free acid in the sample will be simply $\Delta v = v_r - v_s$, provided that the dissociation of the weak acid is negligible at the particular pH value chosen.

The crucial point in this procedure is the correct choice of pH. If too little acid is added, the dissociation of the weak acid will make Δv too large. In contrast, if Δv is small and a large excess of strong acid is added, the determination of Δv will not be very precise. The optimal pH region is found in the following way. By adding increasing amounts of strong acid to both the sample and reference solutions, titration curves of the type shown in Fig. 1 are obtained. From this figure, Δv can be read directly, for any pH value. For each pair of corresponding v_r and v_s values, the two solutions have the same pH, volume and ionic strength. Figure 1 shows that Δv decreases as v is increased, until it finally reaches a constant value, which then corresponds to the amount of strong acid originally present in the sample. As already mentioned, the high values obtained for Δv at low v values are due to the dissociation of the weak acid.

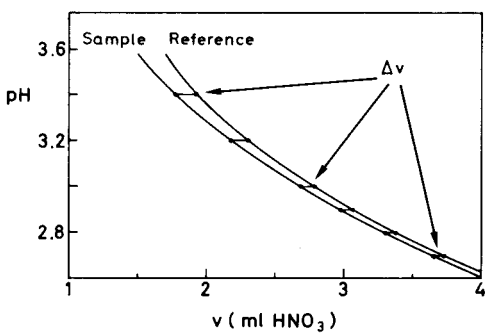

Fig. 1. Illustration of the method. Δv corresponds to the amount of strong acid in the sample. The two curves represent the titration of the sample and reference solutions, respectively, with 0.2 M nitric acid.

The general procedure outlined above was used to determine the amount of free acid in a solution of uranyl nitrate; it is difficult to prepare uranyl salts with an exact stoichiometric composition. 1.5 ml (v_s) of 0.2 M nitric acid and 225 ml of 0.1 M potassium nitrate were added to 25 ml of 0.05 M uranyl nitrate; the pH of this solution was found to be 3.58 and the total volume was 251.5 ml. The reference solution was then made by adding 0.2 M nitric acid and 0.1 M potassium nitrate from separate burettes to 225 ml of 0.1 M potassium nitrate, until the pH and volume of the resulting solution were identical with those of the sample solution. The volume of nitric acid added (v_r) was then 1.7 ml. Titration of the two solutions with additional amounts of nitric acid gave the two curves shown in Fig. 1. As can be seen, a constant Δv was obtained for pH values below ca. 3.0, (corresponding to v values above ca. 2.5), indicating that the hydrolysis of the uranyl ion is insignificant in this region. This last result was confirmed in a separate study of the uranium(VI) hydrolysis [7]: Δv was found to be 0.11 ml, and the concentration of free acid in the uranyl stock solution was therefore 8.8×10^{-4} M, or 1.8 mol % (0.11 ml of 0.2 M acid per 25 ml of 0.05 M uranyl solution).

The method described above is based on precisely matching the pH of two solutions by adding a strong acid. With a modern precision pH meter, this matching can be accomplished with a precision of 0.001—0.002 pH unit, which corresponds to a precision of 0.2—0.4% in the hydrogen ion concentration. The liquid junction potentials should be nearly equal for the two solutions, because they have the same pH, ionic strength and also similar chemical composition, when Δv is measured. It may be pointed out that the accuracy of the pH measurements, in terms of the true activity or concentration of hydrogen ions, is of little interest, because only the relative pH values are considered.

The precision in the determination of Δv depends mainly on v_r and v_s; because these volumes were measured with a precision of ca. 0.003 ml, the precision in Δv was of the order of a few per cent.

The present method has certain advantages compared to the procedure of Ahrland et al. [5]. The pH values are not used to calculate the hydrogen ion concentration, therefore standardization of the pH meter is not critical and the activity coefficient of the hydrogen ion need not be estimated, even if normal standard buffers are used. No correction is made for the liquid junction potential, which will be nearly the same for the sample and reference solutions, as the two solutions have exactly the same pH value and ionic strength when Δv is measured. Furthermore, the optimal pH region, in which dissociation of the weak acid (or the hydrolysis of the uranyl ion) is negligible, is easily found from the curves in Fig. 1, whereas calculations must be carried out at various points on the titration curve, before the optimal pH region is established in the Ahrland procedure.

REFERENCES

1 W. Lund, Talanta, 23 (1976) 619.
2 C. F. Baes and N. J. Meyer, Inorg. Chem., 1 (1962) 780.
3 G. Gran, Analyst, 77 (1952) 661.
4 A. Johansson, Analyst, 95 (1970) 535.
5 S. Ahrland, R. Larsson and K. Rosengren, Acta Chem. Scand., 10 (1956) 705.
6 A. I. Vogel, Quantitative Inorganic Analysis, Longmans, London, 2nd edn. 1951, p. 470.
7 P. A. Overvoll and W. Lund, to be published.

Analytica Chimica Acta, 102 (1978) 215—220

Short Communication

DÉTERMINATION D'HYDRAZINES ET D'HYDRAZIDES À L'AIDE DU CÉRIUM(IV), DU MANGANÈSE(III) ET DE L'ARGENT(II) PRODUITS COULOMÉTRIQUEMENT

(Determination of hydrazines and hydrazides with coulometrically generated cerium(IV), manganese(III) and silver(II))

M. CHATEAU-GOSSELIN et G. J. PATRIARCHE*

Institut de pharmacie, Université Libre de Bruxelles, Campus Plaine 205/1, 1050 Brussels (Belgique)

(Reçu le 10 Avril 1978)

Les possibilités d'utilisation de la coulométrie dans l'analyse des médicaments ont été mises en évidence antérieurement [1—4]. Au cours de ce travail, nous avons fait appel à différents agents coulométriques d'oxydation tels que le cérium(IV), le manganèse(III) et l'argent(II) en vue de dosage d'une série d'hydrazines et d'hydrazides. Parmi les molécules renfermant ces groupements fonctionnels, plusieurs sont susceptibles d'activités thérapeutiques: nous y trouvons principalement des antidépresseurs du type IMAO, mais aussi un antituberculeux, un cytostatique et un analgésique antipyrétique. L'oxydation des fonctions hydrazines et hydrazides se produit très aisément. Lors de cette étude, deux schémas d'oxydation ont été rencontrés. Le premier (eqn. 1) conduit à la formation de dérivés colorés de type diazoïque avec consommation de deux électrons. Ceci s'applique aux cas où la fonction hydrazide est stabilisée par la présence d'un groupement phényl.

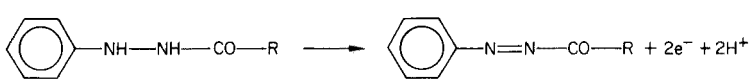

(1)

Le second provoque un dégagement d'azote et consomme 4 électrons par molécule.

$$R—NH—NH—R' + 2\,H_2O \rightarrow ROH + R'OH + N_2 + 4H^+ + 4e^- \quad (2)$$

$$R—CO—NH—NH—R' + 2\,H_2O \rightarrow RCOOH + R'OH + N_2 + 4H^+ + 4e^- \quad (2a)$$

Partie experimentale

Le coulomètre utilisé a déjà été décrit antérieurement [3, 4]. Il est alimenté par un ampérostat avec en série dans le circuit, une forte résistance à décades. Suivant les cas envisagés, nous avons utilisé un système de détection du point

final potentiométrique (Pt-ECS) ou un système ampérométrique à deux électrodes de platine polarisables.

Coulométrie à l'aide du cérium(IV) ou manganèse(III). Les mesures ont été réalisées dans une cellule en H à deux compartiments séparés par un disque en verre fritté (G4). Des électrodes de platine de 1,4 ou 30 cm^2 (pour les deux faces) sont utilisées comme électrodes génératrices. La contre-électrode est constituée par une spirale de platine. Les milieux d'électrogénération sont respectivement constitués par du sulfate cérium(III) pentahydraté 0,05 M dans l'acide sulfurique 3 M, ou par du sulfate de manganèse monohydraté 0,3 M dans de l'acide sulfurique 3 M. Une solution d'acide sulfurique 3 M est utilisée comme catholyte. Avant chaque essai, l'électrolyte de support est prétitré avec une solution de fer(II).

Coulométrie a l'aide de l'argent(II). La cellule utilisée et son système de refroidisement ont déjà été décrits antérieurement [5]. L'anode est constituée de plaques d'or d'une surface de 2 ou 10 cm^2. L'électrode auxiliaire est constituée par une spirale de platine. La solution génératrice est une solution de nitrate d'argent 0,1 M dans de l'acide nitrique 5 M. Le catholyte est constitué d'une solution 5 M en acide nitrique. Toutes les mesures ont été effectuées à −10°C. Un prétitrage de l'électrolyte support est réalisé avant chaque essai avec une solution de vanadium(IV). L'électrode de référence plonge dans la solution par l'intermédiaire d'un tube craquelé de type Perley rempli d'une solution de nitrate de sodium 4 M afin d'éviter toute diffusion des ions chlorures dans le milieu réactionnel.

Echantillons. Les produits utilisés sont de qualité p.a. ou pharmacopées. Les solutions stock de phénylhydrazine et de diphénylcarbazide sont préparées par dissolution dans un minimum d'acétonitrile et diluées ensuite avec de l'eau bidistillée bouillie et refroidie. Les autres produits sont simplement dissous dans de l'eau bidistillée.

Résultats et discussion

La volumétrie cérique classique des hydrazines et hydrazides avait déjà été réalisée par plusieurs auteurs [6, 7]. En ce qui concerne la coulométrie, les conditions d'électrogénération en ont été déterminée par Lingane et al. [3, 8]. Le cérium(IV) est produit à une électrode de platine avec un rendement en courant proche de 100%, à partir d'une solution de sulfate de cérium(III) 0,05 M. Il est nécessaire de travailler à des densités de courant comprises entre 1 et 10 mA cm^{-2}. L'étude théorique et l'optimalisation des conditions expérimentales ont déjà été réalisées précédemment lors de la détermination des phénothiazines [3, 9] et des dérivés du *p*-aminophénol [10].

La phénylhydrazine, la diphénylcarbazide et la phénylsemicarbazide (cryogénine) ont pu être dosées par une méthode coulométrique directe. Notons que pour la cryogénine et la diphénylcarbazide, le saut de potentiel indiquant la fin de la réaction est observé pour la formation d'un dérivé diazoïque. Le Tableau 1 reprend les résultats obtenus. Quant à l'oxalyldihydazide et l'isoniazide, alors que leur oxydation par le cérium(IV) est

TABLEAU 1

Résultats coulométriques

Dérivés étudiés	Nombre d'électrons	Prise d'essai (mg)	Trouvé (mg)	(%)	Nombre d'essais	*s* (mg)
Coulométrie à l'aide du cérium(IV)						
Phénylhydrazine	4	3,042	3,030	99,6	4	0,026
		1,554	1,542	99,2	4	0,005
		0,783	0,779	99,5	4	0,006
		0,385	0,383	99,5	4	0,003
Phénylsemicarbazide	2	1,649	1,651	100,1	3	0,003
		1,300	1,300	100,0	3	0,006
		1,082	1,082	100,0	3	0,006
		3,012	3,060	101,6	4	0,011
Diphénylcarbazide	2 × 2	4,950	4,930	99,6	4	0,033
		1,550	1,567	101,1	4	0,001
		1,260	1,261	100,1	4	0,010
		0,993	1,004	101,1	3	0,001
Oxalyldihydrazide[a]	2 × 4	0,359	0,361	100,6	3	0,002
		0,308	0,311	100,9	3	0,002
		0,251	0,255	101,6	3	0,001
		0,215	0,215	100,0	3	0,001
Isoniazide[b]	4	2,029	2,009	99,0	2	
		1,016	1,014	99,8	3	0,002
		0,505	0,496	98,2	5	0,001
Coulométrie à l'aide du manganèse(III)						
Phénylhydrazine	4	6,000	5,974	99,6	4	0,031
		3,180	3,176	99,9	4	0,020
		1,007	1,004	99,7	4	0,005
		0,608	0,614	101,0	4	0,003
Phénylsemicarbazide	2	1,884	1,903	101,0	5	0,018
		1,020	1,032	101,2	5	0,004
		0,533	0,536	100,6	5	0,004
		0,266	0,269	101,0	4	0,001
Diphénylcarbazide	2 × 2	4,950	4,919	99,4	4	0,016
		1,269	1,285	101,3	5	0,002
		0,635	0,641	100,9	5	0,001

[a]Coulométrie en retour: temps de réaction, 5 min. [b]Coulométrie en retour: temps de réaction, 40 min.

relativement lente, ils sont déterminés par un procédé en retour en utilisant un électrolyte de support additionné de 0,4 mole par litre de sulfate ferrico-ammonique qui n'intervient cependant pas lors de l'oxydation anodique. Après la production d'un excès de cérium(IV) et un temps de contact suffisant, la polarité des électrodes est inversée et le fer(II) électrogénéré réduit le cérium(IV) en excès dans la solution.

Le potentiel du couple Mn(II)/Mn(III) en milieu sulfurique est très proche de celui du couple Ce(III)/Ce(IV) et offre donc des possibilités d'emploi similaires. Les conditions d'électrogénération du manganèse(III) sur platine ont été étudiées par Selim et Lingane [11, 12]. Le rendement de courant de l'électrogénération est très proche des 100% si l'on opère en milieu 0,3 M en sulfate de manganèse et 3 M en acide sulfurique avec des densités de courant comprises entre 1 et 3 mA cm^{-2}. Cette méthode a été appliquée avec succès au dosage de la phénylhydrazine, de la cryogénine et de diphénylcarbazide (Tableau 1). Il faut cependant considérer deux particularités observées lors du dosage de la phénylhydrazine. L'addition d'un catalyseur, en l'occurrence des ions cuivre(II), est nécessaire à l'obtention d'une efficacité de titration correcte. En l'absence de cuivre, la réaction est lente et les résultats obtenus sont inférieurs à 90%. D'autre part, nous avons observé un dédoublement du saut de potentiel enregistré pour la détermination du point d'équivalence. Le premier saut s'établit très lentement et est peu reproductible, le second est très net, reproductible et correspond à un nombre d'électrons égal à quatre. L'écartement entre les deux sauts est d'autant plus marqué que la concentration de l'échantillon à doser est faible. Au-dessus de 6 mg, ce dédoublement disparaît et il ne subsiste que le second saut.

L'ion argent(II) dont le potentiel d'oxydation en milieu nitrique est de +1,9 V vs. ENH, peut être considéré comme un des oxydants les plus puissants utilisés jusqu'ici en chimie analytique. Les conditions d'électrogénération de cet agent très instable et inutilisable en volumétrie ordinaire ont été étudiées par Lingane et Davis [8, 13] et dans nos laboratoires [5, 14]. Nous en avons effectué l'étude théorique et les possibilités d'application à l'analyse organique. L'emploi d'une anode d'or, d'un anolyte constitué de 0,1 M de nitrate d'argent et de 5 M d'acide nitrique, à des températures proches de −10°C, nous a déjà permis le dosage de diphénols et des ions nitrites, notamment dans les eaux de consommation [5, 14].

Les hydrazides sont aisément oxydables par l'argent(II), le plus souvent selon l'éqn. (2), avec consommation de 4 électrons. Quelques exceptions existent cependant à ce schéma réactionnel. Dans le cas de l'oxydation de la procarbazine et de l'oxalyldihydrazide, le point final de la réaction est reproductible mais correspond respectivement à la consommation de 3 et 4,5 électrons par molécule. Quant à l'oxydation de la phénylsemicarbazide, elle conduit à une dislocation totale de la molécule et consomme 12 électrons. Il faut aussi faire remarquer que ces différentes molécules sont susceptibles de subir une oxydation secondaire lente des produits formés lors de la première étape de la réaction. Cela signifie que si l'on procède à l'addition successive d'échantillons à doser comme cela se pratique classiquement en coulométrie, une erreur positive croissante apparaît, augmentant au cours des essais et due à cette oxydation ultérieure. Une seule et unique détermination doit donc être réalisée par portion de l'électrolyte support après prétitrage de celui-ci avec quelques gouttes d'une solution très diluée de sulfate de vanadyle. Malheureusement, pour certains dérivés tels que la phénylhydrazine et la

phenelzine, cette oxydation secondaire s'effectue trop rapidement et les résultats obtenus ne sont pas reproductibles.

Néanmoins, dans les autres cas, cette méthode est applicable aux microdosages de ces hydrazides comme le montrent les résultats figurant dans le Tableau 2.

Nos remerciements vont au Fonds National de la Recherche Scientifique (F.N.R.S.) pour l'aide apportée à l'un d'entre nous (G. J. P.), et aux Firmes Roche, Pfizer et Warner-Lambert qui nous ont fournis bénévolement les échantillons standards.

TABLEAU 2

Coulométrie à l'aide de l'argent(II)

	Théorie (mg)	Trouvé (mg)	Différence (mg)	(%)	Nombre d'essais	s (mg)
Isoniazide 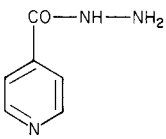	2,913	2,914	+0,001	100,0	4	0,005
	1,713	1,708	−0,005	99,7	4	0,003
	0,857	0,855	−0,002	99,8	4	0,001
	0,513	0,523	+0,010	102,0	4	0,008
Isocarboxazide 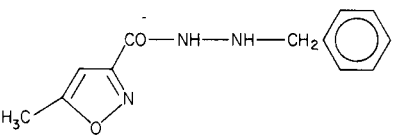	9,996	10,066	+0,070	100,7	4	0,009
	7,440	7,459	+0,019	100,3	5	0,075
	5,094	5,160	+0,066	100,3	4	0,020
	2,008	2,010	+0,002	100,1	5	0,019
Nialamide 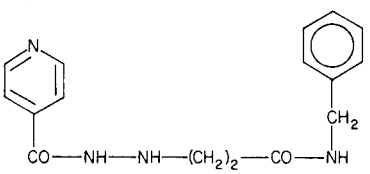	5,310	5,352	+0,042	100,8	4	0,034
	3,186	3,206	+0,020	100,6	5	0,037
	1,520	1,524	+0,004	100,3	4	0,014
Procarbazine 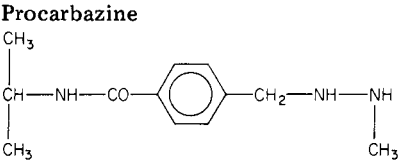	7,608	7,755	+0,147	101,9	5	0,026
	4,836	4,827	−0,009	99,8	5	0,018
	2,472	2,478	+0,006	100,2	4	0,016
Phénylsemicarbazide 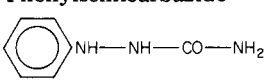	1,512	1,518	+0,006	100,4	5	0,013
	0,933	0,934	+0,001	100,1	5	0,010
	0,400	0,403	+0,003	100,8	4	0,005
Oxalyldihydrazide 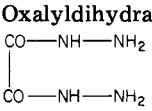	2,008	2,027	+0,019	100,9	4	0,042
	1,514	1,511	−0,003	99,8	5	0,011
	1,001	0,992	−0,009	99,1	4	0,012

BIBLIOGRAPHIE

1 G. J. Patriarche, Contribution à l'analyse coulométrique, Ed. Arscia-Maloine, Paris, 1964.
2 Z. E. Kalinowska, Acta. Pol. Pharm., 21 (1964) 481.
3 G. J. Patriarche et J. J. Lingane, Anal. Chim. Acta, 49 (1969) 25.
4 G. J. Patriarche et J. J. Lingane, Anal. Chem., 39 (1967) 168.
5 M. Chateau-Gosselin, G. J. Patriarche et G. D. Christian, Z. Anal. Chem., 285 (1977) 373.
6 S. Pinzauti, V. Dal Piaz et E. La Porta, Il Farmaco, Ed. Prat., 29 (1974) 136.
7 J. A. Gautier, F. Pellerin et G. Baylocq, Ann. Pharm. Fr., 24 (1966) 405.
8 J. J. Lingane, Electroanalytical Chemistry, 2nd edn. N-Y Interscience, 1958.
9 G. J. Patriarche et J. J. Lingane, Ann. Pharm. Fr., 28 (1970) 511.
10 M. Chateau-Gosselin et G. J. Patriarche, Mikrochim. Acta, 1 (1977) 265.
11 R. G. Selim, Ph. D. Thesis, Harvard University, U.S.A. (1959).
12 R. G. Selim et J. J. Lingane, Anal. Chim Acta, 21 (1959) 536.
13 J. J. Lingane et D. G. Davis, Anal. Chim. Acta, 15 (1956) 207.
14 M. Chateau-Gosselin et G. J. Patriarche, Analusis, 5 (1977) 310.

Analytica Chimica Acta, 102 (1978) 221—224

Short Communication

PRECONCENTRATION OF GOLD AND TUNGSTEN FROM GEOLOGICAL SAMPLES FOR NEUTRON ACTIVATION ANALYSIS

N. R. DAS and S. N. BHATTACHARYYA*

Nuclear Chemistry Division, Saha Institute of Nuclear Physics 92, Acharya Prafulla Chandra Road, Calcutta-700009 (India)

(Received 6th March 1978)

Although the occurrence of tungsten in gold-bearing veins and of gold in tungsten ores, e.g. scheelite, wolframite etc. is well established [1—4] and their co-existence in ore samples has been studied [5], there is no suitable method for their simultaneous determination in natural samples. Unlike many elements, the abundances of both gold and tungsten in most rocks and minerals are well below the limit of detection of conventional analytical procedures. Neutron activation analysis, (n.a.a.) is one of the most powerful instrumental techniques for multi-elemental analysis of trace concentrations, e.g. tungsten [6—11] and gold [12].

The present investigation deals with the development of a simple and reliable chemical method by which both gold and tungsten can be preconcentrated easily and determined subsequently by n.a.a. The method is applicable to rocks that are soluble in HF—aqua regia. To avoid the effects of undesirable radionuclides produced on irradiation, preconcentration of the desired elements in a non-isotopic solid diluent suitable for activation is desirable. For measurements of the overall recoveries of gold and tungsten, ^{198}Au (2.7 d) and ^{185}W (83 d) were used.

Experimental

Reagents. All reagents were of analytical grade. ^{198}Au in hydrochloric acid and ^{185}W, as sodium tungstate in alkaline medium (BARC, Trombay) were used.

Rock samples. The rock samples studied were of gold-bearing quartz veins [13] from the Kunderkocha and Sausel areas, Shinghbhum District, Bihar.

Dissolution of rock samples. Ca. 10 g of rock (100 mesh) along with the requisite amount of the respective tracer solution (^{198}Au or ^{185}W) was digested twice in a polyethylene beaker with 10 ml of hydrofluoric acid, on a hot water bath, until dryness. The residue was dissolved in aqua regia and evaporated to a paste, which was then treated slowly with concentrated alkali solution, to which ca. 1 g of tartaric or citric acid was added. Then the solution was made strongly acidic with ca. 20 ml of dilute aqua regia solution

and filtered. The filtrates incorporating ^{198}Au and ^{185}W were marked 'A' and 'B', respectively.

Solvent extraction. An aliquot (25 ml) of filtrate 'A' was shaken vigorously in a separating funnel with three 25-ml portions of methyl isobutyl ketone (MIBK), each for ca. 5 min. The aqueous and organic phases were separated. The results (Table 1) show that the ^{198}Au was almost completely extracted into MIBK. It was then back-extracted into 10^{-3} M hydrochloric acid solution for further treatment.

Tungsten was extracted with tri-butylphosphate (TBP) after gold had been separated with MIBK. It was therefore necessary to examine whether any significant amount of tungsten is extracted with the gold. An aliquot (25 ml) of filtrate 'B' was treated with MIBK; the separated aqueous phase was treated with further portions (10 ml) of 12 M hydrochloric acid and then with TBP. Table 1 shows that no significant amount of tungsten is taken up by MIBK, but tungsten is almost quantitatively taken up by TBP. The tungsten in the TBP layer may be back-extracted, as required, into an aqueous phase.

Co-precipitation of ^{198}Au and ^{185}W tracers. Gold-198 was taken up completely and distributed uniformly in lead sulfide precipitated from dilute hydrochloric acid medium [14]. For the recovery of ^{185}W in a similar solid support, the aqueous solution containing ^{185}W was neutralized with ammonia solution and then acidified with dilute acetic acid, to which 10 ml of lead nitrate solution (ca. 1 g) was added. From the hot solution, lead was precipitated with hydrogen sulfide. Co-precipitation of ^{185}W by lead sulfide was quantitative. To verify the distribution of ^{185}W in lead sulfide, different fractions of the precipitate were collected, dried and weighed, and their activities were measured (Fig. 1).

TABLE 1

Solvent extraction of gold with MIBK from solution 'A', and of tungsten with MIBK and TBP from solution 'B' in dilute aqua regia

Samples marked 'A'	^{198}Au (%)		Samples marked 'B'	^{185}W (%)		
	MIBK ext.	Aq. phase		MIBK ext.	TBP ext.	Aq. pha
^{198}Au	98.5	1.5	^{185}W	2.0	97.5	0.5
	99.0	1.0		2.0	97.0	1.0
	98.0	2.0		1.5	97.0	1.5
Rock sample[a] + ^{198}Au	97.0	2.0	Rock sample[a] + ^{185}W	2.0	96.0	1.5
	97.5	1.0		2.5	95.5	1.0
Rock sample[a] + Au (10^{-4} M) + ^{198}Au	97.0	2.0	Rock sample[a]	2.5	95.0	1.0
	96.5	2.5	+ W (10^{-2} M) + ^{185}W	2.0	95.5	1.5

[a]The gold and tungsten contents are 1.8×10^{-5} and 1.8×10^{-6}%, respectively.

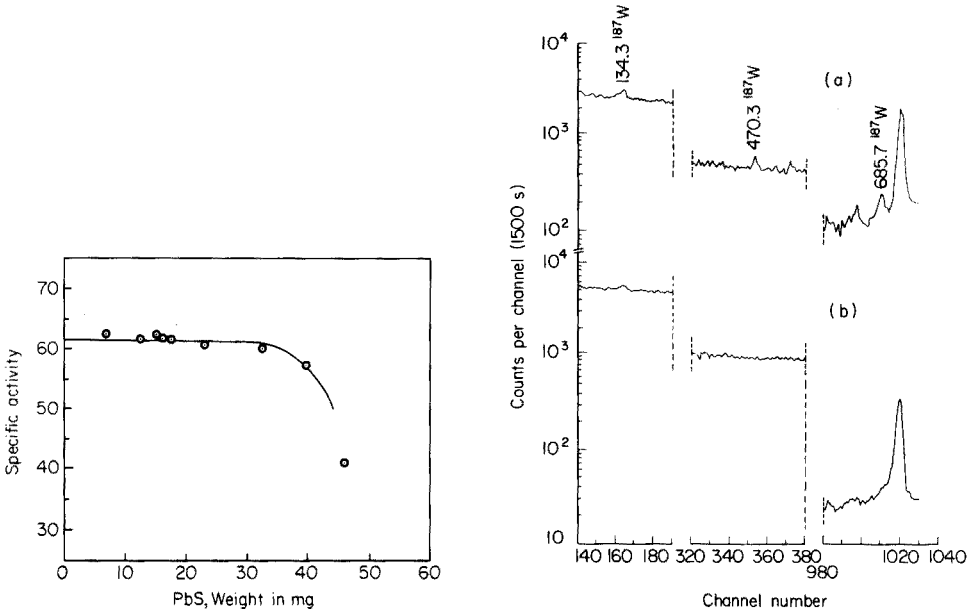

Fig. 1. Distribution of ^{185}W tracer in lead sulfide precipitated from dilute acetic acid medium.

Fig. 2. γ-Spectra of neutron-irradiated mineral samples containing tungsten: (a) 0.75 g of untreated sample; (b) MIBK extract of 10 g of the same sample.

Results and discussion

Although various methods for the decomposition of geological samples are known, digestion of rock samples with hydrofluoric acid and its final dissolution in aqua regia helps to keep the gold in the $HAuCl_4$ state which makes complete extraction into MIBK most favourable [14]. To keep tungsten in solution along with the gold, the procedure described forms a stable complex in alkaline medium with tartaric or citric acid. Gold was then extracted from the acid solution with MIBK; no significant amount of tungsten was taken up, as shown by the γ-spectrum (Fig. 2) of the MIBK extract. No characteristic tungsten peak is evident, although the rock sample contained 1.8×10^{-6}% tungsten. The use of MIBK for partial separation of tungsten from geological samples under different conditions has been described [15, 16].

Extraction of tungsten from hydrochloric acid medium with undiluted TBP has been reported [17, 18]. The extracted species is probably $WO_2Cl_2 \cdot 2$ TBP [18]. Table 1 shows that TBP is a good extractant for tungsten from aqua regia solutions. The extraction of ^{185}W tracer by undiluted TBP becomes complete after hydrochloric acid is added to the aqueous phase left after extraction of gold by MIBK; some hydrochloric acid is extracted by MIBK as $HCl \cdot 5H_2O \cdot 4$MIBK [19] and the efficiency of extraction of tungsten is reduced.

For successful determination by n.a.a., both gold and tungsten require to be preconcentrated in a non-isotopic solid diluent. The uptake of gold by lead sulfide has been reported [14, 20]; the uptake of ^{185}W is quantitative when the precipitation of lead sulfide is carried out from a solution containing ^{185}W in dilute acetic acid medium. Figure 1 shows that the specific activity in different lead sulfide fractions is almost constant over a wide range. The choice of lead sulfide as a solid non-isotopic diluent is well established; undesirable radionuclides are not formed under the experimental conditions during neutron activation.

REFERENCES

1 T. N. Lakshminarayan, Indian Minerals, 26 (1972) 49.
2 I. I. Chetyrbotskoya, V. V. Sakhonenok and L. Ya. Shmuraeva, Mineral Geokhim., Vol'framovykh Mestorozhd, Tr. Vses. Soveshch., 3rd 1971 (Publ. 1975), 393; Chem. Abstr. No. 84: 138504h.
3 G. N. Stepanov, V. M. Kuz'min, D. T. Presich and V. M. Chudinov, Tezisy Dokl. Simp. Mineral Geokhim. Zolota 1, (1974) 96; Chem. Abstr. No. 84: 153246u.
4 V. G. Moiseenko, G. N. Stepanov, M. V. Stepanova and V. M. Chudinov, Tezisy Dokl. Simp. Mineral Geokhim. Zolota, 2, (1974) 46; Chem. Abstr. No. 84: 153419c.
5 G. N. Stepanov, M. V. Stepanova and O. P. Kuryakova, Tezisy Dokl. Simp. Mineral Geokhim. Zolota, 2, (1974) 112; Chem. Asbtr. No. 84: 182472v.
6 H. Zinner, R. Hinkelmann and H. Stark, J. Radioanal. Chem., 16 (1973) 31.
7 R. A. Nadkarni and B. C. Haldar, J. Radioanal. Chem., 8 (1971) 45.
8 D. H. F. Atkins and A. A. Smales, Anal. Chim. Acta, 22 (1960) 462.
9 R. Bachman and C. V. Banks, Anal. Chem., 43 (1971) 120R.
10 F. A. Simon and C. L. Rollinson, J. Res. U.S. Geol. Surv., 3 (1975) 475.
11 O. Johnansen and E. Steinnes, J. Radioanal. Chem., 17 (1970) 407.
12 A. Chow and F. E. Beamish, Talanta, 14 (1967) 219.
13 N. R. Das, P. S. Chakraborty and S. N. Bhattacharyya, J. Radioanal. Chem., 34 (1976) 249.
14 N. R. Das and S. N. Bhattacharyya, Talanta, 21 (1974) 894.
15 G. W. C. Milner, G. A. Barnett and A. A. Smales, Analyst, 80 (1955) 380.
16 C. H. Kim, P. W. Alexander and L. E. Smythe, Talanta, 23 (1976) 573.
17 V. Pfeifer, Mikrochim. Acta, (1960) 518.
18 A. K. De and M. S. Rahaman, Talanta, 11 (1964) 601.
19 H. M. Widmer, J. Phys. Chem., 74 (1970) 3251.
20 P. Schiller and G. B. Cook, Nuclear Techniques for Mineral Exploration and Exploitation, Vienna, IAEA, 1971, pp. 137—142.

Analytica Chimica Acta, 102 (1978) 225—228

Short Communication

THE SORPTION CHARACTERISTICS OF RADIONUCLIDES ON COPPER HEXACYANOFERRATE(II), AND THE DETERMINATION OF ^{137}Cs IN SEA WATER

SHOICHI KAWAMURA*, SADAO SHIBATA, KATSUMI KUROTAKI and HIROSHI TAKESHITA

Chemistry Division, National Institute of Radiological Sciences, 9-1, 4-Chome, Anagawa, Chiba-shi (Japan)

(Received 30th March 1978)

The chemical properties and sorption characteristics of the hexacyanoferrate(II) of many metals have been investigated by many workers [1—14]. The adsorption and ion-exchange behavior of zinc hexacyanoferrate(II) depends on the ratio of the starting materials [4, 13]. In order to confirm such effects, different ratios of copper nitrate and sodium hexacyanoferrate(II) were mixed and analysis of the products showed their composition to be either $Cu_2Fe(CN)_6$ or $Na_2CuFe(CN)_6$.

The present communication reports the relationship between the ratios of copper nitrate and sodium hexacyanoferrate(II) taken, the relative sorption rates of cesium from aqueous solutions with or without the addition of hydrochloric acid, the atomic ratio of sorbed cesium to released copper and sodium, the distribution coefficients of radionuclides in concentrated salt solutions, and a simple and rapid determination of ^{137}Cs in sea water containing ^{59}Fe, ^{60}Co, ^{65}Zn, ^{85}Sr, ^{95}Zr, ^{106}Ru and ^{144}Ce.

Experimental

Preparation of copper hexacyanoferrate(II) analogues. All reagents used were of analytical grade. The copper hexacyanoferrate(II) analogues were prepared by mixing 0.1 M sodium hexacyanoferrate(II) (200—300 ml) and 0.1 M copper nitrate in the ratios 1:10, 1:3, 1:2, 1:1 and 1:0.1. The brown slurries obtained by adding these solutions dropwise to a beaker during 30 min while stirring, were heated with stirring on a boiling water bath for 2 h, allowed to stand for 24 h, filtered or centrifuged, washed thoroughly, and dried at room temperature. Slurries other than that given by the 1:10 ratio were finely dispersed, and were centrifuged for 15 min at 3000 G. Products labelled with ^{22}Na were prepared by the same procedure.

Relative sorption rates and batch distribution coefficient. The relative sorption rates for cesium were determined by mixing 0.1 g of the copper

hexacyanoferrate(II) analogues with 5 ml of a cesium chloride solution labelled with ^{137}Cs (0.01 μCi ml^{-1}) followed by centrifugation at 8000 G for 1 min. The activity of the supernatant solution was measured by a well-type scintillation counter. Distribution coefficients, K_d(ml g^{-1}), for the radionuclides were determined by equilibrating 0.1 g of the analogues with 5 ml of an aqueous solution containing the radionuclides, followed by the same treatment as described for the determination of the relative sorption rates.

Measurement of the Cu—Cs or Na—Cs exchange ratio. Exchanges of Cu—Cs (or Na—Cs) were studied by shaking 5 g of the copper hexacyanoferrate(II) (or the ^{22}Na-labelled) analogue with 100 ml of a ^{137}Cs-labelled cesium chloride solution. After equilibrium had been attained, the mixture was centrifuged, and cesium (or sodium) or copper in the supernates was determined by activity measurement or EDTA titration, respectively. The Cu—Cs or Na—Cs exchange ratio was calculated from the ratio of the amounts of cesium adsorbed to those of copper (or ^{22}Na) released. The amounts of copper or sodium released into the aqueous phase, and the amount of cesium taken up, were obtained by the ^{137}Cs decrease and the copper (or ^{22}Na) increase in the aqueous phase, respectively.

Determination of copper, hexacyanoferrate(II), and sodium. Copper hexacyanoferrate(II) (or ^{22}Na-labelled $Na_2CuFe(CN)_6$) was decomposed by heating with concentrated sulfuric acid and dissolving in 8 M hydrochloric acid, followed by evaporation to dryness. A large portion of the iron in the hydrochloric acid solution was extracted with isopropyl ether saturated with 8 M hydrochloric acid, and evaporated to dryness. After hydrochloric acid was added to give the 8 M solution, the solution was passed through a Bio-Rad AG-X1 column, and the copper (or sodium) and the iron in the hexacyanoferrate(II) were separated by the method of Kraus and Moore [15]. The copper or the iron was determined titrimetrically with EDTA; sodium was determined by the ^{22}Na activity.

Results and discussion

Relationship between mixing ratio and composition. Possible differences in the stoichiometric composition of the resulting copper hexacyanoferrate(II) analogues were checked by varying the mixing ratios of 0.1 M sodium hexacyanoferrate(II) and 0.1 M copper nitrate. The products resulting from the 1:10, 1:3, 1:2 and 1:1 ratios are best represented as $Cu_2Fe(CN)_6$, and that given by the 1:0.1 ratio as $Na_2CuFe(CN)_6$. The x-ray diffraction patterns of the 1:10, 1:3, 1:2 and 1:1 ratios were all identical and different from that given by the 1:0.1 ratio. This supports the two independent chemical formulae Unlike $Na_2CuFe(CN)_6$, $Cu_2Fe(CN)_6$ was easily prepared because of its rapid precipitation. Study of the sorption characteristics was confined to the $Cu_2Fe(CN)_6$.

Relative sorption rate of ^{137}Cs and the Cu—Cs or Na—Cs exchange ratio. The relative sorption rates of ^{137}Cs, or of 10^{-3} M cesium chloride tagged with ^{137}Cs, on $Cu_2Fe(CN)_6$ were determined by varying the shaking time with 0.1 M

hydrochloric acid, water and sea water, respectively. The sorption of cesium was quite rapid; shaking for 10 min gave quantitative sorption. Although quantitative recoveries were not obtained in all cases, many repeated experiments confirmed the rapid sorption equilibrium. In the absence of a mineral acid, such rapid sorption of cesium is rarely observed on the hexacyanoferrate(II) salts of common metals, and the cause of the rapid sorption on $Cu_2Fe(CN)_6$ is obscure.

The exchange of elements for cesium in the external solution was determined by batch experiments. With 10^{-2} or 10^{-3} M cesium chloride and $Cu_2Fe(CN)_6$, the atomic ratio of sorbed cesium to copper released from the $Cu_2Fe(CN)_6$ was 2:1, thus the cesium sorption is controlled by an ion-exchange mechanism. With 10^{-1} M cesium chloride, the ratio of sorbed cesium to released copper was 3:1 which indicates that adsorption of cesium and ion-exchange both occur. The ratio of sorbed cesium to released sodium on $Na_2CuFe(CN)_6$ was determined by the same procedure as for $Cu_2Fe(CN)_6$. With 10^{-3} M cesium chloride, no copper was found in the external solution, which indicates that ion-exchange does not take place between the copper in $Na_2CuFe(CN)_6$ and cesium. The ratio of sorbed cesium to released sodium is 1:1, i.e. ion exchange takes place between the sodium in $Na_2CuFe(CN)_6$ and cesium. However, with 10^{-1} and 10^{-2} M cesium chloride, the ratios of sorbed cesium to released sodium were 8:1 and 6:1, respectively. The sorption therefore involves a retention other than an ion-exchange process; such a retention of cesium has also been observed with zinc or nickel hexacyanoferrate(II) analogues [4, 13].

Relative sorption rates of radionuclides on $Cu_2Fe(CN)_6$. The relative sorption rates of ^{59}Fe, ^{60}Co, ^{65}Zn, ^{85}Sr, ^{95}Zr and ^{144}Ce, with or without the addition of carriers, on $Cu_2Fe(CN)_6$ were determined by shaking with 0.1 M hydrochloric acid. Figure 1 shows that these metal ions are sorbed to some extent. Their

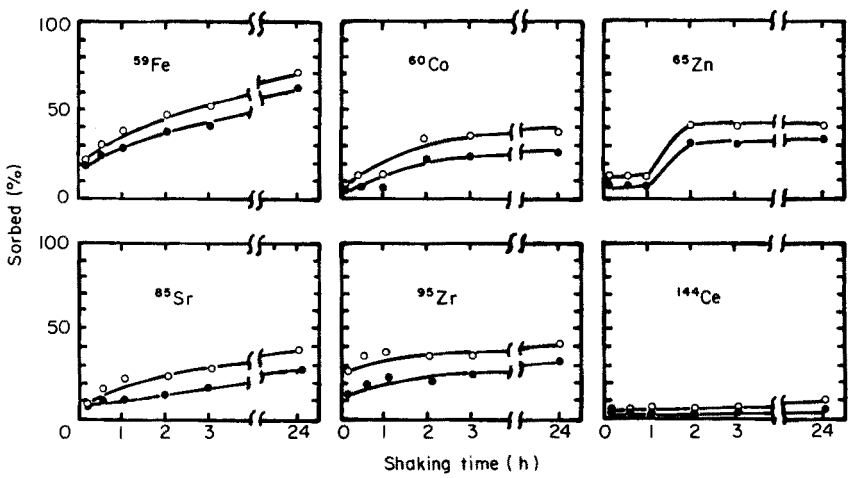

Fig. 1. Relative sorption rates on $Cu_2Fe(CN)_6$. (○) Without carrier, (●) with 10^{-3} M solution.

sorption rates are slow in comparison with that of cesium. The sorption of cerium is extremely low, as is commonly observed on metal hexacyanoferrate(II) salts. The % sorptions of radionuclides, other than cesium, on $Cu_2Fe(CN)_6$ are in general lower than on $Ni_2Fe(CN)_6$ [13].

Determination of ^{137}Cs in sea water containing ^{59}Fe, ^{60}Co, ^{65}Zn, ^{85}Sr, ^{95}Zr, ^{106}Ru and ^{144}Ce. A one-step selective sorption procedure for the γ-emitter ^{137}Cs in sea water containing several radionuclides provides a very simple and rapid analytical method. Accordingly, the feasibility of a selective chromatographic sorption of ^{137}Cs on a $Cu_2Fe(CN)_6$ column was examined by passing sea water containing ^{59}Fe, ^{60}Co, ^{65}Zn, ^{85}Sr, ^{95}Zr, ^{106}Ru, ^{137}Cs and ^{144}Ce and EDTA. These radionuclides, other than cesium, form complexes with the added EDTA. ^{137}Cs is selectively sorbed by the $Cu_2Fe(CN)_6$; the other complexed radionuclides are not sorbed.

Sea water (1 l) adjusted to 0.1 M in hydrochloric acid) was spiked with ^{59}Fe, ^{60}Co, ^{65}Zn, ^{85}Sr, ^{95}Zr, ^{106}Ru, ^{137}Cs and ^{144}Ce (each 1 μCi) and 4 g of Na_4EDTA was added. After the resulting solution was passed through the $Cu_2Fe(CN)_6$ column (20—30 mesh, 7 g, 1.4 × 4.5 cm) at a flow rate of 1 l h^{-1}, the $Cu_2Fe(CN)_6$ packing was transferred to a beaker, to which was added 50 ml of 25% Na_4EDTA solution. After heating for 10 min, the solution was transferred to a polyethylene test tube. The γ-activities were measured on a well-type Ge(Li) detector couple with a 1024-channel pulse-height analyzer. ^{137}Cs was shown to be quantitatively recovered; the activities of ^{59}Fe, ^{60}Co, ^{65}Zn, ^{95}Zr, and the other elements were 4, 1, 2, 1, and less than 1%, respectively. The use of copper hexacyanoferrate(II) for the extraction of ^{137}Cs from sea water is well known [16, 17].

REFERENCES

1 S. Krawczynski and B. Kanellakopulos, Atomkernergie, 6 (1961) 214.
2 G. J. Mohanrao and T. R. Folsom, Analyst, 88 (1963) 105.
3 S. Kawamura, K. Kurotaki and M. Izawa, Bull. Chem. Soc. Jpn., 42 (1969) 3003.
4 S. Kawamura, H. Kuraku and K. Kurotaki, Anal. Chim. Acta, 49 (1970) 317.
5 K. Watari, J. At. Energy Soc. Jpn., 12 (1970) 718.
6 V. V. Vol'khin, E. A. Shul'ga and M. V. Zil'berman, Izv. Akad. Nauk SSSR, Neorg. Mater, 7 (1971) 77; Chem. Abstr., 74 (1971) 91594 p.
7 V. V. Vol'khin and E. A. Shul'ga, Redk. Shchelochnye. Elem., (1969) 352; Chem. Abstr., 74 (1971) 130788b.
8 J. B. Ayers and W. H. Waggoner, J. Inorg. Nucl. Chem., 33 (1971) 721.
9 V. V. Vol'khin, S. A. Kolesova, M. V. Zil'berman and S. A. Onorin, Zh. Neorg. Khim., 16 (1971) 1611; Chem. Abstr., 75 (1971) 53663y.
10 V. Veselý and V. Pekárek, Talanta, 19 (1972) 219, 1245.
11 S. Kawamura, S. Shibata and K. Kurotaki, Anal. Chim. Acta, 56 (1971) 405 and references therein.
12 M. T. Ganzerli Valentini, S. Meloni and V. Maxia, J. Inorg. Nucl. Chem., 34 (1972) 1427
13 S. Kawamura, S. Shibata and K. Kurotaki, Anal. Chim. Acta, 81 (1976) 91.
14 S. Vlasselaer, W. D'olieslager and M. D'hont, J. Radioanal. Chem., 35 (1977) 211.
15 K. A. Kraus and G. E. Moore, J. Am. Chem. Soc., 72 (1950) 5792, 75 (1953) 1460.
16 T. R. S. Wilson, Nature, 248 (1974) 125.
17 J. W. R. Dutton and N. T. Mitchell in J. P. Riley and G. Skirrow (Eds.), Chemical oceanography, Vol. 3, Academic Press, 1975, pp. 450—451.

Analytica Chimica Acta, 102 (1978) 229—231

Short Communication

DETERMINATION OF "TOTAL" CHLOROPHENOLS IN A BRINE BY A MODIFIED 4-AMINOANTIPYRINE TEST AFTER COLUMN CLEANUP

T. RAMSTAD* and D. N. ARMENTROUT
Dow Chemical U.S.A., Midland, Michigan 48640 (U.S.A.)
(Received 10th April 1978)

The determination of phenols in aqueous matrices by reaction with 4-aminoantipyrine (4-AAP) is widely used in situations where a total phenols value is desired [1, 2]. As an alternative to sample cleanup by distillation or extraction, a procedure which utilizes selective column adsorption of chlorophenols from an aqueous sample on XAD-2 macroreticular resin has been developed. After an aqueous wash of the resin column to remove salt completely, the phenols are eluted with alkaline methanol and determined by a modified form of the 4-AAP test. The test, calibrated in terms of 2,4,5-trichlorophenol, was applicable from 0.1 to over 2.0 mg l^{-1} total phenols. Amberlite XAD-2 resin was preferred to other possible adsorbents, including charcoal, and to reversed liquid chromatography phases because of the extensive documentation of its adsorption and elution characteristics [3, 4].

Experimental

"Purified" XAD-2 resin (Applied Science Laboratories, Inc.), sieved to produce a 25—40 mesh cut, was Soxhlet-extracted in methanol for 2 days. This resulted in a smaller absorbance for the blank and improved the flow characteristics of the resin. Thick-walled glass tubes (5.1-cm long, 1.1-cm i.d.) were dry-packed with the Soxhlet-extracted resin. Sample and reagents were pumped through the tubes with a Model 351 Sage syringe pump. Photometric measurements were made on a Bausch-Lomb Spectronic 88 Spectrophotometer.

Phenol-free water, obtained by passing demineralized or distilled water through an activated carbon bed, was used.

Buffer pH 7.8. Into a 2-l volumetric flask, add 172.0 ml of 1 M KH_2PO_4 and fill to the mark with 1 M K_2HPO_4.

2,4,5-Trichlorophenol standard (1 mg l^{-1}). Prepare a stock solution (500 mg l^{-1}) by weighing 50 mg of TCP into a 100-ml volumetric flask, adding 2—3 ml of methanol, and diluting to the mark with water. Refrigerate. This solution need be no more than 3% in methanol. For the working solution, pipet 2.0 ml of stock solution into a 1-l volumetric flask and fill nearly to the mark with water. Adjust to pH 4 with (1 + 9) phosphoric acid. Dilute to the mark with water. Refrigerate in a glass bottle.

Procedure. Blanks, standards and samples are processed separately. For the blank, pass 35 ml of water, with a 50-ml syringe, through the adsorption tube at a flow rate of 15 ml min^{-1}. Reverse the column. With a 10-ml syringe, pass 10 ml of 0.01 M NaOH in methanol through the tube at 4 ml min^{-1}, and collect in a 50-ml volumetric flask. Dry the tube by applying suction. To the 50-ml flask, add 10 ml of water, 20 ml of phosphate buffer pH 7.8, 2 ml of 4-AAP solution (aqueous 0.5% w/v, stored in an amber bottle), 1 ml of $K_3Fe(CN)_6$ solution (aqueous 2.0% w/v, stored in an amber bottle) with shaking after each addition. Dilute to the mark with water, allow to stand for 10 min in the dark (fading begins after 15 min), and measure the absorbance in a 10-cm cell at 500 nm against a water reference.

For the standard (1 mg ml^{-1}), pass 35 ml of water at 15 ml min^{-1} to remove residual methanol. Pass 25 ml of standard at 15 ml min^{-1}. Pass 35 ml of water at 15 ml min^{-1} to remove salt if the sample was a brine and to wash out acid. Then reverse the column, pass 0.01 M NaOH in methanol and continue the procedure described for the blank. Read the absorbance against the blank.

For samples, adjust the pH to 4.0 ± 0.2 with (1 + 9) phosphoric acid. Then continue the analysis as described for the standard, passing 25 ml of sample. The concentration of phenols is calculated from: $(A_{sample}-A_{blank})/(A_{standard}-A_{blank}) \times 1$ mg l^{-1}.

RESULTS AND DISCUSSION

The foregoing procedure was evaluated by comparing the results (Table 1) obtained for six industrial brine samples with the results obtained by liquid chromatography with an electrochemical detector (l.c.—e.c.) which is considered to be the reference technique. L.c. provided quantitation of each component; a total phenols figure, calculated as TCP, is obtained by the XAD-2/4-AAP technique. L.c. showed TCP to be the major constituent in each sample, but phenol, *p*-chlorophenol, 2,5-dichlorophenol, and 2,4-dichloro-5-methoxyphenol were also present. Direct comparison of the methods is thus not possible.

TABLE 1

Comparison of results given by the XAD-2/4-AAP and l.c.—e.c. methods

Sample	XAD-2/4-AAP (μg ml^{-1})	L.c.—e.c. (μg ml^{-1})
1	0.08	0.09
2	0.30	0.37
3	0.35	0.34
4	0.42	0.34
5	0.28	0.34
6	0.58	0.46

Fortifying a relatively clean sample with various amounts of TCP showed virtually complete recovery. The reproducibility of the procedure may be gauged from the absorbances obtained for a 1 mg l^{-1} standard processed four times: 0.443, 0.456, 0.430, and 0.440 (s.d. 0.01).

The recovery of TCP under the conditions described was greater than 95%. The slight loss resulted from incomplete adsorption on XAD-2 and not from incomplete elution with caustic methanol. Although lowering the pH below 4.0 may result in a higher recovery, the cleanup becomes less selective, and interferences may result.

Each time the solvent was switched from water to methanol and vice versa, air bubbles formed in the XAD column. With a short column (5 cm long), the possibility of channelling occurring with time could not be ignored. Application of vacuum to the column to volatilize methanol prior to reintroducing water eliminated this problem.

In this procedure the 4-AAP test is performed in the presence of methanol, which decreases the intensity of color formation. The absorbance of the TCP-antipyrine product increases with decreasing pH. A pH of 7.8 was selected to avoid the self-condensation of 4-AAP to form "red antipyrine" at lower pH. At pH 10, where a strong absorbance is observed for phenol, there is essentially no response for trichlorophenol. The absorbance vs. concentration of the phenol—4-AAP product at pH 7.8 is linear from 0.1 to over 2 mg l^{-1} TCP.

The authors gratefully acknowledge the contributions of J. Ulrich to this work.

REFERENCES

1 Standard Methods for the Examination of Water and Wastewater, 14th edn., 1976, p. 574.
2 ASTM Annual Standards, Part 31, 1976, p. 553.
3 G. A. Junk, J. J. Richard, M. D. Grieser, D. Witiak, J. L. Witiak, M. D. Arguello, R. Vick, H. J. Svec, J. S. Fritz and G. V. Calder, J. Chromatogr., 99 (1974) 745.
4 G. A. Junk, J. J. Richard, J. S. Fritz and H. J. Svec, Resin Sorption Methods for Monitoring Selected Contaminants in Water, in L. H. Keith (Ed.), Identification and Analysis of Organic Pollutants in Water, Ann Arbor Science Publishers, Ann Arbor, Michigan, 1976, pp. 135—153.

Analytica Chimica Acta, 102 (1978) 233—236

Short Communication

AUTOMATIC THERMOMETRIC ANALYSIS FOR CAUSTIC SODA AND ALUMINA IN BAYER LIQUORS

R. MAGRONE, R. JEAN and P. SACCONE

Aluminium Pechiney, Centre de l'Alumine, 13120 Gardanne (France)

R. WEBER*

Technicon International Division S.A., 12—14 Chemin Rieu, 1208 Geneva (Switzerland)

(Received 7th December 1977)

In the production of aluminium by the Bayer process, the concentration of caustic soda (30—250 g l^{-1} as Na_2O) and alumina (15—300 g l^{-1} as Al_2O_3) must be known accurately at several points in the manufacturing circuit. The analysis requires 30 min for a competent technician and in an average plant 30—50 analyses per day are the minimum required. As the samples tend to precipitate on cooling to room temperature, the analyses should be performed as soon as possible after the sample collection. Furthermore, rapid return of results to the factory improves manufacturing efficiency. For these reasons, the analyses were automated by means of the recently described Technicon Thermometric Analyzer [1, 2].

Caustic soda is determined by its heat of neutralization when titrated with sodium hydrogencarbonate (9 kcal mol^{-1}). Aluminium is complexed with tartrate to avoid precipitation and to release completely the caustic soda. "Caustic soda" is defined as the sum of free sodium hydroxide and that combined with alumina. The content expressed as caustic Na_2O in g l^{-1} therefore excludes carbonates, sulphates, vanadates, phosphates, chlorides, etc.

Alumina is determined by its heat of reaction on complexing with sodium tartrate (5—7 kcal mol^{-1} Al_2O_3).

Experimental

Equipment. A Technicon (TA-2) Thermometric Analyzer was used with the flow system shown in Figs. 1 and 2. The TA-2 differs from the Thermometric Analyzer TA-1 in that a refrigeration unit is now employed in place of the tap water cooling. This change has resulted in a significant increase in long-term stability.

Samples. Where samples contain excessive particulate matter, they are filtered through filter paper or centrifuged. If the concentration of Na_2O exceeds 200 g l^{-1}, samples should be diluted 1:1 with water to facilitate filtration when necessary.

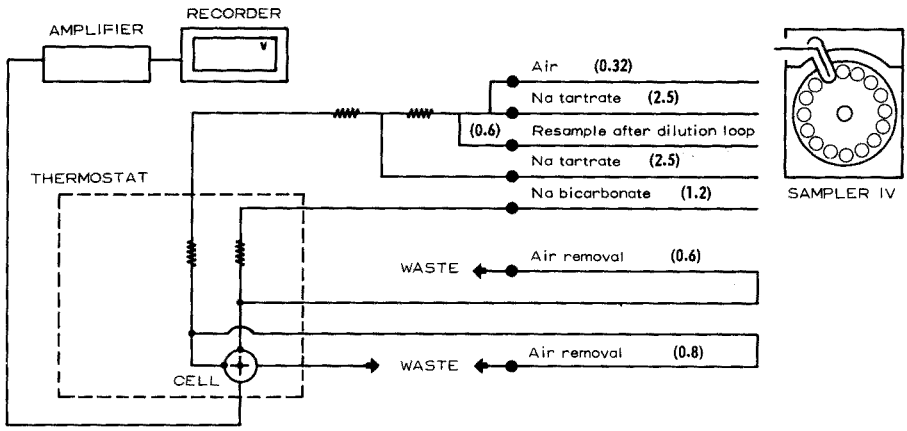

Fig. 1. Flow diagram for the determination of sodium hydroxide. (Figures in parentheses represent flow rates of pump tubes in ml min^{-1}). The dilution loop dilutes the sample 10 times. Sodium tartrate solution is 23% (w/v). Sodium hydrogencarbonate solution is 6.3% (w/v).

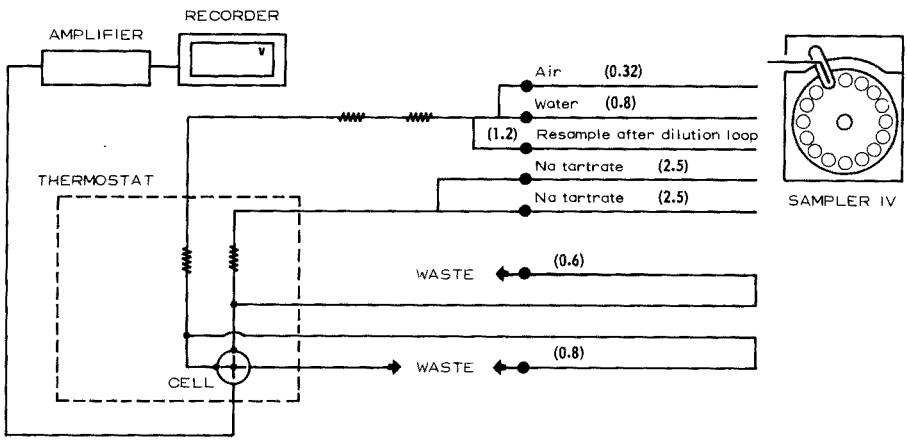

Fig. 2. Flow diagram for the determination of alumina. (Figures in parentheses represent flow rates of pump tubes in ml min^{-1}). The dilution loop dilutes the sample 10 times. Sodium tartrate solution is 23% (w/v).

Calibration

The first step in calibration was to fix an instrument sensitivity (recorder chart division/°C) corresponding to the concentration of soda and alumina in Bayer liquors. Bayer liquor on standing precipitates salts, is unstable and hence is not suitable as a calibration solution.

Experimentally, it was found that an aqueous solution of Na_2O (171 g l^{-1}) and diluted H_2SO_4 (780 g l^{-1}; density, 1.84) used as samples in the determinations of caustic and aluminium, respectively, gave instrument responses corresponding to the upper concentration limits of these substances (170 g l^{-1}

for Na_2O and 170 g l^{-1} for Al_2O_3). With these concentrations of sodium hydroxide and sulphuric acid, recorder readings were set arbitrarily at 90 divisions.

Three samples with Al_2O_3/Na_2O concentration ratios of approximately 1.15, 1.05 and 0.6 were then analyzed manually by reference methods (acid titration for Na_2O and oxinate gravimetry for alumina [3]) daily for at least 10 days. These solutions were diluted with equal volumes and with 3 volumes of water, and the undiluted and diluted samples were analyzed daily on the Thermometric Analyzer over 2 working weeks, so that 90 results were obtained for each substance, caustic and alumina.

Standard methods of regression analysis applied to these results gave the equations

$$Na_2O \text{ (caustic) (g } l^{-1}) = 1.854X + 0.043Y + 2.08 \quad (1)$$

$$Al_2O_3 \quad (\text{g } l^{-1}) = 2.025Y - 0.136X - 0.66 \quad (2)$$

where X and Y are the peak heights for the caustic and alumina determination respectively, when the instrument sensitivity was set to 90 divisions for the caustic and sulphuric acid calibration solutions.

Normal instrument operation would require the instrumental sensitivity to be adjusted before each group of analyses or, at any rate, at set intervals to compensate for normal instrumental fluctuations. Even with skilled staff, the adjustment of the instrument is time-consuming. Where a laboratory is manned by only skeleton crews for 16 h/day, it has been found that a mathematical correction for changes of sensitivity is, overall, the most efficient analytical procedure when the normal staff are not on duty. An obvious prerequisite for mathematical correction of sensitivity changes is long-term instrument stability. Over 5 days (Table 1) the maximum variation in sensitivity, on one day, was 15%.

Data obtained in a typical run are given in Table 2; the peaks are adjusted to the standard sensitivity (90 divisions) by

$$X\ (Na_2O) = [(\text{Sample}_x - \text{Base}_x)/(\text{Standard}_x - \text{Base}_x)] \times 90 = 86.2 \text{ divisions}$$

$$Y\ (Al_2O_3) = [(\text{Sample}_y - \text{Base}_y)/(\text{Standard}_y - \text{Base}_y)] \times 90 = 52.4 \text{ divisions}$$

Substitution of X and Y into eqns. (1) and (2) then gives 164.1 g l^{-1} for Na_2O and 93.5 g l^{-1} for Al_2O_3. Comparison of the results obtained for 300 samples over 4 months on the Thermometric Analyzer with manual analyses

TABLE 1

Variations in sensitivity over 5 days

Day	1	2	3	4	5
Base[a]	0	2	0	5	−2
Standard[a]	90	92	96	83	94

[a]Chart divisions.

TABLE 2

Data used to illustrate the calibration method

	Na_2O (x)	Al_2O_3 (y)
Standard	88.7	93.3
Base	1.0	0.5
Sample	85.0	54.6

as indicated above gave correlation coefficients of 0.99986 (r.s.d. 0.4%) for Na_2O and 0.99976 (r.s.d. 0.6%) for Al_2O_3. Once the instrument has been calibrated, 10—20 samples per hour can be analyzed with a precision better than 1%.

The precision of the technique for Al_2O_3 is being further improved by using two thermometric cells for the simultaneous determination of Al_2O_3 and Na_2O. As Bayer solutions are unstable, the advantages of simultaneous determinations are obvious from eqn. (2) above. Further, for the manufacture of aluminium oxide, the ratio of alumina to caustic is the important parameter. By simultaneous measurements, minor variations in the thermostat temperature will tend to cancel out in the ratio.

REFERENCES

1 F. Hagedorn, G. Peuschel and R. Weber, Analyst, 100 (1975) 810.
2 R. Weber, G. Blanc, G. Peuschel and F. Hagedorn, Anal. Chim. Acta, 86 (1976) 79.
3 M. Jamey and R. Magrone, Analyse des Liqueurs d'Aluminate, XXIème Congrès International de Chimie Pure et Appliquée, Prague, Czechoslovakia 1967.

Analytica Chimica Acta, 102 (1978) 237—240

Short Communication

DIALKYL SULPHITES AS GRAVIMETRIC REAGENTS FOR GOLD BY PRECIPITATION FROM HOMOGENEOUS SOLUTION

S. C. SOUNDAR RAJAN and N. APPALA RAJU*

Department of Chemistry, Sri Venkateswara University, Tirupati-517502 (India)

(Received 15th January 1978)

Except for the case of ethylene glycol, there is no record of a procedure for precipitation from homogeneous solution which involves production of a reducing agent. Ethylene glycol, produced by hydrolysis of 2-hydroxyethyl acetate or ethylene diacetate, reduces periodate to iodate which serves to precipitate thorium or iron as iodates [1, 2]. The present communication describes two new reagents, dimethyl sulphite and diethyl sulphite, as homogeneous precipitants; sulphur dioxide is formed, and a superior separation of gold can be achieved.

Experimental

Gold chloride solution. Pure gold wire (1 g) was dissolved in aqua regia, 1 g of sodium chloride was added and the solution was evaporated on a water bath to near dryness. The evaporation was repeated thrice with additions of 1 ml of concentrated hydrochloric acid to expel nitrogen oxides. The solution was diluted to exactly 1 l with adjustment of the acidity to 0.1 M in hydrochloric acid. The gold content was further checked by standardization with hydroquinone [3].

Alkyl sulphite reagents. Dimethyl sulphite and diethyl sulphite (E. Merck, Darmstadt) were used as supplied.

Preliminary investigations. The reagents were not completely miscible with aqueous solutions, hence semi-alcoholic solutions were employed. Precipitation was satisfactory from solutions containing 25—40% (v/v) alcohol. At lower concentrations, the reagent remained immiscible and at higher concentrations (>70%), the gold particles adhered tenaciously to the beaker wall. Solutions which were 0.4—0.7 M with respect to hydrochloric acid yielded an easily filterable precipitate. Though 0.8 ml of dimethyl sulphite and 1.0 ml of diethyl sulphite should produce sufficient sulphur dioxide to reduce 100 mg of gold (III), it was found that a minimum of 1 ml of the ester had to be added even for smaller amounts of gold in order to obtain a precipitate which settled properly and was easily transferred. However, when 2 ml of the ester were added, the precipitated gold remained colloidal even after digestion for 1 h.

Procedure. To an aliquot of gold solution, add 4—7 ml of concentrated hydrochloric acid and 25—40 ml of alcohol (methanol or ethanol), and dilute the solution to ca. 100 ml. Then add 1.0—1.5 ml of the ester and stir gently. Allow to stand, covered, at room temperature until the yellow colour disappears and gold starts to precipitate; this usually takes about 15 min. Place on a hot water bath for about 40 min with occasional stirring. Metallic gold gradually separates and settles; losses of solution by evaporation are not made up. Filter the supernatant liquid through a Whatman No. 42 (9 cm) filter paper, and transfer the precipitate to the paper with water. Transfer any particles sticking to the beaker to the filter with small pieces of ashless filter paper. Wash the precipitate with about 100 ml of 1% (v/v) hydrochloric acid, dry, ignite at about 800°C in a silica crucible and weigh as the metal.

The results obtained showed that gold could be quantitatively precipitated by the use of the dialkyl sulphites; recoveries of 26.0—97.6 mg of gold were good (cf. Table 1)

Effects of other ions

Co-precipitation of platinum. Sulphur dioxide was one of the earliest reagents employed for the precipitation of gold. Beamish et al. [3] critically compared this reagent with hydroquinone; sulphur dioxide is easily expelled from solutions, and is therefore preferable to hydroquinone when subsequent analyses of the filtrate are required, but significant amounts of platinum are co-precipitated with gold when sulphur dioxide is used. The data of Beamish et al. [1] are inconclusive on this point, and further experiments to define the extent of co-precipitation of platinum were therefore carried out here. The following procedure was adopted because of the small amounts of platinum involved.

Gold was precipitated from solutions containing known amounts of gold and platinum, with dimethyl or diethyl sulphite and with sulphur dioxide [4]. The precipitated gold was separated by using IG-4 filter sticks, and the precipitate was washed similarly with 100 ml of 1% (v/v) HCl solution. Gold in the beaker and on the filter stick was dissolved in the minimum amount of

TABLE 1

Co-precipitation of platinum with gold

Au taken (mg)	Pt added (mg)	Pt co-precipitated (mg)[a]		
		SO_2	DMS	DES
12.0	24.1	0.10, 0.11	0.02, 0.03	0.01, 0.01
12.0	33.9	0.12, 0.10	0.02, 0.03	0.02, 0.02
30.0	24.1	0.20, 0.18	0.05, 0.04	0.02, 0.03
30.0	33.9	0.20, 0.19	0.06, 0.05	0.02, 0.03
30.0	52.0	0.48, 0.39	0.07, 0.06	0.04, 0.05

[a] Duplicate results are given.

aqua regia, the solution was evaporated to near dryness after adding a drop of saturated sodium chloride solution, and the evaporation was repeated twice with addition of a few drops of 11 M HCl. The final residue was extracted five times with 2-ml portions of 10% (v/v) HCl, and the solution was transferred to a 15-ml separatory funnel (constructed from a centrifuge tube, a tap and a ground-glass stopper). The solution was shaken with 5 ml of ethyl acetate; after phase separation, the upper organic phase containing the gold was removed with a capillary dropper until a ca. 5-mm layer remained. This process was repeated 5 or 6 times to ensure complete extraction of gold; tests showed that 3 or 4 extractions sufficed. Finally, the aqueous phase was filtered into a 50-ml calibrated flask through a small wet filter paper (no. 40). This unconventional procedure of phase separation was adopted in order to avoid transference of the aqueous phase and consequent losses of platinum. Platinum from the aqueous portion was determined spectrophotometrically with tin(II) chloride [5]. Table 1 shows that the co-precipitation of platinum is considerably decreased by using precipitation from homogeneous solution.

Effect of tellurium and selenium. Earlier reports on the use of sulphur dioxide as a precipitant for gold indicate that the gold solution must be free of tellurium and selenium, because they are also reduced to the element [4]. The extent of their interference was therefore examined. Different aliquots of tellurium(IV) chloride and selenous acid solutions were added to an aliquot of standard gold solution, and gold was determined by the dimethyl sulphite and sulphur dioxide [4] methods. Tellurium was quantitatively precipitated in both procedures. Most of the tellurium volatilized during the ignition stage, but the final weights showed that significant amounts remained with the gold. In contrast, only part of the selenium was precipitated along with gold, and this volatilized during the ignition. Thus gold can be determined when small amounts of selenium are present (Table 2); the amounts of selenium retained in the dimethyl sulphite procedure are, however, slightly

TABLE 2

Effect of tellurium and selenium on the determination of gold by the sulphur dioxide and dimethyl sulphite methods

Au taken (mg)	Se or Te added (mg)	Au recovered (mg)		Error (mg)	
		DMS	SO_2	DMS	SO_2
28.9	55.0 Te	30.3	30.9	+1.4	+2.0
28.9	27.5 Te	30.0	29.8	+1.1	+0.9
20.6	50.0 Se	20.7	20.6	+0.1	0.0
20.6	75.0 Se	20.7	20.7	+0.1	+0.1
30.1	37.5 Se	30.0	30.1	−0.1	0.0
30.1	50.0 Se	30.1	30.0	0.0	−0.1
30.1	75.0 Se	30.2	30.2	+0.1	+0.1
30.1	100.0 Se	30.4	30.3	+0.3	+0.2

TABLE 3

Precipitation of selenium in the sulphur dioxide and dimethyl sulphite procedures (106 mg Se was used in each test)

Au taken (mg)	Total precipitate obtained (mg)		Se precipitated (mg)	
	DMS	SO_2	DMS	SO_2
20.6	53.6	47.3	33.0	26.7
20.6	55.9	46.9	35.3	26.3
—	38.7	31.2	38.7	31.2
—	80.6[a]	75.4[b]	80.6[a]	75.4[b]

[a]2 ml of dimethyl sulphite were used instead of the usual 1 ml.
[b]The whole solution was saturated with sulphur dioxide instead of adding 25 ml of saturated sulphur dioxide solution.

larger than those in the sulphur dioxide procedure. This was confirmed by filtering the mixed precipitate of gold and selenium through an IG-4 filtering crucible and weighing after washing with water, alcohol and ether and drying at 100°C. The amount of selenium precipitated was much greater when 2 ml of the ester were added instead of the usual 1 ml, because the solution became saturated with sulphur dioxide. This effect was further confirmed by passing sulphur dioxide gas over the surface of the solution with stirring so as to saturate it; again larger amounts of selenium were precipitated (Table 3).

REFERENCES

1 C. R. Stine and L. Gordon, Anal. Chem., 25 (1953) 1519.
2 L. Gordon, M. Salutsky and H. H. Willard, Precipitation from Homogeneous Solution, J. Wiley, New York, 1959.
3 F. E. Beamish, J. J. Russell and J. Seath, Ind. Eng. Chem. Anal. Ed., 9 (1937) 174.
4 F. E. Beamish, The Analytical Chemistry of Noble Metals, Pergamon, Oxford, 1966.
5 E. B. Sandell, Colorimetric Determination of Traces of Metals, 3rd edn., Interscience, New York, 1959.

Analytica Chimica Acta, 102 (1978) 241—244

Short Communication

REPRODUCIBILITY OF ELEMENTAL IMPURITY LEVELS IN MILLIPORE FILTERS (EHWP)

C. McDONALD** and H. J. DUNCAN*

Agricultural Chemistry, Department of Chemistry, University of Glasgow, Glasgow G12 800 (Gt. Britain)

(Received 13th April 1978)

During a survey [1] of atmospheric levels of trace elements, discrepancies were found in impurity levels from one box of filter papers to another. Several reports [2—4] have compared impurity levels between various types and makes of filter papers but none of them refers to the variability of impurity levels between the filter papers in any one box.

At the low levels of elements generally present in the atmosphere, it is important, for meaningful results to be obtained, to have information on the variations in elemental concentrations that occur in one type of filter paper, either from the same or different boxes.

Experimental

Filter papers (EHWP 025, Millipore Corporation) were studied as they were used for collecting atmospheric particulates in a general survey [1]. Filter paper blank values were determined as follows.

Each box of 100 filter papers was sub-divided into four equal segments; five papers were selected at random, omitting the top and bottom three filters from each segment, as it was used. The filter papers were examined either by instrumental neutron activation followed by γ-ray spectrometry as already described [2], or by atomic absorption spectrometry. The filters were dissolved in 5 ml of concentrated "Aristar" nitric acid in a Teflon screw cap dissolution bomb, and made up to 25 ml with distilled water. The solutions were then analysed with a double-beam atomic absorption spectrometer (Perkin-Elmer 306) with a graphite-tube atomizer and deuterium background corrector.

To test the reproducibility of the blank values within separate boxes, two fresh boxes were sampled as follows. One segment (25 filters) was divided into five lots of five filters numbered consecutively from the top. From the remaining three segments, each of 25 papers, five were selected at random from each, omitting the top and bottom three papers in each segment.

**Present address: Public Analyst's Department, Strathclyde Regional Council, Glasgow G3.

The accuracy of the analyses is considered to be as follows: activation analysis for Na, Mn, Br, Sc, Zn, Co, Sb, ± 10%, and for Cr, Fe, Se, ± 20%; atomic absorption analysis for Zn, Cr, Cd, ± 5%; for Ni, ± 10%; Cu, Mn, ± 14%; and for Fe, Pb, Al, ± 18%.

Results and discussion

The results found are shown in Tables 1 and 2. Large discrepancies exist from box to box. Table 3 summarizes the results obtained for the variation that occurs within individual boxes. The nine elements tested reveal a variation which can be summarized as follows: (a) the five outside filters, both top and bottom, have much higher blank values than those in the interior (× 25 in the case of Zn); (b) excluding the five outside filters, the blank values within a segment of 25 are reproducible; (c) in a box of 100 filters, the blank values between all four segments are reproducible if the five outside filters, top and bottom are excluded; (d) blank values vary considerably betwee boxes.

TABLE 1

Variation in blank values measured by instrumental neutron activation analysis (ng cm^{-2})

Element	Box 1	Box 2	Box 3	Box 4
Br	8.6	7.9	9.3	8.4
Co	0.29	0.41	1.10	0.65
Cr	20.0	18.7	14.1	10.5
Fe	376	98	407	133
Mn	4.7	4.9	4.0	4.3
Na	497	99	489	503
Sb	0.2	6.7	14.3	10.4
Sc	0.01	0.03	0.06	0.04
Zn	10.2	9.2	39.5	5.5
Se	8.1	6.2	6.5	7.4

TABLE 2

Variation in blank values measured by atomic absorption spectrometry (ng cm^{-2})

Element	Box 5	Box 6	Box 7	Box 8
Al	31.8	15.5	73.7	51.4
Cd	0.64	0.50	1.50	0.30
Cr	11.8	9.6	26.0	20.3
Cu	21.1	50.5	30.1	30.6
Fe	115	134	93	141
Mn	4.0	8.5	5.5	4.9
Ni	18.2	26.1	27.5	12.8
Pb	10.0	5.0	3.8	1.3
Zn	5.5	44.7	10.9	32.6

TABLE 3

Variation in blank values within separate boxes measured by atomic absorption spectrometry (ng cm^{-2})

	Cu	Zn	Fe	Al	Mn	Cd	Cr	Pb	Ni
Box 1									
Lot 1									
1st 5 Filters	110.0	124.8	183.0	51.4	16.1	26.7	18.1	26.5	31.6
2nd	20.8	5.4	122.0	26.8	3.7	0.7	12.4	8.9	19.5
3rd	20.4	5.6	117.0	20.1	3.7	0.7	10.3	8.3	19.5
4th	20.1	5.6	118.0	20.1	4.0	0.6	11.3	9.6	20.6
5th	60.3	146.6	270.0	93.8	7.7	17.2	15.6	15.9	44.3
Lot 2	20.4	5.6	110.0	31.3	3.6	0.6	12.7	10.8	20.1
Lot 3	22.6	5.5	113.0	38.0	4.3	0.7	11.6	11.5	16.8
Lot 4	20.9	5.5	119.0	35.6	4.2	0.6	11.6	8.9	16.1
Box 2									
Lot 1									
1st 5 Filters	270.0	414.9	916.0	64.8	22.6	44.3	18.5	15.3	51.7
2nd	50.3	43.4	141.0	17.9	8.6	0.4	10.1	5.7	26.4
3rd	50.9	48.8	146.0	17.9	7.4	0.5	9.7	5.1	25.3
4th	51.2	59.7	138.0	13.4	7.7	0.6	9.6	5.7	25.8
5th	470.1	132.4	165.0	46.9	13.0	39.5	10.5	12.1	80.6
Lot 2	49.5	38.6	133.0	15.6	9.1	0.6	9.4	5.1	26.2
Lot 3	51.6	28.0	133.0	13.4	8.6	0.7	9.6	4.6	24.8
Lot 4	50.0	61.7	127.0	16.4	8.4	0.2	9.8	5.0	27.5

It is concluded that, for Millipore (EHWP) filters, blank values vary from box to box. However, within one box, provided that the five outside filters, top and bottom, are discarded, the blank variations are small compared with the atmospheric concentrations of the elements investigated.

Financial assistance was provided by the Science Research Council in the form of a postgraduate studentship (to C. McD.).

REFERENCES

1 C. McDonald, Ph.D. Thesis, University of Glasgow, 1977.
2 I. M. Dale, H. J. Duncan and C. McDonald, Radiochem. Radioanal. Lett., 15 (1973) 77.
3 R. Dams, K. A. Rahn and J. W. Winchester, Environ. Sci. Technol., 6 (1972) 441.
4 W. H. Zoller and G. E. Gordon, Anal. Chem., 42 (1970) 257.

Analytica Chimica Acta, 102 (1978) 245—248

Announcements

The Pittsburgh Conference

Cleveland, Ohio, March 5—9, 1979

The 1979 Pittsburgh Conference on Analytical Chemistry and Applied Spectroscopy will be held on March 5—9, 1979 at the Cleveland Convention Center, Cleveland, Ohio, U.S.A. Symposia have been organized as described below:

(1) (2) Liquid chromatography for environmental regulatory requirements.
(3) Practical applications of glass capillary columns in gas chromatography.
(4) Problems and solutions in capillary gas chromatography.
(5) Ion chromatography.
(6) Photoacoustic spectroscopy.
(7) Laboratory systems management.
(8) Microcomputers/microprocessors and process control automation.
(9) New surface analysis techniques.
(10) Trace analysis in characterization of materials.
(11) Environmental analysis of water and sediment.
(12) Inductively coupled plasma emission.
(13) Symposium on biomedical aspects.
(14) New analytical techniques on the horizon.
(15) 1979 Awards symposium (spectroscopy society of Pittsburgh, Society for Analytical Chemists of Pittsburgh, Hasler award, Dal Nogare award).
(16) Fourier transform/computer dispersive groups symposium
(17) ASTM E-42 — New surface analysis instrumentation.
(18) ASTM E-31 — Computerized laboratory systems.
(19) Coblentz award symposium.

General papers are not restricted to the symposia topics.

In 1978, the Modern Laboratory Equipment presented at the conference totalled about 362 exhibitors occupying approximately 800 booths and 17 seminar rooms in which was displayed the latest equipment available for analytical chemistry and spectroscopic work.

For information regarding the 1979 exposition contact: Mr. Allen J. Sharkins, Exposition Chairman, 1979 Pittsburgh Conference, P.O. Box 2128, Lower Burrell, PA 15068, U.S.A.

Electroanalysis in Hygiene, Environmental, Clinical and Pharmaceutical Chemistry

Chelsea, London, England, April 17—20, 1979

An International Conference will be held at Chelsea College, London, organized by the Electroanalytical Group, Analytical Division, Chemical Society. Plenary lectures will be given by speakers of international repute in these fields. It is expected that the Conference fee (about £100) will cover registration and four nights' accommodation. Further information from: Dr. W. F. Smyth, Department of Chemistry, Chelsea College, Manresa Road, London SW3, England.

XXI Colloquium Spectroscopicum Internationale
8th International Conference on Atomic Spectroscopy

Cambridge, England, July 1—6, 1979

The Conference is organized by the Association of British Spectroscopists and sponsored by the Royal Society, International Union of Pure and Applied Chemistry, Chemical Society, and Institute of Physics.

The scientific programme encompasses all branches of spectroscopy with particular emphasis on the theme of analytical spectroscopy. Symposia will be devoted to particular areas and specific applications of spectroscopy. The provisional timetable incorporates five parallel lecture sessions arranged to minimize overlap of related topics. Each symposium will open with an invited lecture on a topic of special significance. Poster sessions will be featured at the conference for material which is better suited to this manner of presentation. Several large halls will house an Exhibition of large and small instrumentation, equipment, accessories and books. Delegates will be housed in the colleges of the University. There will be a full social and ladies programme every day.

Further details from: Association of British Spectroscopists, P.O. Box 109, Cambridge CB1 2HY, United Kingdom.

27th IUPAC Congress

Helsinki, Finland, August 27—31, 1979

The programme has been planned to include the following main sections and subsections:

(I) Trace element analysis: (a) agricultural and food chemistry; (b) biological and clinical chemistry; (c) environmental chemistry; (d) geochemistry; (e) instrumental techniques in trace element analysis.

(II) Modern methods in clinical chemistry: (a) competitive binding assays; (b) enzymatic kinetic methods for non-enzymatic components; (c) analysis

of tissue specimens by ultramicro methods; (d) gas chromatography-, mass spectrometry and electron spin resonance in clinical chemistry.
(III) Chemistry and biology of cell membrane carbohydrates: (a) symposium on structure and analysis of complex oligosaccharides; (b) analytical developments in the determination of structures of complex carbohydrates; (c) biological functions of membrane carbohydrates; (d) purification of membrane glycoproteins.
(IV) Chemistry and technology of natural polymers and their degradation products: (a) cellulose; (b) starch; (c) other polysaccharides; (d) lignin; (e) other phenolic polymers; (f) physical characterization of natural polymers.
(V) Biotechnology and bioengineering: (a) industrial production of enzymes; (b) biotechnology in pulp and paper industry; (c) design and operation of fermentors; (d) mathematical models of fermentation processes.
(VI) Mineral resources in northern Europe

The scientific programme will consist of six plenary lectures and 24 main lectures given by invited speakers and a large number of contributed papers, which any participant may submit. On the basis of the abstracts the organizers will decide which of the papers conveniently fit together as a thematic group to be presented orally and which will be given as poster sessions. The organizers will be happy to consider proposals for additional subsections. Publication rights are retained on all papers given at the 27th Congress of IUPAC. The invited lectures will be published in "Pure and Applied Chemistry", the official journal of IUPAC, and also made available as a special bound reprint. Other scheduled papers may be published elsewhere after the Congress. Participants of the Congress will receive a booklet containing abstracts of the papers.

The working language of the Congress will be English and simultaneous translations are offered.

Further information from : Dr. J. Larinkari, 27th IUPAC Congress, P.O. Box 13244, SF-00131 Helsinki 13, Finland.

Congressus Pharmaceuticus Hungaricus VII

Budapest, Hungary, September 24—29, 1979

The Hungarian Pharmaceutical Society will hold its 7th Congress of Pharmaceutical Sciences in Budapest, in September, 1979.

Plenary sessions will deal with the efficacy and safety of pharmacotherapy. Lecture and poster sessions will be held on pharmaceutical technology and biopharmacy, pharmaceutical chemistry and pharmacology, drug control, pharmacognosy and phytochemistry, organization and economics of pharmacy, and pharmaceutical history. Round-table conferences will be organized on interdisciplinary problems (for pharmacists and other experts working in public and hospital pharmacies, in the pharmaceutical industry and trade, in public services and in scientific institutes). The official language is Hungarian,

but papers may also be presented in English, German or Russian.

During the plenary sessions and during sessions with high participation rate, simultaneous interpretation will be provided.

Further information from: MOTESZ Congress Bureau, H 1361, POB 32.

27th IUPAC Congress
August 27—31, 1979, Helsinki, Finland

The second circular is now available. Plenary lectures will be given by A. Cottenie (Belgium), N. M. Emanuel (U.S.S.R.), E. Gaden, Jr. (U.S.A.), N. Sharon (Israel), T. E. Timell (U.S.A.), C.-B. Laurell (Sweden). The six sections of the programme, each of which consists of invited lectures, and short communications presented orally or as posters, cover the following fields: Trace element analysis; Modern methods in clinical chemistry; Analysis and structure of cell membrane carbohydrates; Chemistry and technology of natural polymers and their degradation products; Biotechnology and bioengineering; Chemometrics.

Further information from : Dr. J. Larinkari, P. O. Box 244, SF-00131 Helsinki 13, Finland.

International Conference on Flow Analysis
September 11—13, 1979, Amsterdam, The Netherlands

A three-day conference on Flow Analysis will be held in Amsterdam. The progam will cover a wide and representative selection of current research on all aspects of flow analysis, including instrumentation design for flow analysis, possibilities for complete automation, new detection systems, theory of flow analysis, and applications in industrial, environmental and clinical analysis. Further information is available from: Secretary FA-Amsterdam, Laboratory for Analytical Chemistry, University of Amsterdam, Nieuwe Achtergracht 166, 1018 WV Amsterdam, The Netherlands.

Erratum

L. A. Lazarou and T. P. Hadjiioannou, Kinetic study of Iron(II)-Induced Acid reaction with a Perbromate-Selective Electrode. Determination of Tartaric Acid. Anal. Chim. Acta, 100 (1978) 207—214.

Page 209, eqn. (5), for k read K.
Page 213, line 25, for deviation read standard deviation.

ANALYTICA CHIMICA ACTA, VOL. 102 (1978)

AUTHOR INDEX

Ali, M. M., see Emara, M. M. 181
Appala Raju, N., see Soundar Rajan, S. C. 237
Ariel, M., see Wang, J. 99
Armentrout, D. N., see Ramstad, T. 229

Beck, M. T., see El-Defrawy, M. M. M. 185
Bhattacharyya, S. N., see Das, N. R. 221
Bower, E. L.-Y.
— and Winefordner, J. D.
The effect of sample environment on the room-temperature phosphorescence of several polynuclear aromatic hydrocarbons 1

Chateau-Gosselin, M.
— et Patriarche, G. J.
Détermination d'hydrazines et d'hydrazides à l'aide du cérium(IV), du manganese(III) et de l'argent(II) produits coulométriquement 215
Corriveau, L. P. V., see Hawkings, R. C. 61

Davies, I. M.
Determination of methylmercury in the muscle of marine fish by cold-vapour atomic absorption spectrometry 189
Das, N. R.
— and Bhattacharyya, S. N.
Preconcentration of gold and tungsten from geological samples for neutron activation analysis 221
de Boer, H. S.
—, den Hartigh, J., Ploegmakers, H. H. J. L. and van Oort, W. J.
Polarographic analysis for corticosteroids. Part 1. The electroanalytical properties of corticosteroids 141
den Hartigh, J., see de Boer, H. S. 141
Doronin, A. N., see Kabanova, O. L. 91
Duncan, H. J., see McDonald, C. 241

El-Defrawy, M. M. M.
—, Posta, J. and Beck, M. T.
Elimination of ionic interference effects in the atomic absorption spectrometric determination of ruthenium 185
Emara, M. M.
—, Ali, M. M. and Gharib, A. E.-A.
Effect of acids on the determination of nickel by atomic absorption spectrometry 181

Fayad, N., see Fogg, A. G. 205
Fodor, P., see Pungor, E. 15
Fogg, A. G.
— and Fayad, N.
Differential pulse polarographic determination of disodium cromoglycate in urine 205

Gharib, A. E.-A., see Emara, M. M. 181
Goncharov, Yu. A., see Kabanova, O. L. 91
Gratzl, M.
—, Rakiás, F., Horvai, G., Toth, K. and Pungor, E.
Effect of pH on the response of a cyanide ion-selective electrode 85

Hancock, R. G. V., see Hoffman, E. L. 157
Hawkings, R. C.
—, Corriveau, L. P. V., Kushneriuk, S. A. and Wong, P. Y.
Dynamic response of the fluoride ion-selective electrode 61
Headridge, J. B.
— and Thompson, R.
Determination of bismuth in nickel-base alloys by atomic absorption spectrometry with introduction of solid samples into an induction furnace 33
Hepler, B. R.
—, Weber, S. G. and Purdy, W. C.
The behaviour of an electrochemical detector used in liquid chromatography and continuous flow voltammetry. Part 2. Evaluation of low-temperature isotropic carbon for use as an electrode material 41
Hoffman, E. L.
—, Naldrett, A. J., van Loon, J. C., Hancock, R. G. V. and Manson, A.

The determination of all the platinum group elements and gold in rocks and ore by neutron activation analysis after preconcentration by a nickel sulphide fire-assay technique on large samples 157
Horvai, G., see Gratzl, M. 85

Jean, R., see Magrone, R. 233
Johansson, B.-L.
—— and Persson, B.
Polarographic study of an alkyl benzimidazolyl sulfoxide and the corresponding sulfide and sulfone 121

Kabanova, O. L.
——, Goncharov, Yu. A. and Doronin, A. N.
Anodic stripping voltammetry and chronopotentiometry of copper at a rotating carbosital disk electrode 91
Kántor, T.
——, Fodor, P. and Pungor, E.
Determination of traces of lead, cadmium and zinc in copper by an arc-nebulization and flame atomic absorption technique 15
Kawamura, S.,
——, Shibata, S., Kurotaki, K. and Takeshita, H.
The sorption characteristics of radionuclides on copper hexacyanoferrate(II), and the determination of ^{137}Cs in sea water 225
Kruidhof, H.
A general x-ray fluorescence spectrometric technique based on simple corrections for matrix effects 177
Kurotaki, K., see Kawamura, S. 225
Kushneriuk, S. A., see Hawkings, R. C. 61

Lund, W., see Overvoll, P. A. 211

Magrone, R.
——, Jean, R., Saccone, P. and Weber, R.
Automatic thermometric analysis for caustic soda and alumina in Bayer liquors 233
Manson, A., see Hoffman, E. L. 157
McDonald, C.
—— and Duncan, H. J.
Reproducibility of elemental impurity levels in millipore filters (EHWP) 241

Naldrett, A. J., see Hoffman, E. L. 157

Ouziel, E., see Wang, J. 99
Overvoll, P. A.
—— and Lund, W.
The determination of small amounts of strong acid in presence of an excess of weak acid 211

Patriarche, G. J., see Chateau-Gosselin, M. 215
Persson, B., see Johansson, B.-L. 121
Ploegmakers, H. H. J. L., see de Boer, H. S. 141
Poitrenaud, C., see Rodriguez, A. R. 167
Porthault, M., see Shafiqul Alam, A. M. 113
Posta, J., see El-Defrawy, M. M. M. 185
Potter, N. M.
Determination of copper in gasoline by atomic absorption spectrometry with electrothermal atomization 201
Pungor, E., see Gratzl, M. 85
Pungor, E., see Kantor, T. 15
Purdy, W. C., see Hepler, B. R. 41

Rakias, F., see Gratzl, M. 85
Ramstad, T.
—— and Armentrout, D. N.
Determination of 'total' chlorophenols in a brine by a modified 4-amino-antipyrine test after column clean up 229
Rodriguez, A. R.
—— et Poitrenaud, C.
Influence des solvants organiques sur les équilibres d'échange d'ions entre une résine a groupements sulfoniques. I. Partage d'éléments métalliques monovalents et divalents 167

Saccone, P., see Magrone, R. 233
Samuelsson, R.
Pulse polarographic determination of nitrosamines. Part 1. Determination of nitrosodiethanolamines in grinding fluids 133
Shafiqul Alam, A. M.
——, Vittori, O. and Porthault, M.
Determination of germanium(IV) in perchloric acid solution by a.c. polarography and differential pulse polarography in the presence of 3,4-dihydroxybenzaldehyde 113
Shibata, S., see Kawamura, S. 225
Soundar Rajan, S. C.
—— and Appala Raju, N.
Dialkyl sulphites as gravimetric

reagents for gold by precipitation from homogeneous solution 237
Sullivan, J. V.
— and van Loon, J. C.
A demountable boosted-output spectral map for atomic absorption and fluorescence measurements 25

Takeshita, H., see Kawamura, S. 225
Thompson, R., see Headridge, J. B. 33
Tóth, K., see Gratzl, M. 85

Ure, A. M., see Verbeek, A. A. 195

van Loon, J. C., see Sullivan, J. V. 25
van Loon, J. C., see Hoffman, E. L. 157
van Oort, W. J., see de Boer, H. S. 141
Verbeek, A. A.
— and Ure, A. M.
Improved precision by servomechanical stabilization of cyanogen band emission in a nitrous oxide—acetylene flame 195
Vittori, O., see Shafiqul Alam, A. M. 113

Wang, J.
—, Ouziel, E., Yarnitzky, Ch. and Ariel, M.
A flow detector based on square-wave polarography at the dropping mercury electrode 99
Weber, R., see Magrone, R. 233
Weber, S. G., see Hepler, B. R. 41
Winefordner, J. D., see Bower, E. L.-Y. 1
Wong, P. Y., see Hawkings, R. C. 61

Yarnitzky, Ch., see Wang, P. 99

ANALYTICA CHIMICA ACTA
(including COMPUTER TECHNIQUES AND OPTIMIZATION)

INFORMATION FOR AUTHORS

Analytica Chimica Acta publishes original papers, short communications, and reviews dealing with every aspect of modern chemical analysis, both fundamental and applied. The section on *Computer Techniques and Optimization* is devoted to new developments in chemical analysis by the application of computer techniques and by interdisciplinary approaches, including statistics, systems theory and operation research.

Reviews are written by invitation of the editors, who welcome suggestions for subjects. Short communications are usually complete descriptions of limited investigations, and should generally not exceed four printed pages. Preliminary communications of important urgent work can be printed in this category within 4 months of submission, if the authors are prepared to forego proofs.

Submission of papers

Authors should submit three copies of the manuscript in double-spaced typing on one side of the paper only, with a margin of 4 cm, on pages of uniform size. If any variety of machine copying is used (e.g. xerox), authors should ensure that all copies are easily legible and that the paper used can be written on with both ink and pencil. Authors are advised to retain at least one copy of the manuscript. Manuscripts should be preceded by a sheet of paper carrying (a) the title of the paper, (b) the name and full postal address of the person to whom proofs are to be sent, (c) the number of pages, tables and figures. (d) suggested keywords for indexing.

Manuscripts should be sent to the editorial addresses given on the covers of current issues; submission to the publisher leads to delays. Submission of a manuscript implies that the work described has not been, and will not be, published elsewhere (except as an abstract, or as part of a lecture, review or academic thesis). On acceptance of the manuscript, the copyright passes to the publishers, if it has not been previously reserved by a government institution or company.

The preferred language of the journal is English, but French and German manuscripts are also acceptable. For authors whose first language is not English, French or German, linguistic improvement is provided as part of the normal editorial processing.

Notes on the preparation of manuscripts

Authors are given every latitude, consistent with clarity and brevity, in the style and form of their papers. Very useful advice is provided in the Handbook for Authors issued by the Chemical Society and American Chemical Society.

Title and initial layout. All manuscripts should be headed by a concise but informative title. This is followed by the names of the authors, and the address of the laboratory where the work was carried out. The author to whom correspondence should be addressed must be indicated by an asterisk (without a footnote). If the present address of an author is different from that mentioned, it should be given in a footnote. Acknowledgements of financial support should not be made in footnotes.

Summary. Research papers and reviews begin with a Summary (50—250 words) which should comprise a brief factual account of the contents of the paper, with emphasis on new information. Uncommon abbreviations, jargon and reference numbers must not be used. The Summary should be suitable for use by abstracting services without rewriting. Papers in French or German require a Résumé or Zusammenfassung followed by a Title and Summary in English; authors are encouraged to provide translations where necessary. Short communications do not require summaries.

Introduction. The first paragraphs of the paper should contain accounts of the reasons for the work, any essential historical background (as briefly as possible and with key references only) and preliminary experimental work.

Experimental. The experimental methods may be described after the introductory material, or after the discussion of results, depending on the nature of the paper. Detailed experimental descriptions should, however, be restricted to one section of the paper, and not scattered throughout the text. Working procedures should be given in the imperative mood; sufficient detail should be given to allow any reasonably experienced worker to carry out the procedure. Detailed descriptions of well-known techniques and equipment are unnecessary, as are simple preparations of reagents or solutions, and lists of common chemicals. Manufacturers need be named only if the product differs essentially from that of other manufacturers. Local suppliers for multi-national concerns need not be named. In writing, complete sentences should be used, and procedural steps should not be numbered.

Results and Discussion. These may be treated together or separately. In discussing results, unnecessary repetition of experimental detail, unsupported elaboration of hypotheses, and verbose exposition of ideas should be avoided. Chemical formulae should not be used in the text unless confusion is likely to arise from the use of names. Formulae should, however, be used for brevity in Tables and Figures. Calculations well known to specialists are unnecessary. Conclusions should be added only if needed for interpretation; they should not be used as extended summaries.

Acknowledgements. These should be kept as short as possible, and placed, without a heading, at the conclusion of the text.

References

The references should be collected at the end of the paper, numbered in the order of their appearance in the text (*not* arranged alphabetically), and typed on a separate sheet. If the paper forms part of a series, the reference to the previous part should appear as the first reference, the number being cited at the title of the paper. References given in Tables should be numbered according to the position of the Table in the text. Every reference listed must be cited in the text. Reference numbers in the text are set in square brackets on the line. Numerals referring to equations are placed in parentheses.

In the list of references, the following forms should be adopted.

Journals

1 W. Lund and M. Salberg, Anal. Chim. Acta, 76 (1975) 131.
2 M. McDaniel, A. D. Shendrikar, K. D. Reizneir and P. W. West, Anal. Chem., 48 (1976) 2240.

The title of the journal must be abbreviated as in the Bibliographic Guide for Editors and Authors.

Books

1 D. D. Perrin, Masking and Demasking of Chemical Reactions, Interscience-Wiley, New York, 1970, p. 188.
2 G. G. Guilbault, in G. Svehla (Ed.), Wilson and Wilson's Comprehensive Analytical Chemistry, Vol. 8, Elsevier, Amsterdam, 1977, p. 49.

Titles of papers are unnecessary. Citations of reports which are not widely available (e.g. reports from government research centres) should be avoided if possible. Authors' initials should not be used in the text, unless real confusion could be caused by their omission. If the reference cited contains three or more names, only the first author's name followed by et al. (e.g. McDaniel et al.) should be used in the text; but the reference list must contain the initials and names of *all* authors.

Tables, Computer Programs and Figures

Tables and Figures must be essential for the clear and concise presentation of the material. The same information should not be given in Tables and Figures, and material from the published literature should not be reproduced.

Tables. All Tables should be numbered with Arabic numerals, and have brief descriptive headings; they should be typed on separate pages. The layout should be given serious thought, so that the significance of the results can be grasped quickly. Column headings should be brief.

Tables with only two or three headings are printed best horizontally, e.g.

Hg^{2+} added (μg)	1.0	2.0	3.0	5.0
Extraction (%)	95.0	99.8	99.5	89.0

Experimental information which is relevant to all the results in the Table is best given in parentheses immediately after the heading. No column should contain the same number or unit throughout its length. Footnotes to Tables are denoted by superscript a, b, c . . . . The units used should be clearly stated. Confusion can arise from the use of powers in column headings. The following usage is recommended: e.g. if molar absorptivities are listed, the heading should be $\epsilon(\times 10^4\ l\ mol^{-1}\ cm^{-1})$ so that a number 2.32 in the column signifies 23 200.

Alphanumeric computer output is usually unsuitable for reproduction and should therefore be retyped and presented as Tables; capitals can be used to simulate computer output if such simulation is essential for illustration.

Computer programs. Computer algorithms should be described clearly; a standard high-level programming language or a suitable algorithmic notation should be used as necessary. Complete program listings, however, are not normally admissible. Extensive flow charts should be avoided if the material can equally well be given in descriptive or tabular form. Statements on the portability of the software described to other computer systems, as well as on its availability to interested readers, should be given.

Figures. Figures should be prepared in black waterproof drawing ink on drawing or tracing paper of the same size as that on which the manuscript is typed. One original (or sharp glossy print) and two photostat (or other) copies are required. Attention should be given to line thickness, lettering (which should be kept to a minimum) and spacing on axes of graphs, to ensure suitability for reduction during printing. Axes of a graph should be clearly labelled, along the axes, and outside the graph itself.

The following standard symbols should be used in graphs:

▼ ▽ ■ □ + × ● ○ ▲ △

Simple straight-line graphs are not acceptable, because they can readily be described in the text, by means of an equation or a sentence. Explanatory information should be placed not in the figure, but in the legend, which should be typed on a separate sheet of paper. All Figures should be numbered with Arabic numerals, and require descriptive legends.

Photographs should be glossy prints and be as rich in contrast as possible; colour photographs cannot be accepted. In general, line diagrams are more informative than photographs of equipment.

Computer outputs for reproduction as Figures must be of good quality on blank paper, and should preferably be submitted as glossy prints.

Nomenclature, abbreviations and symbols

In general, the recommendations of the International Union of Pure and Applied Chemistry (IUPAC) should be followed, and attention should be given to the recommendations of the Analytical Chemistry Division in the journal *Pure and Applied Chemistry*. (see also *IUPAC Compendium of Analytical Nomenclature*, 1978)

Symbols, formulae and equations should be written with great care, capitals and lower case letters being distinguished where necessary. Particular care should be taken in typing mathematical expressions containing superscripts and subscripts, and in proof-reading such equations. Greek letters and unusual symbols employed for the first time should be defined by name in the left-hand margin.

Basic SI and other accepted metric nomenclature are given in the Appendix. In accordance with IUPAC rules, the mass number, atomic number, number of atoms and ionic charge should be designated by a left upper index, a left lower index, a right lower index and a right upper index, respectively, placed round the atomic symbol. For example, the phosphate ion should be designated as PO_4^{3-} (*not* PO_4^{-3} or PO_4^{---}), and phosphorus-32 as ^{32}P (*not* P^{32} or P-32).

The Stock notation for the indication of stoichiometric valency states (and indirectly the proportion of the constituents) is recommended. Examples are iron(III) chloride in preference to ferric chloride, and potassium hexacyanoferrate(II) in preference to potassium ferrocyanide. These rules are valid for French and German as well as English usage.

The use of nanometre (nm) and micrometre (μm), for the expression of analytical wavelengths has now superseded mμ or Å or μ, all of which should be avoided, although Å is sensibly retained in crystallographic work.

Natural or Naperian logarithms should be denoted by ln and decadic logarithms by log.

In analytical chemistry, the term normality (N) serves many useful purposes and will be retained. It should not however, be used, if no ambiguity is introduced by the use of molarity (M). The term formality (F) should be avoided.

Unusual abbreviations require definition when first used. Abbreviations for long chemical names (e.g. EDTA, HEDTA, TBAH, en, pn, Tris) are useful, especially in equations, Tables or Figures. For ease of distinction, well-known techniques should be abbreviated by using lower-case letters and full stops, such as, g.c.-m.s., u.v., i.r., a.a.s., n.m.r., a.s.v., d.p.p., etc.

Ambiguity in expressing dilution can be avoided by the use of e.g. (1 + 2) rather than 1:2 which could mean either one part diluted with 2 parts or one part diluted to twice its volume.

The solidus / may be used in equations to economize vertical space, but its use should be consistent. For example:

$$A/b = x^2/(u + v)^{5/6}$$

Special attention should be given to correct use of brackets in complicated equations.

Decimal points should be indicated by full stops in papers written in English and by commas in French and German papers.

Appendix

Basic SI units.

metre	m	candela	cd
kilogram	kg	mole	mol
second	s	(an Avogadro number of any	
ampere	A	particle: atoms, molecules,	
degree Kelvin	K	ions, electrons, etc.)	

Derived SI units.

joule	J	$kg\ m^2\ s^{-2}$	farad	F	$A\ s\ V^{-1}$
newton	N	$J\ m^{-1}$	weber	Wb	V s
watt	W	$J\ s^{-1}$	henry	H	$V\ s\ A^{-1}$
coulomb	C	A s	tesla	T	$V\ s\ m^{-2}$
volt	V	$J\ A^{-1}\ s^{-1}$	hertz	Hz	s^{-1}
ohm	Ω	$V\ A^{-1}$	degree Celsius	°C	K − 273.15

Other units.

litre	l	$10^{-3}\ m^3$	hour	h	3.6×10^3 s
gram	g	10^{-3} kg	dyne	dyn	10^{-5} N
poise	P	$10^{-3}\ m^{-1}\ s^{-1}$	atmosphere	atm	101.325 kN m^{-2}
electron volt	eV	1.6021×10^{-19} J	molar	M	$mol\ l^{-1}$
calorie	cal	4.184 J	molal	*m*	$mol\ kg^{-1}$
minute	min	60 s	curie	Ci	$37 \times 10^9\ s^{-1}$

Prefixes to Abbreviations for the names of units indicating

Multiples		Sub-multiples			
tera ($\times 10^{12}$)	T	milli ($\times 10^{-3}$)	m	pico ($\times 10^{-12}$)	p
giga ($\times 10^9$)	G	micro ($\times 10^{-6}$)	μ	femto ($\times 10^{-15}$)	f
mega ($\times 10^6$)	M	nano ($\times 10^{-9}$)	n	atto ($\times 10^{-18}$)	a
kilo ($\times 10^3$)	k				

(continued from outside of cover)

Elimination of ionic interference effects in the atomic absorption spectrometric determination of ruthenium
M. M. M. El-Defrawy, J. Posta and M. T. Beck (Debrecen, Hungary) 185
Determination of methylmercury in the muscle of marine fish by cold-vapour atomic absorption spectrometry
I. M. Davies (Aberdeen, Gt. Britain) 189
Improved precision by servomechanical stabilization of cyanogen band emission in a nitrous oxide–acetylene flame
A. A. Verbeek and A. M. Ure (Aberdeen, Gt. Britain) 195
Determination of copper in gasoline by atomic absorption spectrometry with electrothermal atomization
N. M. Potter (Warren, MI, U.S.A.) 201
Differential pulse polarographic determination of disodium cromoglycate in urine
A. G. Fogg and N. Fayad (Loughborough, Gt. Britain) 205
The determination of small amounts of strong acid in presence of an excess of weak acid
P. A. Overvoll and W. Lund (Oslo, Norway) 211
Détermination d'hydrazines et d'hydrazides à l'aide du cérium(IV), du manganese(III) et de l'argent(II) produits coulométriquement
M. Chateau-Gosselin et G. J. Patriarche (Brussels, Belgique) 215
Preconcentration of gold and tungsten from geological samples for neutron activation analysis
N. R. Das and S. N. Bhattacharyya (Calcutta, India). 221
The sorption characteristics of radionuclides on copper hexacyanoferrate(II), and the determination of ^{137}Cs in sea water
S. Kawamura, S. Shibata, K. Kurotaki and H. Takeshita (Chiba-Shi, Japan) 225
Determination of "total" chlorophenols in a brine by a modified 4-aminoantipyrine test after column clean up
T. Ramstad and D. N. Armentrout (Midland, MI, U.S.A.) 229
Automatric thermometric analysis for caustic soda and alumina in Bayer liquors
R. Magrone, R. Jean, P. Saccone (Gardanne, France) and R. Weber (Geneva, Switzerland) . 233
Dialkyl sulphites as gravimetric reagents for gold by precipitation from homogeneous solution
S. C. Soundar Rajan and N. Appala Raju (Tirupati, India) 237
Reproducibility of elemental impurity levels in Millipore filters (EHWP)
C. McDonald and H. J. Duncan (Glasgow, Gt. Britain) 241

Announcements 245

Erratum 248

Author Index 249

Information for Authors 253

CONTENTS

The effect of sample environment on the room-temperature phosphorescence of several polynuclear aromatic hydrocarbons
E. L.-Y. Bower and J. D. Winefordner (Gainesville, FL, U.S.A.) 1
Determination of traces of lead, cadmium and zinc in copper by an arc-nebulization and flame atomic absorption technique
T. Kántor, P. Fodor and E. Pungor (Budapest, Hungary) 15
A demountable boosted-output spectral lamp for atomic absorption and fluorescence measurements
J. V. Sullivan and J. C. van Loon (Clayton, Victoria, Australia) 25
Determination of bismuth in nickel-base alloys by atomic absorption spectrometry with introduction of solid samples into an induction furnace
J. B. Headridge and R. Thompson (Sheffield, Gt. Britain) 33
The behaviour of an electrochemical detector used in liquid chromatography and continuous flow voltammetry. Part 2. Evaluation of low-temperature isotropic carbon for use as an electrode material
B. R. Hepler, S. G. Weber and W. C. Purdy (Montreal, Quebec, Canada) 41
Dynamic response of the fluoride ion-selective electrode
R. C. Hawkings, L. P. V. Corriveau, S. A. Kushneriuk and P. Y. Wong (Chalk River, Ontario, Canada) 61
Effect of pH on the response of a cyanide ion-selective electrode
M. Gratzl, F. Rakiás, G. Horvai, K. Tóth and E. Pungor (Budapest, Hungary) 85
Anodic stripping voltammetry and chronopotentiometry of copper at a rotating carbosital disk electrode
O. L. Kabanova, Yu. A. Gorcharov and A. N. Doronin (Moscow, U.S.S.R.) 91
A flow detector based on square-wave polarography at the dropping mercury electrode
J. Wang, E. Ouziel, Ch. Yarnitzky and M. Ariel (Haifa, Israel) 99
Determination of germanium(IV) in perchloric acid solution by a.c. polarography and differential pulse polarography in the prescence of 3,4-dihydroxybenzaldehyde
A. M. Shafiqul Alam, O. Vittori and M. Porthault (Villeurbanne, France) 113
Polarographic study of an alkyl benzimidazolyl sulfoxide and the corresponding sulfide and sulfone
B.-L. Johansson and B. Persson (Uppsala, Sweden) 121
Pulse polarographic determination of nitrosamines. Part 1. Determination of nitrosodiethanolamines in grinding fluids
Samuelsson (Umeå, Sweden) 133
Polarographic analysis for corticosteroids. Part 1. The electroanalytical properties of corticosteroids
H. S. de Boer, J. den Hartigh, H. H. J. L. Ploegmakers and W. J. van Oort (Utrecht, The Netherlands) 141
The determination of all the platinum group elements and gold in rocks and ore by neutron activation analysis after preconcentration by a nickel sulphide fire-assay technique on large samples
E. L. Hoffman, A. J. Naldrett, J. C. van Loon, R. G. V. Hancock (Toronto, Ontario, Canada) and A. Manson (Mississauga, Ontario, Canada) 157
Influence des solvants organiques sur les équilibres d'échange d'ions entre une résine a groupements sulfoniques. I. Partage d'éléments métalliques monovalents et divalents
A. R. Rodriquez et C. Poitrenaud (Gif-sur-Yvette, France) 167

Short Communications

A general x-ray fluorescence spectrometric technique based on simple corrections for matrix effects
H. Kruidhof (Enschede, The Netherlands) 177
Effect of acids on the determination of nickel by atomic absorption spectrometry
M. M. Emara, M. M. Ali and A. E.-A. Gharib (Cairo, Egypt) 181

(continued on inside page of the cover)